

https://dspace.org/

Long distance pneumatic conveying

Bettman, Richard

2015-01-08
http://hdl.handle.net/10539/16268

Downloaded from a DSpace repository. https://dspace.org/

LONG DISTANCE PNEUMATIC CONVEYING

Richard Bettman

A dissertation submitted to the Faculty of Engineering, University of the Witwatersrand, Johannesburg, in fulfilment of the requirements for the degree of Master of *Science in Engineering*.

Johannesburg, 1987.

DECLARATION

I, Richard Bettman, hereby declare that this dissertation is my own work and that the material herein has not been submitted by me for the Degree of Master of Science in Engineering to any other University.

R Bettman

RICHARD BETTMAN

9/10/1987

DATE

TO MY PARENTS

MR AND MRS R BETTMAN

SYNOPSIS

Experimental investigations, to determine the effects of conveying pipeline length and pipeline diameter on the performance of a pneumatic conveying system, are discussed.

It was of concern that insufficient information is available in the published literature for the design of stepped pipelines, which are generally used when conveying over long distances.

The effect of pipeline length was investigated by conducting tests through 100, 200 and 400 metre pipelines. The effect of pipe diameter was investigated using three pipelines over a distance of 200 metres with diameters of 105, 156 and 200mm. Various stepped pipelines over distances of 100 and 400 metres were investigated. The performance of a long distance pipeline (i.e. 1358 metres) was also determined from experimental results. Flyash was the only material conveyed in all the tests.

An empirical model was developed to calculate the conveying pressure of the long distance line. The experimental results were then compared to the conveying pressures as derived from the model.

From the investigations it was established that there exists an optimum pipe diameter in terms of the power required to convey the material.

The following proposals have been made:

a) The conveying pressure of a system is related to the area under the curve on the State Diagram.
b) The optimum stepped pipeline can be determined from a design procedure which has been developed.

The above proposals may require verification through further experimentation. The recommendations for future research work highlight the importance of establishing a universally accepted standard test rig and testing procedure.

ACKNOWLEDGEMENTS

The author would like to express his sincere gratitude to the following organizations for so generously supporting this project:

Esser-Brieden.

Mr E Kuhme, Managing Director of Esser-Brieden, for donating the tandem blow vessel system.

Walter-Becker.

For supplying the control system and for kindly assisting when the relevant help was required.

Johannesburg Consolidated Investments.

The financial assistance from JCI, which covered the expenses incurred during the course of this project.

SASOL.

The bursary received from SASOL for the past six years enabled me to study at Cape Town University and to undertake this research project at the University of the Witwatersrand.

CSIR.

The Council for Scientific and Industrial Research for granting the post-graduate scholarship.

University of the Witwatersrand.

In particular the Department of Mechanical Engineering for supporting this project.

Instrotech Load Cell Services.

Mr D Howcroft for his assistance during the calibration of the load cells.

In addition, the author is indebted to the following people:

Professor R D Marcus: my *supervisor, for granting me* the opportunity to undertake this project. His constant optimism, enthusiasm and concern for my well being, was a major contribution to the completion of the project. It was an enjoyable and invaluable experience working under *his guidance.*

Professor A Nedrick: my supervisor, especially for commenting so thoroughly on the draft of this report.

Professor F Rizk: for his hospitality during my visit to Germany. The lengthy discussions held with him made me gain a better understanding of the theoretical implications of pneumatic conveying.

Mr R Carr : for his helpfulness in the workshop.

Frank, Simon, John, Edwin, Petrus and David: the labourers at UWTec who assisted with the *installation of* the pipeline configurations.

Mr S Ratcliff: for introducing me to the basic concepts of pneumatic conveying. The discussions held with him *stimulated many of* the ideas *developed in this project.*

Mr M Evans: for his continuous encouragement and assistance.

Miss K Masters: for the proficient typing of the initial and final drafts of this report.

Mr and Mrs R Bottman: my parents, for their eternal support and encouragement which will always be treasured.

CONTENTS

DECLARATION		i
SYNOPSIS		iii
ACKNOWLEDGEMENTS		iv
CONTENTS		vi
LIST OF FIGURES		xiii
LIST OF TABLES		xix
NOMENCLATURE		xxi
1 INTRODUCTION		1
1.1 PURPOSE OF INVESTIGATION		1
1.2 PROJECT OBJECTIVES		2
1.3 ORGANISATION OF REPORT		2
2 LITERATURE REVIEW		4
2.1 INTRODUCTION		4
2.2 PNEUMATIC CONVEYING		4
2.2.1	Development of Pneumatic Conveying	4
2.2.2	Pneumatic Conveying Theory	6
2.3 EFFECT OF LINE LENGTH		13
2.4 EFFECT OF PIPE DIAMETER		15
2.5 EFFECT OF BENDS		16
2.6 ACCELERATION, LENGTH AND PRESSURE DROP		19
2.7 TELESCOPIC PIPELINES		20
2.8 REDUCTION OF POWER CONSUMPTION		22
2.8.1	Optimum Conveying Conditions	22
2.8.2	Drag Reduction	22

2.9 EFFECT OF MATERIAL PROPERTIES 23
2.10 DESIGN PROCEDURES 26
2.11 CONCLUSIONS 28

3 DESCRIPTION OF EXPERIMENTAL TEST RIG 29

3.1 INTRODUCTION 29
3.2 REQUIREMENTS 29
3.3 OPERATING RANGES 30
3.4 DESCRIPTION OF EQUIPMENT 31
3.4.1 Tandem Pressure Vessels 31
3.4.2 Filter unit and Receiving Hopper 31
3.4.3 Conveying Pipes 31
3.4.4 Compressors 32
3.5 INSTRUMENTATION AND DATA ACQUISITION 33
3.5.1 Air Flowrate 34
3.5.2 Product Mass Flowrate 34
3.5.3 Pressures 35
3.5.4 Data Acquisition System 36
3.6 DESCRIPTION OF PIPELINE CONFIGURATIONS 36
3.7 SYSTEM OPERATING CYCLE 36
3.8 EXPERIMENTAL PROCEDURE 38
3.9 COMPUTER SOFTWARE 39
3.10 FLYASH PROPERTIES 41
3.10.1 Particle Size 41
3.10.2 Bulk Density 42
3.10.3 Geldarts Classification of Flyash 42

4. EXPERIMENTAL PHILOSOPHY 43

4.1 INTRODUCTION 43
4.2 PIPELINE CONFIGURATIONS INVESTIGATED 44

5. RESULTS AND PERFORMANCE CHARACTERISTICS 46

5.1 INTRODUCTION 46
5.2 EQUATIONS FOR RESULTS 46
5.3 PRESSURE PROFILES 50
5.4 PERFORMANCE CHARACTERISTICS 56
5.4.1 Conveying Pressure Versus Air Velocity 57
5.4.2 Conveying Pressure Versus Load Ratio 59
5.4.3 Power Versus Product Mass Flowrate 60
5.4.4 Power Versus Load Ratio 61
5.4.5 Power Versus Air Velocity 62
5.4.6 Product Mass Flowrate Versus Air Mass Flowrate 63
5.5 LONG DISTANCE RESULTS 64
5.6 CONCLUSIONS 65

6 PIPELINE LENGTH AND DIAMETER EFFECTS ON THE SYSTEM PERFORMANCE 67

6.1 INTRODUCTION 67
6.2 PIPELINE LENGTH EFFECTS 67
6.2.1 Introduction 67
6.2.2 The Effect of Line Length onConveying Pressureand Product Mass Flowrate 68
6.2.2.1 Conveying Pressure 68
6.2.2.2 Product Mass Flowrate 69
6.2.3 Effect of Line Length on the Conveying Pressure from the State Diagram 70
6.2.4 Acceleration Zone Effects on Conveying Pressure for Various Line Lengths 71
6.2.5 Conclusions 72
6.3 PIPELINE DIAMETER EFFECTS 75
6.3.1 Introduction 75
6.3.2 The Effect of Pipe Diameter on Conveying Pressure 75
6.3.3 Conclusions 75

7	EFFECTIVENESS OF STEPPED PIPELINES	80
	7.1 INTRODUCTION	80
	7.2 EXPERIMENTAL OBSERVATIONS	82
	7.3 CONCLUSIONS	86
8	OPTIMUM DESIGN OF TELESCOPIC PIPELINES	88
	8.1 INTRODUCTION	88
	8.2 DESIGN PROCEDURE	89
	8.3 COST CONSIDERATIONS	90
	8.4 CONCLUSIONS	92
9	NORMALISATION OF RESULTS	93
	9.1 INTRODUCTION	93
	9.2 DIMENSIONAL ANALYSIS	93
	9.3 NORMALISATION	96
	9.4 CONCLUSIONS	98
10	PERFORMANCE PREDICTING MODEL	109
	10.1 INTRODUCTION	109
	10.2 CALCULATION METHOD	110
	10.3 MODEL EQUATIONS	113
	10.4 LONG DISTANCE LINE CONVEYING PRESSURES	114
	10.5 CONCLUSIONS	115
11	GENERAL OBSERVATIONS	127
	11.1 INTRODUCTION	127
	11.2 ROTARY VALVE PERFORMANCE	127
	11.3 FLOW PATTERNS	128
	11.4 STEPPED SECTION	130

12 CONCLUSIONS AND RECOMMENDATIONS 132

12.1 CONCLUSIONS 132
12.2 RECOMMENDATIONS FOR FUTURE RESEARCH 134
12.2.1 Line Length 134
12.2.2 Pipe Diameter 135
12.2.3 Standardisation 135
12.2.4 Stepped Pipelines 138

APPENDICES

A RESULTS 139

A1 INTRODUCTION 140
A2 TEST RUN PRINTOUT 141
A3 TABLES OF RESULTS 142
A4 AIR ALONE PRESSURE DROP 256
A5 PRESSURE VERSUS PRODUCT MASS FLOWRATE GRAPHS 265

B EQUIPMENT SPECIFICATIONS 290

B1 COMPRESSORS 291
B2 BRIEDEN BLOW VESSELS 293

C INSTRUMENTATION SPECIFICATION AND CALIBRATION 294

C.1 PRODUCT MASS FLOWRATE MEASUREMENT 295
C.1.1 Load Cell Specifications 295
C.1.2 Calibration 296

C.2 AIR MASS FLOWRATE MEASUREMENT 299
C.2.1 Flowmeter Specifications 299
C.2.2 Calibration 300

C.3 PRESSURE MEASUREMENT 302
C.3.1 Specifications 303
C.3.2 Calibrations 304

C.4 TEMPERATURE MEASUREMENT 311
C.4.1 Specifications 311
C.4.2 Calibration 312

D COMPUTER PROGRAMMES 314

D1 INTRODUCTION 315
D2 PROGRAMME I 316
D3 PROGRAMME II 320
D4 PROGRAMME III 323
D5 PROGRAMME IV 326
D6 PROGRAMME V 330

E DIMENSIONS OF PIPELINE CONFIGURATIONS INVESTIGATED 333

F. EFFECTIVE LENGTH OF PIPELINES 337

F.1 INTRODUCTION 338
F.2 EQUIVALENT LENGTH OF BENDS 338
F.3 EFFECTIVE LENGTHS 340

G. PRESSURE DROP FROM FLOWMETER TO ROTARY VALVE 341

G.1 INTRODUCTION 342
G.2 CALCULATION 342
G.3 CONCLUSION 343

H. MAXIMUM FEED RATE OF THE ROTARY VALVES 344

H.1 INTRODUCTION 345
H.2 CALCULATIONS 345

I ERROR ANALYSIS 347

I.1 INTRODUCTION 348
I.2 EXPERIMENTAL ERRORS 348
I.3 REPEATABILITY OF RESULTS 354
I.4 EQUATION ERROR 360
I.5 MODEL ERRORS 369

REFERENCES 376

LIST OF FIGURES

FIGURE		PAGE
2.1	Model of Flow Phases	8
2.2	The State Diagram	11
2.3	Dimensionless State Diagram	12
2.4	General Phase Diagram	12
2.5	Decay in Product Mass Flowrate with Line Length	13
2.6	Trend in the Minimum Transport Velocity with Respect to Pipeline Length	15
2.7	Geldarts Classification	24
2.8	Particle Size Classification Zones	25
3.1	Test Rig Layout	32
3.2	Filter Arrangement at the Pressure Tapping Points along the Conveying Line.	35
3.3	Interaction between Computer Programmes for Recording and Analysing Data	40
3.4	Particle Size Distribution	41
4.1	Pipeline Configurations Investigated	43
4.2	Expected Trend in the Conveying Pressure	44
5.1	Conveying Pressure versus Product Mass Flowrate	47
5.2	Cubic Model for Conveying Pressure	50
5.3	Pressure along the Pipeline	53
5.4	Location of Pressure Tapping Points	53
5.5	Pressure Drop from P(2) to P(3)	54
5.6	Alternative Filter Arrangement at the Pressure Tapping Points	55
5.7	Conveying Pressure versus Air Velocity	58
5.8	Conveying Pressure versus Load Ratio	59
5.9	Air Power versus Product Mass Flowrate	60
5.10	Power versus Load Ratio	61
5.11	Power versus Air Velocity	62

5.12 Product Mass Flowrate versus Air Mass Flowrate 63
5.13 Long Distance Line Results 65
5.14 Mass versus Time Trace of Material being Collected in the Receiving Hopper 65

6.1 Conveying Pressure as a Function of Line Length 69
6.2 Decrease in Conveying Pressure with Increasing Length 69
6.3 Distribution of Available Energy 70
6.4 Pressure Drop per Unit Length as a Function of the Air Velocity 71
6.5 Conveying Pressure as a Function of Line Length 72
6.6 Conveying Pressure versus Line Length 72
6.7 Pressure along the Pipelines 73
6.8 Conveying Pressures in 105 mm and 156 mm Diameter Pipelines over 100 metres 77
6.9 Conveying Pressure versus Pipe Diameter for a Product Mass Flowrate of 10 t/h 78
6.10 Conveying Pressure versus Pipe Diameter for a Product Mass Flowrate of 20 t/h. 78

7.1 A Telescopic Pipeline 80
7.2 Pressure Profiles for Various Pipeline Designs 81
7.3 Comparison of Conveying Pressures 82
7.4 Conveying Pressures for 400A versus 400B Configurations 85

8.1 Air Power across a Pipeline 88
8.2 Required Diagram to Determine the Optimum Pipeline Design 89
8.3 Total Cost of the Pipelines 91
8.4 Horizontal Section of Pipeline 92

9.1 Dimensional Analysis Results 100
9.2 Conveying Pressure versus (Froude Number/Load Ratio) 101
9.3 (Conveying Pressure/Air Volumetric Flowrate) versus Load Ratio 102

9.4 (Conveying Pressure/Product Mass Flowrate) versus Air Velocity 103
9.5 Air Velocity versus (Conveying Pressure/Load Ratio) 104
9.6 (Pressure/Load Ratio) versus Air Velocity 105
9.7 (Pressure/Load Ratio) versus Air Velocity 106
9.8 Normalisation of the Results 107
9.9 Basic Relationship for the Performance Predicting Model 108

10.1 Empirical Model 109
10.2 Basic Relationship for Empirical Model 110
10.3 Illustrating the Effect of Line Length 110
10.4 Alpha versus Effective Line Length 111
10.5 Pipe Diameter Effects 111
10.6 Beta as a Function of Pipe Diameter 112
10.7 $(p / 1+\mu)$ versus $(v_{ave}^2 / g.D)$ [100A] 116
10.8 $(p / 1+\mu)$ versus $(v_{ave}^2 /$ [100D] 117
10.9 $(p / 1+\mu)$ versus $(v_{ave}^2 /$ [200A] 118
10.10 $(p / 1+\mu)$ versus $(v_{ave}^2 / g.D)$ [200B] 119
10.11 $(p / 1+\mu)$ versus $(v_{ave}^2 / g.D)$ [200C] 120
10.12 $(p / 1+\mu)$ versus $(v_{ave}^2 / g.D)$ [400A] 121
10.13 Alpha versus Effective Line Length (105 mm Diameter Pipeline) 122
10.14 Alpha versus Effective Line Length (156 mm Diameter Pipeline) 123
10.15 Alpha versus Effective Line Length (200 mm Diameter Pipeline) 124
10.16 Beta versus Pipe Diameter 125
10.17 Calculated Conveying Pressure (Pmod) versus Experimental Conveying Pressure (Pexp) 126

11.1 Flow Patterns as a Function of Product and Air Mass Flowrate 129
11.2 Pressure across Transition Piece 131

12.1 State Diagram Showing the Effect of Line Length 132
12.2 Power Loss 133
12.3 Recommended Standard Test Rig 137

A.1 Air Alone Pressure Drop [100A] 257
A.2 Air Alone Pressure Drop [100B] 258
A.3 Air Alone Pressure Drop [100C] 259
A.4 Air Alone Pressure Drop [100D] 260
A.5 Air Alone Pressure Drop [200A] 261
A.6 Air Alone Pressure Drop [200B] 262
A.7 Air Alone Pressure Drop [200C] 263
A.8 Air Alone Pressure Drop [400A] 264
A.9.1 P versus $\dot{G}$ [100A] 266
A.9.2 A versus $\dot{Q}$ [100A] 267
A.9.3 B versus $\dot{Q}$ [100A] 268
A.10.1 P versus $\dot{G}$ [100B] 269
A.10.2 A versus $\dot{Q}$ [100B] 270
A.10.3 B versus $\dot{Q}$ [100B] 271
A.11.1 P versus $\dot{G}$ [100C] 272
A.11.2 A versus $\dot{Q}$ [100C] 273
A.11.3 B versus $\dot{Q}$ [100C] 274
A.12.1 P versus $\dot{G}$ [100D] 275
A.12.2 A versus $\dot{Q}$ [100D] 276
A.12.3 B versus $\dot{Q}$ [100D] 277
A.13.1 P versus $\dot{G}$ [200A] 278
A.13.2 A versus $\dot{Q}$ [200A] 279
A.13.3 B versus $\dot{Q}$ [200A] 280
A.14.1 P versus $\dot{G}$ [200B] 281
A.14.2 A versus $\dot{Q}$ [200B] 282
A.14.3 B versus $\dot{Q}$ [200B] 283
A.15.1 P versus $\dot{G}$ [200C] 284
A.15.2 A versus $\dot{Q}$ [200C] 285
A.15.3 B versus $\dot{Q}$ [200C] 286
A.16.1 P versus $\dot{G}$ [400A] 287
A.16.2 A versus $\dot{Q}$ [400A] 288
A.16.3 B versus $\dot{Q}$ [400A] 289

C.1 Load Cells Calibration Curve 298
C.2 Vortex Shedding Phenomenon 300
C.3 Flowmeter Calibration Curve 301
C.4 Circuit Diagram for the Pressure Transducers 302
C.5 Pressure Transducer Calibration Set-Up 304
C.6 Calibration Curve (Pressure Transducer 1) 305
C.7 Calibration Curve (Pressure Transducer 2) 306
C.8 Calibration Curve (Pressure Transducer 3) 307
C.9 Calibration Curve (Pressure Transducer 4) 308
C.10 Calibration Curve (Pressure Transducer 5) 309
C.11 Calibration Curve (Pressure Transducer 6) 310
C.12 Temperature Resistor Circuit Diagram 311
C.13 Temperature Resistor Calibration Set-Up 312
C.14 Calibration Curve (Temperature Resistor) 313

E.1 Dimensions of 100 Metre Loop 334
E.2 Dimensions of 200 Metre Loop 335
E.3 Dimensions of 400 Metre Loop 335
E.4 Dimensions of Long Distance Line 336

H.1 Rotary Valve Dimensions 346

I.1 P(equ) versus P(exp) [100A] 355
I.2 P(equ) versus P(exp) [100B] 356
I.3 P(equ) versus P(exp) [100C] 357
I.4 P(equ) versus P(exp) [200A] 358
I.5 P(equ) versus P(exp) [200C] 359
I.6 P(equ) versus P(exp) [100A] 361
I.7 P(equ) versus P(exp) [100B] 362
I.8 P(equ) versus P(exp) [100C] 363
I.9 P(equ) versus P(exp) [100D] 364
I.10 P(equ) versus P(exp) [200A] 365
I.11 P(equ) versus P(exp) [200B] 366
I.12 P(equ) versus P(exp) [200C] 367
I.13 P(equ) versus P(exp) [400A] 368
I.14 P(mod) versus P(exp) [100A] 370

I.15 P(mod) versus P(exp) [100D] 371
I.16 P(mod) versus P(exp) [200A] 372
I.17 P(mod) versus P(exp) [200B] 373
I.18 P(mod) versus P(exp) [200C] 374
I.19 P(mod) versus P(exp) [400A] 375

LIST OF TABLES

TABLE		PAGE
5.1	Equations for A and B	48
5.2	Correlation of Equations to the Experimental Results	49
6.1	Pipeline Configurations	75
6.2	Conveying Pressures	77
7.1	Calculated Conveying Pressures for the 100 m Pipelines	83
7.2	Conveying Pressures in the 400 m Pipelines	86
9.1	Dimensional Units	94
A.1	Air Alone Pressure Drop [100A]	257
A.2	Air Alone Pressure Drop [100B]	258
A.3	Air Alone Pressure Drop [100C]	259
A.4	Air Alone Pressure Drop [100D]	260
A.5	Air Alone Pressure Drop [200A]	261
A.6	Air Alone Pressure Drop [200B]	262
A.7	Air Alone Pressure Drop [200C]	263
A.8	Air Alone Pressure Drop [400A]	264
C.1	Load Cell Calibration Results	297
C.2	Flowmeter Calibration Results	301
C.3	Pressure Transducer Specifications	303
C.4	Calibration Results (Pressure Transducer 1)	305
C.5	Calibration Results (Pressure Transducer 2)	306
C.6	Calibration Results (Pressure Transducer 3)	307
C.7	Calibration Results (Pressure Transducer 4)	308
C.8	Calibration Results (Pressure Transducer 5)	309
C.9	Calibration Results (Pressure Transducer 6)	310
C.10	Calibration Results (Temperature Resistor)	313

F.1 Effective Length of Bends 339
F.2 Effective Length of Pipeline Configurations 340
F.3 Effective Length of the Long Distance Line 340

I.1 Summary of Experimental Errors 349
I.2 Repeatability of Results 354
I.3 Equation Errors 360
I.4 Model Errors 369

NOMENCLATURE

SYMBOL	DESCRIPTION	UNITS
A	Cross-sectional area of pipe	m^2
c	Average particle velocity	m/s
D	Pipe inner diameter	mm
D_B	Bend curvature diameter	mm
d	Equivalent particle diameter	mm
Fr	Froude number	-
G	Mass of product	kg
G	Product mass flowrate	t/h
g	Acceleration due to gravity	m/s^2
L	Length	m
m_p	Particle mass	g
P	Power	kW
p	Absolute pressure	kPa
Δp	Pressure difference	kPa
Δp_s	Pressure drop due to solids and air	kPa
Δp_1	Pressure drop due to air alone	kPa
Q	Air mass flowrate	kg/s
R	Gas constant	$m^2s^{-2}k^{-1}$
R_B	Bend radius	m
Re	Reynolds number	-
v_p	Particle velocity	m/s
V	Air volumetric flowrate	m^3/h
v	Average air velocity	m/s
W_p	Particle settling velocity in a cloud	m/s
W_s	Slip velocity	m/s

GREEK SYMBOLS

SYMBOL	DESCRIPTION	UNITS
f_w	Particle/wall friction factor	
ε	Voidage	
η	Dynamic viscosity	$N.s/m^2$
λ	Resistance factor	
λ_L	Resistance factor for air alone in pipe	
λ_M	Additional pressure drop factor in pipe due to solids in a flowing air stream	
μ	Load ratio (kg solids / kg air)	
ν	Kinematic viscosity	m^2/s
ρ	Air density	kg/m^3
ρ_p	Particle density	kg/m^3

1. INTRODUCTION

Pneumatic conveying systems in the mining industry have been developed to transport pulverous building material into the working areas of deep-level mines. The building material is generally used in the mines for packing, setting-up of roadways packs and stoping, as well as concrete and backfill work.

Various researchers have investigated long distance pneumatic conveying (Refs. 17, 19, 33, 35). The investigations have been directed at the selection of pipe sizes and the use of a Froude number relationship for selecting critical pipe lengths. The purpose for further investigations is outlined in this chapter. In addition, the organisation of the report and the contents of each chapter are discussed.

1.1 PURPOSE OF INVESTIGATION

The piping systems have a significant influence on the performance of a long distance pneumatic conveying system. Most vendors of pneumatic conveying equipment use arbitrary methods of selecting piping layouts. Little work has been done to develop a method for sizing the piping system to ensure optimum performance of the system (Ref.17).

It has been shown (Ref.33) that long distance transportation of material, by pneumatic means, requires a discipline different to that of short distance conveying. The rules governing long distances need to be established.

Whilst there is no question that there is a large number of long distance conveying systems operating reliably throughout the world, the lack of any sound theoretical or empirical base is of concern (Ref.17).

The possible performance increase of a long distance conveying system by stepping up the pipeline is in some instances greater than 100% while the required specific compressor output in terms of kW/t decreases (Ref.30). The problem is to determine which criteria should be used to identify under what conditions a change in pipe diameter should be effected (Ref.17).

1.2 PROJECT OBJECTIVES

The aims of the investigations described in this report were:

1) To develop an empirical model for calculating the conveying pressure (i.e. the pressure at the beginning of the conveying pipeline) of a long distance pneumatic conveying system taking the pipeline length, pipe diameter, product mass flowrate and air mass flowrate into account.
2) To investigate the performance characteristics of a pneumatic conveying system in terms of the conveying pressure and the required power as a function of various parameters such as load ratio, product mass flowrate and air velocity.
3) To analyse the effect of conveying distance and pipe diameter.
4) To determine the influence of a stepped pipeline on the conveying performance of a system.
5) To develop criteria for stepping up the pipe, taking theoretical and economic considerations into account.
6) To collect accurate data to determine the performance of the existing 1358 metre conveying line.
7) To investigate the possibility of conveying in a dense phase mode over long distances.

1.3 ORGANISATION OF REPORT

Literature relating to the development in pneumatic conveying with emphasis on long distance conveying systems is reviewed in Chapter 2. The purpose of the investigations described in this report was concluded from the literature survey.

The test rig, required to achieve the objectives of the project, is described in Chapter 3. The reasons for conducting the experiments through the various pipeline configurations are discussed in Chapter 4.

The experimental results recorded are discussed in Chapter 5. A set of equations was developed, expressing the conveying pressure in terms of the product and air mass flowrates for each pipeline configuration. The performance characteristics of pneumatic conveying systems are also discussed in Chapter 5.

With the use of the equations derived in Chapter 5, a comparison of the results, with respect to pipe diameter and line length, is given in Chapter 6.

The effect of stepped pipelines is discussed in Chapter 7. The optimum design of a pipeline, taking economic considerations into account is discussed in Chapter 8.

The normalisation of the results is discussed in Chapter 9, which includes a dimensional analysis of the parameters involved.

The model developed to predict the performance of the long distance line is outlined in Chapter 10. The model was based on the curves obtained from the normalisation of the results.

Some general observations made during the course of the experiments are discussed in Chapter 11.

Conclusions drawn from the investigations and recommendations for further research work are discussed in Chapter 12.

The appendices contain information which was referred to in the main body of this report.

The experimental results recorded are discussed in Chapter 5. A set of equations was developed, expressing the conveying pressure in terms of the product and air mass flowrates for each pipeline configuration. The performance characteristics of pneumatic conveying systems are also discussed in Chapter 5.

With the use of the equations derived in Chapter 5, a comparison of the results, with respect to pipe diameter and line length, is given in Chapter 6.

The effect of stepped pipelines is discussed in Chapter 7. The optimum design of a pipeline, taking economic considerations into account is discussed in Chapter 8.

The normalisation of the results is discussed in Chapter 9, which includes a dimensional analysis of the parameters involved.

The model developed to predict the performance of the long distance line is outlined in Chapter 10. The model was based on the curves obtained from the normalisation of the results.

Some general observations made during the course of the experiments are discussed in Chapter 11.

Conclusions drawn from the investigations and recommendations for further research work are discussed in Chapter 12.

The appendices contain information which was referred to in the main body of this report.

2. LITERATURE REVIEW

'THOSE WHO REMEMBER THE PAST WILL INHERIT THE FUTURE' (Ref.4)

2.1 INTRODUCTION

A literature survey was undertaken to cover all the facets of pneumatic conveying. Once an overall view of the 'state of the art' regarding pneumatic conveying was obtained, the parameters relating to long distance pneumatic conveying were reviewed in more detail. Emphasis was placed on the effect of pipeline length, pipe diameter, bends, acceleration and the design of telescopic pipes.

2.2 PNEUMATIC CONVEYING

2.2.1 Development of Pneumatic Conveying

In 1886, Sturtevant (Ref.36) was one of the first engineers to use air in pipelines for the conveying of light materials such as wood shavings and sawdust. These materials were not abrasive and could be passed through the planing mill-type fans (Ref.36). The Allington charger was invented in 1886 by W F Allington which made it possible to convey materials including woodshavings, hogged wood chips and pulp chips over long distances using a pressure-type pneumatic conveying system. The pipeline lengths eventually approached 1000 m.

In 1890, Duckham (Ref.36) produced the prototype of the modern suction grain unloaders and the present-day marine unloaders for chemicals and other materials. He invented the air-sleeve suction nozzle that enabled material to be conveyed in a state of loose suspension (ie. dilute phase). By 1914, 60% of all the imported grain in England and the Continent was handled by pneumatic pipelines.

The development of the Roots Blower, in 1859, increased the overall capabilities of pneumatic pipeline conveying, but its general use for pneumatic conveying did not occur until about 1920 (Ref.36). From the phenomenon that aeration of pulverised materials caused them to become fluidised and to flow at a very slight angle of repose, Alonzo G Kinyon invented the fluid-solid pump. The first commercial installation was made in 1919. After the abrasion problem of the screw pump was solved with the use of stellite welding rods to hard-surface the screw pump, the fluid-solids pump became the prime feeder of pneumatic pipelines in the cement industry. Today, some 50 different materials are transported with the use of the fluid-solids pump.

Most bakeries, large and small, now use pneumatic pipelines to unload their flour and sugar from cars to trucks and deliver them to bulk storage containers. Pneumatic pipelines have replaced the bucket elevators in flour mills. The plastics industry has become one of the largest users of pneumatic pipelines. Single polyethylene plants have total pipeline lengths of up to 8000m with individual lengths of up to 700m.

In 1967, Solt (Ref.36) developed the Modulaire valve. This valve is the heart of a blow tank and pipeline that modulates the rate of material flow into the pipeline in direct response to line conditions, automatically and instantaneously.

The concept of long distance pneumatic conveying in which systems in excess of 1000 metres long has now been readily accepted by many mining organisations (Ref.16). In particular, a number of successful installations are operating in mines throughout the world (Refs. 12, 25, 39).

While it has taken nearly a hundred years to bring pneumatic conveying to the technological base it is today, it will be many years until the science is near complete. The technological advancements made to date as well as continued advancements which can be expected will yield the ability to minimise the error, but it may never be possible to predict the performance absolutely without error.

2.2.2 Pneumatic Conveying Theory

Visual observations of the motion of solids in a glass pipe reveal that the flow patterns are rather complex and are influenced by many factors, including: the solid loading ratio, the Reynolds number of the flow and the specific properties of the solids (Ref 42). In spite of the widespread application of pneumatic conveying systems in industry there is a lack of understanding of the fundamental characteristics and behaviour of the phase gas-solid flows (Ref.41).

Owen (Ref.23) commented that the hope of developing a theory for pneumatic conveying decreases as the pipe diameters increase. This is a distressing situation since it is generally pipelines of larger diameter which are of industrial interest.

A pneumatic conveying system consists of the following four distinct zones, each requiring its own specialised hardware to effect the required operation.

1 The Prime Mover

A wide range of compressors, blowers, fans and vacuum pumps is available for providing the necessary energy to the conveying gas. When designing a pneumatic conveying system it is important to select the correct prime mover which will deliver the required gas flowrate and pressure for reliable transportation.

ii Feeding, Mixing and Acceleration Zone

This is considered one of the most crucial areas in any pneumatic conveying system. Considering that the solids are essentially at rest when introduced into the air stream, a large momentum change occurs as solids accelerate to some 'steady' flow state.

2.2.2 Pneumatic Conveying Theory

Visual observations of the motion of solids in a glass pipe reveal that the flow patterns are rather complex and are influenced by many factors, including: the solid loading ratio, the Reynolds number of the flow and the specific properties of the solids (Ref 42). In spite of the widespread application of pneumatic conveying systems in industry there is a lack of understanding of the fundamental characteristics and behaviour of the phase gas-solid flows (Ref.41).

Owen (Ref.23) commented that the hope of developing a theory for pneumatic conveying decreases as the pipe diameters increase. This is a distressing situation since it is generally pipelines of larger diameter which are of industrial interest.

A pneumatic conveying system consists of the following four distinct zones, each requiring its own specialised hardware to effect the required operation.

i *The Prime Mover*

A wide range of compressors, blowers, fans and vacuum pumps is available for providing the necessary energy to the conveying gas. When designing a pneumatic conveying system it is important to select the correct prime mover which will deliver the required gas flowrate and pressure for reliable transportation.

ii Feeding, Mixing and Acceleration Zone

This is considered one of the most crucial areas in any pneumatic conveying system. Considering that the solids are essentially at rest when introduced into the air stream, a large momentum change occurs as solids accelerate to some 'steady' flow state.

iii The Conveying Zone

The conveying zone consists of piping, the selection of which is based on a number of factors, including the abrasiveness of the product and the static pressure requirements. Little work has been done on methods of sizing the piping system to ensure optimum performance of the system. What is known, however, is that the piping systems can have a significant influence on the performance of a long distance pneumatic conveying system (Ref.17).

A number of bends and diverter valves can be included in the conveying zone. Bends form a critical part of the conveying zone, considering the change in direction of the solids which consist of a deceleration as they move through the bend, and a re-acceleration at the exit of the bend.

iv Gas/Solid Separation Zone

A wide variety of units is available for the separation of the solids from the gas (eg. bag type filters and cyclones). The selection of an adequate gas/solid separation system is dependent upon a number of factors, the prime factor being the size of the solid particles to be separated from the gas stream.

Modes of Pneumatic Conveying

Pneumatic conveying systems are generally classified into two systems: dilute phase systems and dense phase systems.

A model of the flow phases is depicted in Figure 2.1, as the concentration of the solids is increased (Ref.18).

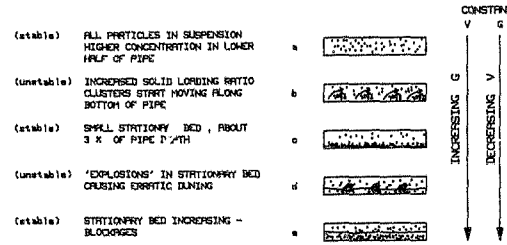


FIGURE 2.1: MODEL OF FLOW PHASES

Of particular importance, is the formation of a so called moving or stationary beds. It will be noted the conditions (c) and (e) in Figure 2.1 are described as being stable in the presence of a stationary bed.

In the past, the modes of pneumatic conveying systems were categorised according to the solids loading ratio. Solids loading of 0-15 were considered *dilute phase systems* and solids loading over 15, dense phase system. A more recent classification is that the pressure minimum curve on the State Diagram forms the boundary between dense and dilute phase conveying (Ref 18). The type of pneumatic conveying system can further be classified in terms of a positive pressure, negative pressure, combined negative postive pressure and closed loop system.

The theory of pneumatic conveying mainly deals with predicting the system conveying pressure. Much progress has been made in developing the theory for *dilute phase conveying*. Dense phase conveying theory is still very much in the elementary stage and is still the subject of intensive investigations (Ref.13). The total pressure drop (Δp_s) is regarded as comprising of the *pressure drop due* to the flowing gas alone (Δp_1) plus the additional pressure drop (Δp_2) due to the presence of the solid particles (Ref.1), as

shown in Equation 2.1.

$$\Delta p_s = \Delta p_1 + \Delta p_z \qquad (2.1)$$

The theory for predicting the pressure drop due to the air alone, p_1, has been readily accepted and is generally expressed as in Equation 2.2 (Ref.20).

$$\Delta p_1 = \lambda_1 \rho v^2 \Delta L \quad . \quad (2.0) \qquad (2.2)$$

The trend is to express the pressure drop due to the solids in terms of Equation 2.3, applicable to dilute phase systems.

$$p_z = \mu \lambda_z \rho v^2 \Delta L \ / \ (2.0) \qquad (2.3)$$

Thus the system pressure drop Δp_s is:

$$\Delta p_s = \mu \lambda \rho \Delta L \ / \ (2.0) \qquad (2.4)$$

where $\lambda = \lambda_1 + \lambda_z$

It has been shown (Ref.13) that the pressure drop for dense phase systems may be described by Equation 2.5.

$$p_1 = p_2 \exp [\xi \mu g L v_f \ / \ (R.T.W_s)] \qquad (2.5)$$

An alternative expression for the pressure drop across a dense phase system is given in Equation 2.6 (Ref.13).

$$\Delta p_s = 2.5 \ L \rho_{ds} u_p^{0.45} (d/D)^{0.25} \qquad (2.6)$$

Konrad et al (Ref.9) derived an equation to quantify the pressure drop required to move an isolated plug in a horizontal pipe. For a cohesionless material, this equation reduces to

$$p / L = 4 \beta_w K_w \sigma_F / D + 2 \rho_B g \beta_w \qquad (2.7)$$

Wen (Ref.42) on the other hand has developed an empirical correlation for the pressure drop in a dense phase system as shown in Equation 2.8.

$$\Delta p_t / (L \rho_{ds}) \cdot D^{0,25} / d_p = 2,5 \cdot u_p^{0,45} \qquad (2.8)$$

Konrad (Ref.10) gives a description of the flow pattern for dense phase conveying. Solid particles travel in plugs which fill the tube at about maximum packing density. Between these plugs the lower portion of the tube is full of stationary layers of particles with air flowing over the top in the form of air 'plugs'. Within the plugs of particles there are interparticle stresses and there appears to be passive failure, ie. the radial compressive stress is greater than the axial stress at every section. The radial stress is transmitted to the tube wall and causes shear stress which balances the pressure drop due to the percolation of air through the interstices of the plug of particles. Konrad developed a quantitative theory to predict the position between air flow, solid flow and pressure drop.

The gas/solid conveying process is perhaps best represented in terms of the so-called State Diagram.

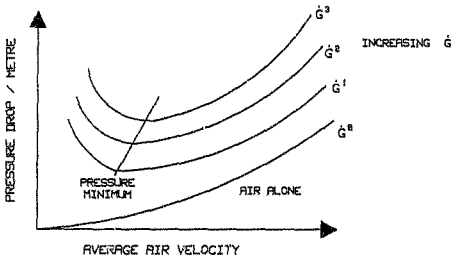


FIGURE 2.2: THE STATE DIAGRAM

The State Diagram shows the pressure drop per unit length for horizontal flow systems as a function of average air velocity for various product mass flowrates. A refinement to the State Diagram is to modify the abscissa to represent a dynamic pressure term ($1/2\rho v^2$). By including a density term, it is possible to obtain a State Diagram which represents all flow conditions in a system, as opposed to the State Diagram depicted in Figure 2.2 which is dependent upon the location in a system where the observations were made.

The Dimensionless State Diagram is shown in Figure 2.3 (Ref.18).

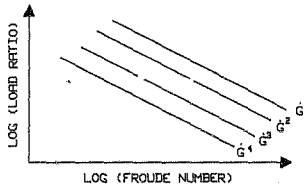


FIGURE 2.3: DIMENSIONLESS STATE DIAGRAM

The diagram is constructed by plotting the load ratio against the Froude number in a log-log plot.

From the general phase diagram in Figure 2.4 it should be noted that the lines of constant flow pattern all slope towards the pressure minimum trace, line III. It has also been shown that the saltation velocity, for fine particles, takes place before the pressure minimum. For coarse particles, on the other hand, the saltation velocity coincides with the pressure minimum (Ref.18).

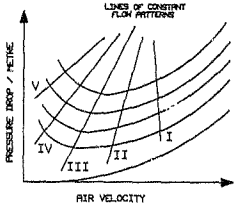


FIGURE 2.4: GENERAL PHASE DIAGRAM

A general method has been developed by Rizk (Ref.27) which illustrates the design and operation of a pneumatic system at optimal conditions, ie. the maximum load ratio at the corresponding Froude number where the pressure is a minimum with the calculated pipe diameter.

Chambers and Marcus (Ref.3) proposed an empirical model to calculate the pipeline pressure loss for a dilute phase pneumatic conveying system.

2.3 EFFECT OF LINE LENGTH

The move towards long-distance conveying systems highlighted the influence of the line length on the discharge rate. Typically, the discharge rate falls off exponentially with increasing line length (Ref.19).

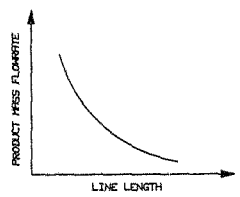


FIGURE 2.5: DECAY IN PRODUCT MASS FLOWRATE WITH LINE LENGTH

The decrease in system throughput with increasing pipeline length is illustrated in Figure 2.5.

It has also been shown by Marcus (Ref.17), from the analysis of the data published by Hunke (Ref.4), that there exists a critical length for conveying material. From the tests conducted over 1000m, 1500m, 2000m, 2500m and 3000m, it is clear that the increase in pipe length results in more energy being required to convey 'air only' through the system with corresponding less blower power available to convey solids.

An increase in length from 1000 metres to 3000 metres resulted in a reduction of product flowrate by 57 times. The conveying rate of 0.347 t/h over the 3000 metres indicated that a critical length was attained for the particular conditions at which the solids mass flow rate was virtually zero.

In laboratory scale equipment for dense phase pneumatic conveying of a particular solid, the pressure drop is usually found to be a linear function of the pipe length (Ref.24). However, Ramachandrac et al (Refs. 22, 26) found that with long pipes, which require conveying pressure drops of up to 6 bar, the pressure drop per unit length decreased continually as the air expanded down the transport line. This effect was also noted by Muschelknautz and Krambrock (Ref.22) who suggested that the overall conveying pressure difference increases exponentially with pipeline length. It can also be related back to the State Diagram for dense phase conveying; as the air expands (ie. the velocity increases) the pressure drop per unit length decreases.

The effect of line length is illustrated in the scaling of pneumatic conveying systems (Ref.14). The scale-up of product mass flow rate with respect to conveying distance can be carried out reasonably accurately, if the extrapolation is not too great, on the following basis:

$$\dot{G}_1 \cdot L_1 = \dot{G}_2 \cdot L_2 \qquad (2.9)$$

where subscripts 1 and 2 refer to the appropriate conveying pipe. The conveying lengths for a given air mass flowrate and conveying pressure drop are then scaled in the ratio G_1/G_2.

For dilute phase conveying over long distances, Snow (Ref.33) concluded that the *minimum* transport velocity increases with increasing line length. The *percentage* change in minimum transport velocity as a function of line length is shown in Figure 2.6.

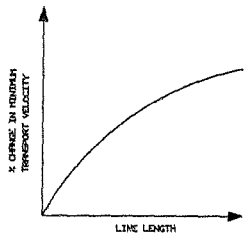


FIGURE 2.6: *TREND IN THE MINIMUM TRANSPORT VELOCITY WITH RESPECT TO PIPELINE LENGTH*

2.4 *EFFECT OF PIPE DIAMETER*

Once a conveying velocity and a load ratio has been selected for the design of a pneumatic conveying system, the pipe diameter can be calculated from Equation 2.13.

Since a system is usually designed for a specific product mass flowrate, the air flow rate Q is given by

$$\dot{Q} = \dot{G} / \mu \qquad (2.10)$$

Assuming an initial pressure, a first approximation of the air density is derived from Equation 2.11.

$$\rho = p / (R.T) \qquad (2.11)$$

Thus the air volume flow rate $\dot{V}$ is

$$\dot{V} = \dot{Q} / \rho \qquad (2.12)$$

The pipe diameter D is thus

$$D = [4 . \dot{V} / (v . \pi)]^{0,5} \qquad (2.13)$$

From Equation 2.4 in Section 2.2.2, for predicting the pressure drop in a horizontal pipe, it can be seen that the pressure drop is inversely proportional to the diameter.

This is supported by the results obtained for conveying waste rock through various pipeline configurations (Ref.19).

2.5 EFFECT OF BENDS

The flow of gas/solid suspensions through bends has been the source of much debate, with many conflicting theories emanating from research work (Ref.16). The bends in a pneumatic conveying system are critical when considering the wear of the piping for the conveying of an abrasive material.

The pressure losses associated with the flow through bends are significant and in many instances the magnitude of these losses is far in excess of any other pressure losses in a total conveying system (Ref.16). Visual observations of the motion of solid particles in bends indicate that there are two basic categories of flow (Ref.1).

i Solid particles sliding around the outer radius.

ii Solid particles colliding several times in traversing the bend, the particle trajectories between the particle-wall impacts sometimes being reported as straight lines and frequently as distinct curves.

Extensive studies (Ref.1) into the paths followed by coarse particles indicate that the particles travel rectilinearly along the straight pipe preceeding a bend until they impinge upon the outer wall of the bend. The particles lose momentum on impact, but are re-accelerated after reflection by the flow medium.

A popular equation for estimating the pressure loss through a bend is that produced by the EEUA (Ref.38). In this equation, a factor B (the ratio of the bend radius to the pipe diameter) is used to account for bends of different radii. The basic equation also includes a term to account for the transport velocity.

$$\Delta P_{bend} = B \rho v^2 / 2 \qquad (2.14)$$

The transport velocity is defined as

$$v = G / (\rho \mu A) \qquad (2.15)$$

and B is obtained from the following table

R_b/D	B
2	1,5
4	0,75
6	0,5

From the table, it can be seen that the pressure loss across the bend increases as the bend radius decreases (Ref.16).

For fine particles, the correlation must be modified in line with the data of Mason and Smith (Ref.32). A suggested format for the effect of particle size is:

$$\frac{P_{bend}}{P_{straight}} = a \left(\frac{2 R_B}{D} \right)^b \cdot \left(\frac{D_p}{D} \right)^c \qquad (2.16)$$

In the case of *fine powders* the data indicates that the pressure losses predicted by existing correlations overestimate the pressure losses that are actually measured. In some cases actual drag reduction may be present (Ref.37).

Schuchart (Ref.32) performed a number of experiments on pressure losses in bends and curves for gas/solid flow. *The experiments* involve the use of glass and plastic particles between 1 and 2 mm in diameter with volumetric concentrations of up to 5%.

Schuchart developed the following expression for bends of varying degrees of curvature.

$$\frac{\Delta p_{bend}}{\Delta p_{straight}} = 210 . \left(\frac{2 R_B}{D} \right)^{-1,15} \qquad (2.17)$$

For a 90° sharp elbow he suggested

$$\Delta p_{bend} = 12 \, (\rho_p / \rho_f)^{0,7} \, (\rho_F u^2 / 2) \, . \, L / D \, . \, c_t \qquad (2.18)$$

where c_t = $\frac{\text{solid volumetric flowrate}}{\text{total volumetric flowrate}}$

$$L = \pi / (4 . D)$$

Another expression suggested for estimating the pressure drop across a bend is (Ref.1):

$$\Delta p_b = 2 f_b \rho_s u_s^2 \qquad (2.19)$$

where ρ_s is the mean density of the flowing suspension and f_b is a coefficient which takes values of 0,375, 0,188 and 0,125 for bend radius/pipe diameter ratios of 2, 4 and 6 or more, respectively.

It has also been shown by Marcus et al (Ref.16) that short radius bends appear to provide the lowest pressure loss over a wide range of mass flow ratios, but it must be kept in mind that only cement was conveyed in those experiments, considering the pressure drop across a bend is largely dependent on the product being conveyed. It was also shown that the pressure loss across a bend is linearly related to the mass flow ratio (Ref.16).

In analysing pressure losses in bends, Rose and Duckworth (Ref.28) suggested a technique that considers only the acceleration portion of the pressure loss which occurs at the exit from the bend.

Marcus et al (Ref.15) emphasised the importance of particle deposition in a bend. It is shown that in some circumstances where bend deposition takes place, deposits might possibly cause blockage of the pipeline. Marcus (Ref.15) also noted that provided sufficient pressure is available a stable situation will be reached where the high flow velocity will result in an erosion rate equal to the deposition rate. It was found that the deposition had a double arch shape formed on the outer side of the bend.

2.6 ACCELERATION, LENGTH AND PRESSURE DROP

The acceleration zone is normally associated with that section of the conveying pipe immediately downstream of the feeding device. A significant momentum change takes place at the feed point resulting in a sharp pressure drop. The importance of this parameter is emphasized by the fact that the magnitude of the associated acceleration pressure loss is in excess of the pressure loss due to friction of solids in this zone (Ref.16).

Scott (Ref.1) gives the pressure-drop caused by the acceleration of the solid particles as:

$$\Delta p_{acc} = m_p \cdot u_p / A \qquad (2.20)$$

Chambers et al (Ref.3) uses the following empirical equation to predict the acceleration pressure drop:

$$P_a = \rho_a v_a^2 \{ 1 + 2\mu v_s / v_a \} / 2 \qquad (2.21)$$

An alternative acceleration pressure loss is given by Marcus (Ref.18)

$$P_a = \mu \cdot v_o \cdot \rho_o \cdot c \qquad (2.22)$$

There is thus considerable uncertainty as to what parameters determine the magnitude of the acceleration pressure loss. From the wide variation in acceleration losses observed in various systems (Ref.23), it is difficult at present to draw any general conclusions.

2.7 TELESCOPIC PIPELINES

Where high air pressures are used in pneumatic conveying systems problems can arise because of the high velocities. For long distance conveying a high initial air pressure is required. As the pressure of the conveying air decreases along the length of the line its density decreases with a corresponding increase in velocity (Ref.1). It has been shown by Konrad (Ref.9) that the expansion of the air in a long pipeline is effectively isothermal, rather than adiabatic and reversible.

In order to keep the velocity to within reasonable limits, stepped pipelines are often employed.

The design of long distance pneumatic conveying systems has received little attention from researchers (Ref.19). These systems commonly operate under extremely dilute conditions, making some arbitrary use of stepped pipes in an attempt to reduce the conveying velocity.

Soo (Ref.35) suggests that for transporting over long distances, an economical design is one in which, as the pressure lowers, the pipe diameter is changed to the next larger standard sized pipe so that the minimum transport velocity is maintained at the inlet of each section of pipe.

Soo (Ref.34), also states that a pneumatic pipeline with minimum pressure drop will be the most economical design.

From observations made by Snow (Ref.33), it was found that a 1600 m line consisting of 900 m, 150 mm diameter pipe followed by 700 m of 200 mm diameter pipe employed a lower pressure to obtain a higher conveying rate when compared to the 1037 m line of 150 mm diameter pipe. Although it must be noted that the air mass flowrate was reduced when conveying through the 1600 m line. This could also explain the improvement in the performance.

From investigations into the effect of stepped pipelines (Ref.19) conveying large lumps of waste rock through four pipeline arrangements, it appeared reasonable to start stepping a pipe immediately after the solids have been accelerated.

Marcus (Ref.19) suggests that the decision to change the pipe diameter is a compromise between the maintenance of low pressure, the Froude number and the availability and economics of the piping itself. It is advised to attain the smallest pressure drop with a minimum number of stages.

Experimental results obtained from full-scale, long distance pneumatic conveying investigations were extensively analysed by Marcus et al (Ref.17). The results indicated that in order to maintain a constant solids mass flowrate at a constant pressure drop, it was necessary to increase the air flowrate as the pipe diameter was increased. The results stressed the importance of being aware of the minimum Froude number. The design process developed by Marcus (Ref.17) is based on dilute phase conditions. The basic philosophy is that the conveying gas expands between a minimum Froude number (Fr_{min}) and a maximum Froude number (Fr_{max}). Once Fr_{max} is achieved, the pipe diameter should be increased such that the conveying conditions on entering the enlargement should not fall below Fr_{min}. From further analysis of the experimental results, for a pipeline with three stages the Froude number was approximately constant and λ_z was constant.

2.8 REDUCTION OF POWER CONSUMPTION

2.8.1 Optimum Conveying Conditions

The determination of the optimal operating point of a pneumatic conveying system assumes the knowledge of the conveying phase of the product involved (Ref.27). Dense phase pneumatic conveying generally result in a low power consumption with reduced attrition and abrasion. However, under certain circumstances, particles wedge together to form immovable plugs. A more dilute phase conveying system is the only alternative.

In general, dense-phase slugging or plug type conveying are ideal systems from the economical, power requirements viewpoint if the conditions prove suitable (Ref.6).

A method has been developed by Rizk (Ref.27) with which one can design and operate a pneumatic system at optimal conditions, ie. the maximum mass flow ratio at the corresponding Froude number where the pressure is a minimum with the calculated pipe diameter. When considering the gas expansion in long lines, it is preferable to use staged pipelines (Ref.27). After each stage care should be taken to ensure that the same Froude number is kept.

2.8.2 Drag Reduction

In most experimental investigations of flow of gas-solid expansions it has been found that the addition of solid particles increases the frictional resistance to flow. However, a few studies reported a decrease in the frictional resistance below that of the pure gas when moving small particles at low load ratios (Ref.42). For example Rossetti and Pfeffer (Ref.31) reported that at a load ratio of 1,5 and a gas Reynolds number of 25,000, the friction factor ratio (i.e. $\Delta p_s / \Delta p_f$) in a vertical test section was as low as 0,27 when transporting 30 m particles in an air stream. This corresponds to a reduction in drag of [illegible] se to 7%. The drag reduction has been explained as being the result of the interaction of the particles with the air turbulence in the vicinity of the pipe wall.

Extensive investigations by Marcus (Ref.11) into drag reducing aids showed that by introducing a complex *pulsating type* flow into the gas-solid suspension drag reducing flow could be effected in a high solid feed rate range, which resulted in significant power savings in the test section.

Further investigations by Marcus (Ref.11) on a second type of drag reducing system utilising a porous type conveying pipe, indicated that in these experiments pulsatile type flow drag reduction effected greater power savings with less hardware requirements.

It has been shown by Kano (Ref.6) that the application of vibration to dense-phase slugging or plug-flow type pneumatic conveying is effective in reducing the power requirements, *holding* especially true in the use of longer pipelines.

2.9 EFFECT OF MATERIAL PROPERTIES

The material properties appear to have the greatest influence on the performance of pneumatic conveying systems (Ref.7). Before any correlation equation can be used, knowledge of the *particle size distribution* is *required*. In addition it is important to know both the maximum and minimum particle sizes. Although characteristics like adhesioness and friability may be considered in specialised applications (eg. transporting carbon black), the *mean particle size* and the size distribution criteria dominate in most industrial applications (Ref.7).

An essential element of particle characterisation is *fluidisation*. The *Geldarts* classification is a useful tool in categorising particles into four regimes. The use of Geldarts classification is the first step in identifying the mode for transporting a product (Ref.32).

The Geldarts Classification, Figure 2.7, isolates four groups of products based on density difference and mean particle size (Ref.32).

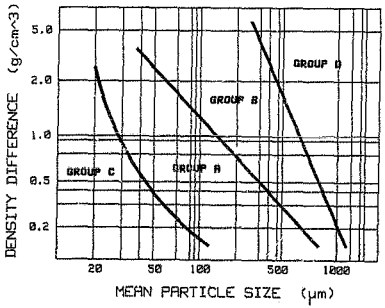


FIGURE 2.7: GELDARTS CLASSIFICATION

Group A - are good candidates for dense phase conveying over a wide range of velocities. They are easily aerated and retain their fluidisation characteristics.

Group B - can be aerated but do not retain the air. They generally require higher transport velocities.

Group C - they are generally too cohesive to fluidise. They are poor candidates for dense phase.

Group D - can be conveyed over a wide range of velocities. Depending upon the size, certain Group D products are good candidates for dense phase. These products break up into natural plugs. In the larger size range (d>10mm) and the irregular shaped products, such natural plug formation does not occur.

A qualitative basis for selecting discontinuous phase system types is given in Figure 2.8 (Ref.7).

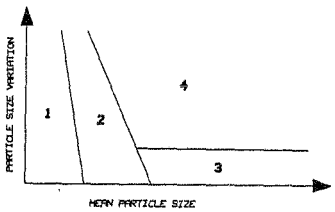


FIGURE 2.8: PARTICLE SIZE CLASSIFICATION ZONES

Material in zone 3, being relatively large and similar in size, will form plugs having pressure drops proportional to their lengths. Since the material cannot form an immovable plug, the system can be stepped at any time, and no separate mechanism is required to break up blockages. Very fine powders like baking flour fall into zone 1, and can also be successfully conveyed using conventional equipment. This relies on the powder's ability to fluidise easily, even if the conveying gas flows at a low velocity. However, if a plug is given any chance to form by increasing the load ratio until a significant bed forms, or by switching off the apparatus when the pipe is full, the resulting plug may be impossible to move (Ref.7).

Materials like flyash and pulverised coal would lie near the border of zones 1 and 2 and while they often exhibit favourable dense-phase conveying characteristics, the materials settle and create unstable plugs. Since the material could be expected to form immovable plugs (being relatively impermeable), the key to high mass load ratios appears to be the promotion of fluidisation.

The problem materials occur in zone 4, where the mean size is relatively large and yet the particle size distribution is wide. In a typical dense-phase conveying situation, the fine particles will remain suspended in the air stream, while the larger particles will form an unstable bed. When the conveying velocity is reduced further, a plug of large particles will form which acts as a filter on the percolating air, and fine particles jam the interstitial spaces, eventually blocking the pipe due to altering the permeability significantly (Ref.7).

2.10 DESIGN PROCEDURES

Various design procedures have been developed, based either on past experience or on laboratory tests to determine the performance of the material.

Stoess (Ref.37)[1] developed a design process based on past experience of conveying various products and with the use of comprehensive tables. First a saturation (i.e. m^3 free air/kg material) is selected from a table which is dependent upon the material and the conveying distance. The volume of free air required is simply derived from the product of the saturations and the conveying rate. The size of the conveying pipe required is next determined by computing for the constant of the particular pipe by dividing the free air required by the velocity which is also given in the table of saturations. Constants for various pipe diameters are also calculated. The operating pressure is determined by multiplying the kW/t factor by the pressure factor which is also tabulated. From the operating pressure and air flow rates required, a suitable blower can be selected.

Perkins (Ref.24) suggests a conveyor sizing procedure which uses empirical data and experimental observations. Various tables are used for selecting correction factors. The air volume flowrate is determined from an empirical relationship.

$$\dot{V} = a (L) + 1,5 \qquad (2.23)$$

where $\dot{V}$ = air flow m^3/kg of material
a = empirical acceleration constant
L = conveying distance

A preliminary blower power is selected from a table. The appropriate load ratio and corresponding flow is listed using data from tables. Alternative pipe diameters corresponding to the appropriate air flow rates are selected. The final selection of pipe size and blower is selected for the most economical system by comparing blower power figures.

A design procedure has been developed by Marcus et al (Ref.18) which is based on a series of laboratory tests to determine the pressure minimum curve (μ vs Fr) and the additional pressure drop curve (λ_z vs Fr) with varying load ratios.

Once the conveying rate, conveying distances and solids loading have been selected, the minimum Froude number (Fr_{min}) is obtained from the laboratory tests. The required air mass flow rate is derived from Equation 2.24.

$$\dot{Q} = \dot{G} / \mu \qquad (2.24)$$

and the volumetric air flowrate is given by

$$\dot{V}_o = \dot{Q} / \rho_o \qquad (2.25)$$

where the ambient air density ρ_o is given by

$$\rho_o = P_{at} / (R . T) \qquad (2.26)$$

Assuming an existing pipe system is to be used, the diameter of the pipeline is known. An initial air velocity can thus be calculated. The pressure losses are calculated using the equations which were proposed by Chambers and Marcus (Ref.3).

2.11 CONCLUSIONS

The literature review provided a background to pneumatic conveying, discussing the important factors related to long distance conveying systems. Various theories to predict the pressure drop along a pipeline were investigated. The theories are generally based on slip velocities and settling velocities which require sophisticated test facilities to measure. This project was aimed at developing a more practical design procedure to determine the pressure losses in a pneumatic conveying system. Thus an attempt was not made to correlate the experimental results to the theories discussed in the literature review.

From the literature review it appears that there still does not exist a sound theoretical or empirical base for the design of long distance pneumatic conveying systems. Especially for long distance conveying where the change in velocity cannot be ignored, the design procedure needs to be further developed.

A more detailed discussion of the purpose for further investigations and the project objectives is given in Section 1.1 and 1.2 respectively.

3 DESCRIPTION OF EXPERIMENTAL TEST RIG AND INSTRUMENTATION

3.1 INTRODUCTION

The experimental investigations described in this report were undertaken at UWTec, the Materials Handling Research Unit of the University of the Witwatersrand, Johannesburg.

Only brief descriptions of the equipment and instruments which were used for the project are given in this chapter. Further details can be found in Appendices B and C.

Most of the equipment had been installed prior to these investigations. All the pipeline configurations, except the long distance line, were assembled for these investigations.

3.2 REQUIREMENTS

In order to meet the objectives of the project as outlined in Section 1.2, it was necessary to convey the material continuously. A high pressure feeding system was required to overcome the high pressure losses over the long conveying pipelines. Variable air and solids mass flowrates were also required in order to vary the solids loading ratio.

Accurate and reliable results had to be recorded. The important parameters being:

a) Conveying pressure.
b) Solids mass flowrate.
c) Air mass flowrate.

Once all the data had been recorded, a detailed analysis of the results was carried out.

3.3 OPERATING RANGES

The corresponding range of the following parameters is outlined below.

a) Air Supply

The maximum delivery pressure from the compressors was 700 kPa. The air flowrate could only be varied by running different combinations of compressors. A continuous variable air mass flowrate supply was thus not available. The minimum air flowrate was 360 m^3/h which was delivered from one compressor. The maximum air mass flow rate was limited by the capacity of the air solids separation unit located at the end of the conveying line. This unit was designed for a maximum air flowrate of 2016 m^3/hr.

b) Product Mass Flowrates

The product mass flowrate could be varied from 0 t/h (i.e. air alone) to a maximum of 20 t/h which was the maximum design capacity of the rotary valves.

c) Pipeline Diameters

A minimum pipe diameter of 105 mm could be used because the outlet from the rotary valves was 105 mm in diameter. It is not recommended to step the pipe to a smaller diameter after the feeding point. High pressure drops and blockages could arise within the range of product mass flowrates to be investigated.

Pipe diameters of 156 mm and 200 mm were also available. The maximum length was 1353 metres which consisted of 355 metres, 105 mm diameter pipe followed by 625 metres, 156 mm diameter and 378 metres of 200 mm diameter pipe.

3.4 DESCRIPTION OF EQUIPMENT

A diagram of the test rig layout is given in Figure 3.1

3.4.1 Tandem Pressure Vessels

Brieden tandem pressure vessels, fitted with rotary valves at the conical section of the vessel, were used for feeding the material into the pipeline. The operating cycle of the system was controlled by a programmable logic controller such that whilst one vessel was in the filling mode, the second vessel was discharging the product. Continuous flow of solids was thus ensured. Details of the operating cycle are given in Section 3.7. The vessel specifications are given in Appendix B.

3.4.2 Filter Unit and Receiving Hopper

A bag type, reverse jet filter unit was located on top of the receiving hopper which in turn was located directly above the intermediate hopper as shown in Figure 3.1. A butterfly valve at the bottom of the receiving hopper enabled material to be collected in the receiving hopper. Flexible rubber pipes were used for all pipes entering the receiving hopper to ensure an accurate response from the load cells.

3.4.3 Conveying Pipes

Mild steel pipes were used in all the pipeline configurations. Rubber gaskets were used to prevent leakage at the flanges. The pipes had to be well secured on the pipe racks, especially when conveying in the dense phase mode.

A sight glass was included in each pipeline configuration such that the flow patterns could be observed.

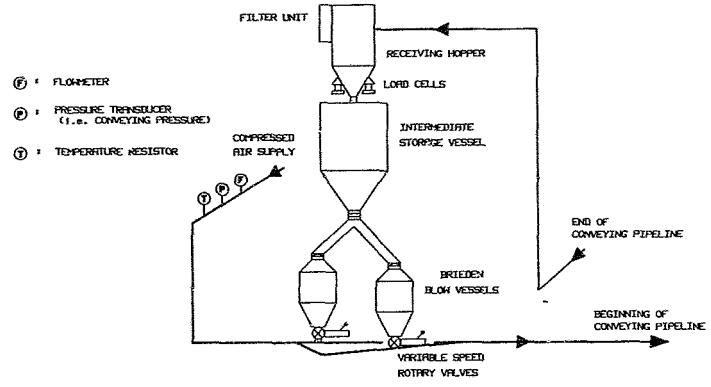
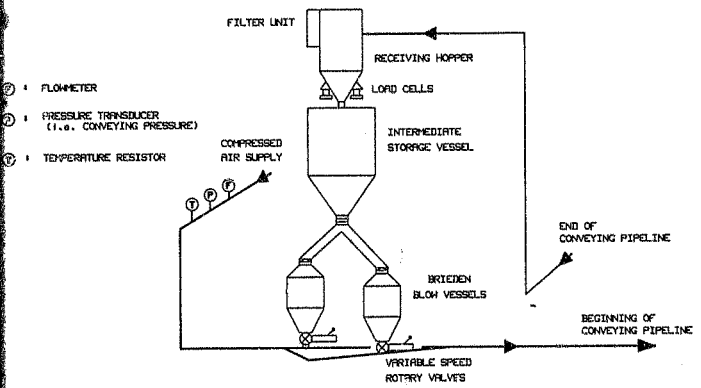


FIGURE 3.1: TEST RIG LAYOUT


FILTER UNIT
RECEIVING HOPPER
LOAD CELLS
INTERMEDIATE
STORAGE VESSEL
COMPRESSED
AIR SUPPLY
END OF
CONVEYING PIPELINE
BRIEDEN
BLOW VESSELS
BEGINNING OF
CONVEYING PIPELINE
VARIABLE SPEED
ROTARY VALVES
F : FLOWMETER
P : PRESSURE TRANSDUCER
(f.e. CONVEYING PRESSURE)
T : TEMPERATURE RESISTOR

3.4.4 Compressors

The following set of cc. .ressors were used to supply the conveying air with the corresponding ra*ed free air deliveries:

COMPRESSOR	FAD (m^3/min)
BM40	11
Demag	8
Hydrovane	10
Atlas	12

The piping arrangements from the compressor house enabled the running of any combination of the compressors in parallel to vary the air mass flowrate delivered to the test rig.

Service air, supplied by a separate compressor to various points in the laboratory, was used to operate the pneumatic actuated valves and the pneumatic system of the control panel. The service air was also used to fluidise the material in the intermediate storage hopper and Briedon vessels. The specifications of the compressors are included in Appendix B.

3.5 INSTRUMENTATION AND DATA ACQUISITION

The important parameters recorded were: conveying pressures, air mass flowrates and product mass flowrate. Initially, the pressure profile along the conveying line was also recorded. Due to poor repeatability and regular blockage of the pressure tappings along the line, further pressures along the conveying lines were not recorded. Only the conveying pressure was considered in the analysis of results.

All the pressure transducers and the air flowmeter have a current output signal opposed to voltage output. As such, it was possible to accurately monitor all parameters without any problems associated with voltage drops in transmission lines.

Details of the calibration procedures and calibration curves for all the instruments are given in Appendix C.

3.5.1 Air Flowrate

A vortex shedding flowmeter was used to record the volumetric flowrate of air. The basic principal of the flowmeter is that vortices are shed from a wedge which is placed in the air stream. The rate at which the vortices are shed is proportional to the air velocity.

The air mass flowrate was derived from the product of the volumetric flow rate and the air density at the flowmeter. The density of the air at the flowmeter was given by Equation 3.1.

$$\rho = p / (R . T) \qquad (3.1)$$

where p was the pressure at the flowmeter and T, the air temperature. A temperature resistor was used to record this temperature at the flowmeter.

The flowmeter was calibrated according to British Standards BS 1042 (Ref 2) *with the use of a pitot static tube.*

3.5.2 Product Mass Flowrate

Material was collected in the receiving hopper at the end of the conveying line. Bridge type, strain gauge, load cells were used to record the mass of material in the hopper. The product mass flowrate was simply obtained from the rate at which material was collected in the hopper. The location of the load cells are shown in Figure 3.1.

All the load cells were joined in parallel to an Instrotech connection box. A voltage output signal from the connection box was recorded which corresponded to a specific mass of material in the hopper.

Calibration weights, each with a mass of forty kilograms, were used to calibrate the load cells. The calibration curve and procedure is given in Appendix C.

3.5.3 Pressures

All pressures were recorded with the use of Fuji pressure transducers. The conveying pressure was defined as the pressure at the flowmeter as shown in Figure 3.1. The milliamp output signals from the transducers were recorded by simply measuring the voltage drop across known resistors.

An illustration of the filter arrangement at the pressure tapping points along the conveying pipeline is shown in Figure 3.2.

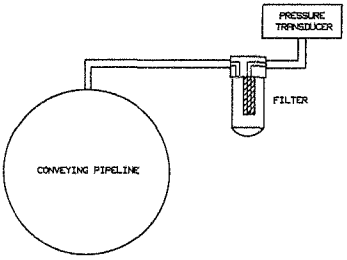


FIGURE 3.2: FILTER ARRANGEMENT AT THE PRESSURE TAPPING POINTS ALONG THE CONVEYING LINE

3.5.4 Data Acquisition System

The computer hardware available for recording data consisted of a personal computer, a double disc drive, the data acquisition and control unit, a printer and a plotter.

The data acquisition and control unit was only used to record data and not for controlling the operation of the test rig. In some cases, a chart recorder was also used to recor the product mass flowrate and the conveying pressure.

The data logger only measured voltage signals. Resistors were used to convert the current signal from the instruments to a voltage signal. The computer programme for collecting data, converted the voltage signals recorded by the data logger to the corresponding parameter with the use of the calibration equations for the specific instrument. A listing of the computer programme is given in Appendix D.

3.6 DESCRIPTION OF PIPELINE CONFIGURATIONS

An illustration of all the pipeline configurations investigated is given in Figures 4.1. Dimensional drawings of the pipelines are given in Appendix E. Figure 3.1 shows details of the equipment at the beginning and at the end of the conveying pipeline.

3.7 SYSTEM OPERATING CYCLE

The Briegen tandem blow vessel system, connected to a programmable logic controller, could either run in an automatic or manual mode.

The basic cycle is outlined below in point form.

1) The vent valve on each blow vessel opened when the cycle was commenced by selecting the automatic mode on the control panel.

2) Once the vessels were completely depressurised the slide valve above the vessels opened and the conical valve of the first vessel opened to fill the vessel with material.
3) The high-level indicator in the vessel signalled that the vessel was full, resulting in the slide valve and conical valve to close.
4) The vessel was then pressurised with service air to the expected conveying pressure.
5) Once the vessel was pressurised the rotary valve fed the material into the conveying line. The material was fluidised in the vessels with service air. The higher pressure in the vessel than in the conveying line ensured that material would not be held up in the vessel.
6) The low-level indicator signalled the rotary valves to stop feeding material.
7) The second blow vessel followed the same operating cycle as the first vessel, as outlined in point 2 to 6.
8) Once the first vessel was empty, the second vessel would immediately start conveying material to ensure a continuous flow of material in the pipeline.
9) Once the rotary valve stopped, the corresponding vent valve opened to depressurise the vessel.

A problem encountered was that the response time of the level indicators was too long, resulting in discontinuous flow of material into the pipeline. The reason being that the indicators operated on a capacitance principle and were not sensitive enough to distinguish between the dielectric constant of fluidised flyash and air.

To overcome the problem, the sensitivity of the indicators had to be manually adjustec during the operating cycle to improve the response time, and ensure continuous conveying.

3.8 EXPERIMENTAL PROCEDURE

Once all the instruments had been calibrated and installed, the procedure outlined below was followed for each test run.

A test run consisted of setting a fixed air mass flowrate and recording data for various different product mass flowrates. For each pipeline configuration, tests were run for a range of air mass flowrates.

It took approximately 45 minutes to record reliable data for each test run. A set of data was recorded about every 12 seconds which consisted of an average of 5 scans from the data logger.

Correct zeroing of all instruments was of utmost importance such that repeatability of results could be assured.

The procedure is given in point form.

1) Check the availability of the computer facilities and the air supply.
2) Load the computer programme which recorded and stored the data (Programme I as listed in Appendix D).
3) Depressurise the air supply line to the test rig.
4) Switch on the power to all the instruments (24 V supply).
5) Record the ambient air temperature and barometric pressure.
6) Start the computer programme, to record the zero values from all the instruments.
7) Switch on the: extraction fan for the filter unit, power to the control panel, compressor for the conveying and service air.
8) Select the automatic mode on the control panel to start the conveying cycle as outlined in Section 3.7.
9) Run the system for 5 minutes to ensure continuous conveying.
10) Close the valve under the receiving hopper, collecting material in the hopper to determine the product mass flowrate.
11) Continue the computer programme to record data for the specific product mass flowrate.

12) Record data for different product mass flowrates, adjusting the speed of the rotary valves in each case.

The repeatability of the results is discussed in Appendix I.

3.9 COMPUTER SOFTWARE

The programmes for recording and analysing the data were written in Hewlett Packard Basic. The diagram in Figure 3.3 illustrates the interaction between the programmes. A listing of the programmes is given in Appendix D.

Voltage signals from the data logger were recorded by Programme I, which printed out all the results recorded during the test. At the end of a test, all the results, as printed out, were stored on a micro disc. A copy of a typical print-out for a test run is given in Appendix A. The print-out also served as a back-up for the information stored on disc.

Programme II read the data from the storage file displaying the data on the screen. The data was processed in Programme III and stored in data files on disc.

In Programme IV the information from selected data files was read. The parameters to be plotted (eg. pressure and load ratio) were stored in a file which was compatible with an existing software package for plotting graphs.

Numerous alterations were made to the programmes in order to analyse the data in different formats (eg. pressure versus velocity, power versus load ratio, etc.). These minor alterations are not shown in Appendix D.

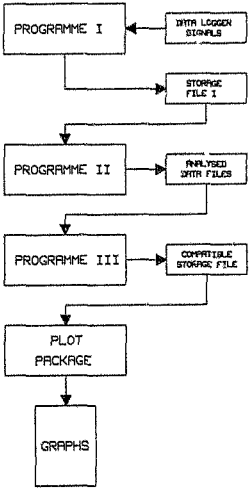


FIGURE 3.3: INTERACTION BETWEEN COMPUTER PROGRAMMES FOR RECORDING AND ANALYSING DATA

3.10 FLYASH PROPERTIES

3.10.1 Particle Size

Generally, flyash is dominated by tiny spherical particles (2 - 80 microns) with occasional separate mineral grains. The particle size distribution of the flyash, used in the experimental investigations described in this report, was obtained by Coulter Counter analysis. In Figure 3.4, the cumulative mass percentage is plotted against the particle diameter. The average particle size (ie. at 50% cumulative mass percentage) corresponds to a particle size of 16 microns.

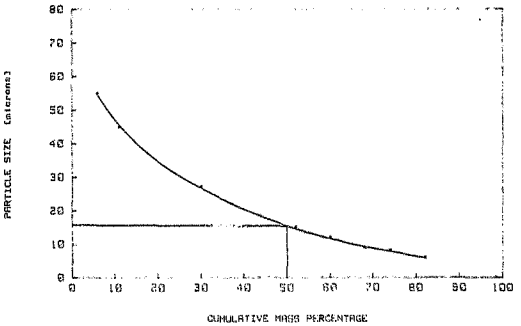


FIGURE 3.4: PARTICLE SIZE DISTRIBUTION

3.10.2 Bulk Density

The bulk density of the flyash was 930 kg/m^3. A container of a known volume was filled with a sample of flyash. Care was taken not to compact the flyash. From the mass of flyash in the container the bulk density was determined.

It has been shown (Ref.5) that the true particle density of flyash, using a picometer, is in the order of 2360 kg/m^3.

3.10.3 Geldarts Classification of Flyash

On the Geldarts Classification, as discussed in Section 2.9, flyash lies on the border of Group A and Group C products. Although Group C products are usually too cohesive to fluidise, flyash fluidises easily and is regarded as a good candidate for dense phase conveying.

4. EXPERIMENTAL PHILOSOPHY

4.1 INTRODUCTION

In this chapter the reasons are outlined for conveying through the various pipeline configurations. A diagram summarising all the pipeline configurations investigated is given in Figure 4.1.

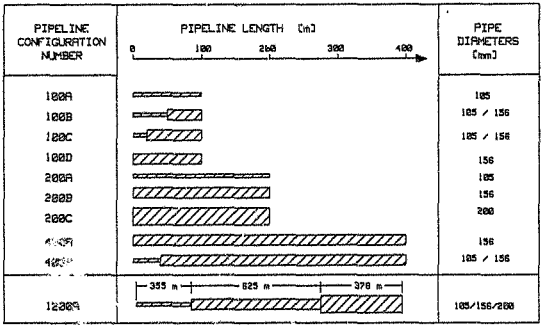


FIGURE 4.1: PIPELINE CONFIGURATIONS INVESTIGATED

4.2 PIPELINE CONFIGURATIONS INVESTIGATED

The effect of stepping a pipeline at various distances along the line was first investigated over a length of 100 metres in configurations 100A, 100B, 100C and 100D, as shown in Figure 4.1. Figure 4.2 illustrates the trend in the conveying pressure which was expected under certain conditions of the load ratios which were to be determined. This figure was derived from the investigations by Snow (Ref.33) who showed that the pressure drop in a stepped pipeline over a distance of 1600 m was lower than the pressure drop over a constant diameter pipeline under the same operating parameters. This trend is illustrated by the conveying pressure of configuration 100D in Figure 4.2 being higher than the conveying pressure of configuration 100C. The conveying pressure in configuration 100B was expected to be lower than 100A due to the decrease in pressure drop per unit length for the larger diameter pipe section in configuration 100B. The decrease in pressure drop per unit length with increasing pipe diameter was discussed in Section 2.4.

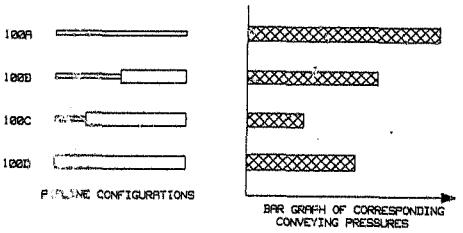


FIGURE 4.2: EXPECTED TREND IN THE CONVEYING PRESSURE

An optimum stepped pipeline would thus correspond to the lowest conveying pressure as shown in Figure 4.2.

From the experimental investigations, the lowest conveying pressure was found to be in the pipeline with a constant diameter of 156 mm [100D]. Thus an optimum stepped pipeline as illustrated by pipeline configuration 100C in Figure 4.2 was not evident. It was concluded that a larger diameter pipe would simply yield a lower conveying pressure.

The advantage of a stepped pipeline was expected to be evident over a longer conveying distance and consequently tests were conducted over 400 metres through configurations 400A and 400B as shown in Figure 4.1. The conveying pressure recorded in the stepped pipeline (400B) was not remarkably less than the constant diameter pipeline (400A). Thus, even over a distance of 400 meters the benefit of a stepped pipeline was not evident.

To determine the effect of pipe diameter, at least three different diameter pipelines had to be investigated.

Tests were therefore conducted over a distance of 200 metres with pipe diameters of 105 mm, 150 mm and 200 mm. Using the results from configurations 100A, 200B and 400A, the effect of line length could be determined.

The experimental results recorded for the long distance line (1200A) were compared to the empirical model developed for predicting the performance of the long distance line. The model was developed from the results of the pipelines with constant diameters (100A, 100D, 200A, 200B, 200C and 400A).

5. RESULTS AND PERFORMANCE CHARACTERISTICS

5.1 INTRODUCTION

A comparison of the results, discussing the effect of pipe diameter, length and stepped pipelines, is given in Chapters 6 and 7. In this chapter, the equations expressing the conveying pressure in terms of product mass flowrate and air mass flowrate are discussed.

An example of a pressure profile along one of the pipelines is also discussed, outlining the problems involved in recording the pressures along the line.

In Section 5.4, typical results from various pipeline configurations show the general trends in the performance of a pneumatic conveying system. The results recorded for the long distance line are briefly discussed in Section 5.5.

5.2 EQUATIONS FOR RESULTS

An equation was found for the conveying pressure as a function of product mass flowrate and air mass flowrate, for each pipeline configuration. Using these equations, the performance of the various configurations were compared, as discussed in Chapters 6 and 7.

Figure 5.1 shows the typical relationship between conveying pressure and product mass flowrate for different air flowrates.

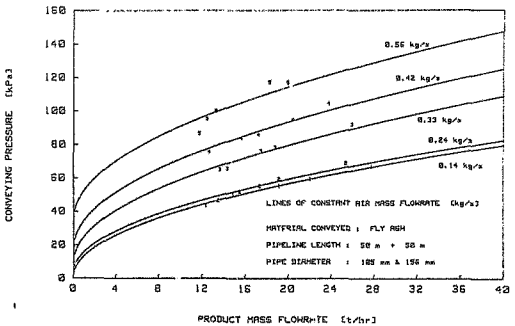


FIGURE 5.1: CONVEYING PRESSURE VERSUS PRODUCT MASS FLOWRATE

Using regression analysis, the following expression for the conveying pressure was found:

$$p = A + B.\sqrt{G} \qquad (5.1)$$

where p is the conveying pressure and G, the product mass flowrate. A and B are functions of the air mass flowrate. For zero product mass flowrate

$$p = A \qquad (5.2)$$

A, thus represents the pressure drop due to air alone.

The square root relationship in Equation 5.1 was chosen because the correlation was better than a simple linear relationship in the form of:

$$p = A + B.\dot{G}$$

The equations for each pipeline configuration are summarised in Table 5.1. The graphs of conveying pressure *versus* product mass flowrate and A and B as a function of air mass flowrate, are included in Appendix A.

Thus: $p = A(\dot{Q}) + B(\dot{Q}) . \sqrt{G}$

TABLE 5.1: EQUATION FOR A AND B

Pipeline Configurations	A $f(\dot{Q})$	B $f(\dot{Q})$
100 A	$A = 133{,}901 . \dot{Q}^2$	$B = 10{,}847 + 23{,}309 . \dot{Q}$
100 B	$A = 105{,}682 . \dot{Q}^2$	$B = 9{,}344 + 16{,}567 . \dot{Q}$
100 C	$A = 45{,}138 . \dot{Q}^2$	$B = 10{,}229 + 7{,}727 . \dot{Q}$
100 D	$A = 48{,}468 . \dot{Q}^2$	$B = 9{,}639 + 9{,}868 . \dot{Q}$
200 A	$A = 257{,}406 . \dot{Q}^2$	$B = 27{,}860 - 3{,}558 . \dot{Q}$
200 B	$A = 60{,}275 . \dot{Q}^2$	$B = 16{,}728 + 0{,}267 . \dot{Q}$
200 C	$A = 77{,}895 . \dot{Q}^2$	$B = 19{,}667 - 4{,}757 . \dot{Q}$
400 A	$A = 102{,}891 . \dot{Q}^2$	$B = 13{,}260 + 17{,}272 . \dot{Q}$

The accuracy of the equations was determined by plotting the experimental pressure drop against the pressure drop derived from the equation for the same product and air mass flowrates, as shown in Appendix I.2. The percentage error, as defined in Equation 5.3, and the correlation coefficient (Ref.40) for all the equations are given in Table 5.2.

$$\% \text{ error} = \left| \frac{P(\text{equ}) - P(\text{exp})}{P \quad p)} \right| . 100 \qquad (5.3)$$

TABLE 5.2: CORRELATION OF EQUATION TO THE EXPERIMENTAL RESULTS

PIPELINE CONFIGURATION	AVERAGE PERCENTAGE ERROR [%]	COEFFICIENT OF CORRELATION
100 A	8,7	0,953
100 B	8,6	0,996
100 C	7,7	0,906
100 D	5,4	0,946
200 A	3,8	0,964
200 B	8,3	0,904
200 C	12,3	0,894
400 A	6,10	0,998

The deviations of the experimental pressure drop from the equations are due to the uncertainties in the experimental results and due to the equation relating the pressure to the product mass flowrate and air mass flowrate, as given by Equation 5.1. As the product mass flowrates increase, the system operates in a more dense phase mode. A cubic model, shown in Figure 5.2 would then probably fit the data more accurately, although at high air mass flowrates, a linear model would be more appropriate.

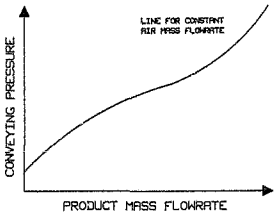


FIGURE 5.2: CUBIC MODEL FOR CONVEYING PRESSURE

5.3 PRESSURE PROFILES

The importance of the static pressure along the pipeline is that parameters such as velocity, Froude number and dynamic pressure are all related to the pressure. The Froude Number for instance is an important parameter for the design of stepped pipelines (Ref. 27).

A typical example of the static pressure profile recorded for the 100 metre line with a diameter of 105 mm (Configuration 100A) is shown in Figure 5.3. An illustration of the pipeline configuration showing the location of the pressure tapping points is given in Figure 5.4.

The first transducer P(1), defined as the conveying pressure, was located at the flowmeter, approximately 6 metres upstream of the rotary valves where the product was fed into the conveying line. The pressure drop from P(1) to the rotary valves was negligible, as shown in Appendix G.

The large pressure drop from P(1) to the second pressure transducer P(2), which was situated 6 metres downstream the rotary valves, is due to the losses across the feeder and the acceleration of the product.

The acceleration pressure drop, which is given by Equation 5.4 (Ref. 18),

$$p_a = \mu \, v_o \, \rho_o \, c \qquad (5.4)$$

only contributes about 15% of this pressure drop.

eg. From the results of test number 100A1, shown in Appendix A

μ = 24,9
v_o = 9,4
ρ_o = 1,57

assuming c = 0,5

thus p_a = 24,9 . 9,4 . 1,57 . 0,5
= 1,7 kPa

and the pressure drop from P(1) to P(2) was recorded as 12,0 kPa.

It thus appears that 85% of the pressure loss across the feeder is due to the resistance of flow through the feeder. The resistance of flow could be due to the vanes of the rotary valves passing through the flow stream and due to additional turbulence. Meijers (Ref.21) emphasized the importance of developing an effecient feeding deveice to reduce the pressure loss across the feeder.

The third transducer was located 29,6 metres away from P(2), along a straight horizontal section of the pipeline, similar to the section between pressure transducers P(5) and P(6). The intention was to analyse the pressure drop per unit length across these two sections in terms of a polytropic expansion of the gas.

From the results shown in Figure 5.5, it can be seen that the effect of product mass flowrate on the pressure drop was inconsistent. Usually the pressure drop increases with increasing product mass flowrate, but from the results recorded the pressure drop was lower in some cases with high product mass flowrate. The repeatability of the results was also unacceptable.

It thus appears to be an unstable flow regime, where there is a continuous fluctuation in pressure due to plug type flow, although the conveying pressure P(1) was stable and could be recorded with an acceptable repeatability.

Another problem in recording the pressures along the conveying line was that the pressure tapping points blocked after about 15 minutes of conveying. The installation of a complete purging system was not practical considering all the pipeline configurations and distance to be investigated.

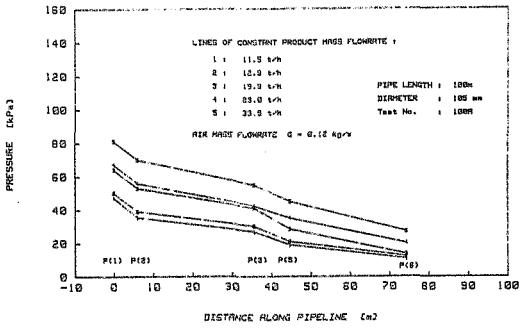


FIGURE 5.3: PRESSURES ALONG THE PIPELINE

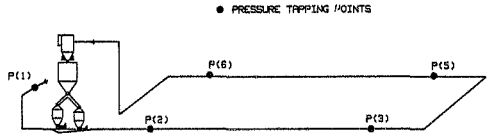


FIGURE 5.4: LOCATION OF THE PRESSURE TAPPING POINTS

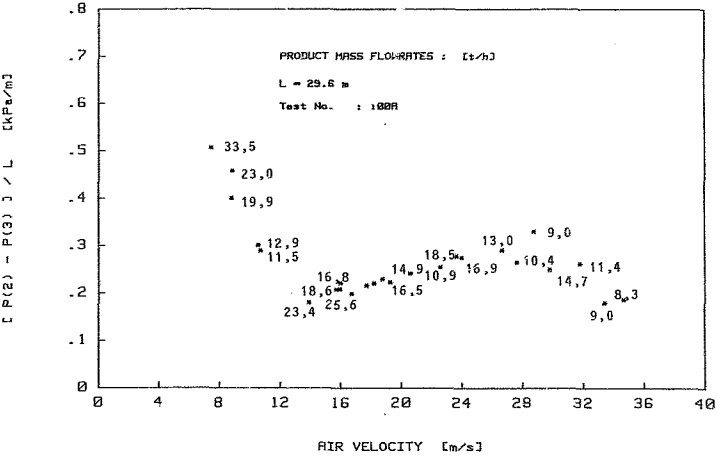


FIGURE 5.5: PRESSURE DROP FROM P(2) TO P(3)

An alternative filter arrangement at the pressure tapping points was developed, as shown in Figure 5.6.

The porous media (sintered bronze) was placed flush with the internal pipe wall. The idea was that the flow of material would prevent the media from blocking.

It was found that the small particles of flyash blocked the porous media after only five minutes of conveying.

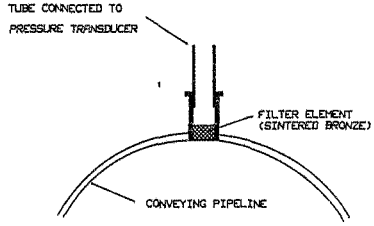


FIGURE 5.6: ALTERNATIVE FILTER ARRANGEMENT OF THE PRESSURE TAPPING POINTS

The only pressure of interest for further analysis was the conveying pressure P(1), which could be recorded accurately with an acceptable repeatability. This pressure was recorded upstream of the feed point in a clean air condition.

5.4 PERFORMANCE CHARACTERISTICS

The power required to convey the material was defined as the air power loss across the conveying system. The expansion of the air in the conveying pipeline is isothermal (Ref.9), thus the power required for isothermal compression, as given by Equation 5.5, was used to calculate the power to convey the material.

$$\text{Power} = p_{at} \cdot v_{fad} \cdot \ln (p_1 / p_{at}) \qquad (5.5)$$

where p_{at} = atmospheric pressure
v_{fad} = free air delivery from the compressor
p_1 = conveying pressure

Usually the performance of a pneumatic conveying system is predicted by considering the pressure losses of the following components individually:

1) acceleration zone
2) bends
3) horizontal conveying line
4) vertical conveying line
5) filter unit

The conveying pressure, which is the summation of all the pressure losses in the system, was of prime interest in this project. The conveying characteristics are thus discussed relative to the point at which the conveying pressure was defined as shown in Figure 3.1.

5.4.1 Conveying Pressure Versus Air Velocity

The State Diagram as discussed in Section 2.2, gives the pressure drop per unit length as a function of the air velocity with the product mass flowrate as a parameter.

In this case the pressure drop over the whole system was plotted against the air velocity at the flowmeter. A so-called 'State Diagram' could thus be drawn, as shown in Figure 5.7. The difference is that the pressure drop includes the losses due to acceleration and bends and that the velocity recorded does not take into account the expansion of the air along the conveying line.

The importance of the so-called 'State Diagram', shown in Figure 5.7, is that the pressure minimum is not evident. Investigations by Meijers (Ref.21) have shown that the pressure minimum on the State Diagram for flyash, with a product mass flowrate greater than 5 t/h, occurs at a velocity greater than 20 m/s. It can be seen in Figure 5.7 that even at an air velocity of 10 m/s, a pressure minimum had not been reached.

The acceleration and bends effects appear to have a significant influence on the overall pressure drop.

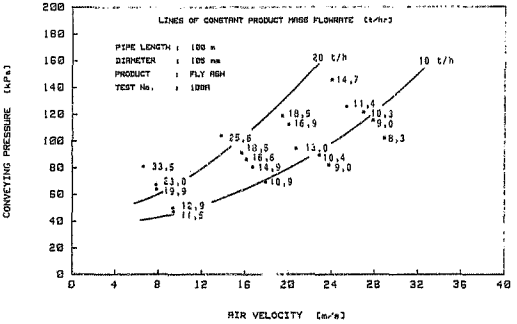


FIGURE 5.7: CONVEYING PRESSURE VERSUS AIR VELOCITY

5.4.2 Conveying Pressure Versus Load Ratio

Figure 5.8 illustrates the conveying pressure as a function of the load ratio with air mass flowrate as a parameter. The advantage of conveying at a minimum air mass flowrate is evident. It is important to note that when conveying at high load ratios, the air mass flowrate should be kept as low as possible. The maximum available pressure could be exceeded if the air flowrate is too high and the load ratio is increased. At low air mass flowrates, the conveying pressure is less sensitive to an increase in load ratio.

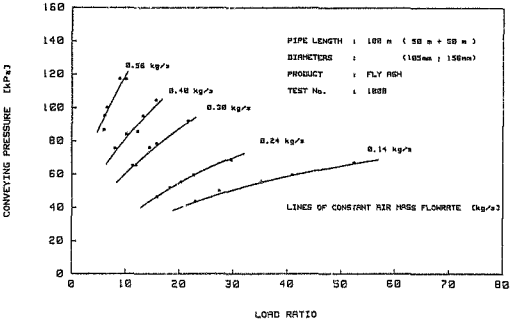


FIGURE 5.8: CONVEYING PRESSURE VERSUS LOAD RATIO

5.4.3 *Power Versus* Product Mass Flowrate

From Figure 5.9 it can be seen that the power required to convey the material is more sensitive to an increase in air mass flowrate than product mass flowrate. A 100% increase in product mass flowrate from 15t/h to 30 t/h at a constant air mass flowrate of 0,3 kg/s results in a power increase of only 33%. When doubling the air mass flowrate from 0,14 to 0,30 kg/s at a constant product mass flowrate of 20 t/h, the power required increases from 5 to 15 kW, a 200% increase.

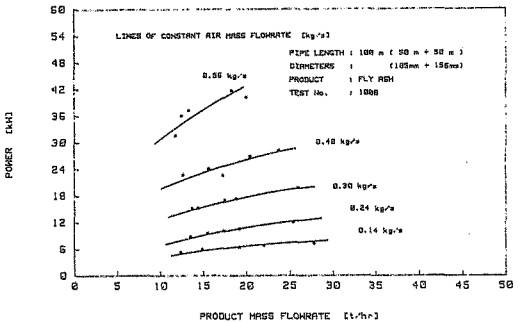


FIGURE 5.9: AIR POWER VERSUS PRODUCT MASS FLOWRATE

5.4.4 Power versus Load Ratio

The lines of constant product mass flowrates in Figure 5.10 illustrate the decrease in power with increasing load ratio. A point of minimum power with increasing load ratio at a constant product mass flowrate was not apparent. If the product could have been conveyed at higher load ratios of the order of 100, by decreasing the air mass flowrate, the pressure term P(1) would eventually dominate in Equation 5.5 from which the power was calculated.

$$\text{Power} = p_{at} \cdot v_{fad} \cdot \text{Ln} \left(P(1) / p_{at} \right) \qquad (5.6)$$

A minimum power will thus appear which would be the optimum point for the design of a system. It is important to consider the maximum available pressure which often limits the system from operating at the power minimum point.

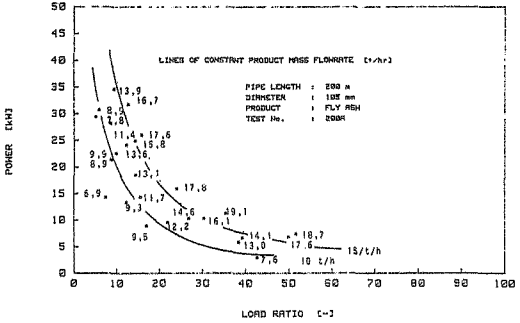


FIGURE 5.10: POWER VERSUS LOAD RATIO

5.4.5 Power versus Air Velocity

The decrease in power as the air velocity decreases for a constant product mass flowrate is shown in Figure 5.11. In the low velocity range the power appears to approach a minimum. The velocity at which the power minimum would occur is expected to increase as the product mass flowrate increases. A power minimum curve could thus be drawn, similar to the pressure minimum curve of the State Diagram as discussed in Section 2.2.

The difference in power required to convey material at a rate of 10 t/h and 20 t/h also decreases as the air velocity decreases. Thus, if the capacity of a conveying system was to be increased, the additional air power required decreases as the conveying air velocity decreases.

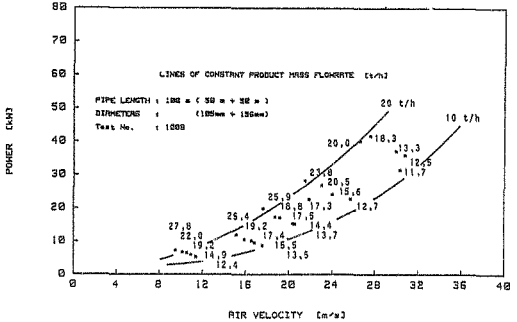


FIGURE 5.11: POWER VERSUS AIR VELOCITY

5.4.6 Product Mass Flowrate versus Air Mass Flowrate

The conveying characteristics of a material are generally given in the graphical form of product throughput versus air flowrate for a specific pipeline layout (Ref.14). Figure 5.12 shows a typical set of results for the 200 metre pipeline with a diameter of 156 mm.

The conveying potential of a pipeline configuration can be determined from these results where the pressure drop across the system is the limiting factor. For a maximum permissible pressure drop across the system, the product mass flowrate decreases as the air mass flowrate increases.

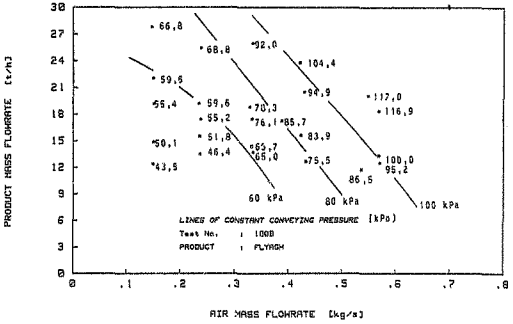


FIGURE 5.12: PRODUCT MASS FLOWRATE VERSUS AIR MASS FLOWRATE

5.5 LONG DISTANCE RESULTS

The problem initially encountered when conveying through the long distance line was that insufficient storage space was available in the intermediate hopper to enable continuous conveying. An additional 3500 kg of flyash was loaded into the system, using the pipeline itself as storage space for the material.

For a minimum air mass flowrate of 0,3 kg/s, the product flowrate had to be less than 5 t/h to ensure continuous conveying. At higher product mass flowrates, insufficient material was available in the storage hopper at the beginning of the conveying line. The installation of larger storage hoppers would have been the only other alternative. At a maximum air flowrate of 0,44 kg/s, the intermediate hopper and the receiving hopper would fill up completely with material if the product mass flowrate was less than 6 t/h. The range of the results recorded was thus constrained by these conditions.

All the results recorded for the long distance line are shown in Figure 5.13.

A typical mass versus time trace of the material collected in the receiving hopper is shown in Figure 5.14. The sudden increase in the mass indicated that plugs of material were entering the hopper. The material was thus being conveyed in a dense phase mode at the end of the pipeline.

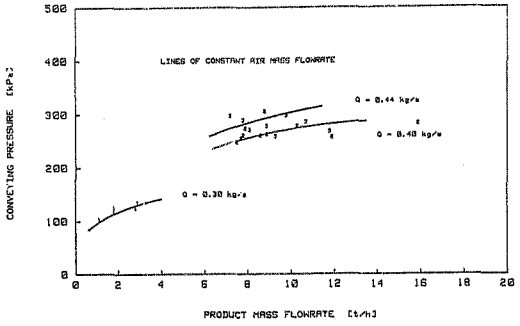


FIGURE 5.13: LONG DISTANCE LINE RESULTS

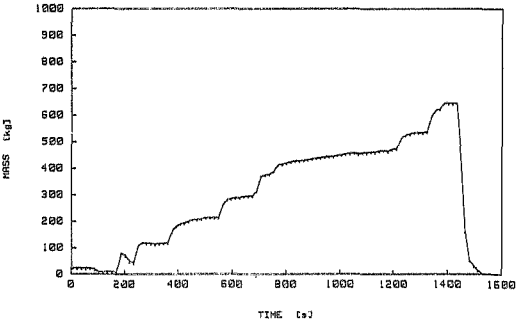


FIGURE 5.14: MASS VERSUS TIME TRACE OF MATERIAL BEING COLLECTED IN THE RECEIVING HOPPER

5.6 CONCLUSIONS

The following conclusions were drawn from discussions in this chapter.

1) From the experimental results it appears that the conveying pressure was related to approximately the square root of the product mass flowrate.
2) The acceleration pressure losses at the feeder are overshadowed by the losses due to the resistance of flow through the feeder.
3) The results show that the conveying pressure is a minimum for the lowest air mass flowrate. Although it appears that there is an optimum load ratio corresponding to a minimum conveying pressure. Higher product mass flowrates are required to verify this optimum load ratio.
4) Under the conditions investigated, the material is conveyed in a dense phase mode at the end of the long distance line.

For future experimental investigations, it should be noted that a purging system is required to measure the pressure along the conveying line to prevent pressure tapping points from blocking. A larger intermediate hopper is also required when conveying through the long distance line. With more storage space available, higher product mass flowrates can be investigated in the low air mass flowrate range.

6. PIPELINE LENGTH AND DIAMETER EFFECTS ON THE SYSTEM PERFORMANCE

6.1 INTRODUCTION

In order to develop criteria for stepping pipelines, one would require a sound understanding of the pipeline length and diameter effects on the system performance. The individual effects of the parameters are discussed in Sections 6.2 and 6.3.

6.2 PIPELINE LENGTH EFFECTS

6.2.1 Introduction

It is commonly known that the conveying distance is one of the major factors influencing the performance of pneumatic conveying systems. The length of pipeline also limits the design of pneumatic conveying systems.

It has been shown (Ref.17) that there exists a critical length of pipeline beyond which it is not possible to convey material. All the energy is required to convey the air, and no additional energy is available to convey material.

The effect of conveying distance on the performance has been established by various researchers (Refs. 5, 33, 35). In Section 6.2.2 the results from the investigations described in this report confirm the effect of line length on the system performance.

A new concept to determine the effect of line length is discussed in Section 6.2.3. The area under the curve on a State Diagram is shown to represent the pressure drop across the system.

6.2.2 The Effect of Line Length on Conveying Pressure and Product Mass Flowrate

6.2.2.1 Conveying Pressure

The equations developed in Section 5.2 were used to plot the conveying pressure as a function of the effective line length. The equivalent horizontal length of the bends, which is discussed in Appendix F, was obtained from investigations by Jardine (Ref.5).

The conveying pressures are shown in Figure 6.1 for the 100, 200 and 400 metre pipelines with constant diameters of 156 mm. The air mass flowrate was kept constant at 0,3 kg/s. The following equation could be used to express the conveying pressure in terms of the effective line length.

$$p = A \cdot L_e^{x} \qquad (6.1)$$

where A is the proportionality constant and a function of air mass flowrate and product mass flowrate. Within the range of effective line lengths investigated, x would be less than 1. Jardine (Ref.5) found that x was of the order of 0,7 for the conveying of flyash over distances of 100, 200 and 400 metres in 102 mm diameter pipelines.

In Section 6.2.3 the relationship between conveying pressure and line length is discussed by considering the area under the curve on the State Diagram. The fact that the value of x in Equation 6.1 is less than 1 is also discussed in Section 6.2.3.

6.2.2.2 Product Mass Flowrate

The exponential decrease in product mass flowrate with increasing line length is shown in Figure 6.2, for a conveying pressure of 100 kPa and an air mass flowrate of 0,3 kg/s. The corresponding product mass flowrates were obtained for the 100, 200 and 400 metre pipelines with a constant diameter of 156 mm using the equations developed in Section 5.2.

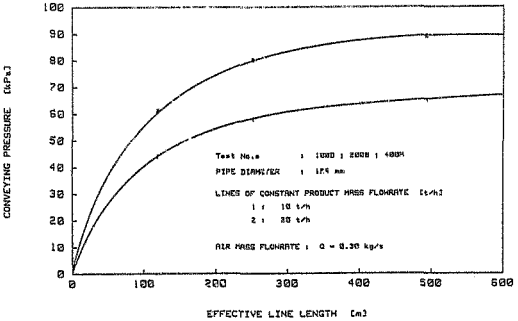


FIGURE 6.1: CONVEYING PRESSURE AS A FUNCTION OF LINE LENGTH

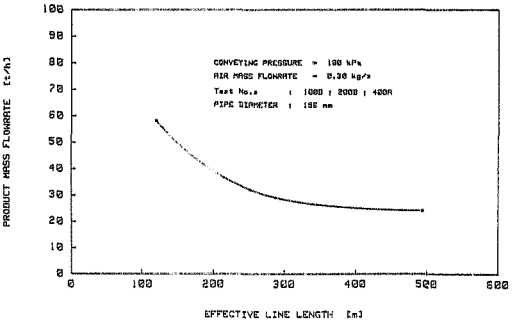


FIGURE 6.2: DECREASE IN CONVEYING PRESSURE WITH INCREASING LENGTH

Figure 6.3 illustrates the decrease in product mass flowrate with increasing line length by considering the total energy available.

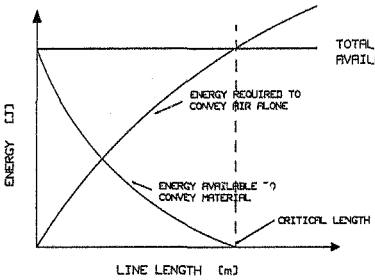


FIGURE 6.3: DISTRIBUTION OF AVAILABLE ENERGY

The energy required to convey the air alone and the additional energy required to convey material make up the total energy available. With increasing line length, more energy is required to convey the air through the pipeline and thus less energy is available to convey the product. The critical line length is shown in Figure 6.3 at the point where all the energy available is required to convey the air alone, thus the product mass flowrate reduces to zero.

6.2.3 The Effect of Line Length on the Conveying Pressure from the State Diagram

The high pressure drop across a long distance pneumatic conveying system is related to the increase in air velocity along the pipeline.

The pressure drop per unit length, as a function of air velocity, is shown in Figure 6.4 for a specific product mass flowrate, ie. a State Diagram as discussed in Section 2.2.

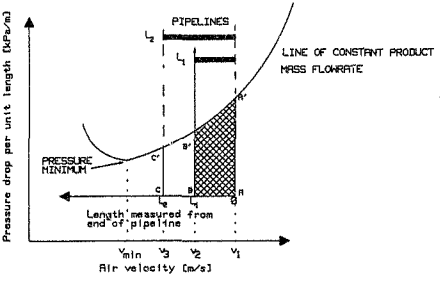


FIGURE 6.4: PRESSURE DROP PER UNIT LENGTH AS A FUNCTION OF THE AIR VELOCITY

For a pipeline with a total length L_1, the velocities at the end and beginning of the pipeline are represented by v_1 and v_2 respectively in Figure 6.4. The second abscissa represents the pipeline length measured from the end of the line. Thus the hatched area ABB'A' shown in Figure 6.4 represents the total pressure drop across the pipeline, ie. the conveying pressure.

The pressure drop across a pipeline of length L_2, where $L_2 = 2.L_1$, is represented by the area ACC'A' in Figure 6.4 for the same product and air mass flowrate considered in the pipeline of length L_1.

It can thus be seen from the areas under the curve that the conveying pressure is not linearly related to the line length. The additional pressure required (area BCC'B') to convey through L_2 is less than the conveying pressure for L_1. This explains the trend of conveying pressure as a function of line length, discussed in Section 6.2.2 and as shown in Figure 6.5.

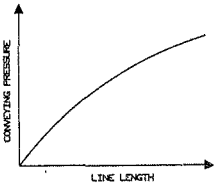


FIGURE 6.5: CONVEYING PRESSURE AS A FUNCTION OF LINE LENGTH

As the pipeline length increases, the velocity at the beginning of the line decreases and if this velocity is less than the velocity at the pressure minimum point v_{min} as shown in Figure 6.4, the following trend shown in Figure 6.6 can be expected.

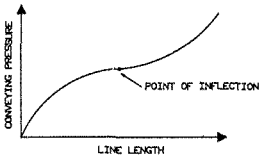


FIGURE 6.6: CONVEYING PRESSURE VERSUS LINE LENGTH

The point of inflection corresponds to the length of pipeline where the velocity at the beginning of the pipeline is equal to the velocity at the pressure minimum point shown in Figure 6.4. The increase in the slope of the curve to the right of the point of inflection shown in Figure 6.6 is due to the dense phase conveying mode at the beginning of the line where the pressure per unit length increases with increasing line length as shown in Figure 6.4.

6.2.4 Acceleration Zone Effect on Conveying Pressure for Various Line Lengths

The pressure profiles along pipelines with lengths of L_1 and L_2 are shown in Figure 6.7. The pressure losses across the feeder consist of a pressure loss due to turbulence and a pressure drop due to the acceleration of the material.

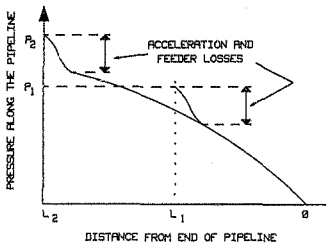


FIGURE 6.7: PRESSURE ALONG THE PIPELINES

The conveying pressures for the line lengths L_1 and L_2 are given by P_1 and P_2 respectively. The acceleration losses can be assumed to be independent of the line length. The conveying pressures are thus not linearly related to the line lengths, due to the effect of the acceleration zone.

6.2.5 Conclusions

From the State Diagram, the effect of line length can be determined by considering the area under the curve. The reasons for the conveying pressure not being linearly related to the line length are as follows:

1. The average pressure drop per unit length decreases as the line length increases.
2. The acceleration pressure losses and losses across the feeder which are independent of line length, effect the conveying pressure.

The product mass flowrate decreases as the line length increases because more of the available energy is required to convey the air through the pipeline.

6.3 PIPELINE DIAMETER EFFECTS

6.3.1 Introduction

The effect of the pipe diameter on the system performance was obtained from the results of the tests conducted through the pipeline configurations as described in Table 6.1.

TABLE 6.1 : PIPELINE CONFIGURATIONS

Pipeline Configuration	Diameter (mm)	Length (m)
100A	105	100
100D	156	100
200A	105	200
200B	156	200
200C	200	200

From the equation expressing the conveying pressure in terms of product and air mass flowrate ($p = A + B\overline{G}^{n}$), as discussed in section 5.2, a comparison was made of the conveying pressures at a specific product mass flowrate and air mass flowrate.

6.3.2 The Effect of Pipe Diameter on Conveying Pressure

The conveying pressures for the 100 metre pipelines with constant diameters of 105 and 156 mm (ie. configurations 100A and 100D) are shown in Table 6.2. The equations from Section 5.2 were used to calculate the conveying pressures with the product mass flowrate ranging of 5 to 15 t/h and the air mass flowrate ranging from 0,1 to 0,5 kg/s.

Plotting the conveying pressure for the 100D configuration against the corveying pressure for 100A multiplied by the ratio of the diameter, as shown in Figure 6.8, illustrates that the conveying pressure was inversely related to the pipe diameter. This is in agreement to the effect of pipe diameter as discussed in Section 2.4. The average percentage difference of the conveying pressures shown in Figure 6.8 was 13,3% with a correlation coefficient of 0,965.

Figures 6.9 and 6.10 give the conveying pressures in the 200 metre pipelines (200A, 200B and 200C) as a function of the pipe diameter, with the air mass flowrate as a parameter.

In Figure 6.9, the conveying pressures were derived from the equation developed in Section 5.2, keeping the product mass flowrate constant at 10 t/h and varying the air mass flowrate from 0,1 to 0,5 kg/s. At an air mass flowrate of 0,5 kg/s, the conveying pressure decreased as the pipe diameter increased although it is not a linear relationship as was concluded from the 100 metre pipelines (100A and 100D).

At low air mass flowrates (i.e. 0,1 kg/s) the conveying pressure in the 200 mm diameter pipe was higher than the conveying pressure in the 156 mm diameter pipe. It thus appears that there exists an optimum pipe diameter corresponding to a minimum conveying pressure. This was only evident at low air mass flowrates (i.e. high load ratios).

In Figure 6.10, the product mass flowrate was increased to 20 t/h. At high air mass flowrates the conveying pressure also decreased with increasing pipe diameter, although there was a definite minimum conveying pressure.

TABLE 6.2: CONVEYING PRESSURES

P1A = Conveying pressure for 100A
P1D = Conveying pressure for 100D

$\dot{Q}$ (kg/s)	$\dot{G}$ (t/h)	P1A (kPa)	P1D (kPa)	P1A.(105/156) (kPa)
0,1	5,0	31	24	21
0,1	10,0	43	34	29
0,1	15,0	52	42	35
0,3	5,0	52	33	35
0,3	10,0	68	44	46
0,3	15,0	81	53	55
0,5	5,0	84	45	56
0,5	10,0	105	58	70
0,5	15,0	121	69	81

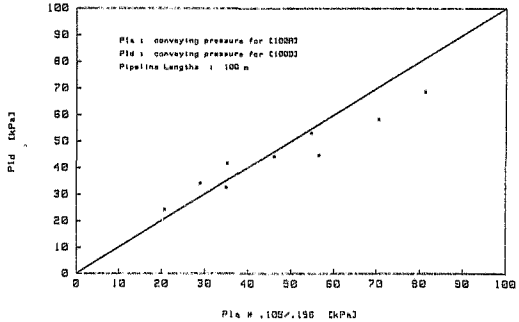


FIGURE 6.8: CONVEYING PRESSURES IN 105 MM AND 156 MM DIAMETER PIPELINES OVER 100 METRES

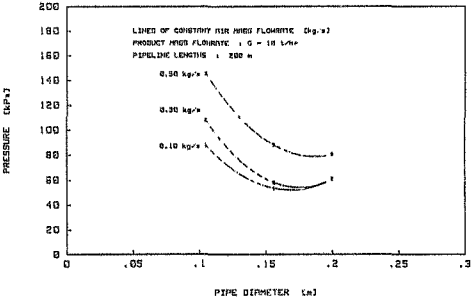


FIGURE 6.9: CONVEYING PRESSURE VERSUS PIPE DIAMETER FOR A PRODUCT MASS FLOWRATE OF 10 t/h

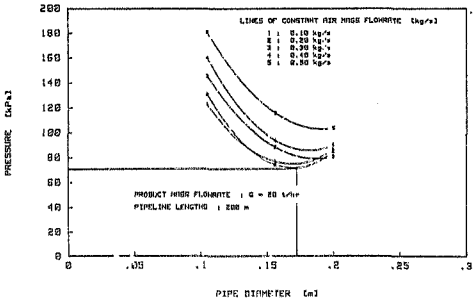


FIGURE 6.10: CONVEYING PRESSURE VERSUS PIPE DIAMETER FOR A PRODUCT MASS FLOWRATE OF 20 t/h

At low air mass flowrates ranging from 0,1 to 0,2 kg/s it also appears that there is an optimum air mass flowrate. The minimum conveying pressure as shown in Figure 6.10 was 70 kPa corresponding to a air mass flowrate of 0,2 kg/s and a pipe diameter in the order of 0,170 m.

Considering that a pipe diameter of 0,170 m is not a standard size, a stepped pipeline consisting of 156 mm and 200 mm diameter pipes would be the optimum pipeline design over 200 metres.

6.3.3 Conclusions

It has been shown that there exists an optimum pipe diameter to convey material, which is a function of product mass flowrate and air mass flowrate. Other parameters which are likely to affect the optimum pipe diameter are the material characteristics and conveying distance.

7. EFFECTIVENESS OF STEPPED PIPELINES

7.1 INTRODUCTION

A stepped pipeline (or telescopic pipeline) consists of a small diameter pipe followed by sections of larger diameter pipes, as shown in Figure 7.1.

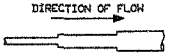


FIGURE 7.1: A TELESCOPIC PIPELINE

The reasons for stepping pipelines in pneumatic conveying systems, as discussed in Section 2.7, include the reduction of power consumption and to ensure a lower conveying pressure, (i.e. the pressure at the beginning of the pipeline). This enables the conveying of the material over longer distances.

The following trend in the performance of stepped pipelines was expected: Stepping the pipe to a larger diameter too close to the feeding point would result in solids deposition with a corresponding higher conveying pressure or even a blockage compared to a pipeline which was stepped further downstream from the feeding point. Figure 7.2 illustrates the pressure profiles expected for various stepped pipelines over a specific distance. Line III would thus be the optimum pipeline design, corresponding to the lowest pressure at the beginning of the pipeline.

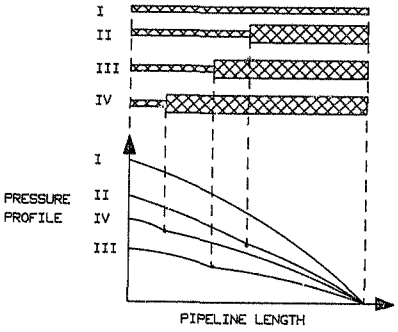


FIGURE 7.2: PRESSURE PROFILE FOR VARIOUS PIPELINE DESIGNS

7.2 EXPERIMENTAL OBSERVATIONS

The bar graph in Figure 7.3 illustrates the magnitude of the conveying pressures in pipeline configurations 100B, 100C and 100D with respect to the conveying pressure in configuration 100A. The equations discussed in Section 5.2 were used to calculate the conveying pressures shown in Table 7.1 for the pipeline configurations 100A, 100B, 100C and 100D. The conveying pressures in Table 7.1 are also expressed as a percentage of the 100A conveying pressure at the corresponding product and air mass flowrates. The averages of these percentages were used to construct the bar graph shown in Figure 7.3.

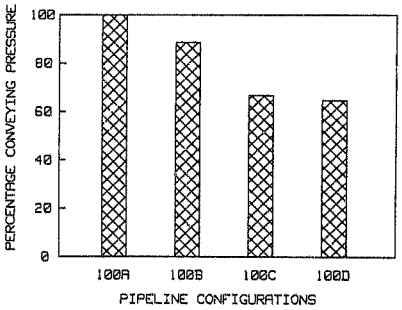


FIGURE 7.3: COMPARISON OF CONVEYING PRESSURES

TABLE 7.1: CALCULATED CONVEYING PRESSURES FOR THE 100 M PIPELINES

		PIPELINE CONFIGURATIONS							
		100A		100B		100C		100D	
$\dot{Q}$ (kg/s)	$\dot{G}$ (t/h)	PA (kPa)	% of PA	PB (kPa)	% of PA	PC (kPa)	% of PA	PD (kPa)	% of PA
0,10	5,0	34,6	100,0	30,5	88,2	25,5	73,8	23,2	67,2
0,10	10,0	48,5	100,0	43,0	88,7	35,9	74,2	33,2	68,6
0,10	15,0	59,1	100,0	52,6	89,0	43,9	74,4	40,9	69,2
0,10	20,0	68,1	100,0	60,7	89,1	50,7	74,5	47,4	69,6
0,20	5,0	39,9	100,0	32,6	81,9	28,0	70,2	27,2	68,1
0,20	10,0	54,5	100,0	45,2	82,9	39,1	71,7	38,1	69,9
0,20	15,0	65,7	100,0	54,8	83,4	47,6	72,4	46,5	70,7
0,20	20,0	75,2	100,0	62,9	83,7	54,7	72,8	53,5	71,2
0,30	5,0	49,8	100,0	38,6	77,4	32,0	64,2	32,3	64,8
0,30	10,0	65,7	100,0	51,2	77,9	43,8	66,6	44,1	67,1
0,30	15,0	77,9	100,0	60,8	78,1	52,8	67,7	53,2	68,3
0,30	20,0	88,2	100,0	69,0	78,2	60,3	68,4	60,8	69,0
0,40	5,0	64,4	100,0	50,3	78,1	38,4	59,5	38,6	59,9
0,40	10,0	82,0	100,0	63,0	76,7	50,7	61,9	51,3	62,5
0,40	15,0	95,6	100,0	72,6	76,0	60,3	63,1	61,1	63,9
0,40	20,0	107,0	100,0	80,0	74,5	68,3	63,8	69,3	64,8
0,50	5,0	83,7	100,0	70,0	83,6	47,8	57,1	46,0	55,0
0,50	10,0	103,5	100,0	82,6	79,8	60,8	58,8	59,7	57,6
0,50	15,0	118,7	100,0	92,3	77,8	70,8	59,7	70,1	59,0
0,50	20,0	131,6	100,0	100,5	76,4	79,3	60,3	78,9	60,0
Average percentages			100,0		81,1		66,7		65,3

The larger diameter pipeline (configurtion 100D) resulted in the lowest conveying pressure. This appears to be due to the dilute phase conveying mode in the pipeline for which it has been shown, in Section 6.3.2, that the pressure drop decreases with increasing pipe diameter. An optimum stepped pipuline as discussed in Section 7.1 was thus not apparent.

Conveying material over a longer distance would result in a larger variation of velocities along the pipeline. Deposition of material at the beginning of the pipeline where the velocity is relatively low would thus have a more significant effect on the performance of the system. The advantage of a stepped pipeline was expected to be more evident over 400 metres than over 100 metres.

The results recorded in the stepped pipeline over 400 metres (configuration 400B) are shown in Table 7.2. The corresponding conveying pressures, as derived from the equations discussed in Section 5.2, for the constant diameter pipeline (configuration 400A) are also shown in Table 7.2. In the last column of Table 7.2 the difference in the conveying pressures is given. No significant difference in the conveying pressures could be established. Figure 7.4 graphically illustrates the similarity of the conveying pressures for the 400A and 400B pipeline configurations. The experimental error was also greater than the differences in the conveying pressures.

Thus a significant gain in the performance of the stepped pipeline over 400 metres was not evident. The effectiveness of a stepped pipeline would also be more evident for a material which is less suitable to be conveyed in a dense phase mode.

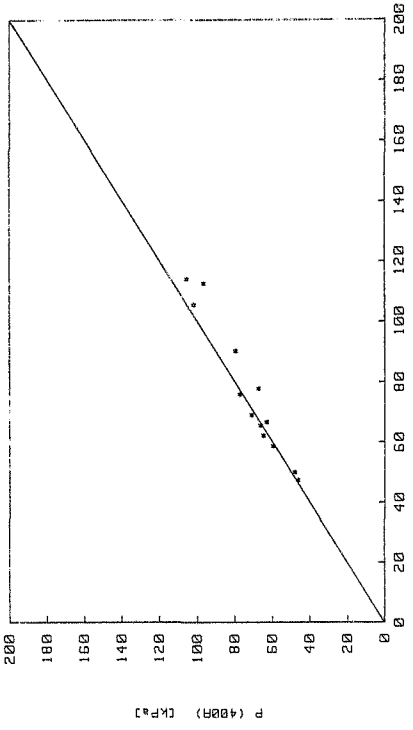


FIGURE 7.4: CONVEYING PRESSURES FOR 400A VERSUS 400B CONFIGURATIONS

TABLE 7.2: CONVEYING PRESSURES IN THE 400 M PIPELINES

$\dot{Q}$ (kg/s)	$\dot{G}$ (t/h)	PIPELINE CONFIGURATION 400A P_A (kPa)	PIPELINE CONFIGURATION 400B P_B (kPa)	DIFFERENCE $P_A - P_B$ (kPa)
0,149	7,7	46,2	47,4	- 1,2
0,149	8,3	47,9	50,0	- 2,1
0,147	16,9	67,2	77,8	-10,6
0,152	14,5	62,9	66,6	- 3,7
0,152	14,5	62,9	66,6	- 3,7
0,309	7,1	59,4	58,6	0,8
0,315	10,5	70,8	69,0	1,8
0,305	8,8	64,6	62,1	2,5
0,307	9,2	65,9	65,5	0,4
0,316	12,8	77,2	75,9	1,3
0,440	8,1	79,3	90,3	-11,0
0,427	17,7	105,5	114,1	- 8,6
0,420	14,6	96,5	112,5	-16,0
0,426	16,2	101,7	105,5	- 3,8
0,426	16,2	101,7	105,5	- 3,8

7.3 CONCLUSIONS

Stepping the pipeline straight after the acceleration zone appears to be the optimum design over distances up to 400 metres within the range of the conveying pressures recorded, although a larger diameter pipeline does not always result in an improved performance.

The results from the 200 metre pipelines show that an optimum pipe diameter exists, as was discussed in Section 5.3.

The optimum pipeline design conveying flyash over 200 metres would consist of a combination of 156 mm diameter and 200 mm diameter pipes, because the 200 mm diameter pipeline over 200 metres had a higher conveying pressure than the 156 mm diameter pipeline.

The effect of stepped pipelines would be more evident at product mass flowrates greater than 20 t/h, which was the minimum product mass flowrate of the experimental test rig.

The effectiveness of a stepped pipeline would be more evident for material which is less suitable, to be conveyed in a dense phase mode, than flyash which conveys well in a dense phase mode.

8. OPTIMUM DESIGN OF TELESCOPIC PIPELINES

8.1 INTRODUCTION

The design procedure discussed in this chapter is based on the power loss across the conveying pipeline (i.e. the power required to convey the material). The optimum pipeline design corresponds to the minimum power loss across the pipeline.

The method developed for the design of the optimum conveying pipeline is based on experimental results. The air power loss across a horizontal section of pipeline, as a function of the air volumetric flowrate and the pipe diameter, has to be determined experimentally.

The experimental results recorded could not be used to illustrate the design procedure, considering that only the conveying pressure was accurately recorded and not the pressure drop across a horizontal section of pipelines which forms the basis of the design method.

The principle of the design method is that the area under the curve, shown in Figure 8.1, represents the power loss across the conveying pipeline.

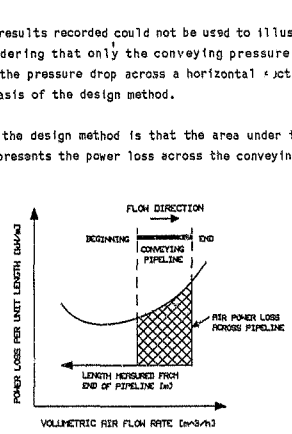


FIGURE 8.1: AIR POWER LOSS ACROSS A PIPELINE

The curve in Figure 8.1 can be derived from experimentally recorded pressure drops across a horizontal section of pipeline for various air mass flowrates. It should be noted that the abscissa representing the pipeline length does not necessarily have a linear scale.

8.2 DESIGN PROCEDURE

The air power loss for different diameter pipelines is shown in Figure 8.2. Once this diagram has been constructed from experimental data, the optimum pipeline design corresponds to a minimum area under the curves for a specific air volumetric flowrate at the end of the conveying line.

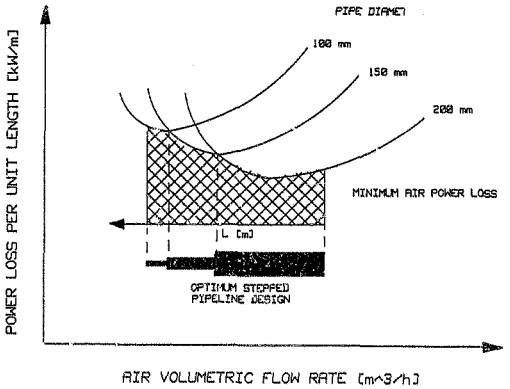


FIGURE 8.2: REQUIRED DIAGRAM TO DETERMINE THE OPTIMUM PIPELINE DESIGN

The optimum volumetric flowrate is determined by selecting a range of volumetric flowrates at the end of the conveying pipeline and calculating the corresponding areas under the curves in Figure 8.2. The optimum volumetric flowrate has a corresponding minimum area under the curves (i.e. a minimum power loss across the pipeline).

8.3 COST CONSIDERATIONS

The cost considerations have been simplified for selecting the optimum pipeline design. Factors such as interest on the initial capital outlay and the cost of the compressor are not considered but can be incorporated. Only the cost of the pipeline is taken into account.

The aim is to minimise the total cost of the system. The total cost, consisting of an initial capital cost plus the running cost which is expressed in Rands per operating hour.

The capital cost is thus simply related to the diameter of the pipes making up the total conveying pipeline.

The air power loss across the system, as discussed in Section 8.2, is equal to the electrical power required by the compressor divided by the efficiency factor of the compressor. Thus the running cost is simply derived from the electrical power cost.

The total cost of the following three pipeline designs is illustrated in Figure 8.3.

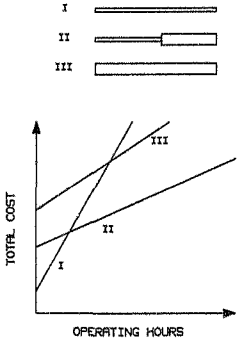


FIGURE 8.3: TOTAL COST OF THE PIPELINES

The capital cost of the pipelines is represented by the total cost in Figure 8.3 at zero operating hours. The slope of the lines in Figure 8.3 is related to the running cost for each pipeline. Thus pipeline I has the lowest capital cost, but the running cost (ie. slope of line I) is high. Line III has the highest capital cost, but the running cost is lower. The optimum pipeline design, line II shown in Figure 8.3, has the lowest running cost and over a number of operating hours has the lowest total cost.

8.4 CONCLUSIONS

It has been generally accepted that the expansion of the air in the conveying pipeline is isothermal (Ref. 2). The air power loss across a horizontal section of pipeline, as shown in Figure 8.4, can thus be derived from Equation 8.1.

$$P_L = p_{at} \cdot V_{fad} \cdot \text{Ln} (p_1 / p_2) \qquad (8.1)$$

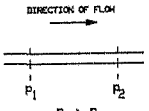


FIGURE 8.4: HORIZONTAL SECTION OF PIPELINE

P_L is the air power loss across the section of pipeline, p_{at} is the atmospheric pressure, V_{fad} is the volumetric free air delivery and p_1 and p_2 are the corresponding pressures in the pipeline.

The maximum available pressure should be considered when designing an optimum pipeline. The pressure drop across a conveying pipeline (i.e. the conveying pressure) can be determined from the area under the curve on the State Diagram, as discussed in Section 6.2.3.

9. NORMALISATION OF RESULTS

9.1 INTRODUCTION

A dimensional analysis of the parameters related to the conveying pressure is discussed in Section 9.2. The functional relationship between the two dimensionless groups which were obtained is also discussed.

Various parameters were plotted against one another in an attempt to normalise all the results onto one line. The normalisation discussed in Section 9.3 also forms the basis of the model developed in Chapter 10 for predicting the performance of the long distance line.

9.2 DIMENSIONAL ANALYSIS

The following list of parameters possibly includes all the factors affecting the pressure drop across a horizontal section of pipeline.

i pipeline length
ii pipe diameter
iii pipe cross-sectional profile (eg. round, square)
iv product mass flowrate
v air mass flowrate
vi air velocity
vii pipe roughness
viii pipe material (eg. steel, plastic)
ix material (eg. powders, rocks, grain)
x material characteristics (eg. particle size, shape, density)
xi conveying air properties (eg. temperature, viscosity, moisture content).
xii conveying medium (eg. air, nitrogen).

All the experimental investigations were assumed to be conducted with similar conveying air properties. The temperature and moisture content varied slightly due to changing atmospheric conditions. The material characteristics were constant considering that only one product (ie. flyash) was used in the experiments.

The air mass flowrate is a function of the velocity and was thus not included in the dimensional analysis.

In the dimensional analysis, the conveying pressure was considered to be a function of the parameters shown in Table 9.1. The dimensional units of the parameters are expressed in terms of:

mass : M
length : L
time : T

TABLE 9.1: DIMENSIONAL UNITS

PARAMETERS	SYMBOL	UNITS
Length	L	L
Diameter	D	L
Product mass flowrate	G	MT^{-1}
Velocity	v	LT^{-1}
Pressure	p	$ML^{-1}T^{-2}$

The following relationship was thus required.

$$p = (L, D, G, v)$$

For dimensional homogeneity

$$[p] = [L^a D^b G^c v^d]$$

ie. $[M L^{-1} T^{-2}] = [L]^a [L]^b [M T^{-1}]^c [L T^{-1}]^d$

$$= [L]^{a+b+d} [M]^c [T]^{-c-d}$$

Equating exponents of [L]:

$$-1 = a + b + d \qquad (9.1)$$

Equating exponents of [M]:

$$1 = c \qquad (9.2)$$

Equating exponents of [T]:

$$-2 = -c - d \qquad (9.3)$$

With four unknowns but only three equations, a complete solution is not possible. However, three exponents can be determined in terms of the *remaining one*. From Equations 9.2 and 9.3, c = 1 and d = 1. Selecting the exponent (a) to remain from Equation 9.1, b = -2 -a.

The values of the exponents were then substituted into the relationship expressing the pressure as a function of the parameters:

$$[p] = [L^a D^{-2-a} G v] = [G v / D^2 (L/D)^a]$$

The group (L/D) is dimensionless, thus any value of (a) is consistent with the requirement of dimensional homogeneity. The second dimensionless group, pD^2/Gv could thus be expressed in terms of a function of $(L/D)^a$.

$$\left(\frac{p D^2}{G v}\right) \propto \left(\frac{L}{D}\right)^a \qquad (9.4)$$

In an attempt to determine the value of (a) , Figure 9.1 shows the graph of

$$p \quad vs \quad v\,G\,/\,D^2\,(\,L/D\,)$$

using the experimentally recorded results from the constant diameter pipeline configurations. The only trend which is evident is that the pressure p seems to increase as the term of the abscissa increases.

An actual value of (a) was not found, but considering the relationship between pressure and length, as discussed in Section 6.2, the value of (a) would be in the order of 0,7. The pressure would then be related to the diameter D as follows:

$$p \propto 1\,/\,(\,D^2\,.\,D^a\,)$$
$$\propto 1\,/\,D^x$$

where x is of the order of 2,7 for (a) equal to 0,7.

9.3 NORMALISATION

In an attempt to normalise the family of curves for constant product mass flowrate on the State Diagram, various parameters were plotted against one another.

At first the conveying pressure versus the ratio of the Froude number and load ratio was plotted, as shown in Figure 9.2. The idea was to keep the parameter on the abscissa dimensionless. The results shows that a set of curves for constant air mass flowrates was generated.

In the graph of pressure divided by air volumetric flowrate versus load ratio, as shown in Figure 9.3, the only trend evident is that the parameter on the ordinate appears to increase as the load ratio increases, although the correlation seems to be poor. In Figure 9.4 the ratio of pressure and product mass flowrate versus air velocity was plotted. The parameter on the ordinate represented the pressure drop per unit product mass flowrate. The points tended to fall on one line, although it was still possible to

distinguish between the lines of constant air mass flowrate.

After reconsidering the State Diagram, it was concluded that the term on the ordinate (i.e. pressure) should be modified in order to normalise the results. The velocity was plotted on the ordinate with the ratio of pressure and load ratio on the abscissa as shown in Figure 9.5. From the graph it is evident that the pressure per unit load ratio is a function of the air velocity.

Plotting the pressure divided by load ratio on the ordinate, the effect of pipeline length was investigated from the results of the 100 and 200 metre pipelines with a constant diameter of 105 mm (i.e. configurations 100A and 200A), as shown in Figure 9.6. The pressure per unit load ratio appeared to be proportional to the pipeline length. The effect of pipe diameter is shown in Figure 9.7. For increasing pipe diameter the pressure per unit load ratio decreases.

Incorporating the effect of length and diameter, the following relationship was plotted in Figure 9.8.

$$p D^2 / (L \mu) \quad vs \quad v$$

The gradient of the line has the dimensional units of dynamic viscosity (i.e. Pa.s). The following equation could thus be used to represent the line

$$p D^2 / (L \mu) = A v^2 \qquad (9.5)$$

where A is the proportionality constant. Comparing Equation 9.5 to Darcy's Law for flow through a porous medium, as given by Massey (Ref.20),

$$p / L = (32 \mu u l_e) / (d^2 e l) \qquad (9.6)$$

the similarity is evident. In Equation 9.6, μ and e are the viscosity and voidage factors respectively.

From Equation 9.5 the pressure is directly proportional to the line length which contradicts the findings as discussed in Section 6.2. In addition, the product mass flowrate tends to zero, the pressure tends to zero. T[illegible] the air alone pressure drop is not incorporated in Equation 9.5.

The term on the ordinate of Figure 9.8 was changed to ($p / [1 + \mu]$).

Thus, as the product mass flowrate reduced to zero, the pressure p would represent the air alone pressure loss. Furthermore instead of plotting the velocity on the abscissa as in Figure 9.8, the Froude number squared (v^2/gD) was plotted. Figure 9.9 illustrates the graph of

$$p / (1 + \mu) \quad \text{vs} \quad v^2 / (g D)$$

A linear relationship is apparent and the slope of the line would be a function of the line length and pipe diameter. This relationship formed the basis of the model developed to predict the performance of the long distance line, discussed in Chapter 10.

9.4 CONCLUSIONS

From the dimensional analysis discussed in Section 9.2, two dimensionless groups were found:

1) $[p D^2 / (\dot{G}.v)]$
2) L / D

The functional relationship between the two groups was not obtained. More experimental data of the pressure drop is required for different diameter pipelines across a horizontal section of pipeline. The pipe roughness and air viscosity which not considered in the dimensional analysis, should be further investigated.

The experimental results were normalised in terms of:

$$p / (1 + \mu) \quad vs \quad v^2 / (g D)$$

These normalised results form the basis of the model discussed in Chapter 10.

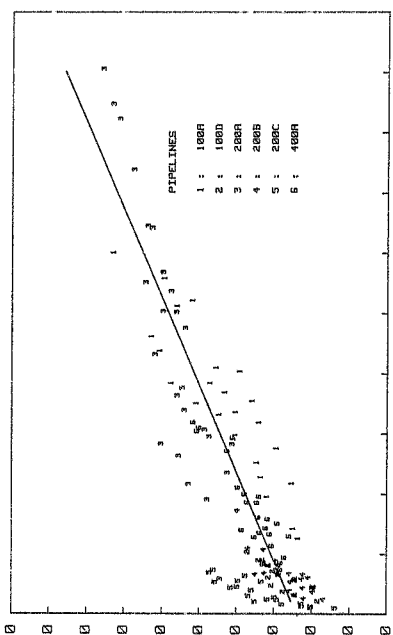


FIGURE 9.1: DIMENSIONAL ANALYSIS RESULTS

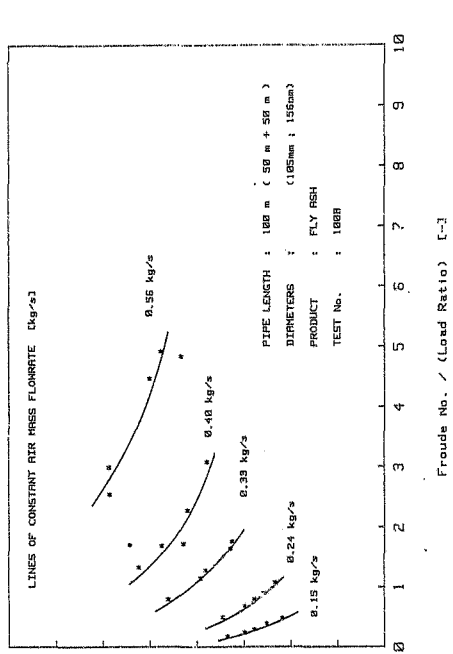


FIGURE 9.2: CONVEYING PRESSURE VERSUS (FROUDE NUMBER/LOAD RATIO)

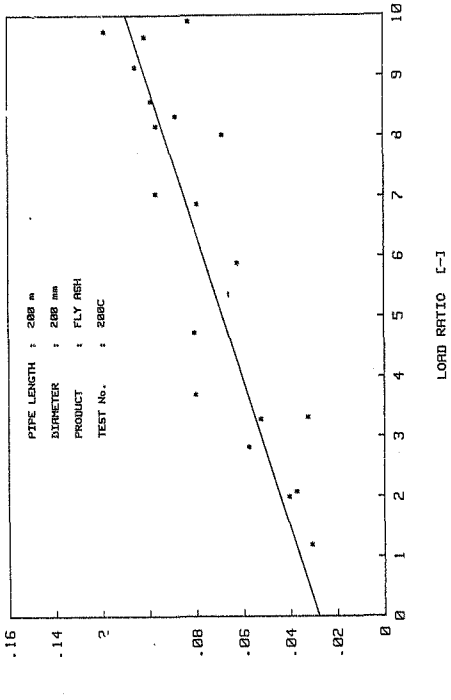


FIGURE 9.3: (CONVEYING PRESSURE/AIR VOLUMETRIC FLOWRATE) VERSUS LOAD RATIO

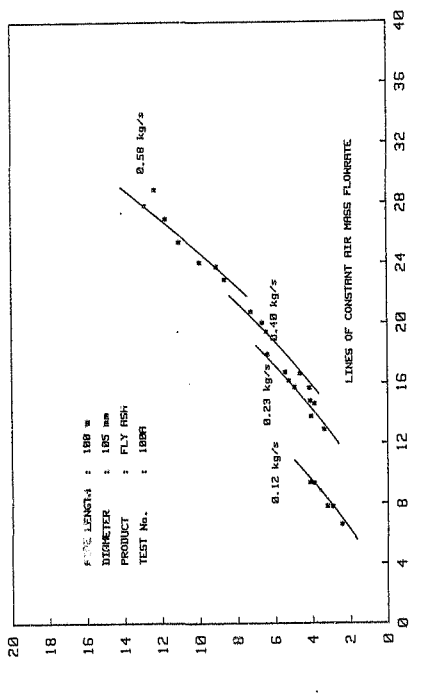


FIGURE 9.4: (CONVEYING PRESSURE/PRODUCT MASS FLOWRATE) VERSUS AIR VELOCITY

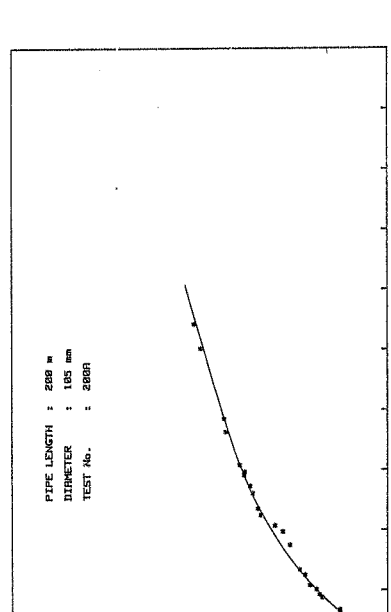


FIGURE 9.5: AIR VELOCITY VERSUS (CONVEYING PRESSURE/LOAD RATIO).

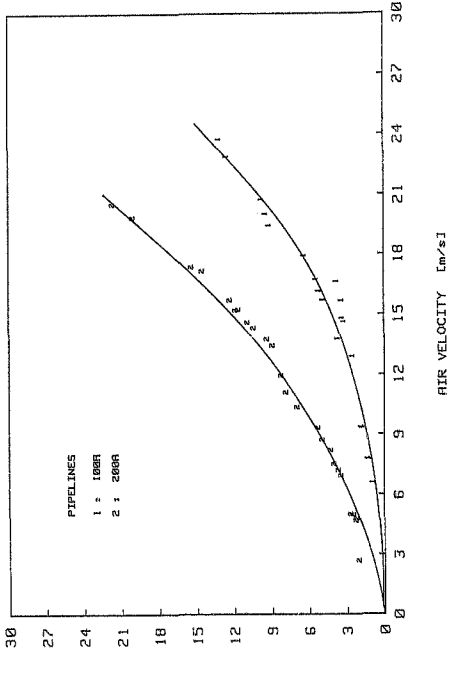


FIGURE 9.6: (PRESSURE/LOAD RATIO) VERSUS AIR VELOCITY

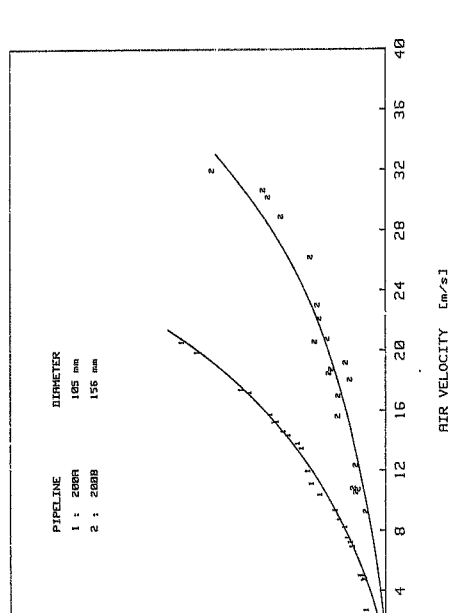


FIGURE 9.7: (PRESSURE/LOAD RATIO) VERSUS AIR VELOCITY

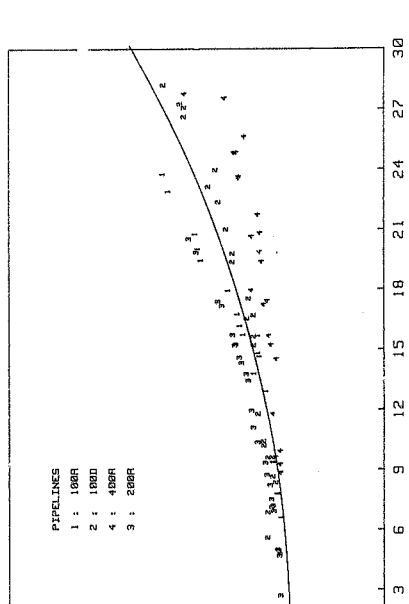


FIGURE 9.8: NORMALISATION OF THE RESULTS

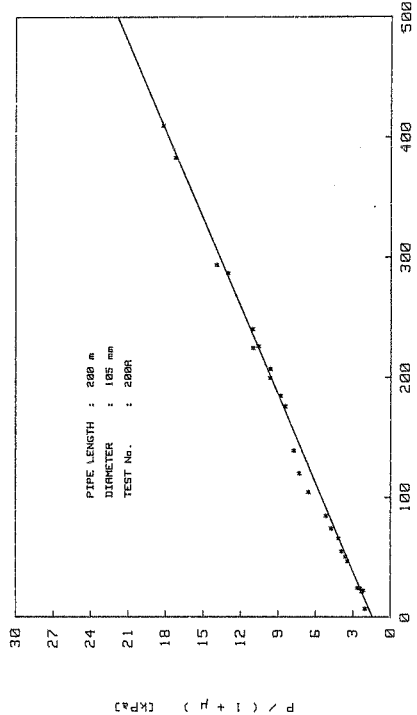


FIGURE 9.9: BASIC RELATIONSHIP FOR THE PERFORMANCE PREDICTING MODEL

10. PERFORMANCE PREDICTING MODEL

10.1 INTRODUCTION

One of the objectives of the project was to develop an empirical model to predict the performance of the long distance line. The results from the constant diameter pipeline configurations were used to establish the effect of pipe diameter and line length on the conveying pressure.

The calculation method, used in the model to determine the conveying pressure, is discussed in Section 10.2. The overall structure of the model, illustrating the required inputs and corresponding output, is shown in Figure 10.1.

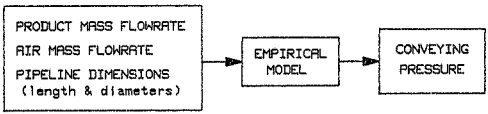


FIGURE 10.1: EMPIRICAL MODEL

In Section 10.4, the experimentally recorded conveying pressures for the long distance line are compared to the corresponding conveying pressures as derived from the empirical model.

10.2 CALCULATION METHOD

The graph illustrated in Figure 10.2 forms the basis of the model. The relationship was derived from the normalisation of the results for a particular pipeline configuration, as discussed in Section 9.3.

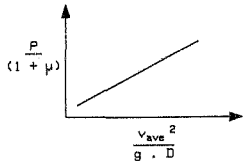


FIGURE 10.2: BASIC RELATIONSHIP FOR EMPIRICAL MODEL

The following equation was derived from the graph:

$$p / (1 + \mu) = k_1 + [\alpha] \; v_{ave}^2 / (gD) \qquad (10.1)$$

where k_1 is the intercept on the ordinate and $[\alpha]$ represents the gradient of the line. The effect of conveying distance on the gradient $[\alpha]$ of the line is shown in Figure 10.3.

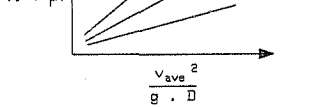


FIGURE 10.3: ILLUSTRATING THE EFFECT OF LINE LENGTH

Thus [α] increases as the pipeline length increases. The experimental results indicated that the conveying pressure was approximately proportional to the square root of the effective line length. Figure 10.4 shows the relationship between [α] and the effective pipeline length for a constant pipe diameter.

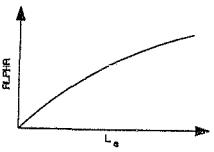


FIGURE 10.4: ALPHA VERSUS EFFECTIVE LINE LENGTH (L_e)

The relationship is expressed by Equation 10.2.

$$\alpha = [\beta] \; L_e^{0,5} \qquad (10.2)$$

where [β] is the proportionality constant.

The effect of pipe diameter on the relationship shown in Figure 10.4 is shown in Figure 10.5.

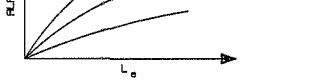


FIGURE 10.5: PIPE DIAMETER EFFECTS

Equation 10.3 expresses $[\beta]$ as a function of pipe diameter. Figure 10.6 shows the graph of $[\beta]$ as a function of pipe diameter.

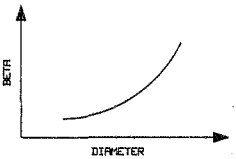


FIGURE 10.6: BETA AS A FUNCTION OF PIPE DIAMETER

$$[\beta] = K_2 . D^6 \qquad (10.3)$$

Substituting $[\beta]$ in Equation 10.2 and substituting $[\alpha]$ in Equation 10.1, the following expression was derived.

$$p / (1 + \mu) = k_1 + k_2 . D^6 . L_e^{0,5} . v_{ave}^2 / (gD) \qquad (10.4)$$

No particular trend was found for k_1 with respect to pipe diameter or line length. The average value of k_1 was used. The average velocity (v_{ave}) was derived from the velocity at the beginning (v_1) and end (v_o) of the line.

Where

$$v_1 = \dot{Q} / (\rho_1 . A) = \dot{Q} . R . T . 4 / [(p_{at} + p_1) . D^2] \qquad (10.5)$$

and

$$v_o = \dot{Q} / (\rho_o A) = \dot{Q} . R . T . 4 / (p_{at} \pi D^2) \qquad (10.6)$$

Thus

$$v_{ave} = \frac{\dot{Q} R T 4}{\pi D^2} \left[\frac{1}{(p_{at} + p)} + \frac{1}{p_{at}} \right] \qquad (10.7)$$

p_{at} is the pressure at the end of the line and p is the conveying pressure, ie. pressure at the beginning of the line.

Substituting the average velocity from Equation 10.7 into Equation 10.4, an implicit equation in terms of conveying pressure (p) was thus derived.

10.3 MODEL EQUATIONS

In this section the equations, derived from the experimental results, are summarised.

The graphs of:

$$\frac{p}{(1 + \mu)} \quad \text{vs} \quad \frac{v^2}{gD}$$

for all the constant diameter pipeline configurations, are shown in Figures 10.7 to 10.12.

The gradient [α] of the lines in Figures 10.7 to 10.12, plotted as a function of pipeline length, is shown in Figures 10.13 to 10.15.

In Figure 10.16 the proportionality constant [β], for the curves from Figures 10.13 to 10.15, is plotted as a function of pipe diameter.

The expression for [β] is given by Equation 10.8.

$$[\beta] = 0{,}5317.E\text{-}3 + 154{,}215 \cdot (D^6) \qquad (10.8)$$

where D is the pipe diameter.

Thus $[\alpha]$ was given by:

$$[\alpha] = [\beta] \cdot L_e^{0,5} \qquad (10.9)$$

where L_e is the effective pipeline length.

The conveying pressure (p) as a function of product mass flowrate, air mass flowrate, pipe diameter and length is given by Equation 10.10.

$$p = [\ 0,813 + (0,5317E\text{-}3 + 154,215.D^6).L_e^{0,5}.v_{ave}^2/(gD)\ ] \cdot [\ 1 + \mu\ ] \qquad (10.10)$$

The average velocity (v_{ave}) as derived in Equation 10.7 is given by

$$v_{ave} = \frac{\dot{Q} R T 4}{D^2} \cdot \left[\frac{1}{(p_{at} + p)} + \frac{1}{p_{at}} \right] \cdot \frac{1}{2} \qquad (10.11)$$

10.4 LONG DISTANCE LINE CONVEYING PRESSURES

The computer programme listed in Appendix D6 was used to calculate the conveying pressure for the long distance line. In Figure 10.17 the calculated conveying pressures are plotted against the experimentally recorded pressures.

The percentage error in P(mod) was defined as follows:

$$\%\ \text{error} = \frac{|P(\text{mod}) - P(\text{exp})|}{P(\text{exp})} \cdot 100$$

where P(exp) is the experimentally recorded conveying pressure. The average percentage error for all the results was 20,4%.

The corresponding correlation coefficient was 0,876. This gives an indication of how well the results lie on the line:

$$P(\text{mod}) = P(\text{exp})$$

A correlation coefficient of 1,000 would thus indicate that all the results lie on the line P(mod) = P(exp). At low product mass flowrates (eg. 2 t/h), corresponding to conveying pressures of the order of 100 kPa, the error is probably due to the fact that the load ratio tends to zero and the model requires further modification to improve the results for calculating the pressure drop due to air alone.

The conveying pressures calculated from the model, P(mod), are generally higher than the experimentally recorded conveying pressures, as illustrated in Figure 10.17.

The higher conveying pressures derived from the model are probably due to the acceleration and feeder losses which were included in the pressure drop across the pipelines from which the model was developed.

10.5 CONCLUSIONS

An empirical model has been developed which can be used to calculate the required air pressure for conveying flyash through a long distance pipeline. The following parameters have been incorporated in the model:

1) Pipeline length.
2) Pipe diameter.
3) Product mass flowrate.
4) Air mass flowrate.

Experimental results show that the average percentage error in the conveying pressures as derived from the model is of the order of 20,4%.

When developing the emperical model the parameter on the ordinate was changed from p / μ to $p / (1 + \mu)$ to include the pressure drop for air alone. A further improvement to the model would be to plot $p / (\phi + \gamma)$ where ϕ represents a friction factor for air alone and γ is a function of the load ratio .

100A

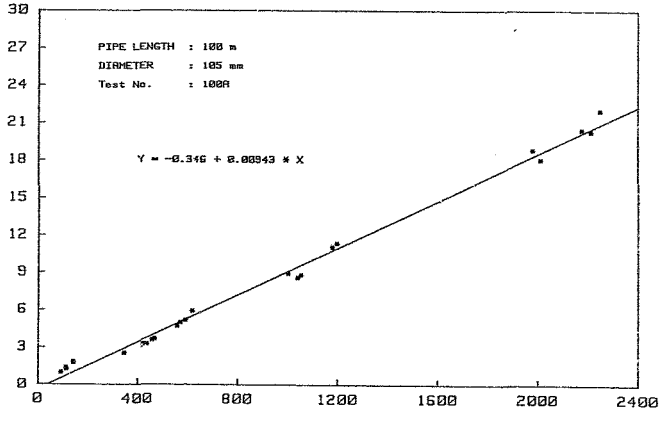


FIGURE 10.7: (p / 1+μ) VERSUS (v_{ave}^2 / g D) [100A]

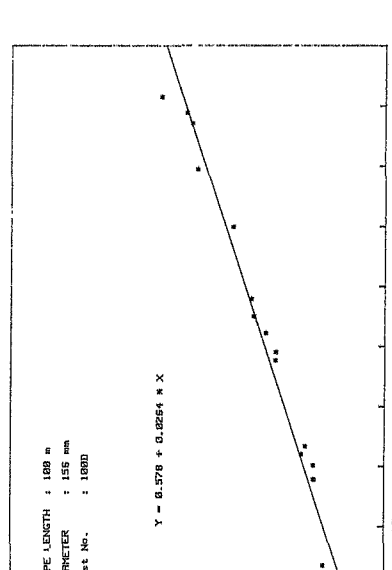


FIGURE 10.8: $(\rho / 1 + \mu)$ VERSUS $(v_{ave}^2 / g D)$ [100D]

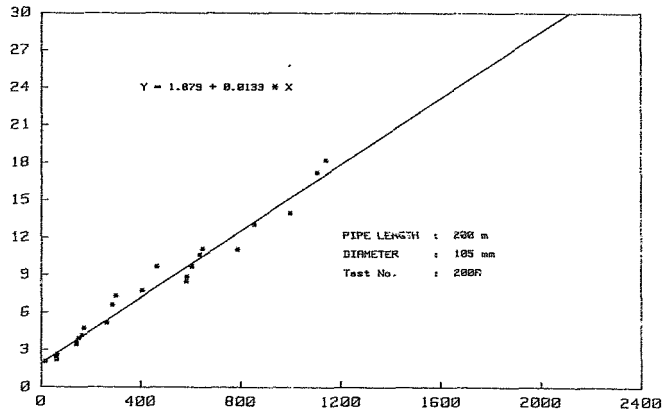


FIGURE 10.9: $(p / 1 + \mu)$ VERSUS $(v_{ave}^2 / g D)$ [200A]

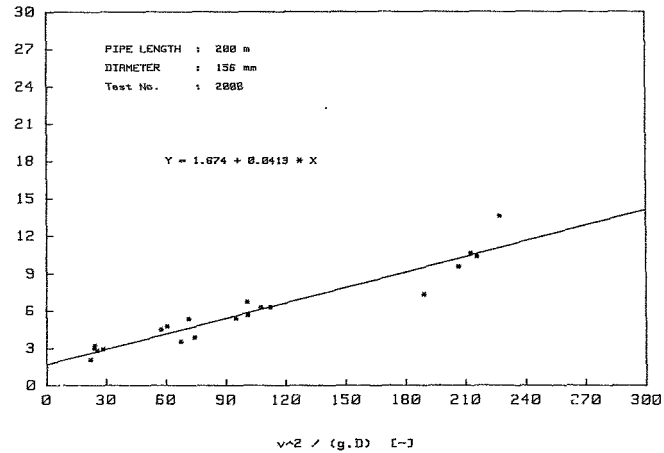


FIGURE 10.10: $(\rho / 1 + \mu)$ VERSUS $(v_{ave}^2 / g D)$ [200B]

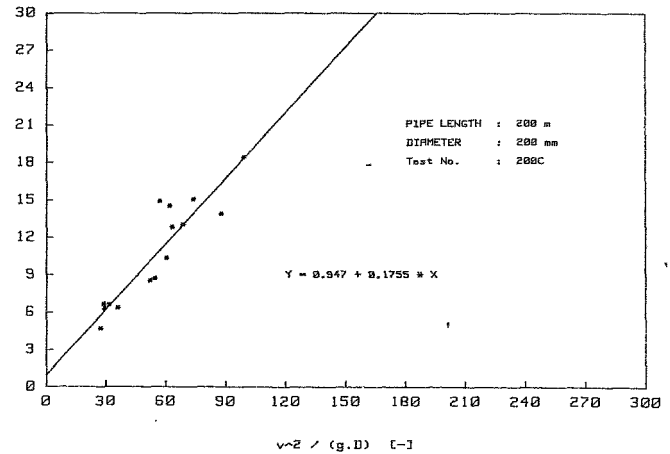


FIGURE 10.11: (p / 1 + μ) VERSUS (v_{ave}^2 / g D) [200C]

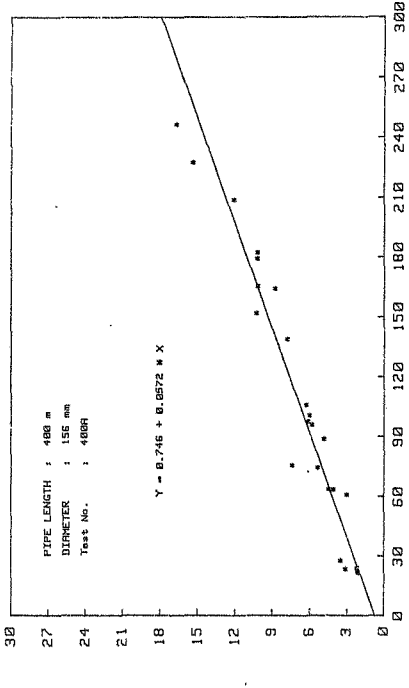


FIGURE 10.12: $(p / 1 + \mu)$ VERSUS $(v_{ave}^2 / g D)$ [400A]

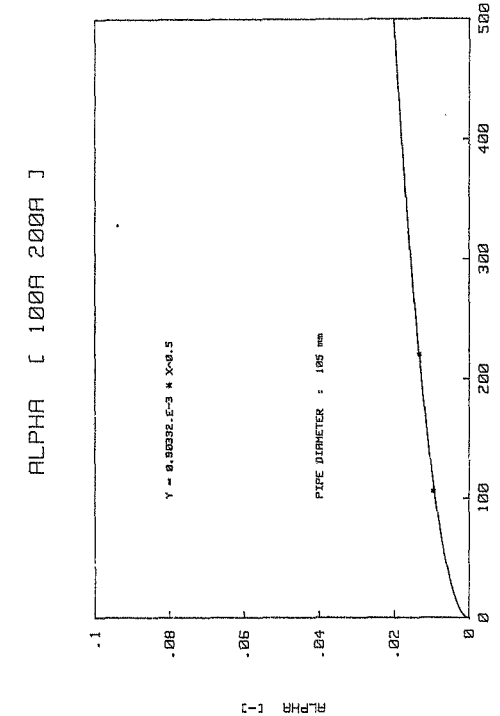


FIGURE 10.13: ALPHA VERSUS EFFECTIVE LINE LENGTH (105 mm DIAMETER PIPELINE)

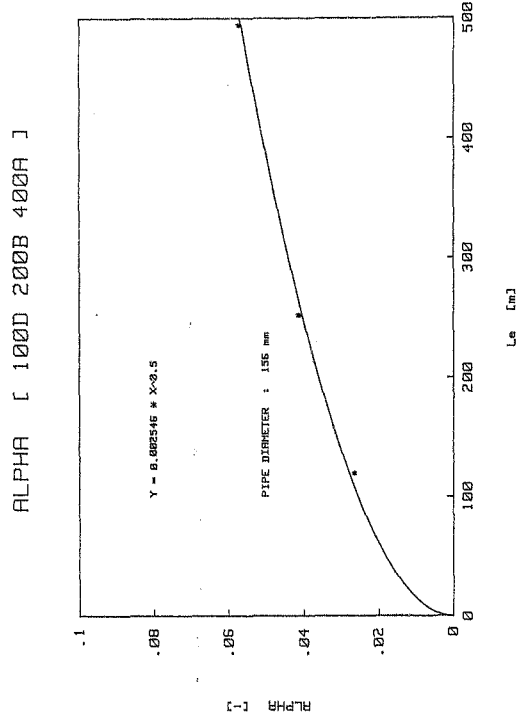


FIGURE 10.14: ALPHA VERSUS EFFECTIVE LINE LENGTH (156 mm DIAMETER PIPELINE)

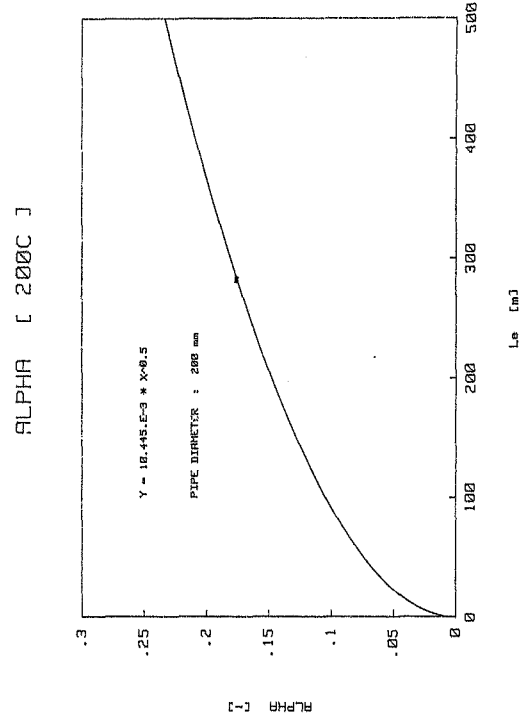


FIGURE 10.15: ALPHA VERSUS EFFECTIVE LINE LENGTH (200 mm DIAMETER PIPELINE)

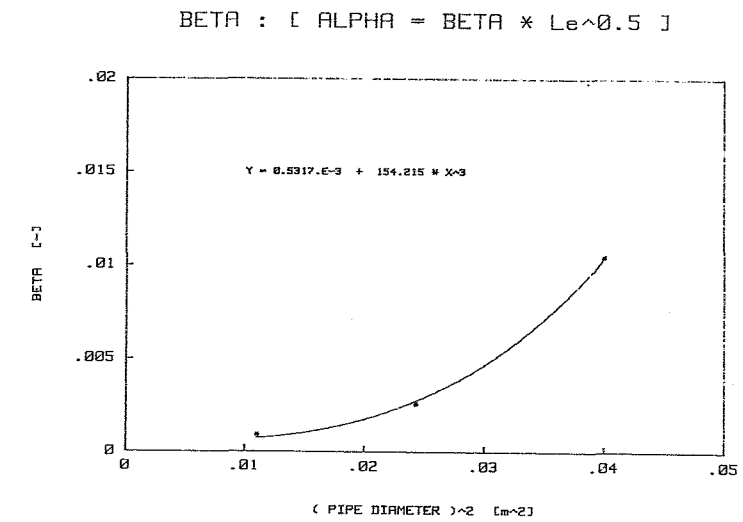


FIGURE 10.16: BETA VERSUS PIPE DIAMETER

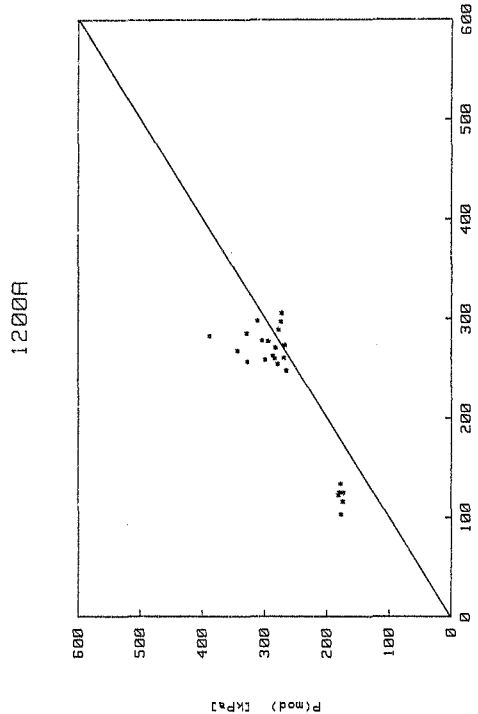


FIGURE 10.17: CALCULATED CONVEYING PRESSURE (Pmod) VERSUS EXPERIMENTAL CONVEYING PRESSURE (Pexp)

11. GENERAL OBSERVATIONS

11.1 INTRODUCTION

In this chapter various secondary observations which were made during the course of the investigations are discussed, although they are not directly related to the objectives of the project as outlined in Section 1.2.

11.2 ROTARY VALVE PERFORMANCE

From the dimensions of the rotary valve and for a maximum speed of 31 rpm a feed rate of 24 t/h was calculated, as shown in Appendix J. The maximum product mass flowrate recorded was in the order of 35 t/h. This was probably due to the pressure in the blow vessels being much larger than the pressure in the conveying pipeline. The material would flow through the leakage spaces of the rotary valve and the bulk density of the material in the rotary valve could have been in the order of 1200 kg/m^3 due to the material being compacted by the pressure in the blow vessels. The bulk density of flyash under normal conditions was 930 kg/m^3 as discussed in Section 3.10.2.

The pressure in the blow vessel could not be reduced to less than 80 kPa because the gauges for setting the pressure had a range of 0-800 kPa, and the slow response of the gauge at pressure below 100 kPa caused a delay in the operating cycle.

As the conveying pressure increased, with increasing air mass flowrate, the maximum product mass flowrates decreased. This was as expected because the differential pressure drop across the rotary valves decreased as the conveying pressure increased.

It was not of concern that the rotary valves operated above design capacity, because the product mass flowrate was recorded accurately with the load cells situated under the receiving hopper at the end of the conveying line.

11.3 FLOW PATTERNS

The flow patterns of the product were observed through the sight glass for each test. The formation and behaviour of the bed when conveying in a dense phase was of interest. A diagram was developed, with product mass flowrate and air mass flowrate on the ordinate and abscissa respectively, as shown in Figure 11.1.

The observations indicated that a moving bed first appeared in the pipeline as the product mass flowrate increased. A further increase in product mass flowrate at a constant air mass flowrate resulted in a fixed bed, with plugs of material moving through the pipe. The rate of the plugs passing through the sight glass was proportional to the product mass flowrate. Reducing the air mass flowrate when conveying in a dilute phase, keeping the product mass flowrate constant, resulted in similar bed formation as outlined above. First, a moving bed appeared and then at lower air mass flowrates, plugs were formed. As the air mass flowrate decreased, the length of the plug appeared to increase.

Although the pipeline never blocked when running the tests, it is reasonable to assume that there exists a minimum air mass flowrate for the product to be conveyed. The minimum air mass flowrate required would also increase for higher product mass flowrates, as shown in Figure 11.1.

A higher air mass flowrate was required to convey material in a dilute phase in the larger diameter pipelines. The saltation point is probably related to the air velocity or a specific Froude number for the material. This corresponds to the findings by Rizk (Ref.27) as discussed in Section 2.2.2.

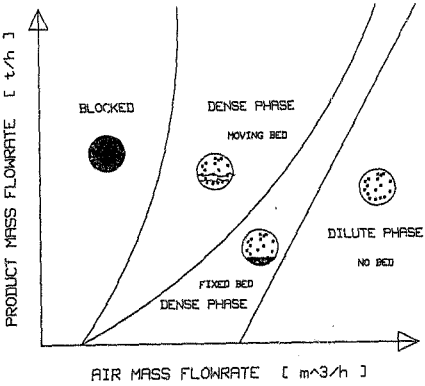


FIGURE 11.1: FLOW PATTERNS AS A FUNCTION OF PRODUCT AND AIR MASS FLOWRATE

11.4 STEPPED SECTION

At present most long distance pneumatic conveying systems have telescopic pipes in terms of a gentle increase in pipe diameter as the line length increases. It was believed that the efficiency of the systems could be increased by having an abrupt increase in pipe diameter. The kinetic energy of the material flowing in the pipe could be transferred to pressure or 'potential' energy in the air.

An attempt at recording the pressure profile across the stepped section was unsuccessful. A typical set of results for air alone is shown in Figure 11.2. The negative values are due to the extraction fan on the filter unit creating a slight vacuum in the conveying line at low air mass flowrates. When product was conveyed in the pipeline, large fluctuations in the pressures along the pipeline resulted in inconsistent data being recorded.

An alternative method to investigate the stepped section would be to compare the performance of a telescopic pipeline with abrupt enlargements and gentle increases in pipe diameter.

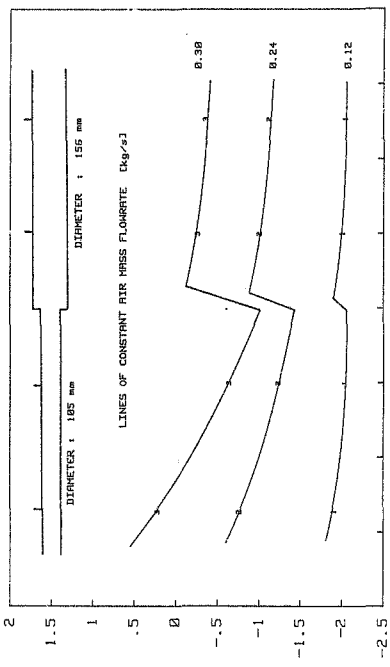


FIGURE 11.2: PRESSURE ACROSS TRANSITION PIECE

12. CONCLUSIONS AND RECOMMENDATIONS

12.1 CONCLUSIONS

The following conclusions were made from the investigations discussed in this report.

1) Reliable data was recorded for the conveying pressure as a function of the product and air mass flowrate in various pipeline configurations. The error in the repeatability of the results was less than 10,5%. The pressures along a section of the conveying pipeline were recorded with an unacceptable repeatability. In order to measure the pressure along the conveying line, a purging system is required at the pressure tapping points to prevent them from blocking. Sophisticated pressure transducers, which will damp the pressure fluctuations in the pipeline, are also required.

2) The principle developed to determine the effect of the pipeline length from the area under the curve on the State Diagram is illustrated in Figure 12.1, although further experimental investigations are required to prove that this principle is correct.

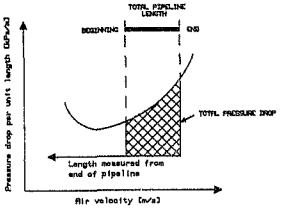


FIGURE 12.1: STATE DIAGRAM SHOWING THE EFFECT OF LINE LENGTH

From the results for different pipe diameters, it was shown that there exists an optimum diameter to convey material at a specific load ratio. A larger diameter does not always result in an improvement in the performance of the system (i.e. a decrease in power requirements).

3) Stepping a pipeline from 105 mm to 156 mm did not significantly improve the performance of the system for conveying distances up to 400 metres. The 200 mm diameter pipeline had a higher conveying pressure than the 156 mm diameter pipeline over a distance of 200 metres at low air mass flowrates. It was thus concluded that the optimum pipeline design may consist of 156 mm and 200 mm diameter pipes for conveying flyash over a distance of 200 m with a low air mass flowrate, of the order of 0,1 kg/s.

4) A design method has been developed to design the optimum conveying pipeline. It is based on the diagram shown in Figure 12.2. Further experimental work is required to verify this design principle.

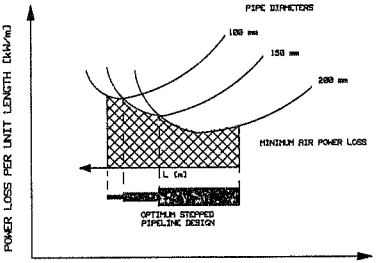


FIGURE 12.2: POWER LOSS

The curves shown in Figure 12.2 are derived from experimental results which determine the air power loss across a horizontal section of pipeline as a function of the air volumetric flowrates. The area under the curves represents the power loss across a pipeline. The optimum pipeline design corresponds to a minimum area under the curves.

5) Material was successfully conveyed through the long distance pipeline (i.e. 1358 m line). From the mass versus time trace of the receiving hopper, it appears that the material was conveyed in a dense phase mode.

6) An empirical model was developed to predict the performance of the long distance line. The average percentage error of the model, with respect to the experimentally recorded conveying pressure, was 20,4%.

12.2 RECOMMENDATIONS FOR FUTURE RESEARCH

The empirical model developed to predict the performance of the long distance line should be used to correlate the performance of existing systems conveying flyash over long distances.

The recommendations for future research work, to establish the theory for the design of the conveying pipeline, are discussed under the following headings: Pipe Length, Pipe Diameter, Standardisation and Stepped Pipelines.

12.2.1 Pipe Length

Once it has been established from future experimental investigations, that the effect of line length can be derived from the State Diagram by considering the area under the curve, no further investigations would be required to determine the effect of line length by conveying over various distances. A State Diagram can simply be derived from the pressure drop across a horizontal section of pipeline as a function of the air velocity.

12.2.2 Pipe Diameter

Further research work is required to establish the effect of the conveying pipe diameter. It has been shown that there exists an optimum diameter to convey material. Now it is required to determine the effect of product mass flowrate and air mass flowrate on the optimum diameter.

12.2.3 Standardisation

The ultimate goal in the research of pneumatic conveying is to develop an equation to predict the pressure drop across a pipeline layout which takes all the influencing factors into account. The following list possibly includes all the factors which influence the pressure drop across a horizontal section of pipeline:

1) pipeline length
2) pipe diameter
3) pipe cross-sectional profile (eg. round, square).
4) product mass flowrate
5) air mass flowrate
6) pipe roughness
7) pipe material (eg. steel, plastic).
8) material (eg. powders, rocks, grain).
9) Material characteristics (eg. particle size, shape, density).
10) Conveying air properties (eg. temperature, viscosity, moisture content).
11) Conveying medium (eg. air, nitrogen).

It is unlikely that the equation, taking all the above mentioned factors into account, will be developed in the near future. For many years to come, a product will always have to undergo a series of tests in order to design the optimum conveying system.

It is essential to establish a universal standard test procedure so that the results for different products in various research institutions throughout the world can form part of a data base. The 'Pneumatic Conveying Equation' can then eventually be derived from this data base.

A recommended standard test rig is illustrated in Figure 12.3.

The following specifications are recommended in the design of the standard test rig.

1) A continuous variable product feeding device which will control the product mass flowrate. The range of the feedrate should be in the order of 0 - 50 m^3/h. A simple slide valve is recommended as a feeding device with a scoop to assist the flow of material into the pipeline, as shown in Figure 12.3.

2) A storage hopper with a capacity of 10 m^3. At the maximum product mass flowrate of 50 m^3/h, 12 minutes will then be available to record the pressure drop along the pipeline.

3) 30 metres of horizontal piping after the feeding point such that the pressure drop recorded along the pipeline is not affected by the acceleration losses. The conveying pipe diameter should range from 50 mm to 300 mm.

4) Load cells to be located under the receiving hopper to determine the product mass flowrate.

5) A data acquisition system connected to a standard computer (eg. Hewlett Packard computer) to record and analyse the following parameters:

   i air mass flowrate
   ii product mass flowrate
   iii pressures

6) A variable air mass flowrate supply is required with a range of 0 - 5000 m^3/h.

Universal consensus is required on a detailed design of the standard test rig and of the experimental procedure.

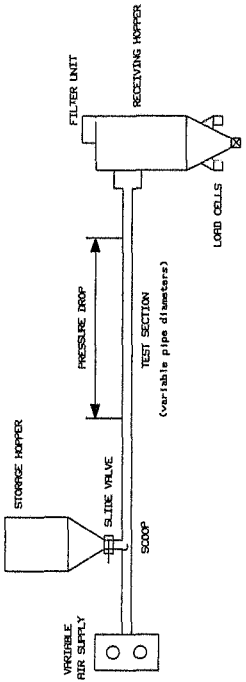


FIGURE 12.3: RECOMMENDED STANDARD TEST RIG

12.2.4 Stepped Pipelines

The results recorded from the standard test rig as discussed in Section 12.2.3 will enable the construction of the diagram as shown in Figure 12.2. The area under the curves can then be calculated for a range of air volumetric flowrates at the end of the pipeline, to determine the optimum air mass flowrate and the corresponding optimum pipeline design.

The cost model of the pipelines, as discussed in Chapter 8, needs to be developed to include factors such as interest on initial capital outlay and the cost of the compressor.

APPENDIX A

RESULTS

A.1 INTRODUCTION

A.2 TEST RUN PRINTOUT

A.3 TABLES OF RESULTS

A.3.1 RESULTS USED FOR ANALYSES
A.3.2 RESULTS TO SHOW REPEATABILITY

A.4 AIR ALONE PRESSURE DROP

A.5 PRESSURE VERSUS PRODUCT MASS FLOWRATE GRAPHS

A.1 INTRODUCTION

A typical computer printout of the data recorded during a test run for a specific product and air mass flowrate, is shown in Appendix A.2. All the data was stored on micro flexible discs and processed at a later stage. The processed data for all the test runs are tabulated in Appendix A.3. The results in Section A.3.2 were used to show the repeatability of the experimental results given in Section A.3.1.

The air alone pressure drops across the pipeline configurations, as a function of air mass flowrate through the pipelines, are graphically shown in Appendix A.4.

The graphs used to develop the equations discussed in Section 5.2 are shown in Appendix A.5. For each of the pipeline configurations, the conveying pressure is plotted against product mass flowrate. The equations for the lines of constant air mass flowrates are tabulated on the graphs. The relationship between the constants in the equations and the air mass flowrate is also graphically represented.

A.2 TEST RUN PRINTOUTS

TEST NUMBER : 20003
DATE : 17/2/87
BAROMETRIC PRESS. : 86
AIR TEMPERATURE : 25
COMPRESSORS USED : B+H+A

PRESSURES ALONG PIPELINE (kPa)							TEMP	AIR	LOAD	TIME	MASS
P 1	P 2	P 7	P 5	P 3	P 4	P 6	(C)	(m^3/hr)	(kg)	(sec)	(t/hr)
73.96	73.96	73.96	73.96	73.96	73.96	73.96	39.8	911.80	-10.0	6.6	
73.84	73.84	73.84	73.84	73.84	73.84	73.84	39.7	897.34	5.4	20.6	3.47
76.25	76.25	76.25	76.25	76.25	76.25	76.25	39.8	888.34	-11.0	38.4	
63.43	63.43	63.43	63.43	63.43	63.43	63.43	39.8	1016.66	32.1	54.3	9.79
78.28	78.28	78.28	78.28	78.28	78.28	78.28	39.9	852.69	166.9	70.1	30.57
87.86	87.86	87.86	87.86	87.86	87.86	87.86	40.0	835.52	121.6	86.1	
86.06	86.06	86.06	86.06	86.06	86.06	86.06	40.1	807.09	228.2	101.9	24.22
88.21	88.21	88.21	88.21	88.21	88.21	88.21	40.2	817.26	274.6	117.7	10.55
90.47	90.47	90.47	90.47	90.47	90.47	90.47	40.2	810.89	260.7	135.6	
92.52	92.52	92.52	92.52	92.52	92.52	92.52	40.3	792.71	328.2	149.4	15.54
79.57	79.57	79.57	79.57	79.57	79.57	79.57	40.4	915.51	448.4	165.3	27.21
82. 2	82.82	82.82	82.82	82.82	82.82	82.82	40.4	859.19	480.4	181.2	7.26
86.55	86.55	86.55	86.55	86.55	86.55	86.55	40.6	821.77	482.1	197.0	.57
85.70	85.70	85.70	85.70	85.70	85.70	85.70	40.6	843.75	546.2	212.9	14.58
85.55	85.55	85.55	85.55	85.55	85.55	85.55	40.7	827.46	476.6	228.7	6.90
78.40	78.40	78.40	78.40	78.40	78.40	78.40	40.8	892.11	306.1	244.6	
71.16	71.16	71.16	71.16	71.16	71.16	71.16	40.9	924.88	14.4	260.5	
69.16	69.16	69.16	69.16	69.16	69.16	69.16	40.9	930.83	-3.7	276.4	
74.84	74.84	74.84	74.84	74.84	74.84	74.84	41.0	880.09	42.5	292.3	10.37
78.10	78.10	78.10	78.10	78.10	78.10	78.10	41.2	876.46	20.2	308.2	
80.18	80.18	80.18	80.18	80.18	80.18	80.18	41.3	871.85	39.6	324.1	4.41
85.32	85.32	85.32	85.32	85.32	85.32	85.32	41.4	826.74	90.6	339.9	2.51
85.21	85.21	85.21	85.21	85.21	85.21	85.21	41.5	850.86	165.9	355.7	24.30
86.15	86.15	86.15	86.15	86.15	86.15	86.15	41.6	844.78	250.0	371.5	14.56
85.05	85.05	85.05	85.05	85.05	85.05	85.05	41.6	845.48	291.7	387.4	14.03
65.25	65.25	65.25	65.25	65.25	65.25	65.25	41.7	1040.11	251.3	403.2	13.43
49.75	49.75	49.75	49.75	49.75	49.75	49.75	41.7	1111.73	359.0	419.1	1.73
60.45	60.45	60.45	60.45	60.45	60.45	60.45	41.8	924.71	472.1	435.0	25.89
60.59	60.59	60.59	60.59	60.59	60.59	60.59	41.9	963.19	468.9	451.2	
66.00	66.00	66.00	66.00	66.00	66.00	66.00	42.0	935.07	411.9	467.1	
67. 4	67.94	67.94	67.94	67.94	67.94	67.94	42.1	931.94	391.7	482.9	
67.93	67.93	67.93	67.93	67.93	67.93	67.93	42.2	937.22	402.2	498.8	2.38
70.74	70.74	70.74	70.74	70.74	70.74	70.74	42.3	908.44	387.7	514.7	
72.54	72.54	72.54	72.54	72.54	72.54	72.54	42.4	910.67	464.8	530.6	17.40
66.27	66.27	66.27	66.27	66.27	66.27	66.27	42.4	923.62	525.4	546.4	13.44
81.30	81.30	81.30	81.30	81.30	81.30	81.30	42.6	860.35	387.8	562.5	14.19
78.36	78.36	78.36	78.36	78.36	78.36	78.36	42.7	883.37	382.0	578.4	
82.44	82.44	82.44	82.44	82.44	82.44	82.44	42.8	867.33	427.8	594.4	10.35
74.49	74.49	74.49	74.49	74.49	74.49	74.49	42.8	917.82	705.4	610.3	17.86
77.10	77.10	77.10	77.10	77.10	77.10	77.10	42.9	894.34	689.0	626.2	
77.25	77.25	77.25	77.25	77.25	77.25	77.25	43.0	895.06	755.7	642.1	15.12
67.59	67.59	67.59	67.59	67.59	67.59	67.59	43.0	964.79	753.5	658.0	
60.10	60.10	60.10	60.10	60.10	60.10	60.10	43.0	994.98	759.1	674.0	1.27
62.08	62.08	62.08	62.08	62.08	62.08	62.08	47	979.75	772.7	689.9	3.30
59.11	59.11	59.11	59.11	59.11	59.11	59.1	.1	1013.67	797.5	705.9	
57.09	57.09	57.09	57.09	57.09	57.09	57.	43.2	1021.37	826.4	721.9	
54.00	54.00	54.00	54.00	54.00	54.00	54.0	43.3	1041.66	45.5	737.9	
55.54	55.54	55.54	55.54	55.54	55.54	55.54	43.3	1024.56	39.2	753.8	
58.49	58.49	58.49	58.49	58.49	58.49	58.49	43.4	1019.29	41.6	769.8	.75
63.61	63.61	63.61	63.61	63.61	63.61	63.61	43.5	920.88	47.2	785.8	1.27
77.61	77.61	77.61	77.61	77.61	77.61	77.61	43.6	865.86	137.0	801.7	20.27
82.43	82.43	82.43	82.43	82.43	82.43	82.43	43.7	855.74	240.0	817.6	23.41
80.14	80.14	80.14	80.14	80.14	80.14	80.14	43.7	865.28	347.9	833.4	24.53

A.3 TABLES OF RESULTS

The page numbers corresponding to the tables of results for the pipeline configuration are given below.

Results used for all analyses		Results to show repeatability	
PIPELINE CONFIGURATION	PAGE NUMBERS	PIPELINE CONFIGURATION	PAGE NUMBERS
100A	144	100A	234
100B	154	100B	239
100C	164	100C	244
100D	174		
200A	184	200A	248
200B	194		
200C	202	200C	253
400A	210		
400B	220		
1200A	226		

An explanation of the numbering system used to identify each set of results is given below:

eg. Read. No. 200B24

200B refers to the pipeline configuration. A summary of all the pipeline configurations investigated is given in Figure 4.1. The 2 following 200B refers to the second air mass flowrate and the 4 refers to the fourth product mass flowrate at the corresponding air mass flowrate.

A.3 TABLES OF RESULTS

The page numbers corresponding to the tables of results for the pipeline configuration are given below.

Results used for all analyses		Results to show repeatability	
PIPELINE CONFIGURATION	PAGE NUMBERS	PIPELINE CONFIGURATION	PAGE NUMBERS
100A	144	100A	234
100B	154	100B	239
100C	164	100C	244
100D	174		
200A	184	200A	248
200B	194		
200C	202	200C	253
400A	210		
400B	220		
1200A	226		

An explanation of the numbering system used to identify each set of results is given below:

eg. Read. No. 200B24

200B refers to the pipeline configuration. A summary of all the pipeline configurations investigated is given in Figure 4.1. The 2 following 200B refers to the second air mass flowrate and the 4 refers to the fourth product mass flowrate at the corresponding air mass flowrate.

The following significant figures are applicable to the data presented in the tables of results.

PARAMETER	SYMBOL AS IN TABLES	SIGNIFICANT FIGURE
Product mass flowrate	$\dot{G}$	1
Air mass flowrate	$\dot{Q}$	2
Load ratio		1
Atmospheric pressure	Pat	1
Pressures	Pi	1
Velocities	Ui	1
Volumetric flowrate	Vi	0
Density	Rho	2
Dynamic pressure	$1/2.\mathrm{Rho}.v^2$	1
Froude number (squared)	$v^2 / g\ D$	0

TEST NUMBER :100A1

Read. No : 100A11
G [t/h]: 11.4
D [kg/s]: .170
Load Ratio : 34.5
Pat [kPa]: 86.2

POINTS ALONG PIPELINE

		1	2	3	5	6
Pi	[kPa]	47.227	35.237	26.728	18.776	10.676
Ui	[m/s]	9.404	10.330	11.111	11.921	12.958
Vi	[m^3/hr]	293.130	321.966	346.340	371.887	403.883
Rho	[kg/m^3]	1.574	1.433	1.332	1.241	1.142
1/2*Rho*v^2	[Pa]	69.595	76.442	82.203	88.294	95.990
Fr	v^2/gD	85.862	103.586	119.861	138.193	163.002

TEST NUMBER :100A1

Read. No : 100A12
G [t/h]: 12.8
D [kg/s]: .109
Load Ratio : 27.5
Pat [kPa]: 86.2

POINTS ALONG PIPELINE

		1	2	3	5	6
Pi	[kPa]	50.652	38.937	30.428	20.882	11.98
Ui	[m/s]	9.344	10.174	10.953	11.838	12.965
Vi	[m^3/hr]	291.233	317.108	341.410	369.072	404.119
Rho	[kg/m^3]	1.594	1.474	1.369	1.261	1.151
1/2*Rho*v^2	[Pa]	70.004	76.256	82.101	89.104	97.181
Fr	v^2/gD	84.755	100.482	116.475	135.193	163.192

TEST NUMBER :100A1

Read. No : 100A13
G [t/h]: 19.9
D [kg/s]: .119
Load Ratio : 46.5
Pat [kPa]: 86.2

POINTS ALONG PIPELINE

		1	2	3	5	6
Pi	[kPa]	62.987	52.847	41.006	28.413	13.413
Ui	[m/s]	7.804	8.424	9.208	10.220	11.759
Vi	[m^3/hr]	243.269	262.574	287.015	318.550	366.518
Rho	[kg/m^3]	1.765	1.635	1.494	1.348	1.171
1/2*Rho*v^2	[Pa]	53.750	58.018	63.418	70.386	80.985
Fr	v^2/gD	59.132	68.895	82.317	101.400	134.237

TEST NUMBER :100A1

Read. No : 100A14
G [t/h]: 23.0
Q [kg/s]: .121
Load Ratio : 52.8
Pat [kPa]: 86.2

		POINTS ALONG PIPELINE				
		1	2	3	5	6
Pi	[kPa]	67.080	55.750	42.195	35.000	20.000
Ui	[m/s]	7.771	8.391	9.277	9.828	11.216
Vi	[m^3/hr]	242.223	261.557	289.169	306.337	349.604
Rho	[kg/m^3]	1.800	1.667	1.508	1.423	1.247
1/2*Rho*v^2	[Pa]	54.347	58.685	64.881	68.772	78.446
Fr	v^2/gD	58.629	68.762	83.557	93.773	122.133

TEST NUMBER :100A1

Read. No : 100A15
G [t/h]: 33.4
Q [kg/s]: .112
Load Ratio : 82.9
Pat [kPa]: 86.2

		POINTS ALONG PIPELINE				
		1	2	3	5	6
Pi	[kPa]	80.947	69.817	54.817	45.000	27.000
Ui	[m/s]	6.603	7.074	7.826	8.412	9.749
Vi	[m^3/hr]	205.800	220.481	243.934	262.185	303.876
Rho	[kg/m^3]	1.961	1.830	1.654	1.539	1.328
1/2*Rho*v^2	[Pa]	42.742	45.792	50.662	54.453	63.112
Fr	v^2/gD	42.323	48.576	59.466	68.691	92.273

TEST NUMBER :100A2

Read. No : 100A21
Ġ [t/h]: 10.6
Q̇ [kg/s]: .280
Load Ratio : 10.7
Pat [kPa]: 85.6

POINTS ALONG PIPELINE

		1	2	3	5	6
Pi	[kPa]	69.327	53.120	45.992	30.000	20.000
Ui	[m/s]	17.936	20.031	21.116	24.028	26.314
Vi	[m^3/hr]	559.053	624.368	658.190	749.241	820.192
Rho	[kg/m^3]	1.804	1.615	1.532	1.346	1.230
1/2*Rho*v^2	[Pa]	290.200	324.105	341.661	388.926	425.756
Fr	v^2/gD	312.511	389.548	432.895	560.950	672.220

TEST NUMBER :100A2

Read. No : 100A22
Ġ [t/h]: 14.8
Q̇ [kg/s]: .280
Load Ratio : 14.7
Pat [kPa]: 85.6

POINTS ALONG PIPELINE

		1	2	3	5	6
Pi	[kPa]	80.673	62.292	55.711	45.000	35.000
Ui	[m/s]	16.744	18.824	19.701	21.317	23.085
Vi	[m^3/hr]	521.890	586.750	614.081	664.444	719.539
Rho	[kg/m^3]	1.933	1.719	1.643	1.518	1.402
1/2*Rho*v^2	[Pa]	270.970	304.646	318.836	344.985	373.891
Fr	v^2/gD	272.169	344.022	376.818	441.161	517.356

TEST NUMBER :100A2

Read. No : 100A23
Ġ [t/h]: 16.5
Q̇ [kg/s]: .278
Load Ratio : 16.4
Pat [kPa]: 85.6

POINTS ALONG PIPELINE

		1	2	3	5	6
Pi	[kPa]	86.460	66.127	59.346	45.067	35.067
Ui	[m/s]	16.161	18.326	19.184	21.280	23.044
Vi	[m^3/hr]	503.720	571.225	597.949	663.291	718.260
Rho	[kg/m^3]	1.990	1.755	1.677	1.512	1.396
1/2*Rho*v^2	[Pa]	259.914	294.746	308.535	342.252	370.615
Fr	v^2/gD	253.547	326.058	357.280	439.472	515.518

TEST NUMBER :100A2

Read. No : 100A24
G [t/h]: 18.5
Q [kg/s]: .277
Load Ratio : 18.5
Pat [kPa]: 85.6

		POINTS ALONG PIPELINE 1	2	3	5	6
Pi	[kPa]	91.237	70.460	63.941	50.000	40.000
Ui	[m/s]	15.757	17.821	18.598	20.510	22.143
Vi	[m^3/hr]	490.707	555.469	579.684	639.261	690.179
Rho	[kg/m^3]	2.038	1.798	1.723	1.562	1.447
1/2*Rho*v^2	[Pa]	251.986	285.533	297.981	328.616	354.780
Fr	v^2/gD	240.126	308.319	335.786	408.380	475.997

TEST NUMBER :100A2

Read. No : 100A25
G [t/h]: 25.6
Q [kg/s]: .259
Load Ratio : 27.4
Pat [kPa]: 85.6

		POINTS ALONG PIPELINE 1	2	3	5	6
Pi	[kPa]	101.827	81.280	75.119	55.000	45.000
Ui	[m/s]	13.787	15.649	16.249	18.574	19.996
Vi	[m^3/hr]	429.720	487.778	506.477	578.950	623.280
Rho	[kg/m^3]	2.172	1.913	1.843	1.612	1.497
1/2*Rho*v^2	[Pa]	206.399	234.206	243.267	278.077	299.369
Fr	v^2/gD	184.524	237.757	256.330	334.937	388.193

TEST NUMBER :100A3

Read. No : 100A31
Q [t/hl]: 10.9
Q [kg/s]: .234
Load Ratio : 13.1
Pat [kPa]: 85.6

POINTS ALONG PIPELINE

		1	2	3	5	6
Pi	[kPa]	50.813	45.973	39.582	30.000	20.000
Ui	[m/s]	16.657	17.270	18.152	19.657	21.518
Vi	[m^3/hr]	519.207	538.306	565.790	612.688	670.708
Rho	[kg/m^3]	1.599	1.542	1.467	1.355	1.238
1/2*Rho*v^2	[Pa]	221.804	229.963	241.704	261.739	286.525
Fr	v^2/gD	269.377	289.560	319.883	375.110	449.518

TEST NUMBER :100A3

Read. No : 100A32
Q [t/hl]: 14.2
Q [kg/s]: .229
Load Ratio : 17.2
Pat [kPa]: 85.6

POINTS ALONG PIPELINE

		1	2	3	5	6
Pi	[kPa]	58.927	52.910	47.043	35.000	25.000
Ui	[m/s]	15.681	16.362	17.086	18.792	20.491
Vi	[m^3/hr]	488.760	509.991	532.547	585.728	638.688
Rho	[kg/m^3]	1.692	1.623	1.554	1.413	1.296
1/2*Rho*v^2	[Pa]	208.197	217.241	226.849	249.502	272.061
Fr	v^2/gD	238.711	259.930	283.398	342.826	407.622

TEST NUMBER :100A3

Read. No : 100A33
Q [t/hl]: 16.7
Q [kg/s]: .231
Load Ratio : 20.1
Pat [kPa]: 85.6

POINTS ALONG PIPELINE

		1	2	3	5	6
Pi	[kPa]	68.307	60.387	53.806	40.000	28.000
Ui	[m/s]	14.814	15.621	16.755	18.153	20.070
Vi	[m^3/hr]	461.742	486.965	509.779	565.967	625.576
Rho	[kg/m^3]	1.803	1.709	1.633	1.471	1.330
1/2*Rho*v^2	[Pa]	197.787	208.565	218.365	242.343	267.965
Fr	v^2/gD	213.050	236.902	259.683	319.902	391.057

TEST NUMBER :100A3

Read. No : 100A34
G [t/h]: 18.5
Q [kg/s]: .233
Load Ratio : 22.0
Pat [kPa]: 85.6

		POINTS ALONG PIPELINE				
		1	2	3	5	6
Pi	[kPa]	71.815	64.400	58.258	45.000	30.000
Ui	[m/s]	14.648	15.372	16.028	17.655	19.946
Vi	[m^3/hr]	456.570	479.135	499.592	550.308	621.715
Rho	[kg/m^3]	1.842	1.755	1.683	1.528	1.353
1/2*Rho*v^2	[Pa]	197.587	207.352	216.206	238.153	269.056
Fr	v^2/gD	208.303	229.401	249.409	302.616	386.245

TEST NUMBER :100A3

Read. No : 100A35
G [t/h]: 23.3
Q [kg/s]: .214
Load Ratio : 30.7
Pat [kPa]: 85.6

		POINTS ALONG PIPELINE				
		1	2	3	5	6
Pi	[kPa]	78.477	69.703	64.376	50.000	35.000
Ui	[m/s]	12.915	13.645	14.150	15.628	17.571
Vi	[m^3/hr]	402.563	425.305	440.411	487.104	547.689
Rho	[kg/m^3]	1.915	1.813	1.751	1.583	1.408
1/2*Rho*v^2	[Pa]	159.734	168.758	174.752	193.279	217.319
Fr	v^2/gD	161.938	180.751	193.819	237.096	299.742

TEST NUMBER :100A4

Read. No : 100A41
G [t/h]: 9.0
Q [kg/s]: .402
Load Ratio : 6.23
Pat [kPa]: 86.12

POINTS ALONG PIPELINE

	1	2	3	5	6
Pi [kPa]	81.963	62.383	54.561	35.000	25.000
Ui [m/s]	23.756	26.888	28.383	32.967	35.934
Vi [m^3/hr]	740.483	838.081	884.683	1027.558	1120.031
Rho [kg/m^3]	1.957	1.729	1.638	1.410	1.294
1/2*Rho*v^2 [Pa]	552.129	624.926	659.676	766.212	835.166
Fr v^2/gD	547.858	701.864	782.090	1055.100	1253.548

TEST NUMBER :100A4

Read. No : 100A42
G [t/h]: 10.3
Q [kg/s]: .405
Load Ratio : 7.12
Pat [kPa]: 86.12

POINTS ALONG PIPELINE

	1	2	3	5	6
Pi [kPa]	89.567	69.167	60.591	45.000	30.000
Ui [m/s]	22.890	25.897	27.411	30.670	34.632
Vi [m^3/hr]	713.467	807.195	854.379	955.968	1079.457
Rho [kg/m^3]	2.045	1.808	1.708	1.536	1.352
1/2*Rho*v^2 [Pa]	535.805	606.193	641.628	717.921	810.659
Fr v^2/gD	508.661	651.084	729.428	913.204	1164.372

TEST NUMBER :100A4

Read. No : 100A43
G [t/h]: 13.0
Q [kg/s]: .376
Load Ratio : 9.61
Pat [kPa]: 86.12

POINTS ALONG PIPELINE

	1	2	3	5	6
Pi [kPa]	94.370	74.333	66.207	55.000	40.000
Ui [m/s]	20.756	23.548	24.893	26.546	29.703
Vi [m^3/hr]	646.947	727.734	766.559	827.433	925.844
Rho [kg/m^3]	2.096	1.864	1.769	1.639	1.465
1/2*Rho*v^2 [Pa]	451.540	507.926	535.024	577.511	646.197
Fr 2/gD	418.232	529.208	587.181	684.143	856.556

TEST NUMBER :100A4

Read. No : 100A44
Ġ [t/h]: 16.8
Q̇ [kg/s]: .397
Load Ratio : 11.8
Pat [kPa]: 86.12

POINTS ALONG PIPELINE

		1	2	3	5	6
Pi	[kPa]	112.203	86.063	77.860	60.000	45.000
Ui	[m/s]	20.023	23.067	24.217	27.177	30.286
Vi	[m^3/hr]	624.110	718.859	754.823	847.082	943.987
Rho	[kg/m^3]	2.292	1.990	1.895	1.689	1.515
1/2*Rho*v^2	[Pa]	459.447	529.198	555.673	623.591	694.920
Fr	v^2/gD	389.227	516.379	569.339	717.020	890.456

TEST NUMBER :100A4

Read. No : 100A45
Ġ [t/h]: 18.5
Q̇ [kg/s]: .398
Load Ratio : 12.8
Pat [kPa]: 86.12

POINTS ALONG PIPELINE

		1	2	3	5	6
Pi	[kPa]	118.857	94.377	86.854	70.000	55.000
Ui	[m/s]	19.443	22.080	23.040	25.527	28.241
Vi	[m^3/hr]	606.023	688.216	718.146	795.674	880.248
Rho	[kg/m^3]	2.368	2.085	1.998	1.804	1.630
1/2*Rho*v^2	[Pa]	447.588	508.293	530.399	587.698	650.122
Fr	v^2/gD	366.994	473.293	515.355	632.632	774.268

TEST NUMBER :100A5

Read. No : 100A51
Ġ [t/h]: 8.27
Q̇ [kg/s]: .570
Load Ratio : 4.02
Pat [a]: 85.21

		POINTS ALONG PIPELINE				
		1	2	3	5	6
		**********	**********	**********	**********	**********
Pi	[kPa]	101.823	73.590	68.075	55.790	44.825
Ui	[m/s]	28.907	34.046	35.271	38.344	41.577
Vi	[m^3/hr]	901.007	1061.198	1099.376	1195.165	1295.949
Rho	[kg/m^3]	2.280	1.936	1.869	1.719	1.585
1/2*Rho*v^2	[Pa]	952.664	1122.040	1162.407	1263.688	1370.250
Fr	v^2/gD	811.216	1125.314	1207.740	1427.370	1678.249

TEST NUMBER :100A5

Read. No : 100A52
Ġ [t/h]: 8.97
Q̇ [kg/s]: .586
Load Ratio : 4.25
Pat [kPa]: 85.21

		POINTS ALONG PIPELINE				
		1	2	3	5	6
		**********	**********	**********	**********	**********
Pi	[kPa]	115.267	84.470	79.163	65.607	54.720
Ui	[m/s]	27.829	32.880	33.941	36.992	39.870
Vi	[m^3/hr]	867.413	1024.848	1057.934	1153.050	1242.734
Rho	[kg/m^3]	2.434	2.060	1.996	1.831	1.699
1/2*Rho*v^2	[Pa]	942.675	1113.769	1149.727	1253.074	1350.561
Fr	v^2/gD	751.853	1049.540	1118.402	1328.501	1543.392

TEST NUMBER :100A5

Read. No : 100A53
Ġ [t/h]: 10.3
Q̇ [kg/s]: .680
Load Ratio : 4.94
Pat [kPa]: 85.21

		POINTS ALONG PIPELINE				
		1	2	3	5	6
		**********	**********	**********	**********	**********
Pi	[kPa]	121.427	93.997	86.248	71.363	60.002
Ui	[m/s]	26.955	31.081	32.486	35.574	38.358
Vi	[m^3/hr]	840.190	968.792	1012.573	1108.835	1195.590
Rho	[kg/m^3]	2.488	2.158	2.064	1.885	1.748
1/2*Rho*v^2	[Pa]	903.839	1042.187	1089.281	1192.835	1284.162
Fr	v^2/gD	705.300	937.869	1024.550	1228.612	1428.385

TEST NUMBER :100A5

Read. No : 100A54
G [t/h]: 11.4
Q [kg/s]: .556
Load Ratio : 5.69
Pat [kPa]: 85.21

	POINTS ALONG PIPELINE 1	2	3	5	6
Pi [kPa]	125.767	98.720	90.938	77.170	65.942
Ui [m/s]	25.388	29.185	30.408	32.986	35.437
Vi [m^3/hr]	791.337	909.680	947.803	1028.166	1104.541
Rho [kg/m^3]	2.531	2.202	2.113	1.948	1.814
1/2*Rho*v^2 [Pa]	815.807	937.8.0	977.1'2	1059.960	1138.676
Fr v^2/gD	625.753	826.909	897.470	1056.348	1219.114

TEST NUMBER :100A5

Read. No : 100A55
G [t/h]: 14.6
Q [kg/s]: .574
Load Ratio : 7.09
Pat [kPa]: 85.21

	POINTS ALONG PIPELINE 1	2	3	5	6
Pi [kPa]	145.777	112.950	103.190	87.303	76.306
Ui [m/s]	24.045	28.028	29.480	32.195	34.387
Vi [m^3/hr]	749.460	873.614	918.871	1003.489	1071.813
Rho [kg/m^3]	2.738	2.366	2.250	2.060	1.929
1/2*Rho*v^2 [Pa]	797.307	929.387	977.533	1067.554	1140.239
Fr v^2/gD	561.277	762.640	843.703	1006.250	1147.938

TEST NUMBER :100B1

Read. No : 100B11
G [t/h]: 12.3
Q [kg/s]: .149
Load Ratio : 22.9
Pat [kPa]: 86.25

POINTS ALONG PIPELINE

		1	2	3	5	6
Pi	[kPa]	43.470	30.167	23.533	16.710	9.829
Ui	[m/s]	11.392	12.694	13.461	14.353	6.968
Vi	[m^3/hr]	350.093	395.671	419.581	447.384	479.427
Rho	[kg/m^3]	1.519	1.363	1.285	1.205	1.125
1/2*Rho*v^2	[Pa]	98.557	109.819	116.455	124.172	27.310
Fr	v^2/gD	125.999	156.441	175.919	200.006	31.728

TEST NUMBER :100B1

Read. No : 100B12
G [t/h]: 14.8
Q [kg/s]: .150
Load Ratio : 27.3
Pat [kPa]: 86.25

POINTS ALONG PIPELINE

		1	2	3	5	6
Pi	[kPa]	50.050	36.313	28.983	21.160	12.647
Ui	[m/s]	10.910	12.133	12.905	13.845	6.812
Vi	[m^3/hr]	340.663	378.177	402.235	431.530	468.677
Rho	[kg/m^3]	1.598	1.437	1.351	1.259	1.159
1/2*Rho*v^2	[Pa]	95.103	105.762	112.490	120.683	26.901
Fr	v^2/gD	115.558	142.913	161.674	186.081	30.322

TEST NUMBER :100B1

Read. No : 100B13
G [t/h]: 19.1
Q [kg/s]: .151
Load Ratio : 35.1
Pat [kPa]: 86.25

POINTS ALONG PIPELINE

		1	2	3	5	6
Pi	[kPa]	55.387	39.690	31.873	21.913	14.285
Ui	[m/s]	10.535	11.848	12.632	13.795	6.724
Vi	[m^3/hr]	328.377	369.304	393.744	429.999	462.627
Rho	[kg/m^3]	1.562	1.477	1.386	1.269	1.179
1/2*Rho*v^2	[Pa]	92.213	103.706	110.569	120.750	26.663
Fr	v^2/gD	107.752	136.285	154.920	184.764	29.544

TEST NUMBER :100B1

Read. No : 100B14
Ġ [t/h]: 22.0
Q̇ [kg/s]: .149
Load Ratio : 40.8
Pat [kPa]: 86.25

		POINTS ALONG PIPELINE				
		1	2	3	5	6
Pi	[kPa]	59.510	43.380	34.545	24.447	16.192
Ui	[m/s]	10.119	11.378	12.211	13.325	6.523
Vi	[m^3/hr]	315.413	354.651	380.601	415.321	448.787
Rho	[kg/m^3]	1.709	1.520	1.417	1.298	1.201
1/2*Rho*v^2	[Pa]	87.523	98.411	105.612	115.246	25.559
Fr	v^2/gD	99.412	125.685	144.750	172.365	27.803

TEST NUMBER :100B1

Read. No : 100B15
Ġ [t/h]: 27.8
Q̇ [kg/s]: .147
Load Ratio : 52.4
Pat [kPa]: 86.25

		POINTS ALONG PIPELINE				
		1	2	3	5	6
Pi	[kPa]	66.803	47.460	38.065	7.320	6.320
Ui	[m/s]	9.483	10.854	11.675	15.511	7.103
Vi	[m^3/hr]	295.570	338.329	362.899	483.467	488.689
Rho	[kg/m^3]	1.793	1.567	1.456	1.096	1.085
1/2*Rho*v^2	[Pa]	80.621	92.284	99.259	131.873	27.358
Fr	v^2/gD	87.297	114.382	132.325	233.568	32.966

TEST NUMBER :100B2

Read. No : 100B21
Ġ [t/h]: 13.5
Q̇ [kg/s]: .236
Load Ratio : 15.8
Pat [kPa]: 86.25

POINTS ALONG PIPELINE

		1	2	3	5	6
Pi	[kPa]	44.410	41.483	32.883	23.807	18.317
Ui	[m/s]	17.596	18.274	19.594	21.209	10.113
Vi	[m^3/hr]	548.450	569.604	610.724	661.090	695.799
Rho	[kg/m^3]	1.554	1.496	1.395	1.289	1.225
1/2*Rho*v^2	[Pa]	240.522	249.799	267.822	289.920	62.627
Fr	v^2/gD	300.576	324.210	372.710	436.719	66.830

TEST NUMBER :100B2

Read. No : 100B22
Ġ [t/h]: 15.5
Q̇ [kg/s]: .236
Load Ratio : 18.2
Pat [kPa]: 86.25

POINTS ALONG PIPELINE

		1	2	3	5	6
Pi	[kPa]	51.813	45.497	37.027	26.737	21.027
Ui	[m/s]	16.848	17.656	18.868	20.589	9.823
Vi	[m^3/hr]	525.137	550.315	588.122	641.744	675.842
Rho	[kg/m^3]	1.619	1.545	1.445	1.325	1.258
1/2*Rho*v^2	[Pa]	229.721	240.735	257.274	280.731	60.678
Fr	v^2/gD	275.566	302.624	345.633	411.533	63.051

TEST NUMBER :100B2

Read. No : 100B23
Ġ [t/h]: 17.4
Q̇ [kg/s]: .238
Load Ratio : 20.2
Pat [kPa]: 86.25

POINTS ALONG PIPELINE

		1	2	3	5	6
Pi	[kPa]	55.200	48.370	39.212	28.957	21.496
Ui	[m/s]	16.589	17.431	18.703	20.728	9.866
Vi	[m^3/hr]	517.070	543.304	582.962	646.071	678.815
Rho	[kg/m^3]	1.659	1.579	1.471	1.328	1.264
1/2*Rho*v^2	[Pa]	228.258	239.839	257.346	285.205	61.502
Fr	v^2/gD	267.185	294.962	339.595	417.101	63.607

TEST NUMBER :100B2

Read. No : 100B24
Ġ [t/h]: 19.1
Q̇ [kg/s]: .235
Load Ratio : 22.6
Pat [kPa]: 86.25

		POINTS ALONG PIPELINE				
		1	2	3	5	6
Pi	[kPa]	59.447	50.640	40.820	29.400	23.697
Ui	[m/s]	15.890	16.912	18.219	20.018	9.539
Vi	[m^3/hr]	495.283	527.147	567.885	623.961	656.328
Rho	[kg/m^3]	1.709	1.606	1.491	1.357	1.290
1/2*Rho*v^2	[Pa]	215.788	229.671	247.420	271.851	58.689
Fr	v^2/gD	245.125	277.680	322.256	389.042	59.463

TEST NUMBER :100B2

Read. No : 100B25
Ġ [t/h]: 25.4
Q̇ [kg/s]: .238
Load Ratio : 29.6
Pat [kPa]: 86.25

		POINTS ALONG PIPELINE				
		1	2	3	5	6
Pi	[kPa]	68.773	56.130	46.897	33.323	28.067
Ui	[m/s]	15.148	16.493	17.637	19.639	9.306
Vi	[m^3/hr]	472.160	514.088	549.736	612.142	640.288
Rho	[kg/m^3]	1.817	1.669	1.561	1.402	1.340
1/2*Rho*v^2	[Pa]	208.523	227.040	242.783	270.344	58.036
Fr	v^2/gD	222.771	264.092	301.987	374.442	56.592

TEST NUMBER :10083

Read. No : 10831
Ġ [t/h]: 13.6
Q̇ [kg/s]: .334
Load Ratio : 11.3
Pat [kPa]: 86.25

		POINTS ALONG PIPELINE 1	2	3	5	6
Pi	[kPa]	64.967	41.153	30.174	16.503	14.088
Ui	[m/s]	20.582	24.430	26.733	30.290	14.053
Vi	[m^3/hr]	641.547	761.460	833.267	944.130	966.858
Rho	[kg/m^3]	1.880	1.584	1.447	1.277	1.247
1/2*Rho*v^2	[Pa]	398.162	472.584	517.149	585.954	123.155
Fr	v^2/gD	411.280	579.395	693.823	890.727	129.041

TEST NUMBER :10083

Read. No : 10832
Ġ [t/h]: 14.3
Q̇ [kg/s]: .331
Load Ratio : 12.0
Pat [kPa]: 86.25

		POINTS ALONG PIPELINE 1	2	3	5	6
Pi	[kPa]	65.670	41.337	31.479	18.133	15.013
Ui	[m/s]	20.370	24.255	26.286	29.646	13.845
Vi	[m^3/hr]	634.917	756.008	819.308	924.061	952.532
Rho	[kg/m^3]	1.882	1.581	1.459	1.293	1.255
1/2*Rho*v^2	[Pa]	390.535	465.018	503.953	568.387	120.249
Fr	v^2/gD	402.823	571.128	670.772	853.261	125.246

TEST NUMBER :10083

Read. No : 10833
Ġ [t/h]: 17.4
Q̇ [kg/s]: .333
Load Ratio : 14.5
Pat [kPa]: 86.25

		POINTS ALONG PIPELINE 1	2	3	5	6
Pi	[kPa]	76.053	48.443	36.847	21.740	18.244
Ui	[m/s]	19.194	23.128	25.307	28.848	13.506
Vi	[m^3/hr]	598.267	720.902	788.816	899.164	929.249
Rho	[kg/m^3]	2.005	1.664	1.520	1.334	1.291
1/2*Rho*v^2	[Pa]	369.267	444.961	486.880	554.990	117.716
Fr	v^2/gD	357.660	519.317	621.774	807.901	119.198

TEST NUMBER :100B3

Read. No : 100B34
Ġ [t/h]: 18.7
ṁ [kg/s]: .328
Load Ratio : 15.8
Pat [kPa]: 86.25

		POINTS ALONG PIPELINE				
		1	2	3	5	6
Pi	[kPa]	78.317	49.630	39.071	23.000	20.219
Ui	[m/s]	18.753	22.712	24.625	28.248	13.131
Vi	[m^3/hr]	584.510	707.910	767.558	880.466	903.461
Rho	[kg/m^3]	2.026	1.673	1.543	1.345	1.311
1/2*Rho*v^2	[Pa]	356.259	431.472	467.827	536.645	113.017
Fr	v^2/gD	341.401	500.769	588.712	774.650	112.674

TEST NUMBER :100B3

Read. No : 100B35
Ġ [t/h]: 25.9
ṁ [kg/s]: .334
Load Ratio : 21.5
Pat [kPa]: 86.25

		POINTS ALONG PIPELINE				
		1	2	3	5	6
Pi	[kPa]	91.963	59.963	48.206	30.207	24.636
Ui	[m/s]	17.647	21.509	23.390	27.005	12.849
Vi	[m^3/hr]	550.037	670.417	729.042	841.720	884.003
Rho	[kg/m^3]	2.186	1.794	1.650	1.429	1.360
1/2*Rho*v^2	[Pa]	340.433	414.940	451.225	520.964	112.393
Fr	v^2/gD	302.318	449.128	531.112	707.971	107.873

TEST NUMBER :100B4

Read. No : 100B41
Q [t/h]: 12.6
Q [kg/s]: .432
Load Ratio : 8.11
Pat [kPa]: 86.25

POINTS ALONG PIPELINE

		1	2	3	5	6
Pi	[kPa]	75.477	47.107	35.931	17.857	16.006
Ui	[m/s]	25.733	31.208	34.662	39.976	18.438
Vi	[m^3/hr]	802.093	972.729	1061.703	1246.029	1268.580
Rho	[kg/m^3]	1.943	1.602	1.468	1.251	1.239
1/2*Rho*v^2	[Pa]	643.370	780.239	851.606	999.456	206.839
Fr	v^2/gD	642.881	945.506	1126.384	1551.446	222.147

TEST NUMBER :100B4

Read. No : 100B42
Q [t/h]: 15.6
Q [kg/s]: .423
Load Ratio : 10.2
Pat [kPa]: 86.25

POINTS ALONG PIPELINE

		1	2	3	5	6
Pi	[kPa]	83.850	53.680	40.239	18.983	18.359
Ui	[m/s]	24.041	29.224	32.329	39.859	17.710
Vi	[m^3/hr]	749.333	910.895	1007.687	1211.228	1218.461
Rho	[kg/m^3]	2.036	1.675	1.514	1.260	1.252
1/2*Rho*v^2	[Pa]	588.355	715.209	791.206	951.021	196.352
Fr	v^2/gD	561.088	829.121	1014.686	1465.996	204.940

TEST NUMBER :100B4

Read. No : 100B43
Q [t/h]: 17.2
Q [kg/s]: .388
Load Ratio : 12.3
Pat [kPa]: 86.25

POINTS ALONG PIPELINE

		1	2	3	5	6
Pi	[kPa]	85.743	54.017	41.363	21.427	19.323
Ui	[m/s]	21.896	26.849	29.511	34.975	16.160
Vi	[m^3/hr]	682.487	836.857	919.839	1090.145	1111.864
Rho	[kg/m^3]	2.050	1.671	1.521	1.283	1.258
1/2*Rho*v^2	[Pa]	491.303	602.430	662.167	784.765	164.273
Fr	v^2/gD	465.446	699.815	845.483	1187.542	170.650

TEST NUMBER :100B4

Read. No : 100B44
G [t/h]: 20.4
Q [kg/s]: .429
Load Ratio : 13.2
Pat [kPa]: 86.25

POINTS ALONG PIPELINE

		1	2	3	5	6
Pi	[kPa]	94.917	61.770	49.177	25.423	23.312
Ui	[m/s]	23.000	28.151	30.769	37.313	17.230
Vi	[m^3/hr]	716.913	877.454	959.044	1163.042	1185.458
Rho	[kg/m^3]	2.155	1.761	1.611	1.328	1.303
1/2*Rho*v^2	[Pa]	570.058	697.714	762.590	924.801	193.463
Fr	v^2/gD	513.587	769.360	919.090	1351.673	193.989

TEST NUMBER :100B4

Read. No : 100B45
G [t/h]: 23.7
Q [kg/s]: .421
Load Ratio : 15.6
Pat [kPa]: 86.25

POINTS ALONG PIPELINE

		1	2	3	5	6
Pi	[kPa]	104.427	67.777	53.819	27.540	25.512
Ui	[m/s]	21.465	26.573	29.220	35.969	16.591
Vi	[m^3/hr]	669.057	828.256	910.788	1121.131	1141.471
Rho	[kg/m^3]	2.266	1.830	1.665	1.352	1.328
1/2*Rho*v^2	[Pa]	522.019	646.231	710.626	874.742	182.788
Fr	v^2/gD	447.308	685.504	828.925	1256.011	179.860

TEST NUMBER :100B5

Read. No : 100B51
G [t/h]: 11.7
Q [kg/s]: .936
Load Ratio : 6.07
Pat [kPa]: 86.25

		POINTS ALONG PIPELINE				
		1	2	3	5	6
Pi	[kPa]	86.513	54.283	42.339	21.857	19.266
Ui	[m/s]	30.311	37.263	40.724	48.439	22.484
Vi	[m^3/hr]	944.780	1161.456	1269.345	1509.836	1346.911
Rho	[kg/m^3]	2.045	1.663	1.522	1.279	1.249
1/2*Rho*v^2	[Pa]	939.295	1154.714	1261.976	1501.071	315.643
Fr	v^2/gD	891.953	1347.989	1610.052	2277.929	330.320

TEST NUMBER :100B5

Read. No : 100B52
G [t/h]: 12.4
Q [kg/s]: .571
Load Ratio : 6.06
Pat [kPa]: 86.25

		POINTS ALONG PIPELINE				
		1	2	3	5	6
Pi	[kPa]	95.210	62.127	48.253	25.267	22.216
Ui	[m/s]	30.770	37.631	41.512	50.069	23.321
Vi	[m^3/hr]	959.087	1172.933	1293.918	1560.627	1604.515
Rho	[kg/m^3]	2.145	1.754	1.590	1.318	1.282
1/2*Rho*v^2	[Pa]	1015.304	1241.685	1369.762	1652.104	348.611
Fr	v^2/gD	919.171	1374.760	1672.993	2433.765	355.379

TEST NUMBER :100B5

Read. No : 100B53
G t/h]: 13.3
Q [kg/s]: .569
Load Ratio : 6.50
Pat [kPa]: 86.25

		POINTS ALONG PIPELINE				
		1	2	3	5	6
Pi	[kPa]	99.973	66.343	51.024	27.177	24.245
Ui	[m/s]	29.944	36.543	40.621	49.162	22.863
Vi	[m^3/hr]	933.340	1139.039	1266.152	1532.353	1577.014
Rho	[kg/m^3]	2.195	1.799	1.618	1.337	1.302
1/2*Rho*v^2	[Pa]	984.094	1200.978	1335.003	1615.680	340.399
Fr	v^2/gD	870.483	1296.455	1601.961	2346.380	341.562

TEST NUMBER :10085

Read. No : 10085A
Ġ [t/h]: 18.3
Q̇ [kg/s]: .569
Load Ratio : 8.93
Pat [kPa]: 86.25

POINTS ALONG PIPELINE

		1	2	3	5	6
Pi	[kPa]	117.117	77.147	62.823	34.220	30.927
Ui	[m/s]	27.557	34.298	37.594	46.520	21.667
Vi	[m^3/hr]	858.947	1069.062	1171.785	1449.997	1490.750
Rho	[kg/m^3]	2.387	1.918	1.749	1.414	1.375
1/2*Rho*v^2	[Pa]	906.210	1127.887	1236.263	1529.783	322.795
Fr	v^2/gD	737.247	1142.053	1372.071	2100.945	306.771

TEST NUMBER :10085

Read. No : 10085B
Ġ [t/h]: 20.0
Q̇ [kg/s]: .548
Load Ratio : 10.1
Pat [kPa]: 86.25

POINTS ALONG PIPELINE

		1	2	3	5	6
Pi	[kPa]	116.963	78.870	62.744	33.967	31.211
Ui	[m/s]	26.578	32.710	36.250	44.927	20.831
Vi	[m^3/hr]	828.427	1019.545	1129.893	1400.366	1433.215
Rho	[kg/m^3]	2.382	1.935	1.746	1.409	1.377
1/2*Rho*v^2	[Pa]	841.187	1035.249	1147.297	1421.936	298.682
Fr	v^2/gD	685.786	1038.709	1275.721	1959.584	283.548

TEST NUMBER :100C

Read. No : 100C11
G [t/h]: 10.5
Q [kg/s]: .146
Load Ratio : 19.9
Pat [kPa]: 85.8

POINTS ALONG PIPELINE

		1	2	3	5	6
		*	**********			
Pi	[kPa]	32.930	21.321	13.926	9.891	4.885
Ui	[m/s]	12.517	13.873	6.751	7.036	7.424
Vi	[m^3/hr]	390.142	432.423	464.490	484.078	510.798
Rho	[kg/m^3]	1.351	1.219	1.135	1.089	1.032
1/2*Rho*v^2	[Pa]	105.829	117.298	25.859	26.950	28.437
Fr	v^2/gD	152.099	186.852	29.782	32.347	36.017

TEST NUMBER :100C

Read. No : 100C12
G [t/h]: 14.1
Q [kg/s]: .144
Load Ratio : 27.1
Pat [kPa]: 85.8

POINTS ALONG PIPELINE

		1	2	3	5	6
		**********				
Pi	[kPa]	38.900	26.219	19.229	12.841	7.625
Ui	[m/s]	11.756	12.858	6.324	6.733	7.109
Vi	[m^3/hr]	366.444	400.772	437.077	463.253	489.116
Rho	[kg/m^3]	1.418	1.296	1.194	1.122	1.062
1/2*Rho*v^2	[Pa]	97.985	107.164	23.877	25.423	26.842
Fr	v^2/gD	134.183	160.500	26.130	29.624	33.024

TEST NUMBER :100C

Read. No : 100C13
G [t/h]: 16.5
Q [kg/s]: .142
Load Ratio : 32.1
Pat [kPa]: 85.8

POINTS ALONG PIPELINE

		1	2	3	5	6
		**********				
Pi	[kPa]	46.887	36.239	25.093	8.802	9.480
Ui	[m/s]	10.901	11.852	5.909	7.154	6.878
Vi	[m^3/hr]	339.789	369.435	406.568	492.187	473.199
Rho	[kg/m^3]	1.512	1.390	1.263	1.044	1.085
1/2*Rho*v^2	[Pa]	89.816	97.652	22.057	24.701	25.671
Fr	v^2/gD	115.372	136.382	22.818	33.440	30.908

TEST NUMBER :100C

Read. No : 100C14
Ġ [t/h]: 24.4
Q [kg/s]: .142
Load Ratio : 47.5
Pat [kPa]: 85.8

POINTS ALONG PIPELINE

		1	2	3	5	6
Pi	[kPa]	55.468	41.546	30.572	21.390	12.113
Ui	[m/s]	10.219	11.336	5.620	6.101	6.679
Vi	[m^3/hr]	318.523	353.346	386.666	419.790	459.561
Rho	[kg/m^3]	1.610	1.451	1.326	1.222	1.116
1/2*Rho*v^2	[Pa]	84.075	93.266	20.947	22.741	24.896
Fr	v^2/gD	101.382	124.762	20.638	24.326	29.153

TEST NUMBER :100C

Read. No : 100C15
Ġ [t/h]: 28.3
Q [kg/s]: .142
Load Ratio : 55.2
Pat [kPa]: 85.8

POINTS ALONG PIPELINE

		1	2	3	5	6
Pi	[kPa]	62.682	46.940	34.848	9.069	16.402
Ui	[m/s]	9.715	10.868	5.417	6.887	6.395
Vi	[m^3/hr]	302.826	338.740	372.689	473.959	439.955
Rho	[kg/m^3]	1.692	1.512	1.375	1.081	1.164
1/2*Rho*v^2	[Pa]	79.836	89.304	20.166	25.645	23.805
Fr	v^2/gD	91.636	114.660	19.173	31.009	26.719

TEST NUMBER :100C2

Read. No : 100C21
Ġ [t/h]: 12.8
Q̇ [kg/s]: .245
Load Ratio : 14.5
Pat [kPa]: 85.7

POINTS ALONG PIPELINE

		1	2	3	5	6
Pi	[kPa]	41.521	23.563	21.547	14.839	8.291
Ui	[m/s]	19.031	22.159	10.227	10.910	11.670
Vi	[m^3/hr]	593.195	690.689	703.470	750.619	802.911
Rho	[kg/m^3]	1.487	1.277	1.254	1.175	1.099
1/2*Rho*v^2	[Pa]	269.336	313.603	65.573	69.948	74.821
Fr	v^2/gD	351.621	476.700	68.351	77.776	88.990

TEST NUMBER :100C2

Read. No : 100C22
Ġ [t/h]: 14
Q̇ [kg/s]: .239
Load Ratio : 16.2
Pat [kPa]: 85.7

POINTS ALONG PIPELINE

		1	2	3	5	6
Pi	[kPa]	49.231	26.837	23.754	15.696	9.088
Ui	[m/s]	17.536	21.025	9.793	10.572	11.309
Vi	[m^3/hr]	546.580	655.344	673.805	727.354	778.058
Rho	[kg/m^3]	1.574	1.314	1.278	1.184	1.107
1/2*Rho*v^2	[Pa]	242.314	290.533	61.308	66.181	70.794
Fr	v^2/gD	298.530	429.161	62.672	73.029	83.566

TEST NUMBER :100C2

Read. No : 100C23
Ġ [t/h]: 16.2
Q̇ [kg/s]: .236
Load Ratio : 18.9
Pat [kPa]: 85.7

POINTS ALONG PIPELINE

		1	2	3	5	6
Pi	[kPa]	52.064	26.527	25.835	16.783	7.412
Ui	[m/s]	17.044	20.922	9.537	10.379	11.424
Vi	[m^3/hr]	531.238	652.118	656.165	714.124	785.993
Rho	[kg/m^3]	1.605	1.318	1.309	1.194	1.085
1/2*Rho*v^2	[Pa]	233.164	286.219	59.108	64.329	70.803
Fr	v^2/gD	282.007	424.945	59.433	70.396	85.279

TEST NUMBER :100C2

Read. No : 100C24
Ġ [t/h]: 22.4
Q̇ [kg/s]: .201
Load Ratio : 30.8
Pat [kPa]: 85.7

	POINTS ALONG PIPELINE 1	2	3	5	6
Pi [kPa]	59.463	33.632	30.027	19.954	4.851
Ui [m/s]	13.804	16.792	7.844	8.592	10.025
Vi [m^3/hr]	430.264	523.404	539.705	591.159	689.764
Rho [kg/m^3]	1.690	1.389	1.347	1.230	1.054
1/2*Rho*v^2 [Pa]	161.005	195.858	41.449	45.401	52.974
Fr v^2/gD	184.991	273.750	40.208	48.241	65.676

TEST NUMBER :100C2

Read. No : 100C25
Ġ [t/h]: 27.2
Q̇ [kg/s]: .238
Load Ratio : 31.7
Pat [kPa]: 85.7

	POINTS ALONG PIPELINE 1	2	3	5	6
Pi [kPa]	66.407	37.552	35.890	24.358	6.567
Ui [m/s]	15.566	19.211	8.822	9.746	11.626
Vi [m^3/hr]	485.198	598.787	606.972	670.570	799.876
Rho [kg/m^3]	1.768	1.433	1.414	1.280	1.073
1/2*Rho*v^2 [Pa]	214.252	264.410	55.009	60.773	72.492
Fr v^2/gD	235.244	358.282	50.856	62.072	88.318

TEST NUMBER :100C3

Read. No : 100C31
G [t/h]: 13
Q [kg/s]: .296
Load Ratio : 12.1
Pat [kPa]: 85.8

		POINTS ALONG PIPELINE				
		1	2	3	5	6
		**********	**********	**********	**********	**********
Pi	[kPa]	44.816	20.904	20.783	13.632	1.186
Ui	[m/s]	22.836	27.952	12.678	13.590	15.534
Vi	[m^3/hr]	711.787	871.296	872.285	935.017	1068.796
Rho	[kg/m^3]	1.509	1.232	1.231	1.148	1.005
1/2*Rho*v^2	[Pa]	393.360	481.511	98.937	106.052	121.226
Fr	v^2/gD	506.264	758.598	105.032	120.682	157.686

TEST NUMBER :100C3

Read. No : 100C32
G [t/h]: 17
Q [kg/s]: .295
Load Ratio : 15.9
Pat [kPa]: 85.8

		POINTS ALONG PIPELINE				
		1	2	3	5	6
		**********	**********	**********	**********	**********
Pi	[kPa]	54.230	26.868	25.939	18.077	4.995
Ui	[m/s]	21.175	26.318	12.022	12.932	14.795
Vi	[m^3/hr]	660.030	820.321	827.144	889.743	1017.938
Rho	[kg/m^3]	1.611	1.296	1.286	1.195	1.045
1/2*Rho*v^2	[Pa]	361.262	448.997	92.918	99.950	114.351
Fr	v^2/gD	435.319	672.432	94.442	109.278	143.037

TEST NUMBER :100C3

Read. No : 100C33
G [t/h]: 19.3
Q [kg/s]: .297
Load Ratio : 18.C
Pat [kPa]: 85.8

		POINTS ALONG PIPELINE				
		1	2	3	5	6
		**********	**********	**********	**********	**********
Pi	[kPa]	58.774	26.511	25.820	17.919	11.180
Ui	[m/s]	20.784	26.755	12.196	13.125	14.037
Vi	[m^3/hr]	647.836	833.936	839.100	903.022	965.771
Rho	[kg/m^3]	1.633	1.284	1.276	1.186	1.109
1/2*Rho*v^2	[Pa]	357.053	459.622	94.916	102.147	109.245
Fr	v^2/gD	419.383	694.938	97.192	112.564	128.752

TEST NUMBER :100C3

Read. No : 100C34
Ġ [t/h]: 24
Q [kg/s]: .296
Load Ratio : 22.4
Pat [kPa]: 85.8

		POINTS ALONG PIPELINE 1	2	3	5	6
Pi	[kPa]	69.386	30.925	30.361	23.285	14.882
Ui	[m/s]	19.496	25.920	11.800	12.565	13.614
Vi	[m^3/hr]	607.687	807.917	811.845	864.502	936.659
Rho	[kg/m^3]	1.756	1.321	1.315	1.235	1.139
1/2*Rho*v^2	[Pa]	333.784	443.764	91.520	97.456	105.591
Fr	v^2/gD	369.012	652.249	90.981	103.166	121.106

TEST NUMBER :100C3

Read. No : 100C35
Ġ [t/h]: 28.6
Q [kg/s]: .294
Load Ratio : 26.9
Pat [kPa]: 85.8

		POINTS 1	2	IPELINE 3	5	6
Pi	[kPa]	73.721	33.518	33.138	25.267	15.994
Ui	[m/s]	18.937	25.318	11.506	12.322	13.444
Vi	[m^3/hr]	590.258	789.138	791.662	847.754	924.994
Rho	[kg/m^3]	1.799	1.345	1.341	1.252	1.148
1/2*Rho*v^2	[Pa]	322.540	431.216	88.785	95.077	103.738
Fr	v^2/gD	348.148	622.281	86.514	99.210	118.109

TEST NUMBER :100C4

Read. No : 100C41
G [t/h]: 12
Q [kg/s]: .404
Load Ratio : 8.241
Pat [kPa]: 85.8

POINTS ALONG PIPELINE

		1	2	3	5	6
Pi	[kPa]	52.477	18.738	19.975	12.597	10.222
Ui	[m/s]	28.605	37.837	16.941	18.211	18.662
Vi	[m^3/hr]	891.600	1179.360	1165.569	1252.965	1283.950
Rho	[kg/m^3]	1.633	1.235	1.249	1.162	1.134
1/2*Rho*v^2	[Pa]	668.136	883.775	179.264	192.705	197.470
Fr	v^2/gD	794.366	1389.867	187.334	216.712	227.562

TEST NUMBER :100C4

Read. No : 100C42
G [t/h]: 15
Q [kg/s]: .371
Load Ratio : 11.21
Pat [kPa]: 85.8

POINTS ALONG PIPELINE

		1	2	3	5	6
Pi	[kPa]	55.863	22.249	21.646	14.923	10.722
Ui	[m/s]	25.663	33.647	15.329	16.352	17.064
Vi	[m^3/hr]	799.911	1048.768	1054.647	1125.046	1174.016
Rho	[kg/m^3]	1.671	1.275	1.268	1.188	1.139
1/2*Rho*v^2	[Pa]	550.419	721.657	148.942	158.884	165.800
Fr	v^2/gD	639.388	1099.106	153.539	174.721	190.262

TEST NUMBER :100C4

Read. No : 100C43
G [t/h]: 16.8
Q [kg/s]: .411[illegible]
Load Ratio : 11.3[illegible]
Pat [kPa]: 85.8

POINTS ALONG PIPELINE

		1	2	3	5	6
Pi	[kPa]	62.049	25.052	26.623	18.473	14.934
Ui	[m/s]	27.514	36.697	16.393	17.674	18.295
Vi	[m^3/hr]	857.610	1143.642	1127.857	1216.002	1258.721
Rho	[kg/m^3]	1.726	1.294	1.312	1.217	1.176
1/2*Rho*v^2	[Pa]	653.185	871.189	176.303	190.081	196.759
Fr	v^2/gD	734.954	1307.412	175.595	204.114	218.707

TEST NUMBER :100C4

Read. No : 100C44
G [t/h]: 18.9
Q [kg/s]: .368
Load Ratio : 14.2
Pat [kPa]: 85.8

POINTS ALONG PIPELINE

		1	2	3	5	6
Pi	[kPa]	67.453	31.945	31.835	24.792	17.849
Ui	[m/s]	23.880	31.077	14.094	14.992	15.996
Vi	[m^3/hr]	744.344	968.648	969.717	1031.477	1100.572
Rho	[kg/m^3]	1.780	1.368	1.367	1.285	1.204
1/2*Rho*v^2	[Pa]	507.647	660.624	135.735	144.380	154.051
Fr	v^2/gD	553.641	937.590	129.806	146.867	167.202

TEST NUMBER :100C4

Read. No : 100C45
G [t/h]: 22.9
Q [kg/s]: .414
Load Ratio : 15.3
Pat [kPa]: 85.8

POINTS ALONG PIPELINE

		1	2	3	5	6
Pi	[kPa]	77.237	32.428	34.548	25.350	20.780
Ui	[m/s]	25.312	34.906	15.535	16.819	17.542
Vi	[m^3/hr]	788.969	1087.991	1066.828	1157.168	1206.898
Rho	[kg/m^3]	1.890	1.370	1.395	1.288	1.235
1/2*Rho*v^2	[Pa]	605.318	834.742	168.302	192.213	190.043
Fr	v^2/gD	622.015	1182.854	157.696	184.840	201.069

TEST NUMBER :100C51

Read. No : 100C51
G [t/h]: 7
Q [kg/s]: .082
Load Ratio : 23.6
Pat [kPa]: 86

	POINTS ALONG PIPELINE 1	2	3	5	6
Pi [kPa]	26.778	22.089	13.594	9.958	5.711
Ui [m/s]	7.076	7.383	3.630	3.767	3.942
Vi [m^3/hr]	220.543	230.110	249.738	259.200	271.204
Rho [kg/m^3]	1.344	1.288	1.187	1.143	1.093
1/2*Rho*v^2 [Pa]	33.640	35.099	7.818	8.114	8.490
Fr v^2/gD	48.603	52.912	8.609	9.274	10.153

TEST NUMBER :100C5

Read. No : 100C52
G [t/h]: 12.5
Q [kg/s]: .100
Load Ratio : 34.5
Pat [kPa]: 86

	POINTS ALONG PIPELINE 1	2	3	5	6
Pi [kPa]	45.485	39.714	26.390	10.488	10.202
Ui [m/s]	7.423	7.764	3.934	4.583	4.596
Vi [m^3/hr]	231.371	241.992	270.682	315.293	316.229
Rho [kg/m^3]	1.564	1.495	1.337	1.148	1.144
1/2*Rho*v^2 [Pa]	42.087	45.061	10.345	12.080	12.085
Fr v^2/gD	53.493	58.517	10.114	13.722	13.804

TEST NUMBER :100C5

Read. No : 100C53
G [t/h]: 28
Q [kg/s]: .098
Load Ratio : 78.5
Pat [kPa]: 86

	POINTS ALONG PIPELINE 1	2	3	5	6
Pi [kPa]	82.352	78.178	56.693	12.072	16.891
Ui [m/s]	5.737	5.887	3.067	4.462	4.253
Vi [m^3/hr]	178.830	183.376	210.987	306.983	292.604
Rho [kg/m^3]	1.992	1.943	1.389	1.161	1.218
1/2*Rho*v^2 [Pa]	32.789	33.623	7.940	11.582	11.011
Fr v^2/gD	31.957	33.602	6.145	13.009	11.819

TEST NUMBER :100C5

Read. No : 100C54
G [t/h]: 34.2
Q [kg/s]: .085
Load Ratio : 111.5
Pat [kPa]: 86

		POINTS ALONG PIPELINE				
		1	2	3	5	6
Pi	[kPa]	83.203	79.960	62.364	9.742	19.754
Ui	[m/s]	4.922	5.018	2.543	3.941	3.568
Vi	[m^3/hr]	153.413	156.410	174.961	271.125	245.455
Rho	[kg/m^3]	1.999	1.960	1.752	1.131	1.249
1/2*Rho*v^2	[Pa]	24.207	24.680	5.666	8.780	7.949
Fr	v^2/gD	23.518	24.446	4.226	10.147	8.317

TEST NUMBER :100C5

Read. No : 100C54
G [t/h]: 34.2
Q [kg/s]: .085
Load Ratio : 111.5
Pat [kPa]: 86

POINTS ALONG PIPELINE
1 2 3 5 6

Pi [kPa] 83.203 79.960 62.364 9.742 19.754
Ui [m/s] 4.922 5.018 2.543 3.941 3.568
Vi [m^3/hr] 153.413 156.410 174.961 271.125 245.455
Rho [kg/m^3] 1.999 1.960 1.752 1.131 1.249
1/2*Rho*v^2 [Pa] 24.207 24.680 5.666 8.780 7.949
Fr v^2/gD 23.518 24.446 4.226 10.147 8.317

TEST NUMBER :100D1

Read. No : 100D11
Q [t/h]: 8.7
Q [kg/s]: .093
Load Ratio : 25.8
Pat [kPa]: 85.6

POINTS ALONG PIPELINE

1
****

Pi	[kPa]	23.928
Ui	[m/s]	8.661
Vi	[m^3/hr]	269.969
Rho	[kg/m^3]	1.246
1/2*Rho*v^2	[Pa]	46.748
Fr	v^2/gD	72.830

TEST NUMBER :100D1

Read. No : 100D12
Q [t/h]: 14.3
Q [kg/s]: .097
Load Ratio : 41.4
Pat [kPa]: 85.6

POINTS ALONG PIPELINE

1
****

Pi	[kPa]	22.293
Ui	[m/s]	8.368
Vi	[m^3/hr]	260.825
Rho	[kg/m^3]	1.341
1/2*Rho*v^2	[Pa]	46.949
Fr	v^2/gD	67.980

TEST NUMBER :100D1

Read. No : 100D13
Q [t/h]: 15
Q [kg/s]: .091
Load Ratio : 45.5
Pat [kPa]: 85.6

POINTS ALONG PIPELINE

1
****

Pi	[kPa]	44.370
Ui	[m/s]	7.147
Vi	[m^3/hr]	222.778
Rho	[kg/m^3]	1.477
1/2*Rho*v^2	[Pa]	37.729
Fr	v^2/gD	49.594

TEST NUMBER :100D1

Read. No : 100D14
G [t/h]: 15.5
Q [kg/s]: .094
Load Ratio : 45.5
Pat [kPa]: 85.6

POINTS ALONG PIPELINE

1

****

Pi	[kPa]	54.111
Ui	[m/s]	6.878
Vi	[m^3/hr]	214.371
Rho	[kg/m^3]	1.588
1/2*Rho*v^2	[Pa]	37.566
Fr	v^2/gD	45.921

TEST NUMBER :100D1

Read. No : 100D15
G [t/h]: 23.5
Q [kg/s]: .093
Load Ratio : 69.9
Pat [kPa]: 85.6

POINTS ALONG PIPELINE

1

****

Pi	[kPa]	82.832
Ui	[m/s]	5.609
Vi	[m^3/hr]	174.824
Rho	[kg/m^3]	1.922
1/2*Rho*v^2	[Pa]	30.239
Fr	v^2/gD	30.541

TEST NUMBER :100D2

Read. No : 100D21
Ġ [t/h]: 11
Q [kg/s]: .142
Load Ratio : 21.4
Pat [kPa]: 85.6

POINTS ALONG PIPELINE

1

****

Pi	[kPa]	36.740
Ui	[m/s]	11.802
Vi	[m^3/hr]	367.875
Rho	[kg/m^3]	1.392
1/2*Rho*v^2	[Pa]	96.918
Fr	v^2/gD	135.233

TEST NUMBER :100D2

Read. No : 100D22
Ġ [t/h]: 17
Q [kg/s]: .137
Load Ratio : 34.2
Pat [kPa]: 85.6

POINTS ALONG PIPELINE

1

****

Pi	[kPa]	48.788
Ui	[m/s]	10.415
Vi	[m^3/hr]	324.632
Rho	[kg/m^3]	1.528
1/2*Rho*v^2	[Pa]	82.897
Fr	v^2/gD	105.309

TEST NUMBER :100D2

Read. No : 100D23
Ġ [t/h]: 20
Q [kg/s]: .141
Load Ratio : 39.3
Pat [kPa]: 85.6

POINTS ALONG PIPELINE

1

****

Pi	[kPa]	53.040
Ui	[m/s]	10.202
Vi	[m^3/hr]	317.986
Rho	[kg/m^3]	1.598
1/2*Rho*v^2	[Pa]	83.182
Fr	v^2/gD	101.041

TEST NUMBER :100D2

Read. No : 100D24
G [t/h]: 26
Q [kg/s]: .138
Load Ratio : 52.0
Pat [kPa]: 85.6

POINTS ALONG PIPELINE

1

****

Pi	[kPa]	61.185
Ui	[m/s]	9.608
Vi	[m^3/hr]	299.486
Rho	[kg/m^3]	1.668
1/2*Rho*v^2	[Pa]	77.009
Fr	v^2/gD	89.626

TEST NUMBER :100D2

Read. No : 100D25
G [t/h]: 33
Q [kg/s]: .140
Load Ratio : 65.3
Pat [kPa]: 85.6

POINTS ALONG PIPELINE

1

****

Pi	[kPa]	62.724
Ui	[m/s]	9.610
Vi	[m^3/hr]	299.530
Rho	[kg/m^3]	1.686
1/2*Rho*v^2	[Pa]	77.845
Fr	v^2/gD	89.652

TEST NUMBER :100D3

Read. No : 100D31
Ġ [t/h]: 15
Q̇ [kg/s]: .206
Load Ratio : 20.1
Pat [kPa]: 85.6

POINTS ALONG PIPELINE

1
****

Pi	[kPa]	39.459
Ui	[m/s]	16.718
Vi	[m^3/hr]	521.099
Rho	[kg/m^3]	1.426
1/2*Rho*v^2	[Pa]	199.280
Fr	v^2/gD	271.345

TEST NUMBER :100D3

Read. No : 100D32
Ġ [t/h]: 18.5
Q̇ [kg/s]: .232
Load Ratio : 22.0
Pat [kPa]: 85.6

POINTS ALONG PIPELINE

1
****

Pi	[kPa]	48.618
Ui	[m/s]	17.557
Vi	[m^3/hr]	547.229
Rho	[kg/m^3]	1.531
1/2*Rho*v^2	[Pa]	235.959
Fr	v^2/gD	299.240

TEST NUMBER :100D3

Read. No : 100D33
Ġ [t/h]: 20.9
Q̇ [kg/s]: .233
Load Ratio : 24.8
Pat [kPa]: 85.6

POINTS ALONG PIPELINE

1
****

Pi	[kPa]	57.299
Ui	[m/s]	16.551
Vi	[m^3/hr]	515.874
Rho	[kg/m^3]	1.629
1/2*Rho*v^2	[Pa]	223.141
Fr	v^2/gD	265.930

TEST NUMBER :100D3

Read. No : 100D34
Ġ [t/h]: 24.5
Q [kg/s]: .219
Load Ratio : 31.0
Pat [kPa]: 85.6

POINTS ALONG PIPELINE

1
:**********

Pi	[kPa]	60.358
Ui	[m/s]	15.220
Vi	[m^3/hr]	474.391
Rho	[kg/m^3]	1.665
1/2*Rho*v^2	[Pa]	192.820
Fr	v^2/gD	224.882

TEST NUMBER :100D3

Read. No : 100D35
Ġ [t/h]: 26.9
Q [kg/s]: .230
Load Ratio : 32.4
Pat [kPa]: 85.6

POINTS ALONG PIPELINE

1
****

Pi	[kPa]	63.227
Ui	[m/s]	15.661
Vi	[m^3/hr]	488.159
Rho	[kg/m^3]	1.697
1/2*Rho*v^2	[Pa]	208.155
Fr	v^2/gD	238.124

TEST NUMBER :100D4

Read. No : 100D41
Ġ [t/h]: 10.8
Q̇ [kg/s]: .299
Load Ratio : 10.0
Pat [kPa]: 85.6

POINTS ALONG PIPELINE

1

****

Pi	[kPa]	39.350
Ui	[m/s]	23.978
Vi	[m^3/hr]	747.385
Rho	[kg/m^3]	1.442
1/2*Rho*v^2	[Pa]	414.393
Fr	v^2/gD	538.174

TEST NUMBER :100D4

Read. No : 100D42
Ġ [t/h]: 14.1
Q̇ [kg/s]: .300
Load Ratio : 13.0
Pat [kPa]: 85.6

POINTS ALONG PIPELINE

1

****

Pi	[kPa]	49.179
Ui	[m/s]	22.380
Vi	[m^3/hr]	697.573
Rho	[kg/m^3]	1.549
1/2*Rho*v^2	[Pa]	387.901
Fr	v^2/gD	486.250

TEST NUMBER :100D4

Read. No : 100D43
Ġ [t/h]: 18.7
Q̇ [kg/s]: .299
Load Ratio : 17.3
Pat [kPa]: 85.6

POINTS ALONG PIPELINE

1

****

Pi	[kPa]	58.339
Ui	[m/s]	21.022
Vi	[m^3/hr]	655.237
Rho	[kg/m^3]	1.644
1/2*Rho*v^2	[Pa]	363.184
Fr	v^2/gD	429.021

TEST NUMBER :100D4

Read. No : 100D44
G [t/h]: 23.1
Q [kg/s]: .294
Load Ratio : 21.7%
Pat [kPa]: 85.6

POINTS ALONG PIPELINE

1

****

Pi	[kPa]	66.018
Ui	[m/s]	19.803
Vi	[m^3/hr]	617.247
Rho	[kg/m^3]	1.720
1/2*Rho*v^2	[Pa]	337.255
Fr	v^2/gD	380.714

TEST NUMBER :100D4

Read. No : 100D45
G [t/h]: 23.5
Q [kg/s]: .292
Load Ratio : 22.3%
Pat [kPa]: 85.6

POINTS ALONG PIPELINE

1

****

Pi	[kPa]	68.049
Ui	[m/s]	19.381
Vi	[m^3/hr]	604.086
Rho	[kg/m^3]	1.740
1/2*Rho*v^2	[Pa]	326.831
Fr	v^2/gD	364.652

TEST NUMBER :100D5

Read. No : 100D51
Ġ [t/h]: 11.3
Q̇ [kg/s]: .359
Load Ratio : 8.73
Pat [kPa]: 85.6

POINTS ALONG PIPELINE

1
****

Pi	[kPa]	48.696
Ui	[m/s]	27.104
Vi	[m^3/hr]	844.812
Rho	[kg/m^3]	1.531
1/2*Rho*v^2	[Pa]	562.355
Fr	v^2/gD	713.183

TEST NUMBER :100D5

Read. No : 100D52
Ġ [t/h]: 12.2
Q̇ [kg/s]: .393
Load Ratio : 8.61
Pat [kPa]: 85.6

POINTS ALONG PIPELINE

1
****

Pi	[kPa]	57.423
Ui	[m/s]	28.220
Vi	[m^3/hr]	879.605
Rho	[kg/m^3]	1.610
1/2*Rho*v^2	[Pa]	640.959
Fr	v^2/gD	773.137

TEST NUMBER :100D5

Read. No : 100D53
Ġ [t/h]: 15.3
Q̇ [kg/s]: .391
Load Ratio : 10.8
Pat [kPa]: 85.6

POINTS ALONG PIPELINE

1
****

Pi	[kPa]	62.677
Ui	[m/s]	27.273
Vi	[m^3/hr]	850.075
Rho	[kg/m^3]	1.660
1/2*Rho*v^2	[Pa]	617.254
Fr	v^2/gD	722.097

TEST NUMBER :100D5

Read. No : 100D54
G [t/h]: 16.5
G [kg/s]: .391
Load Ratio : 11.7
Pat [kPa]: 85.6

POINTS ALONG PIPELINE

1
****

Pi	[kPa]	65.435
Ui	[m/s]	26.636
Vi	[m^3/hr]	830.219
Rho	[kg/m^3]	1.696
1/2*Rho*v^2	[Pa]	601.678
Fr	v^2/gD	688.758

TEST NUMBER :100D5

Read. No : 100D55
G [t/h]: 22.1
G [kg/s]: .556
Load Ratio : 17.2
Pat [kPa]: 85.6

POINTS ALONG PIPELINE

1
****

Pi	[kPa]	73.961
Ui	[m/s]	23.151
Vi	[m^3/hr]	721.594
Rho	[kg/m^3]	1.778
1/2*Rho*v^2	[Pa]	476.540
Fr	v^2/gD	520.314

TEST NUMBER :200A1

Read. No : 200A11
Q [t/h]: 7.6
Q [kg/s]: .049
Load Ratio : 42.7
Pat [kPa]: 86.6

		POINTS ALONG PIPELINE				
		1	2	3	5	6
		**********	**********	**********	**********	**********
Pi	[kPa]	88.638	84.186	22.602	7.857	10.478
Ui	[m/s]	2.713	2.784	4.354	5.033	4.897
Vi	[m^3/hr]	84.563	86.767	135.699	156.882	152.644
Rho	[kg/m^3]	2.104	2.051	1.311	1.134	1.166
1/2*Rho*v^2	[Pa]	7.742	7.945	12.426	14.366	13.978
Fr	v^2/gD	7.146	7.323	18.401	24.594	23.284

TEST NUMBER :200A1

Read. No : 200A12
Q [t/h]: 13
Q [kg/s]: .094
Load Ratio : 38.3
Pat [kPa]: 86.6

		POINTS ALONG PIPELINE				
		1	2	3	5	6
		**********	**********	**********	**********	**********
Pi	[kPa]	95.525	90.487	24.949	16.953	12.244
Ui	[m/s]	5.000	5.142	8.163	8.793	9.212
Vi	[m^3/hr]	155.835	160.248	254.431	274.076	287.134
Rho	[kg/m^3]	2.177	2.117	1.334	1.238	1.182
1/2*Rho*v^2	[Pa]	27.212	27.986	44.429	47.860	50.140
Fr	v^2/gD	24.267	25.667	64.687	75.063	82.385

TEST NUMBER :200A1

Read. No : 200A13
Q [t/h]: 14.1
Q [kg/s]: .099
Load Ratio : 39.1
Pat [kPa]: 86.6

		POINTS ALONG PIPELINE				
		1	2	3	5	6
		**********	**********	**********	**********	**********
Pi	[kPa]	105.535	99.301	33.056	20.435	15.152
Ui	[m/s]	5.031	5.200	7.946	9.031	9.500
Vi	[m^3/hr]	156.814	162.072	247.661	281.491	296.106
Rho	[kg/m^3]	2.294	2.220	1.453	1.278	1.215
1/2*Rho*v^2	[Pa]	29.037	30.011	45.860	52.124	54.830
Fr	v^2/gD	24.572	26.248	61.291	79.179	87.614

TEST NUMBER :200A1

Read. No : 200A14
Q [t/h]: 17.6
Q [kg/s]: .098
Load Ratio : 49.8
Pat [kPa]: 86.6

		POINTS ALONG PIPELINE 1	2	3	5	6
Pi	[kPa]	110.950	103.114	37.618	20.876	15.035
Ui	[m/s]	4.806	5.004	7.643	8.833	9.341
Vi	[m^3/hr]	149.790	155.978	238.219	275.324	291.151
Rho	[kg/m^3]	2.359	2.265	1.483	1.283	1.214
1/2*Rho*v^2	[Pa]	27.239	28.364	43.320	50.067	52.945
Fr	v^2/gD	22.421	24.311	56.706	75.749	84.706

TEST NUMBER :200A1

Read. No : 200A15
Q [t/h]: 18.7
Q [kg/s]: .10C
Load Ratio : 51.5
Pat [kPa]: 86.6

		POINTS ALONG PIPELINE 1	2	3	5	6
Pi	[kPa]	120.416	113.092	42.224	24.884	17.168
Ui	[m/s]	4.707	4.879	7.544	8.740	9.390
Vi	[m^3/hr]	146.711	152.092	235.741	272.430	292.687
Rho	[kg/m^3]	2.470	2.383	1.537	1.330	1.238
1/2*Rho*v^2	[Pa]	27.365	28.369	43.975	50.814	54.593
Fr	v^2/gD	21.508	23.115	55.542	74.163	85.603

TEST NUMBER :200A2

Read. No : 200A21
Ġ [t/h]: 9.5
Q̇ [kg/s]: .155.
Load Ratio : 16.9.
Pat [kPa]: 86.3

		POINTS ALONG PIPELINE				
		1	2	3	5	6
Pi	[kPa]	84.901	10.656	41 361	62.173	15.618
Ui	[m/s]	8.743	8.965	11.725	10.081	14.686
Vi	[m^3/hr]	272.511	79.439	365.451	314.224	457.760
Rho	*[kg/m^3]*	2.052	2.001	1.530	1.780	1.222
1/2*Rho*v^2	[Pa]	76.432	80.426	105.181	90.438	131.749
Fr	v^2/gD	74.207	78.029	133.456	98.664	209.390

TEST NUMBER :200A2

Read. No : 200A22
Ġ [t/h]: 12.2
Q̇ [kg/s]: .154
Load Ratio : 21.9.
Pat [kPa]: 86.3

		POINTS ALONG PIPELINE				
		1	2	3	5	6
Pi	[kPa]	94.612	89.399	42.567	66.074	14.281
Ui	[m/s]	8.231	8.476	11.556	9.773	14.806
Vi	[m^3/hr]	256.568	264.181	360.187	304.620	461.481
Rho	[kg/m^3]	2.168	2.106	1.544	1.826	1.205
1/2*Rho*v^2	[Pa]	73.448	75.627	103.111	87.204	132.109
Fr	v^2/gD	65.779	69.740	129.639	92.725	212.808

TEST NUMBER :200A2

Read. No : 200A23
Ġ [t/h]: 14.4
Q̇ [kg/s]: .151
Load Ratio : 26.7.
Pat [kPa]: 86.3

		POINTS ALONG PIPELINE				
		1	2	3	5	6
Pi	[kPa]	107.965	101.607	45.726	74.382	16.313
Ui	[m/s]	7.526	7.781	11.074	9.099	14.249
Vi	[m^3/hr]	234.591	242.529	345.182	283.621	444.122
Rho	[kg/m^3]	2.326	2.249	1.580	1.924	1.228
1/2*Rho*v^2	[Pa]	65.865	68.094	96.915	79.631	124.694
Fr	v^2/gD	54.993	58.777	119.063	80.382	197.100

TEST NUMBER :200A2

Read. No : 200A24
G [t/h]: 16.1
Q [kg/s]: .147
Load Ratio : 30.2
Pat [kPa]: 86.3

POINTS ALONG PIPELINE

		1	2	3	5	6
Pi	[kPa]	111.776	104.655	41.517	79.764	16.334
Ui	[m/s]	7.218	7.487	11.186	8.610	13.931
Vi	[m^3/hr]	224.989	233.[illegible]	348.661	268.360	434.213
Rho	[kg/m^3]	2.365	2.[illegible]	1.526	1.983	1.226
1/2*Rho*v^2	[Pa]	61.621	63.[illegible]	95.493	73.499	118.924
Fr	v^2/gD	50.583	54.[illegible]	121.475	71.964	188.402

TEST NUMBER :200A2

Read. No : 200A25
G [t/h]: 19.1
Q [kg/s]: .156
Load Ratio : 35.3
Pat [kPa]: 86.3

POINTS ALONG PIPELINE

		1	2	3	5	6
Pi	[kPa]	123.675	[illegible]	[illegible]	88.317	16.938
Ui	[m/s]	6.975	[illegible]	[illegible]	8.337	14.102
Vi	[m^3/hr]	216.151	[illegible]	[illegible]	259.869	439.545
Rho	[kg/m^3]	2.502	[illegible]	1.575	2.081	1.230
1/2*Rho*v^2	[Pa]	60.161	[illegible]	95.594	72.329	122.338
Fr	v^2/gD	46.687	[illegible]	117.877	67.482	193.058

TEST NUMBER :200A3

Read. No : 200A31
Θ [t/h]: 9.3
Q [kg/s]: .210
Load Ratio : 12.2
Pat [kPa]: 86.6

POINTS ALONG PIPELINE

		1	2	3	5	6
Pi	[kPa]	96.964	87.984	46.477	67.223	19.734
Ui	[m/s]	11.123	11.695	15.343	13.274	19.201
Vi	[m^3/hr]	346.690	364.529	478.229	413.730	598.500
Rho	[kg/m^3]	2.184	2.077	1.583	1.830	1.265
1/2*Rho*v^2	[Pa]	135.102	142.050	186.757	161.223	233.224
Fr	v^2/gD	120.111	132.784	228.535	171.047	357.939

TEST NUMBER :200A3

Read. No : 200A32
Θ [t/h]: 6.9
Q [kg/s]: .254
Load Ratio : 7.54
Pat [kPa]: 86.6

POINTS ALONG PIPELINE

		1	2	3	5	6
Pi	[kPa]	82.279	72.187	37.018	57.417	16.663
Ui	[m/s]	14.613	15.541	19.963	17.135	23.898
Vi	[m^3/hr]	455.465	484.414	622.228	534.092	744.878
Rho	[kg/m^3]	2.008	1.888	1.470	1.712	1.228
1/2*Rho*v^2	[Pa]	214.378	228.004	292.870	251.386	350.599
Fr	v^2/gD	207.296	234.485	386.883	285.045	554.435

TEST NUMBER :200A3

Read. No : 200A33
Θ [t/h]: 11.7
Q [kg/s]: .208
Load Ratio : 15.6
Pat [kPa]: 86.6

POINTS ALONG PIPELINE

		1	2	3	5	6
Pi	[kPa]	109.211	100.959	52.557	76.582	21.212
Ui	[m/s]	10.377	10.833	14.601	12.452	18.847
Vi	[m^3/hr]	323.442	337.672	455.122	388.116	587.444
Rho	[kg/m^3]	2.318	2.220	1.647	1.931	1.276
1/2*Rho*v^2	[Pa]	124..82	130.272	175.584	149.733	226.633
Fr	v^2/gD	104.538	113.938	206.984	150.524	344.837

TEST NUMBER :200A3

Read. No : 200A34
G [t/h]: 13.1
Q [kg/s]: .252
Load Ratio : 14.4
Pat [kPa]: 86.6

POINTS ALONG PIPELINE

		1	2	3	5	6
Pi	[kPa]	119.446	108.093	59.915	86.984	27.304
Ui	[m/s]	11.967	12.665	16.829	14.205	21.647
Vi	[m^3/hr]	372.997	394.748	524.551	442.753	674.731
Rho	[kg/m^3]	2.434	2.302	1.732	2.052	1.347
1/2*Rho*v^2	[Pa]	174.435	184.607	245.310	207.057	315.543
Fr	v^2/gD	139.025	155.711	274.952	195.886	454.928

TEST NUMBER :200A3

Read. No : 200A35
G [t/h]: 17.8
Q [kg/s]: .205
Load Ratio : 24.0
Pat [kPa]: 86.6

POINTS ALONG PIPELINE

		1	2	3	5	6
Pi	[kPa]	128.674	118.573	62.297	92.065	28.312
Ui	[m/s]	9.342	9.802	13.506	11.256	17.500
Vi	[m^3/hr]	291.174	305.509	420.979	350.837	545.481
Rho	[kg/m^3]	2.542	2.423	1.758	2.110	1.357
1/2*Rho*v^2	[Pa]	110.921	116.382	160.349	133.649	207.797
Fr	v^2/gD	84.720	93.267	177.093	122.996	297.331

TEST NUMBER :200A4

Read. No : 200A41
Ĝ [t/hJ: 9.8
Q̂ [kg/s]: .311
Load Ratio : 8.73
Pat [kPa]: 86.3

POINTS ALONG PIPELINE

		1	2	3	5	6
Pi	[kPa]	107.499	96.432	58.224	80.941	25.916
Ui	[m/s]	15.736	16.689	21.101	18.235	27.176
Vi	[m^3/hr]	490.473	520.178	657.702	568.361	847.057
Rho	[kg/m^3]	2.288	2.157	1.706	1.974	1.325
1/2*Rho*v^2	[Pa]	283.258	300.414	379.836	328.241	489.193
Fr	v^2/gD	240.387	270.386	432.253	322.797	716.977

TEST NUMBER :200A4

Read. No : 200A42
Ĝ [t/hJ: 11.1
Q̂ [kg/s]: .311
Load Ratio : 9.98
Pat [kPa]: 86.3

POINTS ALONG PIPELINE

		1	2	3	5	6
Pi	[kPa]	115.063	103.747	63.039	85.539	28.814
Ui	[m/s]	15.263	16.172	20.580	17.885	26.699
Vi	[m^3/hr]	475.738	504.064	641.464	557.475	832.186
Rho	[kg/m^3]	2.360	2.227	1.750	2.014	1.349
1/2*Rho*v^2	[Pa]	274.839	291.204	370.581	322.060	480.764
Fr	v^2/gD	226.160	253.894	411.174	310.550	692.024

TEST NUMBER :200A4

Read. No : 200A43
Ĝ [t/hJ: 13.6
Q̂ [kg/s]: .308
Load Ratio : 12.23
Pat [kPa]: 86.3

POINTS ALONG PIPELINE

		1	2	3	5	6
Pi	[kPa]	127.588	114.350	69.956	96.403	32.252
Ui	[m/s]	14.342	15.289	19.632	16.790	25.876
Vi	[m^3/hr]	447.044	476.539	611.930	523.349	806.548
Rho	[kg/m^3]	2.486	2.332	1.816	2.123	1.378
1/2*Rho*v^2	[Pa]	255.644	272.511	349.935	299.280	461.228
Fr	v^2/gD	199.702	226.923	374.183	273.693	650.041

TEST NUMBER :200A4

Read. No : 200A44
Ġ [t/h]: 15.8
Q̇ [kg/s]: .306
Load Ratio : 14.3
Pat [kPa]: 86.3

		POINTS ALONG PIPELINE 1	2	3	5	6
Pi	[kPa]	134.911	122.708	73.483	102.712	33.244
Ui	[m/s]	13.791	14.596	19.093	16.141	25.520
Vi	[m^3/hr]	429.866	454.966	595.128	503.097	795.449
Rho	[kg/m^3]	2.565	2.424	1.853	2.192	1.386
1/2*Rho*v^2	[Pa]	243.931	258.173	337.709	285.486	451.383
Fr	v^2/gD	184.649	206.841	353.917	252.921	632.274

TEST NUMBER :200A4

Read. No : 200A45
Ġ [t/h]: 17.6
Q̇ [kg/s]: .308
Load Ratio : 15.8
Pat [kPa]: 86.3

		POINTS ALONG PIPELINE 1	2	3	5	6
Pi	[kPa]	142.393	130.347	75.162	110.266	35.542
Ui	[m/s]	13.462	14.210	19.067	15.662	25.268
Vi	[m^3/hr]	419.602	442.933	594.321	488.183	787.580
Rho	[kg/m^3]	2.646	2.507	1.868	2.274	1.410
1/2*Rho*v^2	[Pa]	239.774	253.106	339.613	278.963	450.047
Fr	v^2/gD	175.937	196.046	352.957	238.148	619.826

TEST NUMBER :200A5

Read. No : 200A51
G [t/h]: 7.8
Q [kg/s]: .418
Load Ratio : 5.17
Pat [kPa]: 86.6

POINTS ALONG PIPELINE

		1	2	3	5	6
Pi	[kPa]	112.224	98.369	47.085	79.745	32.743
Ui	[m/s]	20.542	22.081	30.551	24.553	34.223
Vi	[m^3/hr]	640.285	688.244	952.267	765.303	1066.710
Rho	[kg/m^3]	2.354	2.190	1.583	1.970	1.413
1/2*Rho*v^2	[Pa]	496.710	533.914	738.734	593.694	827.514
Fr	v^2/gD	409.664	473.331	906.146	585.258	1137.033

TEST NUMBER :200A5

Read. No : 200A52
G [t/h]: 8.9
Q [kg/s]: .415
Load Ratio : 5.95
Pat [kPa]: 86.6

POINTS ALONG PIPELINE

		1	2	3	5	6
Pi	[kPa]	119.382	104.149	57.110	86.011	36.209
Ui	[m/s]	19.864	21.450	28.471	23.704	33.317
Vi	[m^3/hr]	619.150	668.596	887.436	738.850	1038.469
Rho	[kg/m^3]	2.416	2.237	1.685	2.024	1.440
1/2*Rho*v^2	[Pa]	476.607	514.669	683.127	568.749	799.389
Fr	v^2/gD	383.065	446.692	786.964	545.498	1077.626

TEST NUMBER :200A5

Read. No : 200A53
G [t/h]: 11.4
Q [kg/s]: .367
Load Ratio : 8.61
Pat [kPa]: 86.6

POINTS ALONG PIPELINE

		1	2	3	5	6
Pi	[kPa]	125.146	110.211	64.064	92.377	37.967
Ui	[m/s]	17.185	18.489	24.153	20.332	29.212
Vi	[m^3/hr]	535.660	576.307	752.826	633.732	910.540
Rho	[kg/m^3]	2.470	2.296	1.758	2.088	1.453
1/2*Rho*v^2	[Pa]	364.789	392.471	512.682	431.577	620.086
Fr	v^2/gD	286.721	331.886	566.331	401.321	828.474

TEST NUMBER :200A5

Read. No : 200A54
Ġ [t/h]: 13.9
Q̇ [kg/s]: .407
Load Ratio : 9.4ℓ
Pat [kPa]: 86.6

POINTS ALONG PIPELINE

		1	2	3	5	6
Pi	[kPa]	145.938	127.065	76.110	107.785	47.389
Ui	[m/s]	17.394	18.930	24.858	20.808	30.187
Vi	[m^3/hr]	542.153	590.041	774.818	648.563	940.905
Rho	[kg/m^3]	2.704	2.485	1.892	2.261	1.558
1/2*Rho*v^2	[Pa]	409.084	445.218	584.643	489.377	709.965
Fr	v^2/gD	293.714	347.892	599.902	420.325	884.651

TEST NUMBER :200A5

Read. No : 200A55
Ġ [t/h]: 16.7
Q̇ [kg/s]: .363
Load Ratio : 12.7
Pat [kPa]: 86.6

POINTS ALONG PIPELINE

		1	2	3	5	6
Pi	[kPa]	151.347	133.911	83.154	115.635	48.728
Ui	[m/s]	15.214	16.417	21.325	17.900	26.750
Vi	[m^3/hr]	474.201	511.696	664.697	557.938	833.785
Rho	[kg/m^3]	2.789	2.556	1.968	2.345	1.569
1/2*Rho*v^2	[Pa]	319.236	344.478	447.480	375.608	561.311
Fr	v^2/gD	224.701	261.641	441.497	311.066	694.687

TEST NUMBER :200B2

Read. No : 200B21
G [t/h]: 5.5
Q [kg/s]: .145
Load Ratio : 10.5
Pat [kPa]: 85.6

POINTS ALONG PIPELINE

1
****

Pi	[kPa]	33.561
Ui	[m/s]	12.361
Vi	[m^3/hr]	385.289
Rho	[kg/m^3]	1.356
1/2*Rho*v^2	[Pa]	103.607
Fr	v^2/gD	148.339

TEST NUMBER :200B2

Read. No : 200322
G [t/h]: 6.4
Q [kg/s]: .138
Load Ratio : 12.8
Pat [kPa]: 85.6

POINTS ALONG PIPELINE

1
****

Pi	[kPa]	44.050
Ui	[m/s]	10.839
Vi	[m^3/hr]	337.838
Rho	[kg/m^3]	1.476
1/2*Rho*v^2	[Pa]	86.717
Fr	v^2/gD	114.051

TEST NUMBER :200B2

Read. No : 200B23
G [t/h]: 7.9
Q [kg/s]: .140
Load Ratio : 15.4
Pat [kPa]: 85.6

POINTS ALONG PIPELINE

1
****

Pi	[kPa]	49.233
Ui	[m/s]	10.559
Vi	[m^3/hr]	329.115
Rho	[kg/m^3]	1.536
1/2*Rho*v^2	[Pa]	85.646
Fr	v^2/gD	108.237

TEST NUMBER :200B2

Read. No : 200B21
Ġ [t/h]: 5.5
Q [kg/s]: .145
Load Ratio : 10.5
Pat [kPa]: 85.6

POINTS ALONG PIPELINE

1

****

Pi	[kPa]	33.561
Ui	[m/s]	12.361
Vi	[m^3/hr]	385.289
Rho	[kg/m^3]	1.356
1/2*Rho*v^2	[Pa]	103.607
Fr	v^2/gD	148.339

TEST NUMBER :200B2

Read. No : 200B22
Ġ [t/h]: 6.4
Q [kg/s]: .138
Load Ratio : 12.8
Pat [kPa]: 85.6

POINTS ALONG PIPELINE

1

****

Pi	[kPa]	44.050
Ui	[m/s]	10.839
Vi	[m^3/hr]	337.838
Rho	[kg/m^3]	1.476
1/2*Rho*v^2	[Pa]	86.717
Fr	v^2/gD	114.051

TEST NUMBER :200B2

Read. No : 200B23
Ġ [t/h]: 7.9
Q [kg/s]: .140
Load Ratio : 15.1
Pat [kPa]: 85.6

POINTS ALONG PIPELINE

1

****

Pi	[kPa]	49.233
Ui	[m/s]	10.559
Vi	[m^3/hr]	329.115
Rho	[kg/m^3]	1.536
1/2*Rho*v^2	[Pa]	85.646
Fr	v^2/gD	108.237

TEST NUMBER :20082

Read. No : 200824
G [t/h]: 17
Q [kg/s]: .142
Load Ratio : 33.2
Pat [kPa]: 85.6

POINTS ALONG PIPELINE

1

****

Pi	[kPa]	69.789
Ui	[m/s]	9.287
Vi	[m^3/hr]	289.469
Rho	[kg/m^3]	1.767
1/2*Rho*v^2	[Pa]	76.214
Fr	v^2/gD	83.731

TEST NUMBER :20082

Read. No : 200825
G [t/h]: 9.2
Q [kg/s]: .145
Load Ratio : 17.6
Pat [kPa]: 85.6

POINTS ALONG PIPELINE

1

****

Pi	[kPa]	51.630
Ui	[m/s]	10.751
Vi	[m^3/hr]	335.105
Rho	[kg/m^3]	1.559
1/2*Rho*v^2	[Pa]	90.101
Fr	v^2/gD	112.213

TEST NUMBER :200B3

Read. No : 200B31
Q̇ [t/h]: 5.9
ρ̇ [kg/s]: .210
Load Ratio : 7.79
Pat [kPa]: 85.6

POINTS ALONG PIPELINE

1
****

Pi	[kPa]	39.302
Ui	[m/s]	17.007
Vi	[m^3/hr]	530.106
Rho	[kg/m^3]	1.428
1/2*Rho*v^2	[Pa]	206.468
Fr	v^2/gD	280.806

TEST NUMBER :200B3

Read. No : 200B32
Q̇ [t/h]: 6.3
ρ̇ [kg/s]: .237
Load Ratio : 7.36
Pat [kPa]: 85.6

POINTS ALONG PIPELINE

1
****

Pi	[kPa]	44.522
Ui	[m/s]	18.520
Vi	[m^3/hr]	577.262
Rho	[kg/m^3]	1.482
1/2*Rho*v^2	[Pa]	254.215
Fr	v^2/gD	332.986

TEST NUMBER :200B3

Read. No : 200B33
Q̇ [t/h]: 10.6
ρ̇ [kg/s]: .231
Load Ratio : 12.7
Pat [kPa]: 85.6

POINTS ALONG PIPELINE

1
****

Pi	[kPa]	64.912
Ui	[m/s]	15.632
Vi	[m^3/hr]	487.235
Rho	[kg/m^3]	1.709
1/2*Rho*v^2	[Pa]	208.779
Fr	v^2/gD	237.223

TEST NUMBER :200B3

Read. No : 200B34
G [t/h]: 9.7
Q [kg/s]: .230
Load Ratio : 11.6
Pat [kPa]: 85.6

POINTS ALONG PIPELINE

	1
Pi [kPa]	44.410
Ui [m/s]	18.072
Vi [m^3/hr]	563.292
Rho [kg/m^3]	1.475
1/2*Rho*v^2 [Pa]	240.902
Fr v^2/gD	317.065

TEST NUMBER :200B3

Read. No : 200B35
G [t/h]: 8.5
Q [kg/s]: .24
Load Ratio : 9.8
Pat [kPa]: 85.6

POINTS ALONG PIPELINE

	1
Pi [kPa]	41.727
Ui [m/s]	19.202
Vi [m^3/hr]	598.523
Rho [kg/m^3]	1.444
1/2*Rho*v^2 [Pa]	266.232
Fr v^2/gD	357.966

TEST NUMBER :200B4

Read. No : 200B41
G [t/h]: 6.7
Ö [kg/s]: .300
Load Ratio : 6.19
Pat [kPa]: 85.6

POINTS ALONG PIPELINE

1
****

Pi	[kPa]	44.978
Ui	[m/s]	23.026
Vi	[m^3/hr]	717.698
Rho	[kg/m^3]	1.507
1/2*Rho*v^2	[Pa]	399.360
Fr	v^2/gD	514.711

TEST NUMBER :200B4

Read. No : 200B42
G [t/h]: 8.2
Ö [kg/s]: .294
Load Ratio : 7.72
Pat [kPa]: 85.6

POINTS ALONG PIPELINE

1
****

Pi	[kPa]	58.454
Ui	[m/s]	20.581
Vi	[m^3/hr]	641.509
Rho	[kg/m^3]	1.654
1/2*Rho*v^2	[Pa]	350.250
Fr	v^2/gD	411.232

TEST NUMBER :200B4

Read. No : 200B43
G [t/h]: 13.6
Ö [kg/s]: .296
Load Ratio : 12.7
Pat [kPa]: 85.6

POINTS ALONG PIPELINE

1
****

Pi	[kPa]	73.734
Ui	[m/s]	18.768
Vi	[m^3/hr]	584.975
Rho	[kg/m^3]	1.824
1/2*Rho*v^2	[Pa]	321.250
Fr	v^2/gD	341.944

TEST NUMBER :200B44

Read. No : 200B44
G [t/h]: 9.9
Q [kg/s]: .294
Load Ratio : 9.34
Pat [kPa]: 85.6

POINTS ALONG PIPELINE

1

****

Pi	[kPa]	58.108
Ui	[m/s]	20.767
Vi	[m^3/hr]	647.303
Rho	[kg/m^3]	1.636
1/2*Rho*v^2	[Pa]	352.823
Fr	v^2/gD	418.693

TEST NUMBER :200B45

Read. No : 200B45
G [t/h]: 7.8
Q [kg/s]: .297
Load Ratio : 7.28
Pat [kPa]: 85.6

POINTS ALONG PIPELINE

1

****

Pi	[kPa]	51.669
Ui	[m/s]	22.128
Vi	[m^3/hr]	689.715
Rho	[kg/m^3]	1.552
1/2*Rho*v^2	[Pa]	379.994
Fr	v^2/gD	475.337

TEST NUMBER :20085

Read. No : 20085
Q [t/h]: 4.3
Q [kg/s]: .433
Load Ratio : 2.75
Pat [kPa]: 85.5

POINTS ALONG PIPELINE

1

****

Pi	[kPa]	50.926
Ui	[m/s]	31.969
Vi	[m^3/hr]	996.448
Rho	[kg/m^3]	1.565
1/2*Rho*v^2	[Pa]	799.582
Fr	v^2/gD	992.178

TEST NUMBER :20085

Read. No : 20085
Q [t/h]: 7.3
Q [kg/s]: .430
Load Ratio : 4.71
Pat [kPa]: 85.5

POINTS ALONG PIPELINE

1

****

Pi	[kPa]	58.951
Ui	[m/s]	30.211
Vi	[m^3/hr]	941.673
Rho	[kg/m^3]	1.644
1/2*Rho*v^2	[Pa]	750.406
Fr	v^2/gD	836.096

TEST NUMBER :20085

Read. No : 20085
Q [t/h]: 9
Q [kg/s]: .426
Load Ratio : 5.86
Pat [kPa]: 85.5

POINTS ALONG PIPELINE

1

****

Pi	[kPa]	65.315
Ui	[m/s]	28.923
Vi	[m^3/hr]	901.502
Rho	[kg/m^3]	1.703
1/2*Rho*v^2	[Pa]	712.461
Fr	v^2/gD	812.108

TEST NUMBER :20085

Read. No : 200854
Ġ [t/h]: 15
Ḋ [kg/s]: .420
Load Ratio : 9.90
Pat [kPa]: 85.5

POINTS ALONG PIPELINE

1
****

Pi	[kPa]	79.421
Ui	[m/s]	26.209
Vi	[m^3/hr]	816.908
Rho	[kg/m^3]	1.854
1/2*Rho*v^2	[Pa]	636.627
Fr	v^2/gD	666.848

TEST NUMBER :20085

Read. No : 200855
Ġ [t/h]: 6.6
Ḋ [kg/s]: .421
Load Ratio : 4.35
Pat [kPa]: 85.5

POINTS ALONG PIPELINE

1
****

Pi	[kPa]	56.798
Ui	[m/s]	30.685
Vi	[m^3/hr]	956.441
Rho	[kg/m^3]	1.585
1/2*Rho*v^2	[Pa]	746.107
Fr	v^2/gD	914.106

TEST NUMBER :200C2

Read. No : 200C21
G [t/h]: 8.8
Q [kg/s]: .293
Load Ratio : 8.32
Pat [kPa]: 85.9

POINTS ALONG PIPELINE

1

****

Pi	[kPa]	58.285
Ui	[m/s]	21.193
Vi	[m^3/hr]	660.586
Rho	[kg/m^3]	1.599
1/2*Rho*v^2	[Pa]	359.197
Fr	v^2/gD	436.053

TEST NUMBER :200C2

Read. No : 200C22
G [t/h]: 9.1
Q [kg/s]: .294
Load Ratio : 8.57
Pat [kPa]: 85.9

POINTS ALONG PIPELINE

1

****

Pi	[kPa]	63.309
Ui	[m/s]	20.596
Vi	[m^3/hr]	641.980
Rho	[kg/m^3]	1.653
1/2*Rho*v^2	[Pa]	350.663
Fr	v^2/gD	411.835

TEST NUMBER :200C2

Read. No : 200C23
G [t/h]: 6.2
Q [kg/s]: .292
Load Ratio : 5.88
Pat [kPa]: 85.9

POINTS ALONG PIPELINE

1

****

Pi	[kPa]	45.223
Ui	[m/s]	23.334
Vi	[m^3/hr]	727.383
Rho	[kg/m^3]	1.449
1/2*Rho*v^2	[Pa]	394.430
Fr	v^2 gD	528.697

TEST NUMBER :200C2

Read. No : 200C24
G [t/h]: 3.5
Q [kg/s]: .293
Load Ratio : 3.31
Pat [kPa]: 85.9

POINTS ALONG PIPELINE

1
**********v**********

Pi	[kPa]	27.316
Ui	[m/s]	27.143
Vi	[m^3/hr]	846.027
Rho	[kg/m^3]	1.247
1/2*Rho*v^2	[Pa]	459.505
Fr	v^2/gD	715.235

TEST NUMBER :200C2

Read. No : 200C25
G [t/h]: 15.1
Q [kg/s]: .291
Load Ratio : 14.4
Pat [kPa]: 85.9

POINTS ALONG PIPELINE

1
****

Pi	[kPa]	71.708
Ui	[m/s]	19.306
Vi	[m^3/hr]	604.244
Rho	[kg/m^3]	1.734
1/2*Rho*v^2	[Pa]	325.784
Fr	v^2/gD	364.842

TEST NUMBER :200C3

Read. No : 200C31
G [t/h]: 11.3
Q [kg/s]: .446
Load Ratio : 7.03
Pat [kPa]: 86

POINTS ALONG PIPELINE

1

****

Pi	[kPa]	82.809
Ui	[m/s]	27.437
Vi	[m^3/hr]	855.198
Rho	[kg/m^3]	1.878
1/2*Rho*v^2	[Pa]	706.870
Fr	v^2/gD	730.826

TEST NUMBER :200C3

Read. No : 200C32
G [t/h]: 7.6
Q [kg/s]: .446
Load Ratio : 4.72
Pat [kPa]: 86

POINTS ALONG PIPELINE

1

****

Pi	[kPa]	73.319
Ui	[m/s]	29.258
Vi	[m^3/hr]	911.963
Rho	[kg/m^3]	1.762
1/2*Rho*v^2	[Pa]	754.220
Fr	v^2/gD	831.065

TEST NUMBER :200C3

Read. No : 200C33
G [t/h]: 15.9
Q [kg/s]: .445
Load Ratio : 9.90
Pat [kPa]: 86

POINTS ALONG PIPELINE

1

****

Pi	[kPa]	75.039
Ui	[m/s]	29.067
Vi	[m^3/hr]	905.998
Rho	[kg/m^3]	1.772
1/2*Rho*v^2	[Pa]	748.382
Fr	v^2/gD	820.229

TEST NUMBER :200C3

Read. No : 200C34
G [t/h]: 13
Q [kg/s]: .450
Load Ratio : 8.01
Pat [kPa]: 86

POINTS ALONG PIPELINE

1
****

Pi	[kPa]	66.380
Ui	[m/s]	31.133
Vi	[m^3/hr]	970.391
Rho	[kg/m^3]	1 672
1/2*Rho*v^2	[Pa]	810.183
Fr	v^2/gD	940.967

TEST NUMBER :200C3

Read. No : 200C35
G [t/h]: 3.2
Q [kg/s]: .445
Load Ratio : 1.99
Pat [kPa]: 86

POINTS ALONG PIPELINE

1
****

Pi	[kPa]	45.034
Ui	[m/s]	35.883
Vi	[m^3/hr]	1118.471
Rho	[kg/m^3]	1.434
1/2*Rho*v^2	[Pa]	923.480
Fr	v^2/gD	1250.058

TEST NUMBER :200C4

Read. No : 200C41
G [t/h]: 3.2
Q [kg/s]: .427
Load Ratio : 2.08
Pat [kPa]: 85.7

POINTS ALONG PIPELINE

1

****

Pi	[kPa]	40.072
Ui	[m/s]	34.707
Vi	[m^3/hr]	1081.809
Rho	[kg/m^3]	1.421
1/2*Rho*v^2	[Pa]	856.160
Fr	v^2/gD	1169.451

TEST NUMBER :200C4

Read. No : 200C42
G [t/h]: 4.3
Q [kg/s]: .422
Load Ratio : 2.82
Pat [kPa]: 85.7

POINTS ALONG PIPELINE

1

****

Pi	[kPa]	55.430
Ui	[m/s]	30.947
Vi	[m^3/hr]	964.613
Rho	[kg/m^3]	1.579
1/2*Rho*v^2	[Pa]	755.943
Fr	v^2/gD	929.795

TEST NUMBER :200C4

Read. No : 200C43
G [t/h]: 5.6
Q [kg/s]: .420
Load Ratio : 3.70
Pat [kPa]: 85.7

POINTS ALONG PIPELINE

1

****

Pi	[kPa]	69.950
Ui	[m/s]	28.010
Vi	[m^3/hr]	873.055
Rho	[kg/m^3]	1.733
1/2*Rho*v^2	[Pa]	679.667
Fr	v^2/gD	761.666

TEST NUMBER :200C4

Read. No : 200C44
G [t/h]: 12.3
Q [kg/s]: .418
Load Ratio : 8.16
Pat [kPa]: 85.7

POINTS ALONG PIPELINE

1

****

Pi	[kPa]	79.336
Ui	[m/s]	26.393
Vi	[m^3/hr]	822.e53
Rho	[kg/m^3]	1.832
1/2*Rho*v^2	[Pa]	638.064
Fr	v^2/gD	676.260

TEST NUMBER :200C4

Read. No : 200C45
G [t/h]: 14.7
Q [kg/s]: .419
Load Ratio : 9.73
Pat [kPa]: 85.7

POINTS ALONG PIPELINE

1

****

Pi	[kPa]	91.231
Ui	[m/s]	24.700
Vi	[m^3/hr]	769.891
Rho	[kg/m^3]	1.960
1/2*Rho*v^2	[Pa]	598.000
Fr	v^2/gD	592.296

TEST NUMBER :200C51

Read. No : 200C51
G [t/hl]: 2.2
Q [kg/s]: .511
Load Ratio : 1.19
Pat [kPa]: 85.7

POINTS ALONG PIPELINE

1
****

Pi	[kPa]	40.299
Ui	[m/s]	41.867
Vi	[m^3/hr]	1304.970
Rho	[kg/m^3]	1.410
1/2*Rho*v^2	[Pa]	1235.746
Fr	v^2/gD	1701.696

TEST NUMBER :200C52

Read. No : 200C52
G [t/hl]: 6
Q [kg/s]: .507
Load Ratio : 3.28
Pat [kPa]: 85.7

POINTS ALONG PIPELINE

1
****

Pi	[kPa]	59.427
Ui	[m/s]	36.397
Vi	[m^3/hr]	1134.489
Rho	[kg/m^3]	1.609
1/2*Rho*v^2	[Pa]	1065.812
Fr	v^2/gD	1286.118

TEST NUMBER :200C53

Read. No : 200C53
G [t/hl]: 12.4
Q [kg/s]: .501
Load Ratio : 6.87
Pat [kPa]: 85.7

POINTS ALONG PIPELINE

1
****

Pi	[kPa]	78.816
Ui	[m/s]	31.881
Vi	[m^3/hr]	993.705
Rho	[kg/m^3]	1.816
1/2*Rho*v^2	[Pa]	923.059
Fr	v^2/gD	986.724

TEST NUMBER :200C5

Read. No : 200C54
G [t/h]: 16.2
Q [kg/s]: .492
Load Ratio : 9.14
Pat [kPa]: 85.7

POINTS ALONG PIPELINE

1
****

Pi	[kPa]	94.264
Ui	[m/s]	28.718
Vi	[m^3/hr]	895.139
Rho	[kg/m^3]	1.979
1/2*Rho*v^2	[Pa]	816.217
Fr	v^2/gD	800.685

TEST NUMBER :200C5

Read. No : 200C55
G [t/h]: 17.1
Q [kg/s]: .492
Load Ratio : 9.64
Pat [kPa]: 85.7

POINTS ALONG PIPELINE

1
****

Pi	[kPa]	91.995
Ui	[m/s]	29.152
Vi	[m^3/hr]	908.643
Rho	[kg/m^3]	1.951
1/2*Rho*v^2	[Pa]	829.015
Fr	v^2/gD	825.025

TEST NUMBER :400A11

Read. No : 400A11
Ġ [t/h]: 5.4
Q̇ [kg/s]: .147
Load Ratio : 10.1
Pat [kPa]: 86

POINTS ALONG PIPELINE

1
****

Pi	[kPa]	38.697
Ui	[m/s]	11.800
Vi	[m^3/hr]	367.796
Rho	[kg/m^3]	1.441
1/2*Rho*v^2	[Pa]	100.296
Fr	v^2/gD	135.175

TEST NUMBER :400A12

Read. No : 400A12
Ġ [t/h]: 10.7
Q̇ [kg/s]: .145
Load Ratio : 20.3
Pat [kPa]: 86

POINTS ALONG PIPELINE

1
****

Pi	[kPa]	65.646
Ui	[m/s]	9.635
Vi	[m^3/hr]	300.331
Rho	[kg/m^3]	1.747
1/2*Rho*v^2	[Pa]	81.093
Fr	v^2/gD	90.132

TEST NUMBER :400A13

Read. No : 400A13
Ġ [t/h]: 14.4
Q̇ [kg/s]: .145
Load Ratio : 27.4
Pat [kPa]: 86

POINTS ALONG PIPELINE

1
****

Pi	[kPa]	61.015
Ui	[m/s]	9.939
Vi	[m^3/hr]	309.781
Rho	[kg/m^3]	1.696
1/2*Rho*v^2	[Pa]	83.757
Fr	v^2/gD	95.893

TEST NUMBER :400A1

Read. No : 400A14
G [t/h]: 16.8
Q [kg/s]: .144
Load Rati : 32.2
Pat [kPa]: 86

POINTS ALONG PIPELINE

1
****

Pi	[kPa]	70.375
Ui	[m/s]	9.266
Vi	[m^3/hr]	288.810
Rho	[kg/m^3]	1.802
1/2*Rho*v^2	[Pa]	77.343
Fr	v^2/gD	83.350

TEST NUMBER :400A1

Read. No : 400A15
G [t/h]: 18.7
Q [kg/s]: .143
Load Ratio : 36.1
Pat [kPa]: 96

POINTS ALONG PIPELINE

1
****

Pi	[kPa]	77.032
Ui	[m/s]	8.839
Vi	[m^3/hr]	275.523
Rho	[kg/m^3]	1.878
1/2*Rho*v^2	[Pa]	73.360
Fr	v^2/gD	75.857

TEST NUMBER :400A2

Read. No : 400A21
G [t/h]: 6.1
Q [kg/s]: .255
Load Ratio : 6.63
Pat [kPa]: 86

POINTS ALONG PIPELINE

1

****

Pi	[kPa]	56.274
Ui	[m/s]	17.977
Vi	[m^3/hr]	560.339
Rho	[kg/m^3]	1.640
1/2*Rho*v^2	[Pa]	265.057
Fr	v^2/gD	313.749

TEST NUMBER :400A2

Read. No : 400A22
G [t/h]: 10.3
Q [kg/s]: .258
Load Ratio : 11.07
Pat [kPa]: 86

POINTS ALONG PIPELINE

1

****

Pi	[kPa]	64.316
Ui	[m/s]	17.246
Vi	[m^3/hr]	537.559
Rho	[kg/m^3]	1.729
1/2*Rho*v^2	[Pa]	257.201
Fr	v^2/gD	288.757

TEST NUMBER :400A2

Read. No : 400A23
G [t/h]: 12.5
Q [kg/s]: .240
Load Ratio : 14.4
Pat [kPa]: 86

POINTS ALONG PIPELINE

1

****

Pi	[kPa]	68.367
Ui	[m/s]	15.699
Vi	[m^3/hr]	489.343
Rho	[kg/m^3]	1.773
1/2*Rho*v^2	[Pa]	218.466
Fr	v^2/gD	239.280

TEST NUMBER :400A2

Read. No : 400A24
Ġ [t/h]: 15.3
Q [kg/s]: .244
Load Ratio : 17.6
Pat [kPa]: 86

POINTS ALONG PIPELINE

1
****

Pi	[kPa]	75.524
Ui	[m/s]	15.242
Vi	[m^3/hr]	475.078
Rho	[kg/m^3]	1.854
1/2*Rho*v^2	[Pa]	215.295
Fr	v^2/gD	225.533

TEST NUMBER :400A2

Read. No : 400A25
Ġ [t/h]: 23.2
Q [kg/s]: .242
Load Ratio : 26.5
Pat [kPa]: 86

POINTS ALONG PIPELINE

1
****

Pi	[kPa]	82.002
Ui	[m/s]	14.545
Vi	[m^3/hr]	453.363
Rho	[kg/m^3]	1.926
1/2*Rho*v^2	[Pa]	203.695
Fr	v^2/gD	205.387

TEST NUMBER :400A3

Read. No : 400A31
Ġ [t/h]: 7.9
Q̇ [kg/s]: .29
Load Ratio : 7.27
Pat [kPa]: 86

POINTS ALONG PIPELINE

1
****

Pi	[kPa]	51.816
Ui	[m/s]	21.760
Vi	[m^3/hr]	678.262
Rho	[kg/m^3]	1.581
1/2*Rho*v^2	[Pa]	374.300
Fr	v^2/gD	459.702

TEST NUMBER :400A3

Read. No : 400A32
Ġ [t/h]: 9.9
Q̇ [kg/s]: .294
Load Ratio : 9.35
Pat [kPa]: 86

POINTS ALONG PIPELINE

1
****

Pi	[kPa]	63.249
Ui	[m/s]	19.900
Vi	[m^3/hr]	620.279
Rho	[kg/m^3]	1.707
1/2*Rho*v^2	[Pa]	337.979
Fr	v^2/gD	384.464

TEST NUMBER :400A3

Read. No : 400A33
Ġ [t/h]: 11.7
Q̇ [kg/s]: .293
Load Ratio : 16.7
Pat [kPa]: 86

POINTS ALONG PIPELINE

1
****

Pi	[kPa]	85.058
Ui	[m/s]	17.435
Vi	[m^3/hr]	543.430
Rho	[kg/m^3]	1.948
1/2*Rho*v^2	[Pa]	295.994
Fr	v^2/gD	295.099

TEST NUMBER :400A3

Read. No : 400A34
Ġ [t/h]: 11.6
Q̇ [kg/s]: .294
Load Ratio : 10.9
Pat [kPa]: 86

POINTS ALONG PIPELINE

1

****

Pi	[kPa]	69.019
Ui	[m/s]	19.414
Vi	[m^3/hr]	605.118
Rho	[kg/m^3]	1.753
1/2*Rho*v^2	[Pa]	330.387
Fr	v^2/gD	365.899

TEST NUMBER :400A3

Read. No : 400A35
Ġ [t/h]: 9.2
Q̇ [kg/s]: .293
Load Ratio : 8.71
Pat [kPa]: 86

POINTS ALONG PIPELINE

1

****

Pi	[kPa]	58.114
Ui	[m/s]	20.851
Vi	[m^3/hr]	649.902
Rho	[kg/m^3]	1.625
1/2*Rho*v^2	[Pa]	353.240
Fr	v^2/gD	422.062

TEST NUMBER :400A4

Read. No : 400A41
G [t/h]: 3.4
Q [kg/s]: .384
Load Ratio : 2.45
Pat [kPa]: 85.8

POINTS ALONG PIPELINE

1
****

Pi	[kPa]	56.464
Ui	[m/s]	27.786
Vi	[m^3/hr]	866.078
Rho	[kg/m^3]	1.597
1/2*Rho*v^2	[Pa]	616.551
Fr	v^2/gD	749.540

TEST NUMBER :400A4

Read. No : 400A42
G [t/h]: 6.7
Q [kg/s]: .366
Load Ratio : 5.07
Pat [kPa]: 85.8

POINTS ALONG PIPELINE

1
****

Pi	[kPa]	62.157
Ui	[m/s]	24.834
Vi	[m^3/hr]	774.073
Rho	[kg/m^3]	1.705
1/2*Rho*v^2	[Pa]	525.745
Fr	v^2/gD	576.748

TEST NUMBER :400A4

Read. No : 400A43
G [t/h]: 8.9
Q [kg/s]: .391
Load Ratio : 6.31
Pat [kPa]: 85.8

POINTS ALONG PIPELINE

1
****

Pi	[kPa]	74.149
Ui	[m/s]	24.848
Vi	[m^3/hr]	774.494
Rho	[kg/m^3]	1.820
1/2*Rho*v^2	[Pa]	561.905
Fr	v^2/gD	599.399

TEST NUMBER :400A4

Read. No : 400A41
G [t/h]: 3.4
Q [kg/s]: .384
Load Ratio : 2.45
Pat [kPa]: 85.8

POINTS ALONG PIPELINE

1
****

Pi	[kPa]	56.464
Ui	[m/s]	27.786
Vi	[m^3/hr]	866.078
Rho	[kg/m^3]	1.597
1/2*Rho*v^2	[Pa]	616.551
Fr	v^2/gD	749.540

TEST NUMBER :400A4

Read. No : 400A42
G [t/h]: 6.7
Q [kg/s]: .366
Load Ratio : 5.07
Pat [kPa]: 85.8

POINTS ALONG PIPELINE

1
****

Pi	[kPa]	62.157
Ui	[m/s]	24.834
Vi	[m^3/hr]	774.073
Rho	[kg/m^3]	1.705
1/2*Rho*v^2	[Pa]	525.745
Fr	v^2/gD	598.748

TEST NUMBER :400A4

Read. No : 400A43
G [t/h]: 8.9
Q [kg/s]: .391
Load Ratio : 6.31
Pat [kPa]: 85.8

POINTS ALONG PIPELINE

1
****

Pi	[kPa]	74.149
Ui	[m/s]	24.848
Vi	[m^3/hr]	774.494
Rho	[kg/m^3]	1.820
1/2*Rho*v^2	[Pa]	561.905
Fr	v^2/gD	599.399

TEST NUMBER :400A4

Read. No : 400A44
G [t/h]: 9.3
Q [kg/s]: .382
Load Ratio : 6.75
Pat [kPa]: 85.8

POINTS ALONG PIPELINE

1
****

Pi	[kPa]	67.871
Ui	[m/s]	25.650
Vi	[m^3/hr]	799.498
Rho	[kg/m^3]	1.722
1/2*Rho*v^2	[Pa]	566.525
Fr	v^2/gD	638.727

TEST NUMBER :400A4

Read. No : 400A45
G [t/h]: 16.1
Q [kg/s]: .377
Load Ratio : 11.8
Pat [kPa]: 85.8

POINTS ALONG PIPELINE

1
****

Pi	[kPa]	100.157
Ui	[m/s]	20.660
Vi	[m^3/hr]	643.968
Rho	[kg/m^3]	2.105
1/2*Rho*v^2	[Pa]	449.980
Fr	v^2/gD	414.390

TEST NUMBER :400A5

Read. No : 400A51
G [t/h]: 3.7
Q [kg/s]: .455
Load Ratio : 2.25
Pat [kPa]: 85.8

POINTS ALONG PIPELINE

1
****

Pi	[kPa]	54.331
Ui	[m/s]	33.009
Vi	[m^3/hr]	1028.881
Rho	[kg/m^3]	1.592
1/2*Rho*v^2	[Pa]	867.551
Fr	v^2/gD	1057.818

TEST NUMBER :400A5

Read. No : 400A52
G [t/h]: 5.5
Q [kg/s]: .450
Load Ratio : 3.38
Pat [kPa]: 85.8

POINTS ALONG PIPELINE

1
****

Pi	[kPa]	67.474
Ui	[m/s]	30.103
Vi	[m^3/hr]	938.302
Rho	[kg/m^3]	1.730
1/2*Rho*v^2	[Pa]	783.985
Fr	v^2/gD	879.763

TEST NUMBER :400A5

Read. No : 400A53
G [t/h]: 8.9
Q [kg/s]: .443
Load Ratio : 5.580
Pat [kPa]: 85.8

POINTS ALONG PIPELINE

1
****

Pi	[kPa]	79.211
Ui	[m/s]	27.560
Vi	[m^3/hr]	859.026
Rho	[kg/m^3]	1.857
1/2*Rho*v^2	[Pa]	705.068
Fr	v^2/gD	737.382

TEST NUMBER :400A5

Read. No : 400A54
G [t/h]: 13.8
Q [kg/s]: .427
Load Ratio : 8.96
Pat [kPa]: 85.8

POINTS ALONG PIPELINE

1

****

Pi	[kPa]	101.185
Ui	[m/s]	23.563
Vi	[m^3/hr]	734.452
Rho	[kg/m^3]	2.095
1/2*Rho*v^2	[Pa]	581.543
Fr	v^2/gD	539.023

TEST NUMBER :400A5

Read. No : 400A55
G [t/h]: 14.3
Q [kg/s]: .432
Load Ratio : 9.19
Pat [kPa]: 85.8

POINTS ALONG PIPELINE

1

****

Pi	[kPa]	103.334
Ui	[m/s]	23.657
Vi	[m^3/hr]	737.370
Rho	[kg/m^3]	2.109
1/2*Rho*v^2	[Pa]	590.266
Fr	v^2/gD	543.315

TEST NUMBER :400B1

Read. No : 400B11
Q [t/h]: 7.7
Q [kg/s]: .148
Load Ratio : 14.3
Pat [kPa]: 85.8

POINTS ALONG PIPELINE

1

****

Pi	[kPa]	47.353
Ui	[m/s]	11.085
Vi	[m^3/hr]	345.518
Rho	[kg/m^3]	1.549
1/2*Rho*v^2	[Pa]	95.174
Fr	v^2/gD	119.295

TEST NUMBER :400B1

Read. No : 400B12
Q [t/h]: 8.3
Q [kg/s]: .149
Load Ratio : 15.4
Pat [kPa]: 85.8

POINTS ALONG PIPELINE

1

****

Pi	[kPa]	49.962
Ui	[m/s]	10.948
Vi	[m^3/hr]	341.236
Rho	[kg/m^3]	1.572
1/2*Rho*v^2	[Pa]	94.210
Fr	v^2/gD	116.336

TEST NUMBER :400B1

Read. No : 400B13
Q [t/h]: 16.0
Q [kg/s]: .147
Load Ratio : 31.6
Pat [kPa]: 85.8

POINTS ALONG PIPELINE

1

****

Pi	[kPa]	77.775
Ui	[m/s]	9.021
Vi	[m^3/hr]	281.182
Rho	[kg/m^3]	1.888
1/2*Rho*v^2	[Pa]	76.823
Fr	v^2/gD	79.005

TEST NUMBER :400B1

Read. No : 400B14
Ġ [t/h]: 14.5
Q̇ [kg/s]: .152
Load Ratio : 26.4
Pat [kPa]: 85.8

POINTS ALONG PIPELINE

1
****

Pi	[kPa]	66.597
Ui	[m/s]	10.025
Vi	[m^3/hr]	312.481
Rho	[kg/m^3]	1.756
1/2*Rho*v^2	[Pa]	88.268
Fr	v^2/gD	97.572

TEST NUMBER :400B1

Read. No : 400B15
Ġ [t/h]: 14.5
Q̇ [kg/s]: .152
Load Ratio : 26.4
Pat [kPa]: 85.8

POINTS ALONG PIPELINE

1
****

Pi	[kPa]	66.597
Ui	[m/s]	10.025
Vi	[m^3/hr]	312.481
Rho	[kg/m^3]	1.756
1/2*Rho*v^2	[Pa]	88.268
Fr	v^2/gD	97.572

TEST NUMBER :400B3

Read. No : 400B31
G [t/h]: 7.1
Q [kg/s]: .709
Load Ratio : 6.37
Pat [kPa]: 86

POINTS ALONG PIPELINE

1

****

Pi	[kPa]	58.600
Ui	[m/s]	21.175
Vi	[m^3/hr]	660.000
Rho	[kg/m^3]	1.687
1/2*Rho*v^2	[Pa]	378.263
Fr	v^2/gD	435.280

TEST NUMBER :400B3

Read. No : 400B32
G [t/h]: 10.5
Q [kg/s]: .315
Load Ratio : 9.25
Pat [kPa]: 86

POINTS ALONG PIPELINE

1

****

Pi	[kPa]	69.000
Ui	[m/s]	20.340
Vi	[m^3/hr]	634.000
Rho	[kg/m^3]	1.790
1/2*Rho*v^2	[Pa]	370.307
Fr	v^2/gD	401.661

TEST NUMBER :400B3

Read. No : 400B33
G [t/h]: 3.8
Q [kg/s]: .305
Load Ratio : 8.00
Pat [kPa]: 86

POINTS ALONG PIPELINE

1

****

Pi	[kPa]	62.100
Ui	[m/s]	20.790
Vi	[m^3/hr]	648.000
Rho	[kg/m^3]	1.696
1/2*Rho*v^2	[Pa]	366.463
Fr	v^2/gD	419.595

TEST NUMBER :40083

Read. No : 40083
G [t/h]: 9.2
Q [kg/s]: .306
Load Ratio : 8.32
Pat [kPa]: 86

POINTS ALONG PIPELINE

1

****

Pi	[kPa]	65.500
Ui	[m/s]	20.437
Vi	[m^3/hr]	637.000
Rho	[kg/m^3]	1.734
1/2*Rho*v^2	[Pa]	362.158
Fr	v^2/gD	405.471

TEST NUMBER :40083

Read. No : 40083
G [t/h]: 12.8
Q [kg/s]: .315
Load Ratio : 11.2
Pat [kPa]: 86

POINTS ALONG PIPELINE

1

****

Pi	[kPa]	75.900
Ui	[m/s]	19.731
Vi	[m^3/hr]	615.000
Rho	[kg/m^3]	1.848
1/2*Rho*v^2	[Pa]	359.664
Fr	v^2/gD	377.947

TEST NUMBER :40085

Read. No : 400851
θ [t/h]: 8.1
Q [kg/s]: .440
Load Ratio : 5.109
Pat [kPa]: 85.8

POINTS ALONG PIPELINE

1

****

Pi	[kPa]	90.283
Ui	[m/s]	25.131
Vi	[m^3/hr]	783.308
Rho	[kg/m^3]	2.024
1/2*Rho*v^2	[Pa]	639.083
Fr	v^2/gD	613.121

TEST NUMBER :40085

Read. No : 400852
θ [t/h]: 17.7
Q [kg/s]: .426
Load Ratio : 11.5
Pat [kPa]: 85.8

POINTS ALONG PIPELINE

1

****

Pi	[kPa]	114.064
Ui	[m/s]	21.833
Vi	[m^3/hr]	680.527
Rho	[kg/m^3]	2.257
1/2*Rho*v^2	[Pa]	537.981
Fr	v^2/gD	462.776

TEST NUMBER :40085

Read. No : 400853
θ [t/h]: 14.6
Q [kg/s]: .419
Load Ratio : 9.65
Pat [kPa]: 85.8

POINTS ALONG PIPELINE

1

****

Pi	[kPa]	112.548
Ui	[m/s]	21.796
Vi	[m^3/hr]	679.361
Rho	[kg/m^3]	2.225
1/2*Rho*v^2	[Pa]	528.544
Fr	v^2/gD	461.193

TEST NUMBER :40085

Read. No : 40085A
Q [t/h]: 16.2
Q [kg/s]: .426
Load Ratio : 10.5
Pat [kPa]: 85.8

POINTS ALONG PIPELINE

1
****

Pi	[kPa]	105.482
Ui	[m/s]	23.053
Vi	[m^3/hr]	718.547
Rho	[kg/m^3]	2.137
1/2*Rho*v^2	[Pa]	567.739
Fr	v^2/gD	515.930

TEST NUMBER :40085

Read. No : 40085B
Q [t/h]: 16.2
Q [kg/s]: .426
Load Ratio : 10.5
Pat [kPa]: 85.8

POINTS ALONG PIPELINE

1
****

Pi	[kPa]	105.482
Ui	[m/s]	23.053
Vi	[m^3/hr]	718.547
Rho	[kg/m^3]	2.137
1/2*Rho*v^2	[Pa]	567.739
Fr	v^2/gD	515.930

TEST NUMBER :1200A1

Read. No : 1200A11
Q [t/h]: 1.8
Q [kg/s]: .310
Load Ratio : 1.61
Pat [kPa]: 85.8

POINTS ALONG PIPELINE

1
****

Pi	[kPa]	116.224
Ui	[m/s]	15.528
Vi	[m^3/hr]	483.993
Rho	[kg/m^3]	2.307
1/2*Rho*v^2	[Pa]	278.101
Fr	v^2/gD	234.077

TEST NUMBER :1200A1

Read. No : 1200A12
Q [t/h]: 3
Q [kg/s]: .306
Load Ratio : 2.71
Pat [kPa]: 85.8

POINTS ALONG PIPELINE

1
****

Pi	[kPa]	122.918
Ui	[m/s]	15.054
Vi	[m^3/hr]	469.223
Rho	[kg/m^3]	2.353
1/2*Rho*v^2	[Pa]	266.617
Fr	v^2/gD	220.008

TEST NUMBER :1200A1

Read. No : 1200A13
Q [t/h]: 2.8
Q [kg/s]: .304
Load Ratio : 2.55
Pat [kPa]: 85.8

POINTS ALONG PIPELINE

1
****

Pi	[kPa]	125.293
Ui	[m/s]	14.831
Vi	[m^3/hr]	462.278
Rho	[kg/m^3]	2.374
1/2*Rho*v^2	[Pa]	261.100
Fr	v^2/gD	213.544

TEST NUMBER :1200A2

Read. No : 1200A21
Ġ [t/h]: 10.3
Q̇ [kg/s]: .396
Load Ratio : 7.20
Pat [kPa]: 85.8

POINTS ALONG PIPELINE

1
****

Pi	[kPa]	278.062
Ui	[m/s]	11.119
Vi	[m^3/hr]	346.578
Rho	[kg/m^3]	4.123
1/2*Rho*v^2	[Pa]	254.853
Fr	v^2/gD	120.028

TEST NUMBER :1200A2

Read. No : 1200A22
Ġ [t/h]: 11.9
Q̇ [kg/s]: .398
Load Ratio : 8.29
Pat [kPa]: 85.8

POINTS ALONG PIPELINE

1
****

Pi	[kPa]	256.987
Ui	[m/s]	11.945
Vi	[m^3/hr]	372.315
Rho	[kg/m^3]	3.854
1/2*Rho*v^2	[Pa]	274.934
Fr	v^2/gD	138.517

TEST NUMBER :1200A2

Read. No : 1200A23
Ġ [t/h]: 8.8
Q̇ [kg/s]: .370
Load Ratio : 6.59
Pat [kPa]: 85.8

POINTS ALONG PIPELINE

1
****

Pi	[kPa]	305.527
Ui	[m/s]	9.804
Vi	[m^3/hr]	305.576
Rho	[kg/m^3]	4.370
1/2*Rho*v^2	[Pa]	209.985
Fr	v^2/gD	93.308

TEST NUMBER :1200A3

Read. No : 1200A31
G [t/h]: 11.8
Q [kg/s]: .437
Load Ratio : 7.49
Pat [kPa]: 85.8

POINTS ALONG PIPELINE

1
****

Pi	[kPa]	267.770
Ui	[m/s]	12.750
Vi	[m^3/hr]	397.417
Rho	[kg/m^3]	3.960
1/2*Rho*v^2	[Pa]	321.876
Fr	v^2/gD	157.824

TEST NUMBER :1200A3

Read. No : 1200A32
G [t/h]: 7.7
Q [kg/s]: .43
Load Ratio : 4.93
Pat [kPa]: 85.8

POINTS ALONG PIPELINE

1
****

Pi	[kPa]	254.464
Ui	[m/s]	13.227
Vi	[m^3/hr]	412.268
Rho	[kg/m^3]	3.786
1/2*Rho*v^2	[Pa]	331.157
Fr	v^2/gD	169.840

TEST NUMBER :1200A3

Read. No : 1200A33
G [t/h]: 9.3
Q [kg/s]: .421
Load Ratio : 6.13
Pat [kPa]: 85.8

POINTS ALONG PIPELINE

1
****

Pi	[kPa]	258.781
Ui	[m/s]	12.738
Vi	[m^3/hr]	397.035
Rho	[kg/m^3]	3.819
1/2*Rho*v^2	[Pa]	309.847
Fr	v^2/gD	157.521

TEST NUMBER :1200A1

Read. No : 1200A11R
Ġ [t/h]: 1.8
Q̇ [kg/s]: .288
Load Ratio : 1.73
Pat [kPa]: 86

POINTS ALONG PIPELINE

1

****

Pi	[kPa]	125.165
Ui	[m/s]	13.796
Vi	[m^3/hr]	430.006
Rho	[kg/m^3]	2.419
1/2*Rho*v^2	[Pa]	230.205
Fr	v^2/gD	184.769

TEST NUMBER :1200A1

Read. No : 1200A12R
Ġ [t/h]: 2.9
Q̇ [kg/s]: .287
Load Ratio : 2.79
Pat [kPa]: 86

POINTS ALONG PIPELINE

1

****

Pi	[kPa]	134.067
Ui	[m/s]	13.276
Vi	[m^3/hr]	413.806
Rho	[kg/m^3]	2.504
1/2*Rho*v^2	[Pa]	220.631
Fr	v^2/gD	171.109

TEST NUMBER :1200A1

Read. No : 1200A13R
Ġ [t/h]: 1.1
Q̇ [kg/s]: .292
Load Ratio : 1.04
Pat [kPa]: 86

POINTS ALONG PIPELINE

1

****

Pi	[kPa]	103.116
Ui	[m/s]	15.866
Vi	[m^3/hr]	494.524
Rho	[kg/m^3]	2.129
1/2*Rho*v^2	[Pa]	267.911
Fr	v^2/gD	244.375

TEST NUMBER :1200A2

Read. No : 1200A21R
Ġ [t/h]: 15.9
Q̇ [kg/s]: .409
Load Ratio : 10.7
Pat [kPa]: 86

POINTS ALONG PIPELINE

1

****

Pi	[kPa]	282.757
Ui	[m/s]	10.946
Vi	[m^3/hr]	341.191
Rho	[kg/m^3]	4.316
1/2*Rho*v^2	[Pa]	258.566
Fr	v^2/gD	116.326

TEST NUMBER :1200A2

Read. No : 1200A22R
Ġ [t/h]: 8.6
Q̇ [kg/s]: .408
Load Ratio : 5.84
Pat [kPa]: 86

POINTS ALONG PIPELINE

1

****

Pi	[kPa]	260.139
Ui	[m/s]	11.837
Vi	[m^3/hr]	368.964
Rho	[kg/m^3]	3.989
1/2*Rho*v^2	[Pa]	279.509
Fr	v^2/gD	136.035

TEST NUMBER :1200A2

Read. No : 1200A23R
Ġ [t/h]: 8.9
Q̇ [kg/s]: .404
Load Ratio : 6.10
Pat [kPa]: 86

POINTS ALONG PIPELINE

1

****

Pi	[kPa]	262.640
Ui	[m/s]	11.783
Vi	[m^3/hr]	367.273
Rho	[kg/m^3]	3.969
1/2*Rho*v^2	[Pa]	275.587
Fr	v^2/gD	134.790

TEST NUMBER :1200A3

Read. No : 1200A31R
ṁ [t/h]: 7.2
Q̇ [kg/s]: .441
Load Ratio : 4.52
Pat [kPa]: 85.7

POINTS ALONG PIPELINE

1
****

Pi	[kPa]	296.983
Ui	[m/s]	11.668
Vi	[m^3/hr]	363.678
Rho	[kg/m^3]	4.370
1/2*Rho*v^2	[Pa]	297.483
Fr	v^2/gD	132.164

TEST NUMBER :1200A3

Read. No : 1200A32R
ṁ [t/h]: 9.8
Q̇ [kg/s]: .434
Load Ratio : 6.27
Pat [kPa]: 85.7

POINTS ALONG PIPELINE

1
****

Pi	[kPa]	297.941
Ui	[m/s]	11.537
Vi	[m^3/hr]	359.589
Rho	[kg/m^3]	4.346
1/2*Rho*v^2	[Pa]	289.189
Fr	v^2/gD	129.209

TEST NUMBER :1200A3

Read. No : 1200A33R
ṁ [t/h]: 10.7
Q̇ [kg/s]: .441
Load Ratio : 6.73
Pat [kPa]: 85.7

POINTS ALONG PIPELINE

1
****

Pi	[kPa]	285.377
Ui	[m/s]	12.178
Vi	[m^3/hr]	379.588
Rho	[kg/m^3]	4.187
1/2*Rho*v^2	[Pa]	310.454
Fr	v^2/gD	143.981

TEST NUMBER :1200A2

Read. No : 1200A21RR
G [t/h]: 7.9
Q [kg/s]: .392
Load Ratio : 5.59
Pat [kPa]: 85.8

POINTS ALONG PIPELINE

1

****

Pi	[kPa]	273.378
Ui	[m/s]	11.202
Vi	[m^3/hr]	349.150
Rho	[kg/m^3]	4.043
1/2*Rho*v^2	[Pa]	253.641
Fr	v^2/gD	121.816

TEST NUMBER :1200A2

Read. No : 1200A22RR
G [t/h]: 7.8
Q [kg/s]: .400
Load Ratio : 5.41
Pat [kPa]: 85.8

POINTS ALONG PIPELINE

1

****

Pi	[kPa]	260.519
Ui	[m/s]	11.926
Vi	[m^3/hr]	371.738
Rho	[kg/m^3]	3.874
1/2*Rho*v^2	[Pa]	275.511
Fr	v^2/gD	138.088

TEST NUMBER :1200A2

Read. No : 1200A23RR
G [t/h]: 7.5
Q [kg/s]: .401
Load Ratio : 5.18
Pat [kPa]: 85.8

POINTS ALONG PIPELINE

1

****

Pi	[kPa]	247.706
Ui	[m/s]	12.499
Vi	[m^3/hr]	389.576
Rho	[kg/m^3]	3.710
1/2*Rho*v^2	[Pa]	289.791
Fr	v^2/gD	151.658

TEST NUMBER :1200A3

Read. No : 1200A31RR
G [t/h]: 7.8
Q [kg/s]: .425
Load Ratio : 5.08
Pat [kPa]: 85.8

POINTS ALONG PIPELINE

1
*...**********

Pi	[kPa]	288.726
Ui	[m/s]	11.877
Vi	[m^3/hr]	370.197
Rho	[kg/m^3]	4.140
1/2*Rho*v^2	[Pa]	292.006
Fr	v^2/gD	136.945

TEST NUMBER :1200A3

Read. No : 1200A32RR
G [t/h]: 8.1
Q [kg/s]: .425
Load Ratio : 5.29
Pat [kPa]: 85.8

POINTS ALONG PIPELINE

1
****

Pi	[kPa]	270.927
Ui	[m/s]	12.518
Vi	[m^3/hr]	390.195
Rho	[kg/m^3]	3.922
1/2*Rho*v^2	[Pa]	307.342
Fr	v^2/gD	152.140

TEST NUMBER :1200A3

Read. No : 1200A33RR
G [t/h]: 8.9
Q [kg/s]: .424
Load Ratio : 5.82
Pat [kPa]: 85.8

POINTS ALONG PIPELINE

1
****

Pi	[kPa]	277.564
Ui	[m/s]	12.306
Vi	[m^3/hr]	383.587
Rho	[kg/m^3]	3.984
1/2*Rho*v^2	[Pa]	301.707
Fr	v^2/gD	147.031

TEST NUMBER :100A1r

Read. No : 100A11r
G [t/h]: 13.09
Q [kg/s]: .163
Load Ratio : 22.26
Pat [kPa]: 86.31

POINTS ALONG PIPELINE

	1	2	3	5	6
Pi [kPa]	59.620	50.070	40.093	31.873	22.687
Ui [m/s]	10.623	11.367	12.264	13.117	14.222
Vi [m^3/hr]	331.110	354.296	382.260	408.847	443.306
Rho [kg/m^3]	1.775	1.659	1.538	1.438	1.326
1/2*Rho*v^2 [Pa]	100.171	107.186	115.646	123.689	134.114
Fr v^2/gD	109.553	125.433	146.015	167.033	196.376

TEST NUMBER :100A1r

Read. No : 100A12r
G [t/h]: 13.9
Q [kg/s]: .163
Load Ratio : 23.6
Pat [kPa]: 86.31

POINTS ALONG PIPELINE

	1	2	3	5	6
Pi [kPa]	60.253	50.553	41.794	33.647	23.526
Ui [m/s]	10.581	11.331	12.105	12.928	14.119
Vi [m^3/hr]	329.797	353.171	377.319	402.946	440.077
Rho [kg/m^3]	1.787	1.669	1.562	1.463	1.340
1/2*Rho*v^2 [Pa]	100.054	107.145	114.471	122.246	133.511
Fr v^2/gD	108.686	124.638	142.265	162.246	193.525

TEST NUMBER :100A1r

Read. No : 100A13r
G [t/h]: 16.29
Q [kg/s]: .160
Load Ratio : 28.1
Pat [kPa]: 86.31

POINTS ALONG PIPELINE

	1	2	3	5	6
Pi [kPa]	69.470	57.940	47.163	38.540	25.283
Ui [m/s]	9.772	10.533	11.405	12.492	13.641
Vi [m^3/hr]	304.573	328.918	355.476	389.384	425.175
Rho [kg/m^3]	1.901	1.760	1.629	1.487	1.362
1/2*Rho*v^2 [Pa]	90.765	98.019	105.934	116.039	126.705
Fr v^2/gD	92.697	108.108	126.270	151.508	180.641

TEST NUMBER :100A1r

Read. No : 100A14r
Ġ [t/h]: 19.1
Q̇ [kg/s]: .159
Load Ratio : 33.3
Pat [kPa]: 86.31

POINTS ALONG PIPELINE

		1	2	3	5	6
Pi	[kPa]	75.307	62.417	50.389	45.000	35.000
Ui	[m/s]	9.321	10.141	11.034	11.487	12.433
Vi	[m^3/hr]	290.533	316.104	343.917	358.032	387.545
Rho	[kg/m^3]	1.973	1.813	1.647	1.601	1.479
1/2*Rho*v^2	[Pa]	85.700	93.243	101.447	105.610	114.316
Fr	v^2/gD	84.348	99.848	118.192	128.092	150.081

TEST NUMBER :100A1r

Read. No : 100A15r
Ġ [t/h]: 23.8
Q̇ [kg/s]: .152
Load Ratio : 43.5
Pat [kPa]: 86.31

POINTS ALONG PIPELINE

		1	2	3	5	6
Pi	[kPa]	72.333	63.157	50.172	34.128	24.128
Ui	[m/s]	9.134	9.695	10.617	12.031	13.121
Vi	[m^3/hr]	284.697	302.176	330.924	375.009	408.966
Rho	[kg/m^3]	1.925	1.813	1.656	1.461	1.340
1/2*Rho*v^2	[Pa]	80.284	85.213	93.320	105.752	115.328
Fr	v^2/gD	80.993	91.243	109.430	140.528	167.130

TEST NUMBER :100A21r

Read. No : 100A21r
Q [t/h]: 12.0
Q [kg/s]: .319
Load Ratio : 10.4
Pat [kPa]: 86.31

		POINTS ALONG PIPELINE				
		1	2	3	5	6
Pi	[kPa]	79.217	65.010	56.042	47.377	36.376
Ui	[m/s]	18.617	20.365	21.648	23.051	25.118
Vi	[m^3/hr]	580.287	634.767	674.756	718.493	782.919
Rho	[kg/m^3]	1.983	1.812	1.705	1.601	1.469
1/2*Rho*v^2	[Pa]	343.587	375.844	399.522	425.418	463.565
Fr	v^2/gD	336.485	402.633	454.961	515.853	612.511

TEST NUMBER :100A22r

Read. No : 100A22r
Q [t/h]: 13.82
Q [kg/s]: .316
Load Ratio : 12.1
Pat [kPa]: 86.31

		POINTS ALONG PIPELINE				
		1	2	3	5	6
Pi	[kPa]	84.640	69.047	60.748	51.050	39.525
Ui	[m/s]	18.003	19.810	20.928	22.406	24.458
Vi	[m^3/hr]	561.147	617.470	652.316	698.369	762.334
Rho	[kg/m^3]	2.032	1.846	1.748	1.632	1.495
1/2*Rho*v^2	[Pa]	329.219	362.263	382.707	409.726	447.254
Fr	v^2/gD	314.654	380.988	425.203	487.361	580.726

TEST NUMBER :100A23r

Read. No : 100A23r
Q [t/h]: 16.85
Q [kg/s]: .318
Load Ratio : 14.7
Pat [kPa]: 86.31

		POINTS ALONG PIPELINE				
		1	2	3	5	6
Pi	[kPa]	96.150	77.697	68.826	59.293	47.639
Ui	[m/s]	16.997	18.910	19.991	21.300	23.153
Vi	[m^3/hr]	529.800	589.411	623.113	663.909	721.671
Rho	[kg/m^3]	2.162	1.944	1.839	1.726	1.587
1/2*Rho*v^2	[Pa]	312.371	347.518	367.389	391.442	425.499
Fr	v^2/gD	280.482	347.150	387.985	440.451	520.426

TEST NUMBER :100A2r

Read. No : 100A24r
Ġ [t/h]: 18.6
Q̇ [kg/s]: .319
Load Ratio : 16.1
Pat [kPa]: 86.31

		POINTS ALONG PIPELINE				
		1	2	3	5	6
Pi	[kPa]	97.970	79.597	71.242	60.770	49.943
Ui	[m/s]	16.976	18.856	19.856	21.269	22.959
Vi	[m^3/hr]	529.127	587.725	619.889	662.955	715.637
Rho	[kg/m^3]	2.177	1.960	1.861	1.737	1.609
1/2*Rho*v^2	[Pa]	313.619	348.351	366.822	392.941	424.166
Fr	v^2/gD	279.769	345.167	382.742	439.187	511.760

TEST NUMBER :100A2r

Read. No : 100A25r
Ġ [t/h]: 20.C
Q̇ [kg/s]: .365
Load Ratio : 15.2
Pat [kPa]: 86.31

		POINTS ALONG PIPELINE				
		1	2	3	5	6
Pi	[kPa]	132.523	83.820	75.330	64.390	53.903
Ui	[m/s]	16.362	21.045	22.151	23.759	25.536
Vi	[m^3/hr]	509.983	655.977	690.430	740.553	795.942
Rho	[kg/m^3]	2.578	2.004	1.904	1.775	1.652
1/2*Rho*v^2	[Pa]	345.028	443.800	467.109	501.019	538.492
Fr	v^2/gD	259.892	429.989	476.343	548.016	633.057

TEST NUMBER :100A5r

Read. No : 100A51r
Q [t/h]: 7.6
Q [kg/s]: .54
Load Ratio : 3.72
Pat [kPa]: 86.31

		POINTS ALONG PIPELINE 1	2	3	5	6
Pi	[kPa]	100.537	76.730	68.902	55.950	45.448
Ui	[m/s]	29.463	33.765	35.468	38.697	41.781
Vi	[m^3/hr]	918.343	1052.437	1105.514	1206.168	1302.307
Rho	[kg/m^3]	2.223	1.940	1.846	1.692	1.567
1/2*Rho*v^2	[Pa]	964.724	1105.591	1161.348	1267.085	1368.080
Fr	v^2/gD	842.735	1106.810	1221.263	1453.771	1694.757

TEST NUMBER :100A5r

Read. No : 100A53r
Q [t/h]: 10.1
Q [kg/s]: .524
Load Ratio : 5.38
Pat [kPa]: 86.31

		POINTS ALONG PIPELINE 1	2	3	5	6
Pi	[kPa]	113.503	89.417	81.026	66.913	55.287
Ui	[m/s]	25.828	29.368	30.841	33.681	36.447
Vi	[m^3/hr]	805.047	915.394	961.296	1049.834	1136.037
Rho	[kg/m^3]	2.347	2.064	1.966	1.800	1.643
1/2*Rho*v^2	[Pa]	782.929	990.244	934.886	1020.991	1104.826
Fr	v^2/gD	647.624	837.329	923.410	1101.341	1289.631

TEST NUMBER :100A5r

Read. No : 100A55r
Q [t/h]: 13.2
Q [kg/s]: .514
Load Ratio : 8.23
Pat [kPa]: 86.31

		POINTS ALONG PIPELINE 1	2	3	5	6
Pi	[kPa]	133.960	104.203	95.643	81.160	69.675
Ui	[m/s]	23.146	26.762	28.021	30.444	32.686
Vi	[m^3/hr]	721.460	834.146	873.390	948.922	1018.792
Rho	[kg/m^3]	2.567	2.220	2.120	1.952	1.818
1/2*Rho*v^2	[Pa]	687.600	794.997	832.400	904.387	970.978
Fr	v^2/gD	520.122	695.289	762.250	899.791	1037.175

TEST NUMBER :100B1r

Read. No : 100B11R
G [t/h]: 21
Q [kg/s]: .141
Load Ratio : 41.3
Pat [kPa]: 85.86

POINTS ALONG PIPELINE

		1	2	3	5	6
Pi	[kPa]	50.196	41.105	50.000	22.475	12.898
Ui	[m/s]	10.139	10.845	10.153	12.733	6.328
Vi	[m^3/hr]	316.015	338.644	316.471	396.879	435.366
Rho	[kg/m^3]	1.608	1.501	1.606	1.280	1.167
1/2*Rho*v^2	[Pa]	82.651	88.570	82.771	103.801	23.370
Fr	v^2/gD	99.792	114.595	100.080	157.397	26.165

TEST NUMBER :100B1r

Read. No : 100B12R
G [t/h]: 24.2
Q [kg/s]: .140
Load Ratio : 47.7
Pat [kPa]: 85.86

POINTS ALONG PIPELINE

		1	2	3	5	6
Pi	[kPa]	54.663	44.507	50.000	22.372	13.001
Ui	[m/s]	9.785	10.548	10.121	12.705	6.301
Vi	[m^3/hr]	305.002	328.761	315.470	395.998	433.537
Rho	[kg/m^3]	1.661	1.541	1.606	1.279	1.169
1/2*Rho*v^2	[Pa]	79.519	85.714	82.249	103.244	23.198
Fr	v^2/gD	92.958	108.004	99.448	156.699	25.945

TEST NUMBER :100B1r

Read. No : 100B13R
G [t/h]: 28.2
Q [kg/s]: .139
Load Ratio : 56.1
Pat [kPa]: 85.86

POINTS ALONG PIPELINE

		1	2	3	5	6
Pi	[kPa]	58.396	52.432	50.000	28.546	17.101
Ui	[m/s]	9.452	9.840	10.036	11.918	5.999
Vi	[m^3/hr]	294.612	307.319	312.819	371.480	412.775
Rho	[kg/m^3]	1.705	1.634	1.606	1.352	1.217
1/2*Rho*v^2	[Pa]	76.149	79.433	80.855	96.017	21.897
Fr	v^2/gD	86.732	94.376	97.784	137.896	23.520

TEST NUMBER :100B1r

Read. No : 100B14R
Ĝ [t/h]: 31.6
Q̇ [kg/s]: .141
Load Ratio : 61.8
Pat [kPa]: 85.86

		POINTS ALONG PIPELINE 1	2	3	5	6
Pi	[kPa]	58.358	46.250	50.000	23.687	15.839
Ui	[m/s]	9.620	10.502	10.212	12.665	6.180
Vi	[m^3/hr]	299.853	327.336	318.300	394.757	425.220
Rho	[kg/m^3]	1.704	1.561	1.605	1.294	1.202
1/2*Rho*v^2	[Pa]	78.851	86.079	83.702	103.808	22.950
Fr	v^2/gD	89.846	107.070	101.241	155.719	24.959

TEST NUMBER :100B1r

Read. No : 100B15R
Ĝ [t/h]: 43
Q̇ [kg/s]: .136
Load Ratio : 87.6
Pat [kPa]: 85.86

		POINTS ALONG PIPELINE 1	2	3	5	6
Pi	[kPa]	69.837	59.568	50.000	34.927	26.804
Ui	[m/s]	8.563	9.167	9.813	11.037	5.361
Vi	[m^3/hr]	266.891	285.736	305.859	344.028	368.831
Rho	[kg/m^3]	1.838	1.717	1.604	1.426	1.330
1/2*Rho*v^2	[Pa]	67.391	72.150	77.231	86.869	19.114
Fr	v^2/gD	71.178	81.585	93.481	118.268	18.778

TEST NUMBER :100B3r

Read. No : 100B31R
G [t/h]: 15.3
Q [kg/s]: .312
Load Ratio : 13.5
Pat [kPa]: 85.6

POINTS ALONG PIPELINE

		1	2	3	5	6
Pi	[kPa]	63.690	38.760	50.000	14.203	12.108
Ui	[m/s]	19.918	23.910	21.928	29.794	13.787
Vi	[m^3/hr]	620.823	745.279	683.501	928.652	948.568
Rho	[kg/m^3]	1.813	1.510	1.647	1.212	1.187
1/2*Rho*v^2	[Pa]	359.640	431.737	395.949	537.965	112.779
Fr	v^2/gD	385.137	555.032	466.830	861.761	124.205

TEST NUMBER :100B3r

Read. No : 100B32R
G [t/h]: 17.1
Q [kg/s]: .312
Load Ratio : 15.2
Pat [kPa]: 85.6

POINTS ALONG PIPELINE

		1	2	3	5	6
Pi	[kPa]	67.516	42.122	50.000	16.724	14.932
Ui	[m/s]	19.481	23.354	21.998	29.151	13.442
Vi	[m^3/hr]	607.219	727.948	685.657	908.637	924.833
Rho	[kg/m^3]	1.852	1.544	1.640	1.237	1.216
1/2*Rho*v^2	[Pa]	351.350	421.206	394.734	525.757	109.829
Fr	v^2/gD	368.444	529.518	469.780	825.014	116.068

TEST NUMBER :100B3r

Read. No : 100B33R
G [t/h]: 21.5
Q [kg/s]: .310
Load Ratio : 19.2
Pat [kPa]: 85.6

POINTS ALONG PIPELINE

		1	2	3	5	6
Pi	[kPa]	78.935	50.255	50.000	19.029	16.836
Ui	[m/s]	18.054	21.866	21.907	28.391	13.138
Vi	[m^3/hr]	562.747	681.544	682.827	884.946	903.897
Rho	[kg/m^3]	1.985	1.639	1.636	1.262	1.236
1/2*Rho*v^2	[Pa]	323.514	391.808	392.546	508.741	106.649
Fr	v^2/gD	316.451	464.161	465.910	782.554	112.783

TEST NUMBER :100B3r

Read. No : 100B34R
Q [t/h]: 23.3
Q [kg/s]: .308
Load Ratio : 20.9
Pat [kPa]: 85.6

		POINTS ALONG PIPELINE 1.	2	3	5	6
Pi	[kPa]	82.657	52.714	50.000	19.812	18.159
Ui	[m/s]	17.657	21.480	21.910	28.184	12.972
Vi	[m^3/hr]	550.373	669.324	682.722	878.490	892.490
Rho	[kg/m^3]	2.019	1.660	1.628	1.265	1.245
1/2*Rho*v^2	[Pa]	314.819	382.975	390.639	502.508	104.777
Fr	v^2/gD	302.688	447.933	466.040	771.186	109.954

TEST NUMBER :100B3r

Read. No : 100B35R
Q [t/h]: 26.8
Q [kg/s]: .310
Load Ratio : 24.0
Pat [kPa]: 85.6

		POINTS ALONG PIPELINE 1	2	3	5	6
Pi	[kPa]	90.419	56.582	50.000	24.444	16.676
Ui	[m/s]	17.036	21.090	22.114	27.249	13.283
Vi	[m^3/hr]	531.003	657.371	689.281	849.352	913.867
Rho	[kg/m^3]	2.102	1.698	1.620	1.314	1.222
1/2*Rho*v^2	[Pa]	305.090	377.695	396.029	487.998	107.764
Fr	v^2/gD	281.757	431.818	474.789	720.868	115.284

TEST NUMBER :100B5r

Read. No : 100B51R
G [t/h]: 12.9
Q [kg/s]: .546
Load Ratio : 6.55
Pat [kPa]: 85.6

		POINTS ALONG PIPELINE				
		1	2	3	5	6
*		**********	**********	**********	**********	**********
Pi	[kPa]	98.984	59.866	50.000	22.583	25.511
Ui	[m/s]	29.168	37.011	39.704	49.767	21.452
Vi	[m^3/hr]	909.146	1153.625	1237.563	1551.206	1510.325
Rho	[kg/m^3]	2.164	1.705	1.590	1.268	1.303
1/2*Rho*v^2	[Pa]	920.462	1167.984	1252.968	1570.514	313.835
Fr	v^2/gD	825.939	1329.872	1530.437	2404.470	314.880

TEST NUMBER :100B5r

Read. No : 100B52R
G [t/h]: 15.9
Q [kg/s]: .539
Load Ratio : 8.18
Pat [kPa]: 85.6

		POINTS ALONG PIPELINE				
		1	2	3	5	6
*		**********	**********	**********	**********	**********
Pi	[kPa]	105.693	67.252	50.000	25.184	28.725
Ui	[m/s]	27.949	34.978	39.428	48.259	21.186
Vi	[m^3/hr]	871.161	1090.252	1228.958	1504.219	1457.659
Rho	[kg/m^3]	2.229	1.781	1.580	1.291	1.332
1/2*Rho*v^2	[Pa]	870.646	1089.608	1228.232	1503.330	298.991
Fr	v^2/gD	758.364	1187.776	1509.229	2261.012	293.303

TEST NUMBER :100B5r

Read. No : 100B53R
G [t/h]: 17.2
Q [kg/s]: .540
Load Ratio : 8.6
Pat [kPa]: 85.6

		POINTS ALONG PIPELINE				
		1	2	3	5	6
*		**********	**********	**********	**********	**********
Pi	[kPa]	111.147	70.422	50.000	28.539	30.452
Ui	[m/s]	27.236	34.345	39.518	46.948	20.919
Vi	[m^3/hr]	848.933	1070.528	1231.751	1463.353	1439.235
Rho	[kg/m^3]	2.293	1.818	1.580	1.330	1.352
1/2*Rho*v^2	[Pa]	850.310	1072.263	1233.748	1465.725	295.845
Fr	v^2/gD	720.158	1145.187	1516.095	2139.827	285.935

TEST NUMBER :100C11R

Read. No : 100C11R
Ġ [t/h]: 12.4
Q̇ [kg/s]: .145
Load Ratio : 23.7
Pat [kPa]: 86

POINTS ALONG PIPELINE

		1	2	3	5	6
Pi	[kPa]	40.073	30.519	20.372	14.930	7.281
Ui	[m/s]	11.244	12.164	6.037	6.363	6.885
Vi	[m^3/hr]	350.469	379.204	415.377	437.774	473.673
Rho	[kg/m^3]	1.492	1.379	1.259	1.195	1.104
1/2*Rho*v^2	[Pa]	94.323	103.056	22.944	24.181	26.164
Fr	v^2/gD	122.738	143.690	23.817	26.455	30.971

TEST NUMBER :100C12R

Read. No : 100C12R
Ġ [t/h]: 14.4
Q̇ [kg/s]: .143
Load Ratio : 27.8
Pat [kPa]: 86

POINTS ALONG PIPELINE

		1	2	3	5	6
Pi	[kPa]	46.310	35.997	24.797	6.802	9.009
Ui	[m/s]	10.606	11.502	5.738	6.850	6.691
Vi	[m^3/hr]	330.569	358.515	394.756	471.299	460.352
Rho	[kg/m^3]	1.565	1.443	1.311	1.098	1.124
1/2*Rho*v^2	[Pa]	88.030	95.471	21.575	25.759	25.160
Fr	v^2/gD	109.196	128.438	21.511	30.662	29.254

TEST NUMBER :100C13R

Read. No : 100C13R
Ġ [t/h]: 18.2
Q̇ [kg/s]: .147
Load Ratio : 34.2
Pat [kPa]: 86

POINTS ALONG PIPELINE

		1	2	3	5	6
Pi	[kPa]	50.263	40.218	28.708	21.204	9.626
Ui	[m/s]	10.574	11.416	5.691	6.089	6.826
Vi	[m^3/hr]	329.591	355.822	391.527	418.931	469.657
Rho	[kg/m^3]	1.612	1.493	1.357	1.268	1.131
1/2*Rho*v^2	[Pa]	90.120	97.292	21.972	23.510	26.356
Fr	v^2/gD	108.550	126.516	21.161	24.226	30.448

TEST NUMBER :100C1R

Read. No : 100C14R
Ġ [t/h]: 21.1
Q [kg/s]: .145
Load Ratio : 40.3
Pat [kPa]: 86

		POINTS ALONG PIPELINE				
		1	2	3	5	6
Pi	[kPa]	53.996	42.071	30.263	20.437	4.430
Ui	[m/s]	10.134	11.078	5.228	6.039	7.107
Vi	[m^3/hr]	315.872	345.263	380.732	415.464	489.006
Rho	[kg/m^3]	1.656	1.515	1.375	1.259	1.069
1/2*Rho*v^2	[Pa]	85.013	92.929	21.010	22.949	27.011
Fr	v^2/gD	99.702	119.153	19.970	23.827	33.009

TEST NUMBER :100C1R

Read. No : 100C15R
Ġ [t/h]: 22.7
Q [kg/s]: .145
Load Ratio : 47.4
Pat [kPa]: 86

		POINTS ALONG PIPELINE				
		1	2	3	5	6
Pi	[kPa]	58.095	44.727	30.156	14.279	6.027
Ui	[m/s]	9.839	10.829	5.530	6.403	6.980
Vi	[m^3/hr]	306.690	337.574	380.458	440.772	480.213
Rho	[kg/m^3]	1.703	1.547	1.373	1.185	1.088
1/2*Rho*v^2	[Pa]	82.444	90.772	20.991	24.316	26.494
Fr	v^2/gD	93.990	117.847	19.981	26.814	31.833

TEST NUMBER :100C3R

Read. No : 100C31R
G [t/h]: 13.4
Q [kg/s]: .320
Load Ratio : 11.6
Pat [kPa]: 86

		POINTS ALONG PIPELINE				
		1	2	3	5	6
		**********	**********	**********	**********	**********
Pi	[kPa]	47.053	22.086	22.345	13.732	7.334
Ui	[m/s]	23.528	28.963	13.090	14.220	15.195
Vi	[m^3/hr]	733.362	902.764	900.607	976.380	1045.448
Rho	[kg/m^3]	1.573	1.278	1.281	1.179	1.103
1/2*Rho*v^2	[Pa]	435.345	535.907	109.726	119.202	127.373
Fr	v^2/gD	537.424	814.384	111.963	132.135	150.872

TEST NUMBER :100C3R

Read. No : 100C32R
G [t/h]: 13.8
Q [kg/s]: .314
Load Ratio : 12.1
Pat [kPa]: 86

		POINTS ALONG PIPELINE				
		1	2	3	5	6
		**********	**********	**********	**********	**********
Pi	[kPa]	48.429	22.477	22.068	14.971	7.444
Ui	[m/s]	22.874	28.347	12.891	13.797	14.908
Vi	[m^3/hr]	712.981	883.550	886.896	949.240	1025.699
Rho	[kg/m^3]	1.588	1.282	1.277	1.193	1.104
1/2*Rho*v^2	[Pa]	415.535	514.946	106.087	113.544	122.690
Fr	v^2/gD	507.968	780.087	108.580	124.382	145.226

TEST NUMBER :100C3R

Read. No : 100C33R
G [t/h]: 14.4
Q [kg/s]: .310
Load Ratio : 12.8
Pat [kPa]: 86

		POINTS ALONG PIPELINE				
		1	2	3	5	6
		**********	**********	**********	**********	**********
Pi	[kPa]	50.176	22.621	23.228	15.977	7.672
Ui	[m/s]	22.337	28.003	12.616	13.513	14.711
Vi	[m^3/hr]	696.229	872.653	867.999	929.713	1012.146
Rho	[kg/m^3]	1.607	1.282	1.289	1.204	1.105
1/2*Rho*v^2	[Pa]	400.922	502.630	102.585	109.879	119.622
Fr	v^2/gD	484.379	761.311	104.002	119.317	141.413

TEST NUMBER :100C3R

Read. No : 100C34R
G [t/h]: 17.1
Q [kg/s]: .313
Load Ratio : 15.1.
Pat [kPa]: 86

POINTS ALONG PIPELINE

		1	2	3	5	6
Pi	[kPa]	52.907	27.108	26.789	17.777	7.728
Ui	[m/s]	22.081	27.118	12.320	13.390	14.826
Vi	[m^3/hr]	688.266	845.251	847.640	921.249	1020.026
Rho	[kg/m^3]	1.638	1.333	1.330	1.223	1.105
1/2*Rho*v^2	[Pa]	399.236	490.297	100.912	109.675	121.435
Fr	v^2/gD	473.34	713.925	99.181	117.154	143.624

TEST NUMBER :100C3R

Read. No : 100C35R
G [t/h]: 23.4
Q [kg/s]: .313
Load Ratio : 20.7
Pat [kPa]: 86

POINTS ALONG PIPELINE

		1	2	3	5	6
Pi	[kPa]	59.896	26.982	28.333	19.212	7.763
Ui	[m/s]	21.087	27.230	12.190	13.247	14.865
Vi	[m^3/hr]	657.277	848.752	838.727	911.432	1022.726
Rho	[kg/m^3]	1.717	1.330	1.346	1.238	1.104
1/2*Rho*v^2	[Pa]	381.761	492.974	99.982	109.649	121.916
Fr	v^2/gD	431.696	719.851	97.106	114.671	144.385

TEST NUMBER :200A21R

Read. No : 200A21R
G [t/h]: 9.7
Q [kg/s]: .139
Load Ratio : 19.2
Pat [kPa]: 86.1

POINTS ALONG PIPELINE

		1	2	3	5	6
Pi	[kPa]	81.429	83.526	12.062	59.107	10.610
Ui	[m/s]	7.848	7.751	13.394	9.055	13.595
Vi	[m^3/hr]	244.626	241.602	417.495	282.232	423.763
Rho	[kg/m^3]	2.057	2.083	1.205	1.783	1.188
1/2*Rho*v^2	[Pa]	63.355	62.571	108.125	73.094	109.748
Fr	v^2/gD	59.798	58.329	174.174	79.597	179.443

TEST NUMBER :200A22R

Read. No : 200A22R
G [t/h]: 12.6
Q [kg/s]: .135
Load Ratio : 25.8
Pat [kPa]: 86.1

POINTS ALONG PIPELINE

		1	2	3	5	6
Pi	[kPa]	96.376	103.217	25.599	74.789	7.865
Ui	[m/s]	6.978	6.725	11.399	7.914	13.550
Vi	[m^3/hr]	217.490	209.630	355.300	246.670	422.355
Rho	[kg/m^3]	2.241	2.325	1.372	1.976	1.154
1/2*Rho*v^2	[Pa]	54.563	52.392	89.137	61.884	105.959
Fr	v^2/gD	47.267	43.912	126.145	60.802	178.282

TEST NUMBER :200A23R

Read. No : 200A23R
G [t/h]: 16.2
Q [kg/s]: .135
Load Ratio : 33.2
Pat [kPa]: 86.1

POINTS ALONG PIPELINE

		1	2	3	5	6
Pi	[kPa]	107.711	114.074	29.706	70.922	12.434
Ui	[m/s]	6.575	6.366	11.003	8.115	12.932
Vi	[m^3/hr]	204.925	198.411	342.959	252.937	403.076
Rho	[kg/m^3]	2.381	2.459	1.423	1.929	1.210
1/2*Rho*v^2	[Pa]	51.452	49.816	86.109	63.507	101.203
Fr	v^2/gD	41.963	39.338	117.535	63.930	162.351

TEST NUMBER :200A3R

Read. No : 200A31R
Ġ [t/h]: 8.4
Q̇ [kg/s]: .247
Load Ratio : 9.44
Pat [kPa]: 85.8

		POINTS ALONG PIPELINE				
		1	2	3	5	6
Pi	[kPa]	90.232	80.794	44.458	64.839	18.952
Ui	[m/s]	13.916	14.704	18.806	16.261	23.385
Vi	[m^3/hr]	433.745	458.318	586.168	506.860	728.895
Rho	[kg/m^3]	2.051	1.941	1.518	1.755	1.220
1/2*Rho*v^2	[Pa]	198.581	209.831	268.365	232.055	333.709
Fr	v^2/gD	187.996	209.901	343.340	256.719	530.897

TEST NUMBER :200A3R

Read. No : 200A32R
Ġ [t/h]: 11.5
Q̇ [kg/s]: .211
Load Ratio : 13.0
Pat [kPa]: 85.8

		POINTS ALONG PIPELINE				
		1	2	3	5	6
Pi	[kPa]	104.867	96.845	45.408	74.249	19.885
Ui	[m/s]	11.015	11.499	16.006	13.122	19.872
Vi	[m^3/hr]	343.324	358.403	498.908	409.005	619.397
Rho	[kg/m^3]	2.220	2.127	1.528	1.864	1.231
1/2*Rho*v^2	[Pa]	134.682	140.597	195.716	160.448	242.982
Fr	v^2/gD	117.785	128.359	248.726	167.163	383.371

TEST NUMBER :200A3R

Read. No : 200A33R
Ġ [t/h]: 12.9
Q̇ [kg/s]: .242
Load Ratio : 14.7
Pat [kPa]: 85.8

		POINTS ALONG PIPELINE				
		1	2	3	5	6
Pi	[kPa]	118.331	104.263	51.527	84.556	26.511
Ui	[m/s]	11.852	12.730	17.618	14.202	21.542
Vi	[m^3/hr]	369.433	396.779	549.149	442.478	671.443
Rho	[kg/m^3]	2.368	2.205	1.593	1.974	1.303
1/2*Rho*v^2	[Pa]	166.309	178.619	247.212	199.282	302.275
Fr	v^2/gD	136.380	157.317	301.343	195.820	450.532

TEST NUMBER :200A3R

Read. No : 200A34R
G [t/h]: 15.7
Q̇ [kg/s]: .249
Load Ratio : 17.4
Pat [kPa]: 85.8

		POINTS ALONG PIPELINE				
		1	2	3	5	6
Pi	[kPa]	130.502	118.019	52.986	94.326	31.656
Ui	[m/s]	11.473	12.176	17.881	13.777	21.128
Vi	[m^3/hr]	357.605	379.507	557.340	429.426	658.552
Rho	[kg/m^3]	2.511	2.366	1.611	2.091	1.363
1/2*Rho*v^2	[Pa]	165.228	175.347	257.513	198.412	304.277
Fr	v^2/gD	127.788	143.919	310.400	184.271	433.372

TEST NUMBER :200A3R

Read. No : 200A35R
G [t/h]: 17.5
Q̇ [kg/s]: .208
Load Ratio : 23.2
Pat [kPa]: 85.8

		POINTS ALONG PIPELINE				
		1	2	3	5	6
Pi	[kPa]	128.152	116.056	55.815	93.569	27.776
Ui	[m/s]	9.645	10.223	14.571	11.504	18.169
Vi	[m^3/hr]	300.623	318.637	454.180	358.582	566.308
Rho	[kg/m^3]	2.500	2.359	1.655	2.096	1.327
1/2*Rho*v^2	[Pa]	116.293	123.262	175.696	138.715	219.072
Fr	v^2/gD	90.308	101.455	206.128	128.487	320.469

TEST NUMBER :200A5

Read. No : 200A51R
G [t/h]: 6.8
Q [kg/s]: .431
Load Ratio : 4.37
Pat [kPa]: 86.3

POINTS ALONG PIPELINE

		1	2	3	5	6
Pi	[kPa]	109.569	88.733	53.410	71.901	28.534
Ui	[m/s]	21.751	24.341	30.495	26.930	37.100
Vi	[m^3/hr]	677.976	758.684	950.501	839.404	1156.403
Rho	[kg/m^3]	2.291	2.047	1.634	1.851	1.343
1/2*Rho*v^2	[Pa]	541.983	606.503	759.844	671.031	924.444
Fr	v^2/gD	459.314	575.179	902.789	704.082	1336.284

TEST NUMBER :200A5

Read. No : 200A52R
G [t/h]: 9.9
Q [kg/s]: .388
Load Ratio : 7.07
Pat [kPa]: 86.3

POINTS ALONG PIPELINE

		1	2	3	5	6
Pi	[kPa]	127.073	105.156	67.141	87.735	35.461
Ui	[m/s]	18.022	20.085	25.061	22.095	31.581
Vi	[m^3/hr]	561.726	626.030	781.132	688.696	984.366
Rho	[kg/m^3]	2.491	2.235	1.791	2.032	1.422
1/2*Rho*v^2	[Pa]	404.530	450.839	562.536	495.968	708.897
Fr	v^2/gD	315.304	391.626	609.718	473.953	968.264

TEST NUMBER :200A5

Read. No : 200A53R
G [t/h]: 11
Q [kg/s]: .428
Load Ratio : 7.1
Pat [kPa]: 86.3

POINTS ALONG PIPELINE

		1	2	3	5	6
Pi	[kPa]	143.517	119.097	78.256	100.096	43.961
Ui	[m/s]	18.512	20.713	25.853	22.824	32.660
Vi	[m^3/hr]	577.007	645.608	805.839	711.421	1018.005
Rho	[kg/m^3]	2.674	2.390	1.915	2.169	1.516
1/2*Rho*v^2	[Pa]	458.180	512.654	639.887	564.913	808.360
Fr	v^2/gD	332.693	416.504	648.899	505.748	1035.572

TEST NUMBER :200A5

Read. No : 200A54R
Q [t/h]: 12.7
Q [kg/s]: .430
Load Ratio : 8.18
Pat [kPa]: 86.3

		POINTS ALONG PIPELINE				
		1	2	3	5	6
Pi	[kPa]	154.654	128.205	83.552	109.296	48.352
Ui	[m/s]	17.875	20.080	25.358	22.021	31.987
Vi	[m^3/hr]	557.168	625.870	790.405	686.375	997.028
Rho	[kg/m^3]	2.784	2.479	1.963	2.260	1.556
1/2*Rho*v^2	[Pa]	444.830	499.680	631.041	547.986	796.004
Fr	v^2/gD	310.208	391.425	624.280	470.765	993.334

TEST NUMBER :200A5

Read. No : 200A55R
Q [t/h]: 16.6
Q [kg/s]: .427
Load Ratio : 10.7
Pat [kPa]: 86.3

		POINTS ALONG PIPELINE				
		1	2	3	5	6
Pi	[kPa]	171.146	142.475	98.325	123.568	58.202
Ui	[m/s]	16.664	18.753	23.237	20.442	29.490
Vi	[m^3/hr]	519.423	584.519	724.298	637.179	925.411
Rho	[kg/m^3]	2.966	2.636	2.127	2.418	1.665
1/2*Rho*v^2	[Pa]	411.854	463.470	574.301	505.224	733.765
Fr	v^2/gD	269.602	341.412	524.222	405.699	855.756

TEST NUMBER :200C2R

Read. No : 200C21R
Q [t/h]: .6
Q [kg/s]: .317
Load Ratio : .524
Pat [kPa]: 85.8

POINTS ALONG PIPELINE

1

****

Pi	[kPa]	37.473
Ui	[m/s]	26.399
Vi	[m^3/hr]	822.846
Rho	[kg/m^3]	1.390
1/2*Rho*v^2	[Pa]	484.439
Fr	v^2/gD	676.579

TEST NUMBER :200C2R

Read. No : 200C22R
Q [t/h]: 3.1
Q [kg/s]: .308
Load Ratio : 2.791
Pat [kPa]: 85.8

POINTS ALONG PIPELINE

1

****

Pi	[kPa]	56.266
Ui	[m/s]	22.462
Vi	[m^3/hr]	700.144
Rho	[kg/m^3]	1.586
1/2*Rho*v^2	[Pa]	400.105
Fr	v^2/gD	489.841

TEST NUMBER :200C2R

Read. No : 200C23R
Q [t/h]: 10.3
Q [kg/s]: .306
Load Ratio : 9.32
Pat [kPa]: 85.8

POINTS ALONG PIPELINE

1

****

Pi	[kPa]	75.488
Ui	[m/s]	19.737
Vi	[m^3/hr]	615.192
Rho	[kg/m^3]	1.795
1/2*Rho*v^2	[Pa]	349.601
Fr	v^2/gD	378.183

TEST NUMBER :200C3R

Read. No : 200C31R
Ġ [t/h]: .9
Q [kg/s]: .436
Load Ratio : .573
Pat [kPa]: 85.7

POINTS ALONG PIPELINE

1

****

Pi	[kPa]	33.897
Ui	[m/s]	37.684
Vi	[m^3/hr]	1174.586
Rho	[kg/m^3]	1.337
1/2*Rho*v^2	[Pa]	949.293
Fr	v^2/gD	1378.639

TEST NUMBER :200C3R

Read. No : 200C32R
Ġ [t/h]: 9.1
Q [kg/s]: .435
Load Ratio : 5.80
Pat [kPa]: 85.7

POINTS ALONG PIPELINE

1

****

Pi	[kPa]	58.535
Ui	[m/s]	31.362
Vi	[m^3/hr]	977.547
Rho	[kg/m^3]	1.605
1/2*Rho*v^2	[Pa]	789.177
Fr	v^2/gD	954.896

TEST NUMBER :200C3R

Read. No : 200C33R
Ġ [t/h]: 9.6
Q [kg/s]: .432
Load Ratio : 6.17
Pat [kPa]: 85.7

POINTS ALONG PIPELINE

1

****

Pi	[kPa]	74.050
Ui	[m/s]	28.183
Vi	[m^3/hr]	878.449
Rho	[kg/m^3]	1.771
1/2*Rho*v^2	[Pa]	703.296
Fr	v^2/gD	771.105

TEST NUMBER :200C41R

Read. No : 200C41R
G [t/h]: 1.3
Q [kg/s]: .529
Load Ratio : .681
Pat [kPa]: 85.7

POINTS ALONG PIPELINE

1
****

Pi	[kPa]	40.030
Ui	[m/s]	43.583
Vi	[m^3/hr]	1358.452
Rho	[kg/m^3]	1.404
1/2*Rho*v^2	[Pa]	1333.019
Fr	v^2/gD	1844.036

TEST NUMBER :200C42R

Read. No : 200C42R
G [t/h]: 8.5
Q [kg/s]: .528
Load Ratio : 4.46
Pat [kPa]: 85.7

POINTS ALONG PIPELINE

1
****

Pi	[kPa]	67.157
Ui	[m/s]	35.824
Vi	[m^3/hr]	1116.421
Rho	[kg/m^3]	1.704
1/2*Rho*v^2	[Pa]	1093.224
Fr	v^2/gD	1245.925

TEST NUMBER :200C43R

Read. No : 200C43R
G [t/h]: 11.3
Q [kg/s]: .544
Load Ratio : 5.76
Pat [kPa]: 85.7

POINTS ALONG PIPELINE

1
****

Pi	[kPa]	84.475
Ui	[m/s]	33.176
Vi	[m^3/hr]	1034.068
Rho	[kg/m^3]	1.897
1/2*Rho*v^2	[Pa]	1043.756
Fr	v^2/gD	1068.510

A.4 AIR ALONE PRESSURE DROP

The air alone pressure drop was required for the developing of the equations expressing the conveying pressure as a function of product mass flowrate and air mass flowrate.

The pressure transducer (P1) located at the beginning of the pipeline, which was defined as the conveying pressure of the system, could not accurately measure the pressure drop due to air alone. The pressure transducer had a range of 0 - 700 kPa and the air alone pressure drop for all the pipelines investigated only ranged from 0 - 50 kPa.

The air alone pressure drop was thus measured with a mercury manometer. A correction factor of 1,02 had to be included, because 100 units on the scale of the manometer represented 102 mm in reality.

Using regression analysis, an equation was derived for the pressure drop due to air alone as a function of air mass flowrate. The equations are shown on the graphs in Figures A.1 to A.9. With the use of the equations the conveying pressure for zero product mass flowrate could be included in Figures A.10 to A.19 where the conveying pressure is plotted as a function of the product mass flowrate.

The negative values of pressure drop recorded in some cases are due to the extraction fan on the filter unit creating a vacuum in the pipeline at low air mass flowrates.

The air alone pressure drop was not recorded for configurations 400B and 1200A, because the equation for pressure as a function of product and air mass flowrate was not required in the analysis of the results.

TABLE A.1: AIR ALONE PRESSURE DROP [100A]

Pipeline Configuration : 100A
Barometric Pressure : 86,0 kPa

PRESSURE mmHg (x1,02)	kPa	AIR TEMPERATURE °C	AIR VOLUMETRIC FLOWRATE m^3/h	AIR MASS FLOWRATE kg/s
2,1	2,9	33	538	0,15
83	11,3	29	830	0,26
120	17,4	26	970	0,32
214	29,1	23	1151	0,43
356	48,4	15	1348	0,61

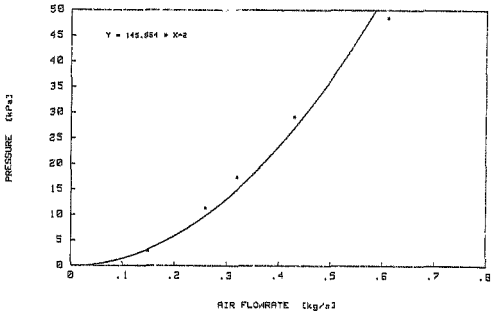


FIGURE A.1: AIR ALONE PRESSURE DROP [100A]

TABLE A.2: AIR ALONE PRESSURE DROP [100B]

Pipeline Configuration : 100B
Barometric Pressure : 86,3

PRESSURE mmHg (x1,02)	kPa	AIR TEMPERATURE °C	AIR VOLUMETRIC FLOWRATE m^3/h	AIR MASS FLOWRATE kg/s
10	1,4	34	539	0,15
56	7,6	30	832	0,25
95	12,9	26	1006	0,32
156	21,2	22	1204	0,42
218	29,7	17	1352	0,52

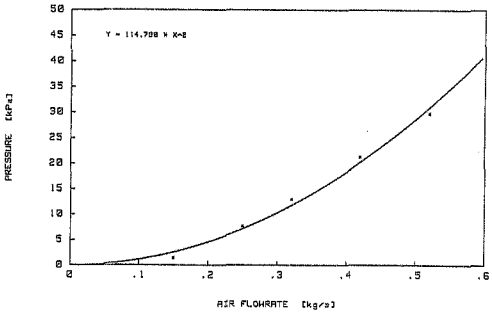


FIGURE A.2: AIR ALONE PRESSURE DROP [100B]

TABLE A.3: AIR ALONE PRESSURE DROP [100C]

Pipeline Configuration : 100C
Barometric Pressure : 86,2

PRESSURE mmHg (x1,02)	kPa	AIR TEMPERATURE °C	AIR VOLUMETRIC FLOWRATE m^3/h	AIR MASS FLOWRATE kg/s
4	0,5	23	533	0,15
29	3,9	23	867	0,26
51	6,9	23	1066	0,33
88	12,0	22	1309	0,42
14o	20,1	22	1592	0,56

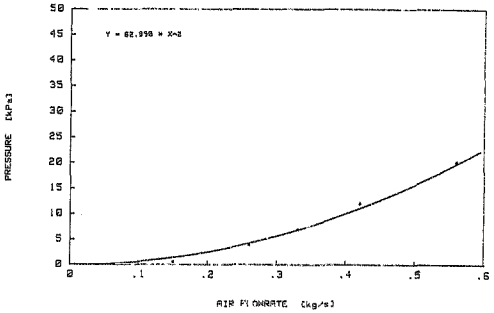


FIGURE A.3: AIR ALONE PRESSURE DROP [100C]

FIGURE A.4: AIR ALONE PRESSURE DROP [100D]

Pipeline Configuration : 100D
Barometric Pressure : 85,8

PRESSURE mmHg (x1,02)	kPa	AIR TEMPERATURE °C	AIR VOLUMETRIC FLOWRATE m^3/h	AIR MASS FLOWRATE kg/s
26	3,5	20	889	0,26
82	11,2	20	1270	0,41
80	10,9	20	1268	0,40
184	25,0	21	1686	0,62
81	11,0	21	1279	0,41
56	7,1	22	1060	0,33
6	1,8	22	596	0,17

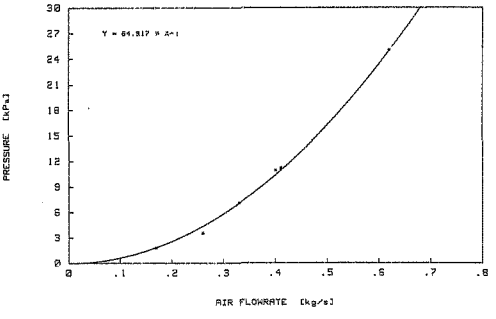


FIGURE A.4: AIR ALONE PRESSURE DROP [100D]

TABLE A.5: AIR ALONE PRESSURE DROP [200A]

Pipeline Configuration : 200A
Barometric Pressure :

PRESSURE mmHg (x1,02)	kPa	AIR TEMPERATURE °C	AIR VOLUMETRIC FLOWRATE m^3/h	AIR MASS FLOWRATE kg/s
18	2,5	17	359	0,10
46	6,3	17	449	0,15
132	18,0	17	743	0,25
199	27,8	18	859	0,31
276	37,6	19	954	0,38

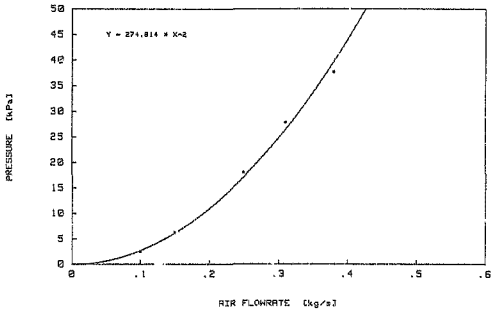


FIGURE A.5: AIR ALONE PRESSURE DROP [200A]

TABLE A.6: AIR ALONE PRESSURE DROP [200B]

Pipeline Configuration : 200B
Barometric Pressure : 85,6

PRESSURE mmHg (x1,02)	kPa	AIR TEMPERATURE °C	AIR VOLUMETRIC FLOWRATE m^3/h	AIR MASS FLOWRATE kg/s
- 18	-2,4	23	0	0,00
- 6	-0,8	31	393	0,11
5	0,7	32	573	0,16
65	8,8	32	1086	0,33
120	16,3	31	1343	0,44
220	29,9	30	1650	0,61

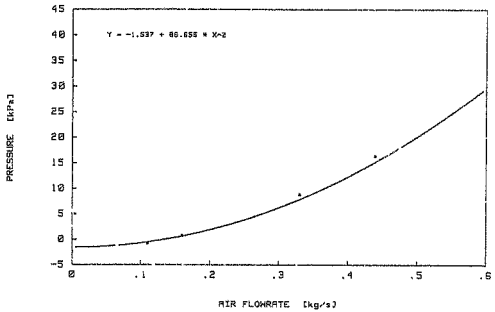


FIGURE A.6: AIR ALONE PRESSURE DROP [200B]

TABLE A.7: AIR ALONE PRESSURE DROP [200C]

Pipeline Configuration : 200C
Barometric Pressure : 85,9 kPa

PRESSURE mmHg (x1,02)	kPa	AIR TEMPERATURE °C	AIR VOLUMETRIC FLOWRATE m^3/h	AIR MASS FLOWRATE kg/s
-17	-2,3	32	0	0,00
0	0,0	33	548	0,15
3	0,4	34	595	0,16
50	6,8	34	1035	0,30
138	18,8	35	1408	0,46

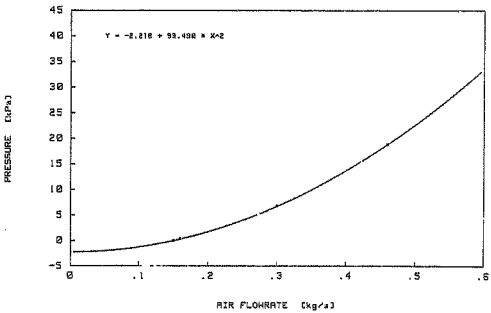


FIGURE A.7: AIR ALONE PRESSURE DROP [200C]

TABLE A.8: AIR ALONE PRESSURE DROP [400A]

Pipeline Configuration : 400A
Barometric Pressure : 85,8

PRESSURE mmHg (x1,02)	kPa	AIR TEMPERATURE °C	AIR VOLUMETRIC FLOWRATE m^3/h	AIR MASS FLOWRATE kg/s
-5	-0,7	35	390	0,10
14	1,9	36	579	0,16
82	11,2	35	1002	0,31
184	25,0	34	1327	0,46
261	35,5	32	1477	0,57

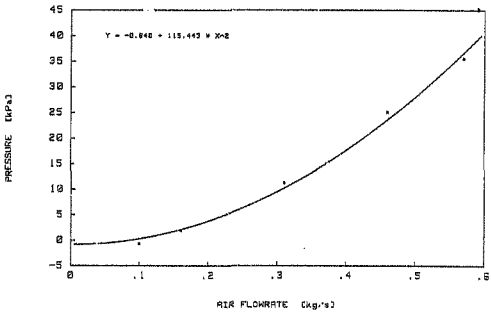


FIGURE A.8: AIR ALONE PRESSURE DROP [400A]

A.5 PRESSURE VERSUS PRODUCT MASS FLOWRATE GRAPHS

The equations expressing the conveying pressure as a function of product and air mass flowrates, as discussed in Section 5.2 of this report, were derived from the graphs given in this Appendix.

For each of the pipeline configurations the following graphs were drawn.

1) P vs $\dot{G}$
2) A vs $\dot{Q}$
3) B vs $\dot{Q}$

The abbreviations shown above represent the following parameters.

P : conveying pressure
$\dot{G}$: product mass flowrate
$\dot{Q}$: air mass flowrate
A : constants from Equation A.1
B : constants from Equation A.1

The form of the equation expressing the conveying pressure as a function of product mass flowrate and air mass flowrate is shown in Equation A.1.

$$P = A + B.\sqrt{\dot{G}} \qquad (A.1)$$

A and B are thus functions of the air mass flowrate.

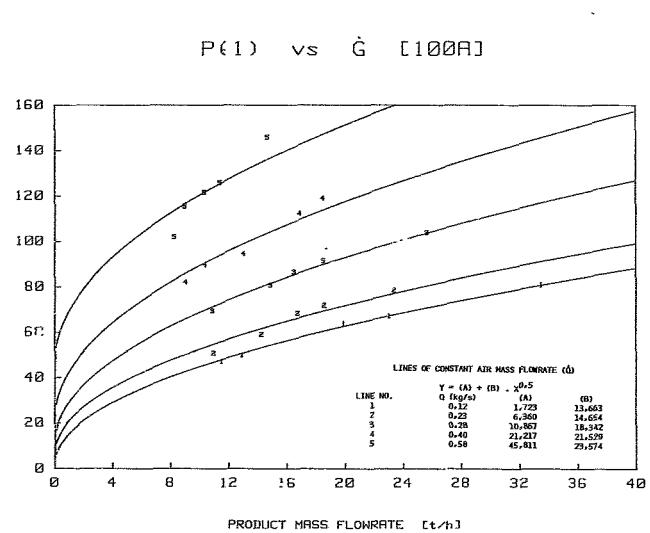


FIGURE A.9.1: P VERSUS Ġ [100A]

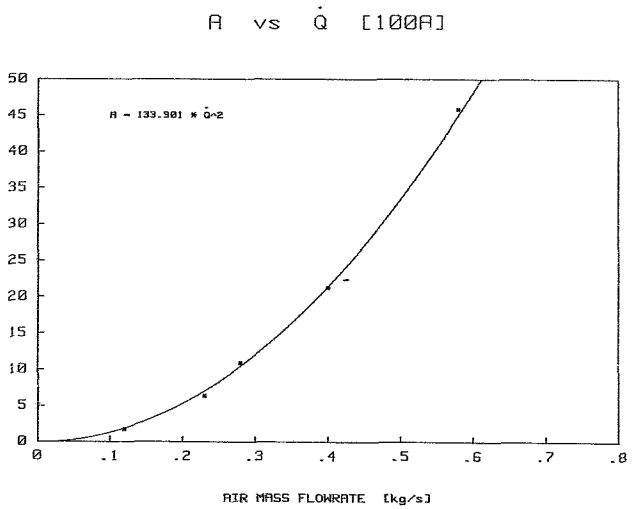


FIGURE A.9.2: A VERSUS Q̇ [100A]

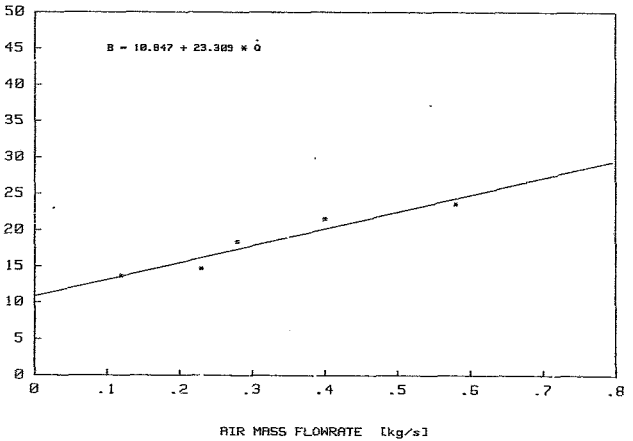


FIGURE A.9.3: B VERSUS Q̇ [100A]

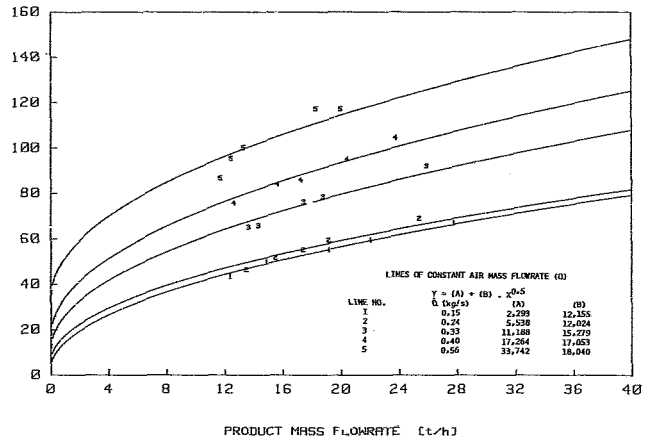


FIGURE A.10.1: P VERSUS Ġ [100B]

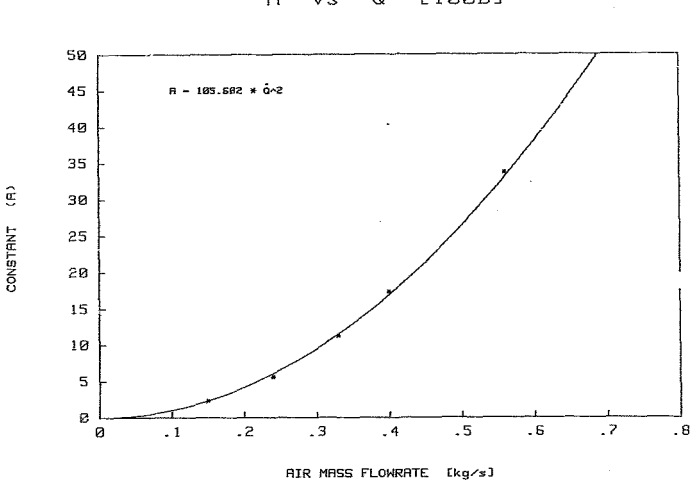


FIGURE A.10.2: A VERSUS Q [100B]

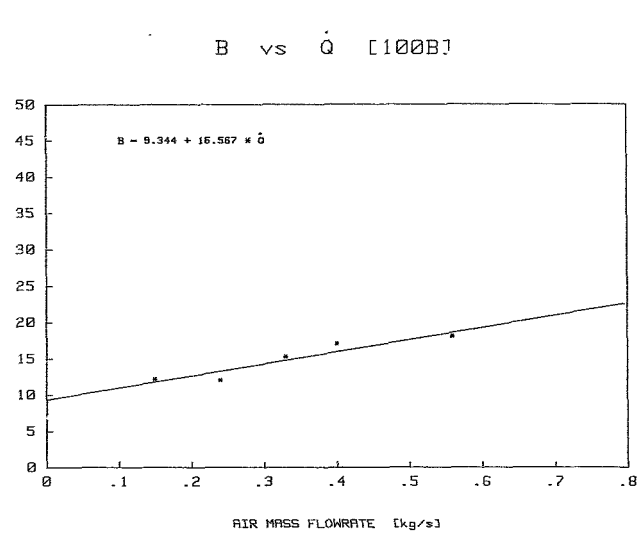


FIGURE A.10.3: B VERSUS Q̇ [100B]

P(1) vs Ġ [100C]

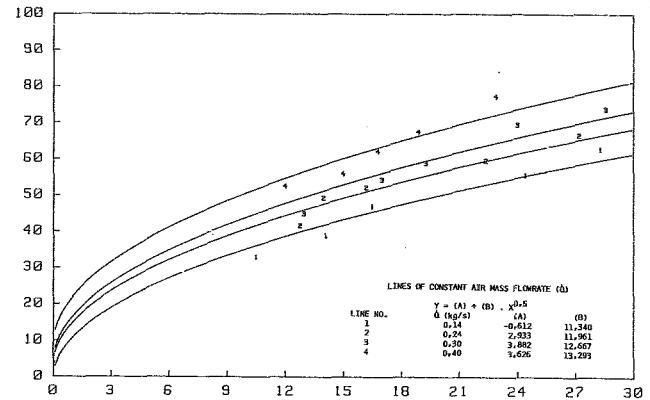


FIGURE A.III.1: P VERSUS Ġ [100C]

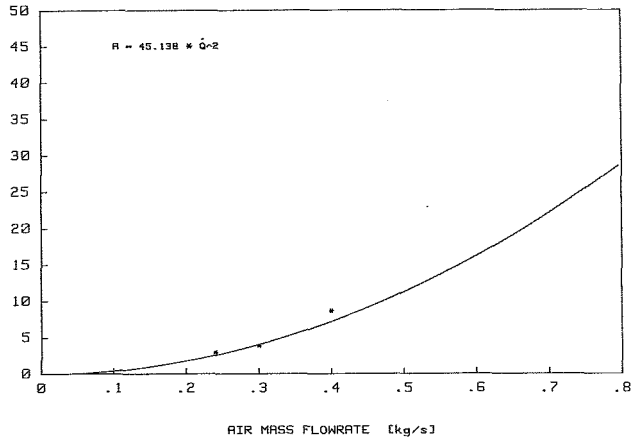


FIGURE A.11.2: A VERSUS Q̇ [100C]

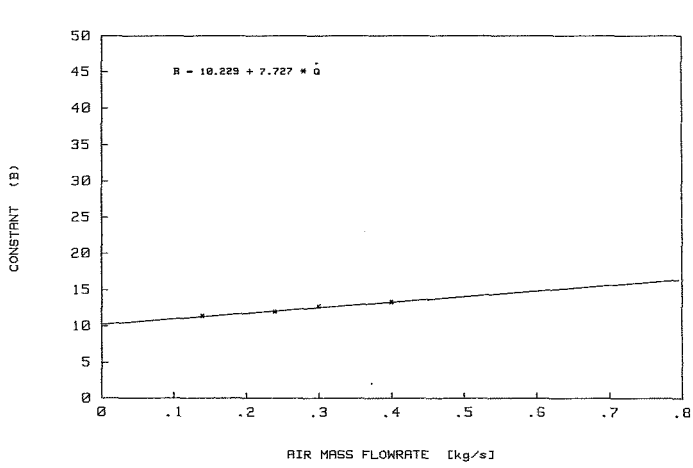


FIGURE A.11.3: B VERSUS Q̇ [100C]

P(1) vs $\dot{G}$ [100D]

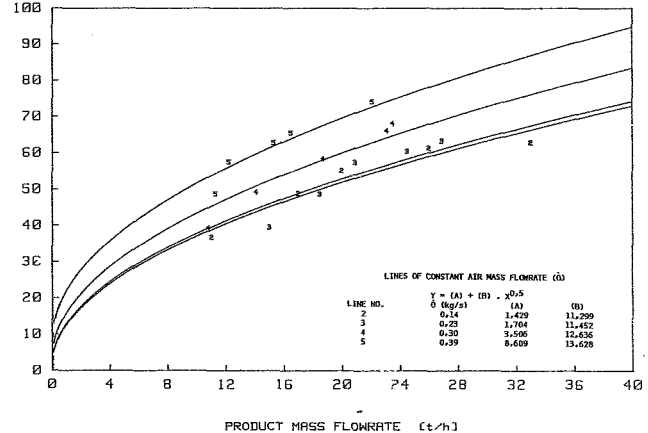


FIGURE A.12.1: P VERSUS $\dot{G}$ [100D]

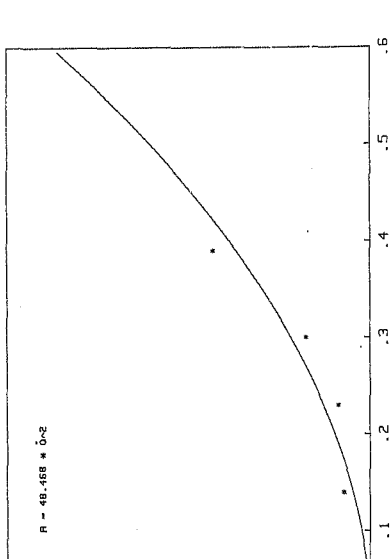


FIGURE A.12.2: A VERSUS $\dot{Q}$ [100D]

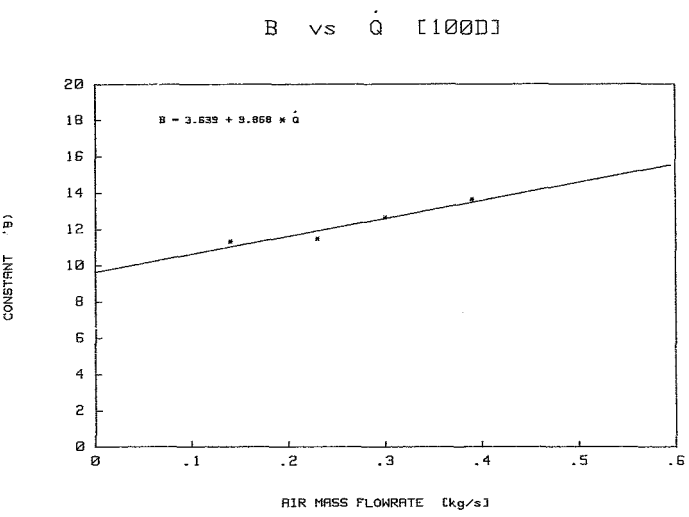


FIGURE A.12.3: B VERSUS Q̇ [100D]

P(1) vs $\dot{G}$ [200A]

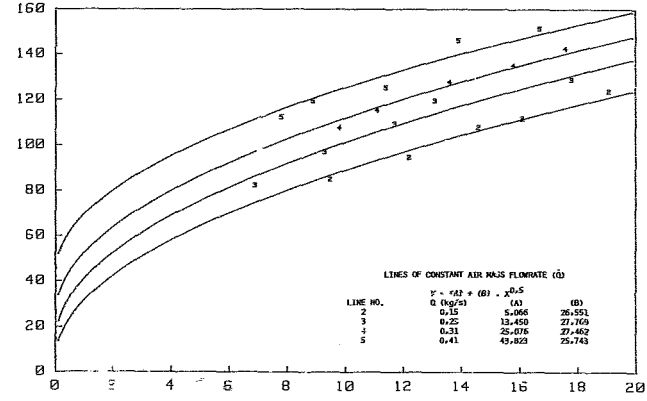


FIGURE A.13.1: P VERSUS G [200A]

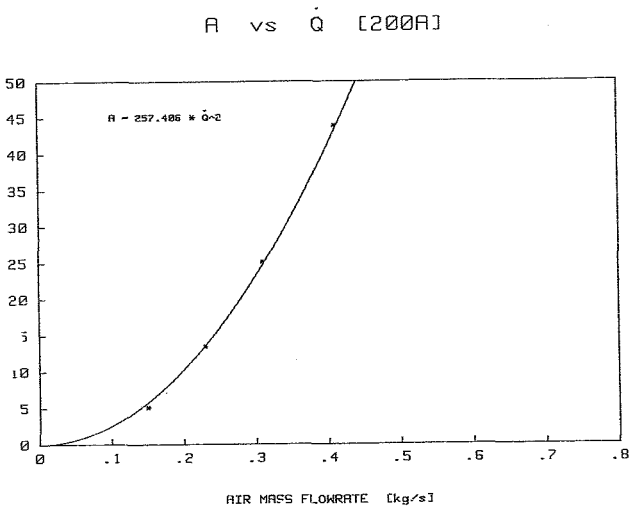


FIGURE A.13.2: A VERSUS $\dot{Q}$ [200A]

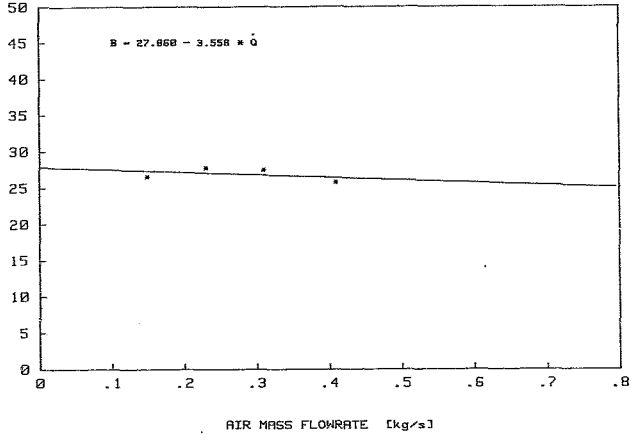


FIGURE A.13.3: B VERSUS Q̇ [200A]

P(1) vs $\dot{G}$ [200B]

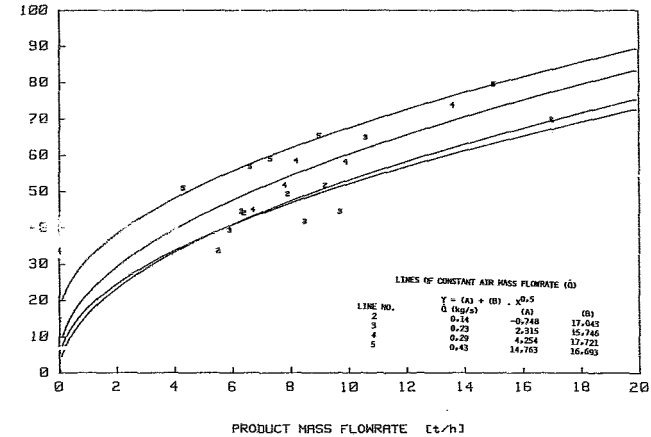


FIGURE A1.4.1: P VERSUS $\dot{G}$ [200B]

A vs $\dot{Q}$ [200B]

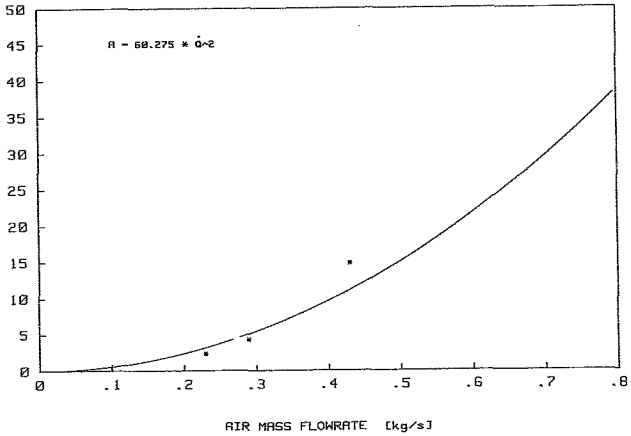


FIGURE A.14.2: A VERSUS $\dot{Q}$ [200B]

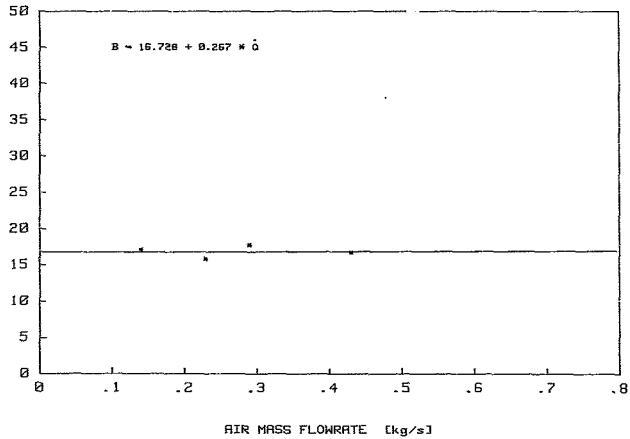


FIGURE A.14.3: B VERSUS Q̇ [200B]

P(1) vs $\dot{G}$ [200C]

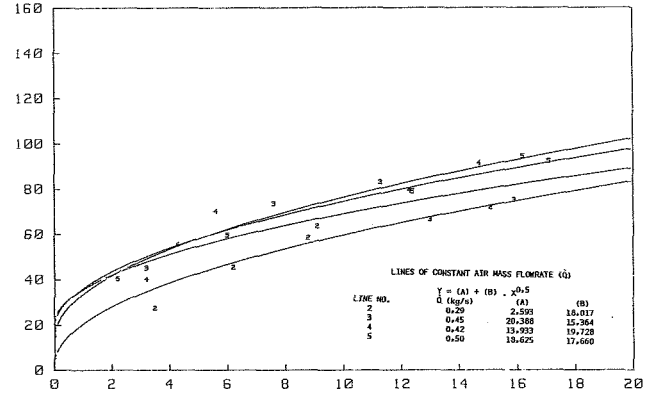


FIGURE A.15.1: P VERSUS $\dot{G}$ [200C]

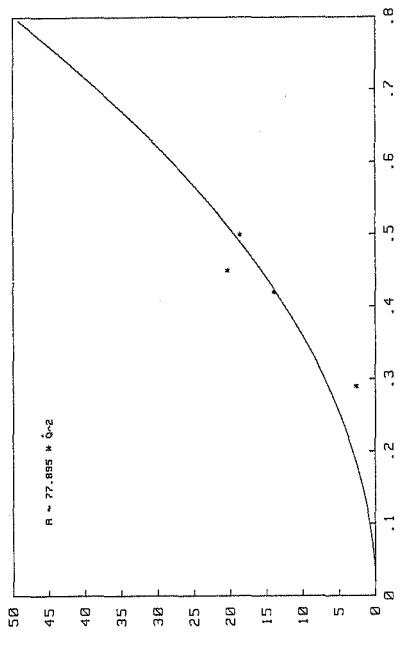


FIGURE A.15.2: A VERSUS Q [200C]

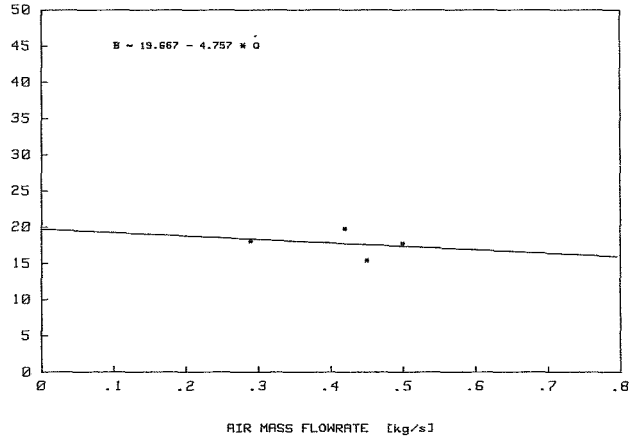


FIGURE A.15.3: B VERSUS Q [200C]

P(1) vs $\dot{G}$ [400A]

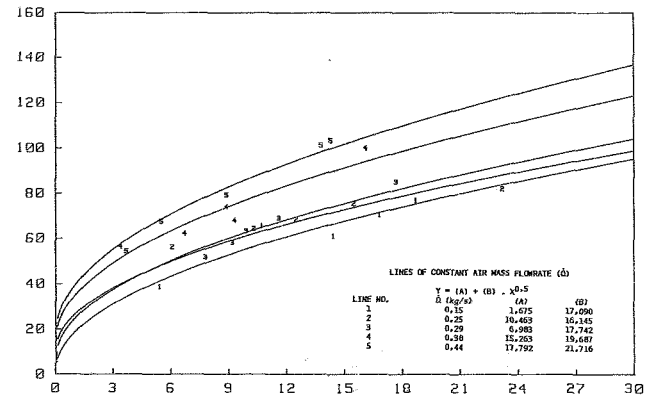


FIGURE A.16.1: P VERSUS $\dot{G}$ [400A]

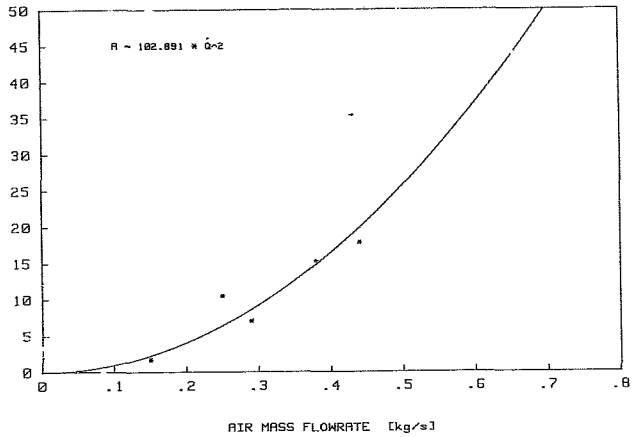


FIGURE A.16.2: A VERSUS Q̇ [400A]

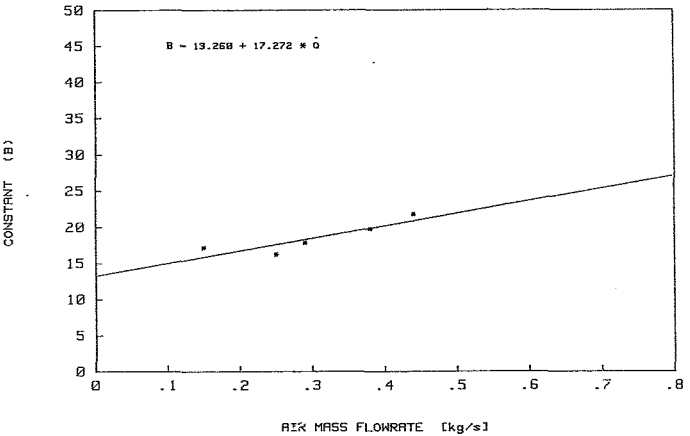


FIGURE A.16.3: B VERSUS $\dot{Q}$ [400A]

APPENDIX B

EQUIPMENT SPECIFICATIONS

B.1 COMPRESSORS

B.1.1 CONVEYING AIR COMPRESSORS

B.1.2 SERVICE AIR COMPRESSORS

B.2 BRIEDEN BLOW VESSELS

B. EQUIPMENT SPECIFICATIONS

B.1 COMPRESSORS

The specifications of the four compressors used to supply the conveying air are given below.

The service air for the control system, pneumatic actuating valves and the reverse jet filter was supplied by two additional compressors.

B.1.1 CONVEYING AIR COMPRESSORS

COMPRESSOR 1

Make	: Bellis and Morcom MFG Ltd.
Serial No.	: 0278/2
Type	: BM40
Operating pressure	: 885 kPa
Free air delivery	: 11,0 m^3/min
Motor	: 75 kW

COMPRESSOR 2

Make	: Hydrovane
Serial No.	: ERR450 P.U.
Operating pressure	: 700 kPa
Free air delivery	: 10,0 m^3/min
Motor	: 75 kW

COMPRESSOR 3

Make	: Mannesmann Demag
Type	: SE 75 EKS
Operating pressure	: 700 kPa
Free air delivery	: 7,7 m^3/min
Motor	: 54,5 kW

COMPRESSOR 4

Make	: Atlas Copco
Type	: ZT 290
Operating pressure	: 800 kPa
Free air delivery	: 12 m^3/min
Motor	: 90 kW

B.1.2 SERVICE AIR COMPRESSORS

COMPRESSOR 5

Make	: Mahle
Type	: MSK D 30
Operating pressure	: 1000 kPa
Free air delivery	: 4,3 m^3/min
Motor	: 30 kW

COMPRESSOR 6

Make	: Hydrovane
Type	: 66 PU
Operating pressure	: 700 kPa
Free air delivery	: 1,53 m^3/min
Motor	: 11 kW

B.2 BRIEDEN BLOW VESSELS

The Brieden blow vessels fed the material into the conveying pipeline. Rotary valves at the bottom conical end of the blow vessels controlled the product mass flowrate.

The specifications of the vessels are given below.

Make	: Brieden
Vessel No.	: 97118
Capacity	: $1m^3$
Maximum operating pressure	: 10 bar
Operating temperature	: 20 °C

APPENDIX C

INSTRUMENTATION SPECIFICATION AND CALIBRATION

C.1 PRODUCT MASS FLOWRATE MEASUREMENT

C.1.1 LOAD CELL SPECIFICATIONS
C.1.2 CALIBRATION

C.2 AIR MASS FLOWRATE MEASUREMENT

C.2.1 FLOWMETER SPECIFICATIONS
C.2.2 CALIBRATION

C.3 PRESSURE MEASUREMENT

C.3.1 SPECIFICATIONS
C.3.2 CALIBRATION

C.4 TEMPERATURE MEASUREMENT

C.4.1 SPECIFICATIONS
C.4.2 CALIBRATIONS

C. INSTRUMENTATION SPECIFICATION AND CALIBRATION

C.1 *PRODUCT MASS FLOWRATE MEASUREMENT*

The receiving hopper at the end of the conveying line was located on three strain gauge type load cells, as shown in Figure 3.1. When closing the valve under the receiving hopper the rate at which the mass of the hopper increased, corresponded to the product mass flowrate of the material being conveyed.

Flexible hoses connected all the piping to the receiving hopper to ensure that the total load was taken up by the load cells.

The load cells consisted of two full wheatstone bridges in series, each assembled on four separate bending beams.

The three load cells were connected in parallel to a junction box which compensated for any uneven loading in the hopper. The data logger recorded the voltage output signal from the junction box, corresponding to the mass of the receiving hopper.

The computer in-built clock recorded the time at which the mass of the receiving hopper was measured.

C.1.1 LOAD CELL SPECIFICATIONS

MAKE	: Ametek
TYPE	: LPE Series (low profile)
RATED CAPACITY	: 2500 lb (each)
EXCITATION VOLTAGE	: 20 v dc
OUTPUT SIGNAL	: 4 to 20 mA
COMPENSATED TEMP.RANGE	: 50 to 150^{o}F

C.1.2 CALIBRATION

The procedure for calibrating the load cells was as follows:

a) The 220 V ac power supply to the junction box was switched on. The transformer and rectifier in the junction box supplied the excitation voltage to the load cells.
b) The output voltage signals from the junction box was recorded from the display panel of the data logger.
c) Calibration weights were loaded onto the receiving hopper. At steps of 40 kg the corresponding voltage signal was recorded. A total mass of 600 kg was loaded onto the receiving hopper.
d) The loading of the weight onto the receiving hopper was repeated 3 times. The average of these results were plotted on a graph of mass versus volt.

The mass was linearly related to the output voltage signal. The calibration equation was thus in the form of

$$G = (a) + (b) \cdot V$$

where (a) was the voltage signal corresponding to a zero mass in the filter unit. Due to a slight drift in the output signal from the junction box, a zero reading to determine the value of (a) was taken at the beginning of each test run.

TABLE C.1: LOAD CELL CALIBRATION RESULTS

MASS kg	AVERAGE OUTPUT V
0	0,713
40	0,761
80	0,806
120	0,847
160	0,891
200	0,938
240	0,981
280	1,029
320	1,074
360	1,116
400	1,160
440	1,205
480	1,247
520	1,290
560	1,330
600	1,371

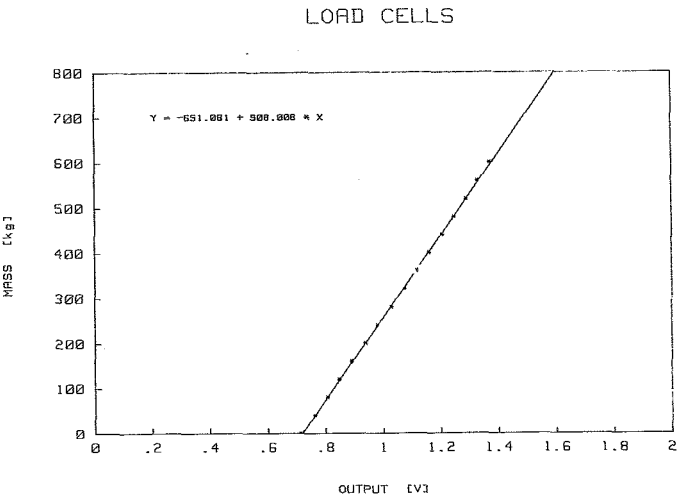


FIGURE C.1: LOAD CELLS CALIBRATION CURVE

C.2 AIR MASS FLOWRATE MEASUREMENT

C.2.1 FLOWMETER SPECIFICATIONS

MAKE	:	Foxboro
TYPE	:	E83 W - Vortex Flowmeter
SIZE	:	100 mm NB
RANGE	:	548 - 2020 m^3/hr
SUPPLY VOLTAGE	:	14 ~ 30 V dc
OUTPUT SIGNAL	:	4 - 20 mA

The principle of operation was as follows. Fluid flowing through the flowmeter body passes a specially shaped vortex shedding element which causes vortices to form and shed (separate) from alternate sides of the element at a rate proportional to the flow velocity of the fluid. These shedding vortices create an alternating differential pressure which is sensed by the detector located in the tail of the shedding element. This vortex shedding phenomenom is shown in Figure C.2.

The alternating differential pressure produces an alternating voltage with a frequency synchronous to the vortex shedding frequency and directly related to the flowrate. The alternating voltage is passed through the electronics of the flowmeter which produces a final 4 to 20 mA analog output signal. The milliamp output signal was passed through a 200 resistor across which the corresponding voltage drop was recorded.

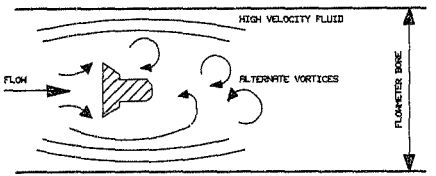


FIGURE C.2: VORTEX SHEDDING PHENOMENON

C.2.2 CALIBRATION

The flowmeter was calibrated with a pitot-static tube, using the Ten Point Log Linear method according to BS 1042 Part 2 of 1973 (Ref.2).

This involved taking two pressure traverses perpendicular to one another moving the pitot-static tube a specified depth at a time across the pipe section as layed out in BS 1042.

TABLE C.2: FLOWMETER CALIBRATION RESULTS

OUTPUT SIGNAL V	FLOWRATE m^3/hr
1,365	388,0
1,775	661,3
2,200	946,6
2,888	1369,8
3,250	1652,4

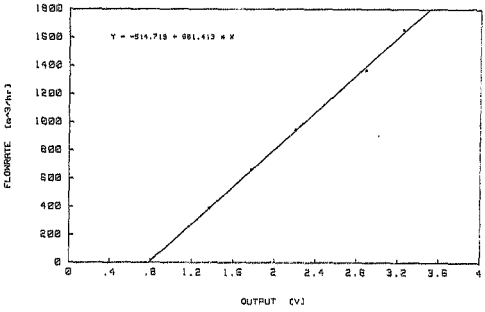


FIGURE C.3: FLOWMETER CALIBRATION CURVE

C.3 PRESSURE MEASUREMENT

Six pressure transducers were used to record the relevant pressure along the conveying pipeline, although only the conveying pressure was measured with an acceptable repeatibility. Due to the pressure fluctuation in the conveying pipeline caused by plugs of material flowing through the pipeline, a consistent pressure could not be measured along the pipeline. A more sophisticated filter arrangement with a purging system, to prevent the pressure tapping points from blocking, was required.

After reconsidering the objective of the project as outlined in Section 1.2, it was decided that the analysis of the results would only be in terms of the conveying pressure.

The circuit diagram used for all the pressure transducers is shown below.

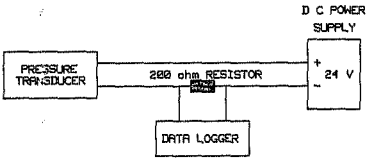


FIGURE C.4: CIRCUIT DIAGRAM FOR THE PRESSURE TRANSDUCERS

The data logger recorded the voltage drop across the resistor.

C.3.1 SPECIFICATIONS

The specifications of the three types of transducers used are given in Table C.3.

TABLE C.3: PRESSURE TRANSDUCER SPECIFICATIONS

SPECIFICATIONS	PRESSURE TRANSDUCERS		
MEASURES	A GAUGE PRESSURE	B GAUGE PRESSURE	C DIFFERENTIAL PRESSURE
MAKE	Fuji Electric	Fuji Electric	Fuji Electric
TYPE	FCP A	FBC 2	FFC 44
RANGE	0 - 600 kPa	Adjustable: min 0-200kPa Max 0-2000kPa	Adjustable: min 0-640 mm H_2O max 0-6400 mm H_2O
OUTPUT	4-20 mA dc	4-20 mA dc	4-20 mA dc
POWER SUPPLY	14-30 V dc	12-45 V dc	12 - 45 V dc
LOAD LIMITATION	500 ohms	600 ohms	350 ohms
TEMPERATURE LIMIT	-20 - 60oC	-30 - 80oC	-10 - 60oC
STEP RESPONSE	0,05 s	Adjustable (0,1; 0,4; 0,2; 6) s	Adjustable (0,2; 0,3; 1,3) s

C.3.2 CALIBRATION

The pressure transducers were calibrated in situ. Figure C.5 shows the set-up of the facilities for calibrating the pressure transducers.

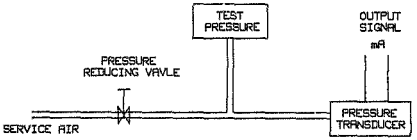


FIGURE C.5: PRESSURE TRANSDUCER CALIBRATION SET-UP

The service air was throttled with the pressure reducing valve such that a range of voltages signals from the pressure transducer could be recorded corresponding to the test pressures.

The test pressures were recorded with either a mercury manometer or a Budenburg Standard Test Gauge.

For the mercury manometer a correction of 1,02 was included because 100 units on the scale represented 102 mm in reality.

PRESSURE TRANSDUCER 1

Specifications (see Table C.4) : A

Location *(see Figure 3.1)* : PT 1

Test pressure instrument : mercury manometer

TABLE C.4 : CALIBRATION RESULTS (PRESSURE TRANSDUCER 1)

TEST PRESSURE mmHg (x1,02)	TEST PRESSURE kPa	VOLTAGE SIGNAL V
0	0	0,818
150	20,4	0,928
296	40,2	1,034
482	65,6	1,174
648	88,2	1,294
900	122,5	1,481
559	76,1	1,232
168	22,9	0,941
0	0	0,818

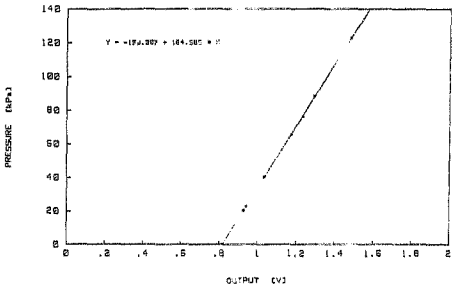


FIGURE C.6: CALIBRATION CURVE (PRESSURE TRANSDUCER 1)

PRESSURE TRANSDUCER 2

Specifications (see Table C.4) : B

Location (see Figure 3.1) : PT 2

Test pressure instrument : mercury manometer

TABLE C.5: CALIBRATION RESULTS (PRESSURE TRANSDUCER 2)

TEST PRESSURE mmHg (x1,02)	TEST PRESSURE kPa	VOLTAGE SIGNAL V
0	0	0,780
120	16,3	1,062
282	38,4	1,438
484	65,9	1,909
622	84,6	2,220
762	103,7	2,530
300	40,8	1,470
90	12,3	0,985
0	0	0,781

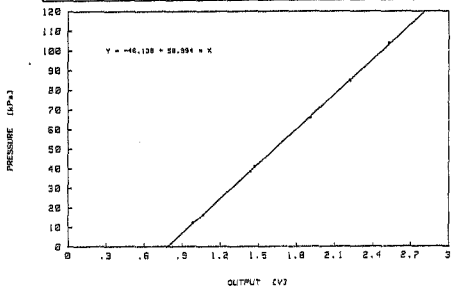


FIGURE C.7: CALIBRATION CURVE (PRESSURE TRANSDUCER 2)

PRESSURE TRANSDUCER 3

Specifications (see Table C.4) : C

Location (see Figure 3.1) : PT 3

Test pressure instrument : Budenberg gauge

TABLE 3.6 : CALIBRATION RESULTS (PRESSURE TRANSDUCER 3)

TEST PRESSURE kP	VOLTAGE SIGNAL V
0	0,797
50	1,522
100	2,280
150	3,102
200	3,901
175	3,452
125	2,663
75	1,879
25	1,119

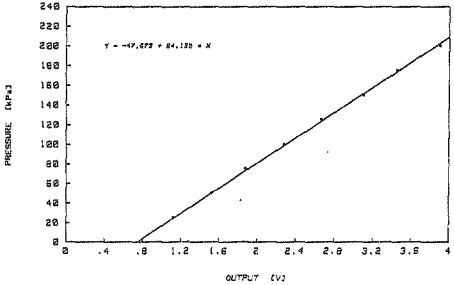


FIGURE C.8: CALIBRATION CURVE (PRESSURE TRANSDUCER 3)

PRESSURE TRANSDUCER 4

Specifications (see Table C.4) : B

Location (see Figure 3.1) : PT 4

Test pressure instrument : Budenberg gauge

TABLE C.7 : CALIBRATION RESULTS (PRESSURE TRANSD ER 4)

TEST PRESSURE kPa	VOLTAGE SIGNAL V
0	0,457
50	1,162
100	1,918
150	2,598
200	3,303
175	2,957
125	2,227
75	1,526

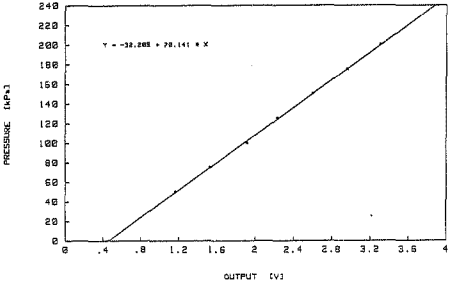


FIGURE C.9: CALIBRATION CURVE (PRESSURE TRANSDUCER 4)

PRESSURE TRANSDUCER 5

Specifications (see Table C.4) : B

Location (see Figure 3.1) : PT 5

Test pressure instrument : Budenberg gauge

TABLE C.8 : CALIBRATION RESULTS (PRESSURE TRANSDUCER 5)

TEST PRESSURE kPa	VOLTAGE SIGNAL V
0	0,802
50	1,528
100	2,314
150	3,118
200	4,015
175	3,600
125	2,742
75	1,960
25	1,116

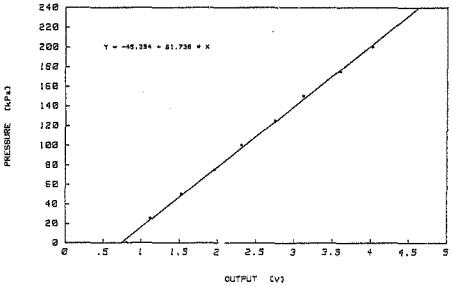


FIGURE C.10: CALIBRATION CURVE (PRESSURE TRANSDUCER 5)

PRESSURE TRANSDUCER 6

Specifications (see Table C.4) : C

Location (see Figure 3.1) : PT 6

Test pressure instrument : Budenberg gauge

TABLE C.9 : CALIBRATION RESULTS (PRESSURE TRANSDUCER 6)

TEST PRESSURE kPa	VOLTAGE SIGNAL V
0	0,803
50	1,531
100	2,446
150	3,302
200	4,188
175	3,785
125	2,853
75	2,001
25	1,178

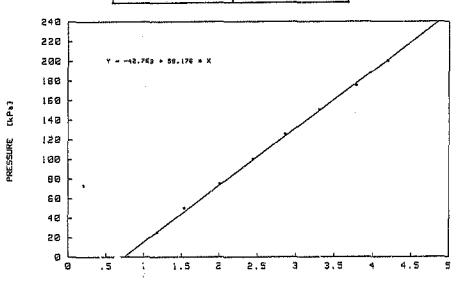


FIGURE C.11: CALIBRATION CURVE (PRESSURE TRANSDUCER 6)

C.4 TEMPERATURE MEASUREMENT

The conveying air temperature was recorded with a temperature resistor at the flowmeter, as shown in Figure 3.1. The air mass flowrate was derived from the temperature, pressure and volumetric flowrate at the flowmeter.

C.4.1 SPECIFICATIONS

MAKE : Ultracust
TYPE : Thermometer resistance

A circuit diagram of the temperature resistor is shown in Figure C.12.

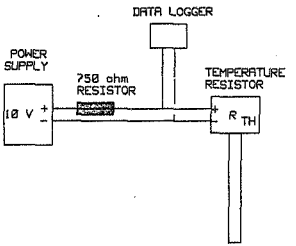


FIGURE C.12: TEMPERATURE RESISTOR CIRCUIT DIAGRAM

The resistance (R_{TH}) is a function of temperature.

C.4.2 CALIBRATION

The temperature resistor and a standard test alcohol thermometer were placed in a beaker of water as shown in Figure C.13.

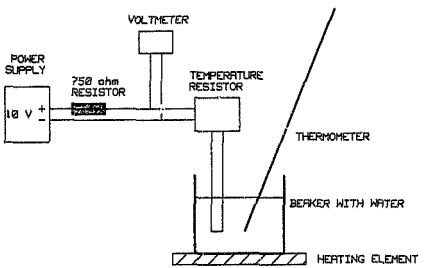


FIGURE C.13: TEMPERATURE RESISTOR CALIBRATION SET-UP

The voltage drop across the temperature resistor was recorded at various water temperatures, as measured with the alcohol thermometer.

TABLE C.10: CALIBRATION RESULTS (TEMPERATURE RESISTOR)

TEMPERATURE °C	VOLTAGE V
3,5	1,170
11,0	1,196
21,0	1,229
30,0	1,264
31,0	1,271
42,0	1,310
55,0	1,352
61,0	1,357

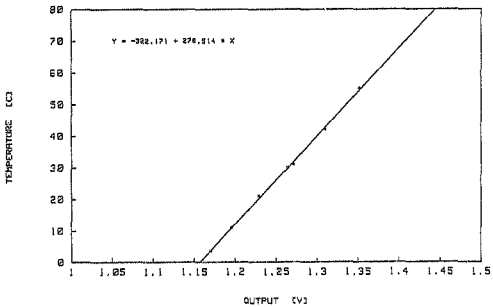


FIGURE C.14: CALIBRATION CURVE (TEMPERATURE RESISTOR)

APPENDIX D

COMPUTER PROGRAMMES

D1 INTRODUCTION
D2 PROGRAMME 1
D3 PROGRAMME II
D4 PROGRAMME III
D5 PROGRAMME IV
D6 PROGRAMME V

D.1 INTRODUCTION

The programmes listed in this Appendix were used for recording and analysis of the data. All the programmes were written in BASIC for the Hewlett Packard (9816) personal computer.

The interaction between Programmes I, II and III is shown in Figure 3.4. Programme IV was used to compare the conveying pressures derived from the equation discussed in Section 5.2 for the various pipeline configurations investigated.

In Appendix D.6 the programme is listed which was used to calculate the performance of the long distance line with the empirical model as discussed in Chapter 10.

02 PROGRAMME I

```
10 OPTION BASE 1
20 PRINTER IS 1
30 PRINT CHR$(12);
40  ON KEY 5 LABEL "STOP" GOTO 1400
50  DIM P(10),Pn(10),S(12,200),Zero(10)
60  PRINT TAB(20);"****************************************"
70  PRINT TAB(20);"*                PROGRAMME I           *"
80  PRINT TAB(20);"****************************************"
90  PRINT TAB(20):
100 PRINT TAB(20);"*****************************************"
110 PRINT TAB(20);"* Programme for the collecting of    *"
120 PRINT TAB(20);"* data during a test run. Voltage    *"
130 PRINT TAB(20);"* signals from the data logger ware *"
140 PRINT TAB(20);"* converted to the corresponding    *"
150 PRINT TAB(20);"* parameters with the calibration   *"
160 PRINT TAB(20);"* curves. All the data was store on *"
170 PRINT TAB(20);"* micro fiexible discs.             *"
180 PRINT TAB(20);"*****************************************"
190 Aa=0
200 BEEP
210 PRINTER IS 1
220 INPUT "TEST NUMBER",Tn$
230 INPUT "DATE eg. 23/5/86",D$
240 INPUT "BAROMETRIC PRESS. (kPa)",Pat
250 INPUT "AIR TEMP. (Deg. C)",T$
260 INPUT "COMPRESSORS USED ",C$
270 INPUT "PRINTER IS ... (1 or 701) :",Pis
280 PRINTER IS Pis
290 PRINT TAB(15);"          TEST NUMBER : ";Tn$
300 PRINT TAB(15);"                 DATE : ";D$
310 PRINT TAB(15);"   BAROMETRIC PRESS. : ";Pat
320 PRINT TAB(15);"     AIR TEMPERATURE : ";T$
330 PRINT TAB(15);"    COMPRESSORS USED : ";C$
340 PRINT
350 PRINTER IS 1
360 IF Aa=1 THEN GOTO 380
370 INPUT "USING STORED ZERO'S  (Y/N)",Z$
380 PRINT "PRESS CONT"
390 PAUSE
400 PRINTER IS Pis
410 PRINT TAB(5);"   PRESSURES ALONG PIPELINE (kPa)        TEMP   AIR     LOAD
TIME   MASS  "
420 PRINT USING 430;"P 1","P 2","P 7","P 5","P 3","P 4","P 6","(C)  ","(m^3/hr)"
,"(kg) ","(sec)","(t/hr)"
430 IMAGE 2X,AAAA,2X,AAAA,2X,AAAA,2X,AAAA,2X,AAAA,2X,AAAA,2X,AAAA,2X,AAAA,1X,AAA
AAAA,1X,AAAAAAA,1X,AAAAA,1X,AAAAAAA
440 PRINT
450 L2=0
460 T3=0
470 T0=TIMEDATE
480   OUTPUT 709;"SIS:1SD0S00VRSVA0VF1VN1VS0VW0VC0"
490   OUTPUT 709;"ARAE2"
500   OUTPUT 709;"AFJOAL39"
510 FOR I=1 TO 500
520  FOR L=1 TO 7
530   Pn(L)=0
540  NEXT L
550  Pn=0
560  Ln=0
```

```
570  Tn=0
580  FOR J=1 TO 5
590   OUTPUT 709;"ASVT3"
600   ENTER 709;P(1)
610   OUTPUT 709;"ASVT3"
620   ENTER 709;P(2)
630   OUTPUT 709;"ASVT3"
640   ENTER 709;P(7)
650   OUTPUT 709;"ASVT3"
660   ENTER 709;P(3)
670   OUTPUT 709;"ASVT3"
680   ENTER 709;F
690   OUTPUT 709;"ASVT3"
700   ENTER 709;P(5)
710   OUTPUT 709;"ASVT3"
720   ENTER 709;P(6)
730   OUTPUT 709;"ASVT3"
740   ENTER 709;L
750   OUTPUT 709;"ASVT3"
760   ENTER 709;T
770   OUTPUT 709;"ASVT3"
780   ENTER 709;P(4)
790   FOR K=1 TO 7
800    Pn(K)=Pn(K)+P(K)
810   NEXT K
820   Fn=Fn+F
830   Ln=Ln+L
840   Tn=Tn+T
850  NEXT J
860  IF A=1 THEN
870   GOTO 1280
880  END IF
890  IF I=1 THEN
900   IF Z$="Y" THEN
910   ASSIGN @Path TO "ZERO"
920   ENTER @Path;Zero(*)
930   FOR M=1 TO 7
940    Pn(M)=Zero(M)*5
950   NEXT M
960   Fn=Zero(8)*5
970   Ln=Zero(9)*5
980   END IF
990   C1=-184.585*Pn(1)/5
1000  C2=-58.994*Pn(2)/5
1010  C3=-64.159*Pn(3)/5
1020  C4=-70.141*Pn(4)/5
1030  C5=-61.758*Pn(5)/5
1040  C6=-58.176*Pn(6)/5
1050  C7=-661.41*Fn/5
1060  C8=-908.008*Ln/5
1070  IF Z$="Y" THEN GOTO 1180
1080  FOR M=1 TO 7
1090  Zero(M)=Pn(M)/5
1100  NEXT M
1110  Zero(8)=Fn/5
1120  Zero(9)=Ln/5
1130  INPUT "CREATE ZERO FILE (Y/N)",Z$
1140  IF Z$="N" THEN GOTO 1160
1150  CREATE BDAT "ZERO",1,100
1160  ASSIGN @Path TO "ZERO"
1170  OUTPUT @Path;Zero
```

```
1180    PRINT "ZERO VOLTAGES ARE"
1190    PRINT "*****************"
1200    PRINT Zero(*)
1210    PRINT
1220    PRINT
1230  ELSE
1240    GOTO 1260
1250  END IF
1260  Fa=C7+651.413*Fn/5
1270  La=C8+908.008*Ln/5
1280  Ta=-322.171+278.514*Tn/5
1290  P1a=C1+184.585*Pn(1)/5
1300  P2a=C2+59.994*Pn(2)/5
1310  P3a=C3+61.159*Pn(3)/5
1320  P4a=C4+70.141*Pn(4)/5
1330  P5a=C5+61.779*Pn(5)/5
1340  P6a=C6+58.176*Pn(6)/5
1350  F1=(P1a+Pat)*Fa/(.287*(Ta+273))
1360  T1=TIMEDATE
1370  T2=T1-T0
1380  IF La<L0 THEN
1390    PRINT USING 1400;P1a,P2a,P3a,P4a,P5a,P6a,Ta,Fa,La,T2,(La-L2)*3.600/(T2-T3
      )
1400    IMAGE DDD.DD,DDD.DD,DDD.DD,DDD.DD,DDD.DD,DDD.DD,DDD.DD,DDD.DD,2X,DD.D,1X,DDDD.DD
      ,1X,DDDD.D,1X,DDDDD.D,1X,DDD.DD
1410  ELSE
1420    PRINT USING 1400;P1a,P2a,P3a,P4a,P5a,P6a,Ta,Fa,La,T2
1430  END IF
1440  S(1,I)=P1a
1450  S(2,I)=P2a
1460  S(3,I)=P3a
1470  S(4,I)=P4a
1480  S(5,I)=P5a
1490  S(6,I)=P6a
1500  S(7,I)=P7a
1510  S(8,I)=Ta
1520  S(9,I)=Fa
1530  S(10,I)=La
1540  S(11,I)=T2
1550  S(12,I)=(La-L2)*3.600/(T2-T3)
1560  L0=La
1570  T3=T2
1580  WAIT 10
1590  NEXT I
1600  INPUT "STORE DATA ? (Y/N)",Sd$
1610  IF Sd$="N" THEN GOTO 1670
1620  INPUT "STORAGE FILE NAME",St$
1630  Bytes=100*(400*I)
1640  CREATE BDAT St$,10,6000
1650  ASSIGN @Path TO St$
1660  OUTPUT @Path;Tn$,Pat,S(*)
1670  INPUT "MORE TESTS ?  Y/N)",Q$
1680  PRINT
1690  IF Q$="Y" THEN
1700    As=1
```

```
1700  &amp;amp;wi
1710  GOTO 200
1720 END IF
1730 PRINT
1740   ASSIGN @Path TO "ZERO"
1750   ENTER @Path;Zero(*)
1760   PRINTER IS Pis
1770   PRINT "ZERO VOLTAGES WERE"
1780   PRINT "**********************"
1790   PRINT Zero(*)
1800   PRINTER IS 1
1810 END
```

D3 PROGRAMME II

```
10    OPTION BASE 1
20    PRINT TAB(20);"**********************************"
30    PRINT TAB(20);"*          PROGRAMME II          *"
40    PRINT TAB(20);"**********************************"
50    PRINT TAB(20);
60    PRINT TAB(20);"**********************************"
70    PRINT TAB(20);"* Programme to retrieve data as *"
80    PRINT TAB(20);"* stored from Programme I and   *"
90    PRINT TAB(20);"* select data to be processed.  *"
100   PRINT TAB(20);"**********************************"
110   ON KEY 5 LABEL "STOP" GOTO 350
120   COM S(11,200),Rn$(10),A,Tn$(10),Pat
130   PRINTER IS 1
140   INPUT "RECORDED DATA STORAGE FILE NAME  :",Rn$
150   ASSIGN @Path TO Rn$
160   ENTER @Path;Tn$,Pat,S(*)
170   PRINT "Test No    : ";Tn$
180 PRINT TAB(5);"PRESSURES ALONG PIPELINE (kPa)     TEMP  AIR FLOW   LOAD    TIM
E   MASS FLOW "
190 PRINT USING 200;"P 1","P 2","P 3","P 4","P 5","P 6","(C)  ","(m^3/hr)","(kg
) ","(sec)","( t/hr )"
200 IMAGE 2X,AAAA,2X,AAAA,2X,AAAA,2X,AAAA,2X,AAAA,2X,AAAA,2X,AAAA,3X,AAAA,2X,AAAAAAAA,2X
,AAAAAAA,1X,AAAAAA,2X,AAAAAAAA
210   INPUT "RANGE OF RECORDED DATA LINE (eg. 50,100) max 50",U,V
220   FOR I=U TO V
230    PRINT USING 250;I,S(1,I),S(2,I),S(4,I),S(7,I),S(10,I),S(11,I)
240   NEXT I
250   IMAGE 7(X,DDDD.DD)
260   PRINT "                          ****************                    "
270   INPUT "SATISFIED WITH RANGE (Y/N)",G$
280   IF G$<>"Y" THEN GOTO 210
290   INPUT "READING NUMBER OF DATA POINTS TO BE PROCESSED (eg. 100B24)",Rn$
300   INPUT "LINE NUMBERS OF READIND NUMBER SPECIFIED ABOVE (eg. 4,5)",A,B
310   FOR I=A TO B
320    PRINT USING 250;I,S(1,I),S(2,I),S(4,I),S(7,I),S(10,I),S(11,I)
330   NEXT I
340   LOAD "ANAG"
350   END
```

```
10    OPTION BASE 1
20    PRINT TAB(20);"*************************************"
30    PRINT TAB(20);"*  CONTINUATION OF PROGRAMME II  *"
40    PRINT TAB(20);"*************************************"
50    PRINT TAB(20);
60    PRINT TAB(20);"*************************************"
70    PRINT TAB(20);"*This Programme was store under  *"
80    PRINT TAB(20);"* the name 'ANAA' and loaded     *"
90    PRINT TAB(20);"* as instructed in LINE 340 in   *"
100   PRINT TAB(20);"* Programme II.                   *"
110   PRINT TAB(20);"*************************************"
120   PRINT TAB(20);
130   DIM P(10),U(10),V(10),Rho(10),Ma(10),Fr(10),D(15,5)
140   COM S(11,200),R$(10),A,Tn$(10),Pat
150   ON KEY 5 LABEL "STOP" GOTO 1150
160   PRINTER IS 1
170   PRINT "Test No. (eg.100A1):";
180   PRINT Tn$
190   PRINT "Res. No.(eg.100A11):";
200   PRINT Re$
210   PRINT "BARO. PRESS.  (kPa):";
220   PRINT Pat
230   FOR K=1 TO 11
240    FOR L=1 TO 2
250     D(K,L)=S(K,A+L-1)
260    NEXT L
270   NEXT K
280   PRINT "P1              (kPa):";
290   P(1)=(D(1,1)+D(1,2))/2
300   PRINT P(1)
310   PRINT "P2              (kPa):";S(2,2);
320   P(2)=(D(2,1)+D(2,2))/2
330   PRINT P(2)
340   PRINT "P3              (kPa):";
350   P(3)=(D(3,1)+D(3,2))/2
360   PRINT P(3)
370   PRINT "P4              (kPa):";
380   P(4)=(D(4,1)+D(4,2))/2
390   PRINT P(4)
400   PRINT "P5              (kPa):";
410   P(5)=(D(5,1)+D(5,2))/2
420   PRINT P(5)
430   PRINT "P6              (kPa):";
440   P(6)=(D(6,1)+D(6,2))/2
450   PRINT P(6)
460   PRINT "TEMP          (Deg C):";
470   T=(D(7,1)+D(7,2))/2
480   PRINT T
490   PRINT "AIR FLOW   (m^3/hr):";
500   F=(D(8,1)+D(8,2))/2
510   PRINT F
520   PRINT "MASS FLOW     (t/hr):";
530   Mas=(D(11,1)+D(11,2))/2
540   PRINT Mas
      INPUT "Ms=",Ms
```

```
550   INPUT "Ms[illegible]",Ms
560   PRINT Ms
570   F=F/3600
580   T=T+273
590   MASS STORAGE IS ":HP8290X,700,1"
600   PRINT "STORAGE FILE NAME  :";Rn$
610   CREATE BDAT Rn$,1,1
620   ASSIGN @Path TO Rn$
630   OUTPUT @Path;Tn$,Pat,P(1),P(2),P(3),P(4),P(5),P(6),T,F,Ms
640   ASSIGN @Path TO Rn$
650   ENTER @Path;Tn$,Pat,P(1),P(2),P(3),P(4),P(5),P(6),T,F,Ms
660   PRINT "Test No    : ";Tn$
670   PRINT "Pat    [kPa]: ";Pat
680   PRINT "P1     [kPa]: ";P(1)
690   PRINT "P2     [kPa]: ";P(2)
700   PRINT "P3     [kPa]: ";P(3)
710   PRINT "P4     [kPa]: ";P(4)
720   PRINT "P5     [kPa]: ";P(5)
730   PRINT "P6     [kPa]: ";P(6)
740   PRINT "TEMP   [ K ]: ";T
750   PRINT "F  [m^3/hr]: ";F*3600
760   PRINT "Ms    [t/hr]: ";Ms
770   PRINT
780   MASS STORAGE IS ":HP8290X,700,0"
790   PRINT "PRESS CONT"
800   PAUSE
810   PRINT
820   FOR I=1 TO 6
830    P(I)=P(I)+Pat
840    Rho(I)=P(I)/(.287*T)
850    Ui(I)=F*(P(1)/P(I))/(3.1415*.0525^2)
860    Vi(I)=Ui(I)*3.1415*.0525^2*3600
870    Mo(I)=.5*Rho(I)*Ui(I)^2
880    Fr(I)=Ui(I)^2/(9.81*.105)
890   NEXT I
900   Ma=Vi(1)*Rho(1)
910   PRINTER IS 701
920   PRINT TAB(33);"TEST NUMBER :";Tn$
930   PRINT
940   PRINT TAB(20);"Read. No    : ";Rn$
950   PRINT TAB(20);"M(a)  [t/hr]:";Ms
960   PRINT TAB(20);"M(a)  [kg/a]:";Ma/3600
970   PRINT TAB(20);"Load Ratio  :";Ma/3.6)/(Ma/3600)
980   PRINT
990   PRINT TAB(33);"POINTS ALONG PIPELINE"
1000  PRINT USING 1030;"1","2","3","5","6"
1010  PRINT TAB(20);"*****************/*************"
1020  PRINT
1030  IMAGE 22X,AAAAA,5X,AAAAA,5X,AAAAA,5X,AAAAA,5X,AAAAA
1040  IMAGE 1X,AAAAAAAAAAAAAAAA,DDDD.DDD,2X,DDDD.DDD,2X,DDDD.DDD,2X,DDDD.DDD,2X
,DDDD.DDD
1050  PRINT USING 1040;"P1 (abs.)    [kPa]",P(1),P(2),P(3),P(5),P(6)
1060  PRINT USING 1040;"Ui           [m/s]",Ui(1),Ui(2),Ui(3),Ui(5),Ui(6)
1070  PRINT USING 1040;"Vi        [m^3/hr]",Vi(1),Vi(2),Vi(3),Vi(5),Vi(6)
1080  PRINT USING 1040;"Rho       [kg/m^3]",Rho(1),Rho(2),Rho(3),Rho(5),Rho(6)
1090  PRINT USING 1040;"1/2*Rho*v^2  [Pa]",Mo(1),Mo(2),Mo(3),Mo(5),Mo(6)
1100  PRINT USING 1040;"Fr           v^2/gD",Fr(1),Fr(2),Fr(3),Fr(5),Fr(6)
1110  PRINT
1120  PRINT
1130  PRINTER IS 1
1140  LOAD "ANAS",163
1150  END
```

D4 PROGRAMME III

```
10    OPTION BASE 1
20    PRINT TAB(20);"*************************************"
30    PRINT TAB(20);"*              PROGRAMME III          *"
40    PRINT TAB(20);"*************************************"
50    PRINT TAB(20);
60    PRINT TAB(20);"*************************************"
70    PRINT TAB(20);"* The data from selected storage *"
80    PRINT TAB(20);"* files was retrieved and the    *"
90    PRINT TAB(20);"* parameters which were plotted  *"
100   PRINT TAB(20);"* on the abcissa and ordinate of *"
110   PRINT TAB(20);"* graph were selected and stored *"
120   PRINT TAB(20);"* in file compatable to the PLOT *"
130   PRINT TAB(20);"* PROGRAMME PACKAGE              *"
140   PRINT TAB(20);"*************************************"
150   PRINT TAB(20);
160   DIM P(10),Rho(10),Ui(10),Vi(10),Mo(10),Fr(10),X(30),Y(30)
170   DIM Mat$(18),Head$[40],Xhead$[40],Yhead$[40]
180   INPUT "No. OF POINTS TO BE PLOTTED",N
190   FOR J=1 TO N
200   READ Rn$
210   DATA 100A11,100A12,100A13,100A14,100A15
220   DATA 100A21,100A22,100A23,100A24,100A25
230   DATA 100A31,100A32,100A33,100A34,100A35
240   DATA 100A41,100A42,100A43,100A44,100A45
250   DATA 100A51,100A52,100A53,100A54,100A55
260   DATA 100B11,100B12,100B13,100B14,100B15
270   DATA 100B21,100B22,100B23,100B24,100B25
280   DATA 100B31,100B32,100B33,100B34,100B35
290   DATA 100B41,100B42,100B43,100B44,100B45
300   DATA 100B51,100B52,100B53,100B54,100B55
310   DATA 100C11,100C12,100C13,100C14,100C15
320   DATA 100C21,100C22,100C23,100C24,100C25
330   DATA 100C31,100C32,100C33,100C34,100C35
340   DATA 100C41,100C42,100C43,100C44,100C45
350   DATA 100C51,100C52,100C53,100C54,100C55
360   DATA 100D11,100D12,100D13,100D14,100D15
370   DATA 100D21,100D22,100D23,100D24,100D25
380   DATA 100D31,100D32,100D33,100D34,100D35
390   DATA 100D41,100D42,100D43,100D44,100D45
400   DATA 100D51,100D52,100D53,100D54,100D55
410   DATA 200A11,200A12,200A13,200A14,200A15
420   DATA 200A21,200A22,200A23,200A24,200A25
430   DATA 200A31,200A32,200A33,200A34,200A35
440   DATA 200A41,200A42,200A43,200A44,200A45
450   DATA 200A51,200A52,200A53,200A54,200A55
460   DATA 400A11,400A12,400A13,400A14,400A15
470   DATA 400A21,400A22,400A23,400A24,400A25
480   DATA 400A31,400A32,400A33,400A34,400A35
490   DATA 400A41,400A42,400A43,400A44,400A45
500   DATA 400A51,400A52,400A53,400A54,400A55
510   MASS STORAGE IS ":HP82290X,700,1"
520   ASSIGN @Path TO Rn$
530   ENTER @Path;Tn$,Pat,P(1),P(2),P(3),P(4),P(5),P(6),T,F,Ms
540   PRINT "Test No      : ";Tn$
550   PRINT "Pat   (kPa): ";Pat
```

```
560   PRINT "P1     (kPa): ";P(1)
570   PRINT "P2     (kPa): ";P(2)
580   PRINT "P3     (kPa): ";P(3)
590   PRINT "P5     (kPa): ";P(5)
600   PRINT "P6     (kPa): ";P(6)
610   PRINT "P7     (kPa): ";P(7)
620   PRINT "TEMP   ( K ): "!T
630   PRINT "F  (m^3/hr): ";F*3600
640   PRINT "Ms    (lb/hr): ";Ms
650   PRINT
660   Ma=Fx(P(1)+Pat)/(.287*T)
670   FOR I=1 TO 7
680    P(I)=P(I)+Pat
690    Rho(I)=P(I)/(.287*T)
700    Ui(I)=Fx.P(1)/P(I)/(3.14159*.0525^2)
710    Vi(I)=Ui(I)*3.14159*.0525^2*3600
720    Mo(I)=.5*Rho(I)*Ui(I)^2
730    Fr(I)=Ui(I)^2/(9.81*.105)
740   NEXT I
750   U=Ms/(3.6*Ma)
760   Pow=Pat*(Ma/(Pat/(.287*T)))*LOG(P(1)/Pat)
770   Lam=(P(2)-P(3))*2*.105/((Rho(2)+Rho(3))/2*((Ui(2)+Ui(3))/2)^2*29.6)
780   Leq=2*3.1415*1.85/4
790   Dpb=(P(2)-P(3))*Leq/29.6
800   Dpb=Dpb*210/(2*1.85/.105)^1.15
810   REM                                    *** VARIABLES SELECTION ***
820   X(J)=Ui(1)
830   Y(J)=(P(1)-Pat)/U
840   NEXT J
850   FOR I=1 TO N
860   PRINT "X=";X(I),"Y=";Y(I)
870   NEXT I
880   INPUT "HEADING OF GRAPH",Head$
890   INPUT "X axis HEADING",Xhead$
900   INPUT "Y axis HEADING",Yhead$
910   INPUT "RANGE OF X",Matr(1),Matr(2)
920   INPUT "RANGE OF Y",Matr(3),Matr(4)
930   INPUT "X TICK",Matr(5)
940   INPUT "Y TICK",Matr(6)
950   INPUT "Y CUTS X @",Matr(7)
960   INPUT "X CUTS Y @",Matr(8)
970   Matr(9)=.1
980   Answer$="1"
990   Matr(10)=2
1000  Matr(11)=2
1010  Matr(12)=2
1020  Matr(13)=2
1030  Matr(14)=2
1040  INPUT "CREATE STORAGE FILE ? (Y/N)",Yn$
1050  INPUT "STORAGE FILE NAME",File$
1060  IF Yn$="N" THEN GOTO 1080
1070  CREATE ASCII File$,50
1080  ASSIGN @File TO File$
1090  OUTPUT @File;N
1100  FOR I=1 TO N
1110  OUTPUT @File;X(I),Y(I)
1120  NEXT I
1130  OUTPUT @File;Matr(*),Head$,Xhead$,Yhead$,Answer$
1140  ASSIGN @File TO *
1150  ASSIGN @File TO File$
```

```
1160  ENTER @File;N
1170  FOR I=1 TO N
1180  ENTER @File;X(I),Y(I)
1190  NEXT I
1200  ENTER @File;Matr(*),Head$,Xhead$,Yhead$,Answer$
1210  ASSIGN @File TO *
1220  FOR I=1 TO N
1230  PRINT I,X(I),Y(I)
1240  NEXT I
1250  PRINT "Matr(1)=";Matr(1)
1260  PRINT "Matr(2)=";Matr(2)
1270  PRINT "Matr(3)=";Matr(3)
1280  PRINT "Matr(4)=";Matr(4)
1290  PRINT "Matr(5)=";Matr(5)
1300  PRINT "Matr(6)=";Matr(6)
1310  PRINT "Matr(7)=";Matr(7)
1320  PRINT "Matr(8)=";Matr(8)
1330  PRINT "Matr(9)=";Matr(9)
1340  PRINT "Matr(10)=";Matr(10)
1350  PRINT "Matr(11)=";Matr(11)
1360  PRINT "Matr(12)=";Matr(12)
1370  PRINT "Matr(13)=";Matr(13)
1380  PRINT "Matr(14)=";Matr(14)
1390  PRINT "Head$      ";Head$
1400  PRINT "XHead$     ";Xhead$
1410  PRINT "YHead$     ";Yhead$
1420  PRINT "Answer$    ";Answer$
1430  PRINT
1440  PRINT "PROGRAM DONE"
1450  MASS STORAGE IS ":HP82901X,700,0"
1460  LOAD "PLOT"
1470  END
```

D5 PROGRAMME IV

```
10    OPTION BASE 1
20    COM X(50),Y(50),N
30    PRINT TAB(20);"***************************************"
40    PRINT TAB(20);"                PROGRAMME IV           *"
50    PRINT TAB(20);"***************************************"
60    PRI NT TAB(20);
70    INPUT "PRINTER IS  ..(1 or 701)",P
80    PRINTER IS P
90    PRINT "          COMPARING 100A,100D,200A,200B,200C  and 400A TO DETERMINE
THE   "
100   PRINT "                        EFFECT OF THE PIPE DIAMETER
 "
110   PRINT "                              AND LINE LENGTH
 "
120   PRINT
130   PRINT "          P1a  :     100 m of 105 mm Diamater Pipeline   "
140   PRINT "          P1b  :     50 m / 105 mm  +  50m / 156 mm      "
150   PRINT "          P1c  :     20 m / 105 mm  +  80m / 156 mm      "
160   PRINT "          P1d  :     100 m of 156 mm Diamater Pipeline   "
170   PRINT "          P2a  :     200 m of 105 mm Diamater Pipeline   "
180   PRINT "          P2b  :     200 m of 156 mm Diamater Pipeline   "
190   PRINT "          P2c  :     200 m of 200 mm Diameter Pipeline   "
200   PRINT "          V1   :     Ave. AIR VELOCITY          : P2a    "
210   PRINT "          V2   :     Ave. AIR VELOCITY          : P2b
220   PRINT "          V3   :     Ave. AIR VELOCITY          : P2c
230   PRINT "          Po1  :     POWER REQUIRED FOR : P2a         "
240   PRINT "          Po2  :     POWER REQUIRED FOR : P2b         "
250   PRINT "          Po3  :     POWER REQUIRED FOR : P2c         "
260   PRINT
270   PRINT "        Q       B          V1       V2       V3       P1d      Po1      Po
2     Po3"
280   PRINT "     [kg/s] [t/hr]      [m/s]    [m/s]    [m/s]    [kPa]    [kW]     [kW
]     [kW]"
290   PRINT "*************************************************************************
*************"
300   PRINT
310   D1=.105
320   D2=.156
330   PRINT "     AIR MASS FLOWRATE [kg/s] : ";
340   INPUT Q
350   PRINT Q
360   PRINT "PRODUCT MASS FLOWRATE [t/hr] : ";
370   INPUT B
380   PRINT B
390   A1a=133.901*Q^2
400   B1a=10.847+23.309*Q
410   A1b=105.682*Q^2
420   B1b=9.344+14.567*Q
430   A1c=45.138*Q^2
440   B1c=10.229+7.727*Q
450   A1d=48.468*Q^2
460   B1d=9.639+9.868*Q
470   A2a=257.406*Q^2
480   B2a=27.866-2.558*Q
490   A2b=60.273*Q^2
500   B2b=16.728+4.267*Q
510   A2c=77.895*Q^2
520   B2c=19.667-4.757*Q
530   A4a=102.891*Q^2
540   B4a=15.264+17.272*Q
550   P1a=A1a*B1a^3.5
```

```
560   P1b=A1b+B1b*G^.5
570   P1c=A1c+B1c*G^.5
580   P1d=A1d+B1d*G^.5
590   P2a=A2a+B2a*G^.5
600   P2b=A2b+B2b*G^.5
610   P2c=A2c+B2c*G^.5
620   P4a=A4a+B4a*G^.5
630   IMAGE 3X,DD.DD,3X,DDD.D.7X,DDDDD.2X,DDDDDD,2X,DDDDDD,3X,DDD.D,3X,DDD.D,3X,
DDD.D,3X,DDD.D
640   V1=Q*.287*300*(1/(B4+P2a)+1/B6)/2*3600
650   V2=Q*.287*300*(1/(B4+P2b)+1/B6)/2*3600
660   V3=Q*.287*300*(1/(B4+P2c)+1/B6)/2*3600
670   Ve11=Q*.287*300*(1/(B4+P2a)+1/B6)/2/(3.14159*.105^2/4)
680   Ve12=Q*.287*300*(1/(B4+P2b)+1/B6)/2/(3.14159*.156^2/4)
690   Ve13=Q*.287*300*(1/(B4+P2c)+1/B6)/2/(3.14159*.206^2/4)
700   Ps1=Q*.287*300*LOG((B4+P2a)/B6)
710   Ps2=Q*.287*300*LOG((B4+P2b)/B6)
720   Ps3=Q*.287*300*LOG((B4+P2c)/B6)
730   REM                                        *****  SELECT VARIABLE  *****
740   X(1)=119.8
750   X(2)=252.1
760   X(3)=494.3
770   Y(1)=P1d
780   Y(2)=P2b
790   Y(3)=P4a
800   PRINT USING 630;Q,B,Ve11,Ve12,Ve13,P1d,P2a,P2b,P2c
810   C=C+1
820   IMAGE 24X,DDD.D,4X,DDD.D,3X,DDDD.D,3X,DDDD.D,4X,DDD.D,4X,DDD.D,4X,DDD.D,4X
,DDD.D
830   PRINT "**********************************************************************
**********"
840   INPUT "PLOT GRAPH ? (Y/N)",P$
850   IF P$="N" THEN GOTO 910
860   PRINT "N=";N
870   FOR I=1 TO N
880   PRINT X(I),Y(I)
890   NEXT I
900   LOAD 'ANA20"
910   PRINTER IS 1
920   END
```

```
10    PRINT TAB(20);"**********************************"
20    PRINT TAB(20);"*  CONTINUATION OF PROGRAMME IV  *"
30    PRINT TAB(20);"**********************************"
40    PRINT TAB(20);
50    PRINT TAB(20);"**********************************"
60    PRINT TAB(20);"* This Programme was stored under *"
70    PRINT TAB(20);"* the name 'ANA20' and was loaded *"
80    PRINT TAB(20);"* as instructed in LINE 900 of    *"
90    PRINT TAB(20);"* PROGRAMME IV                    *"
100   PRINT TAB(20);"**********************************"
110   PRINT TAB(20);
120   OPTION BASE 1
130   DIM P(10),Rho(10),Ui(10),Vi(10),M0(10),Fr(10)
140   DIM Matr(18),Head$[40],Xhead$[40],Yhead$[40]
150   COM X(50),Y(50),N
160   PRINT "N=";N
170   FOR I=1 TO N
180   PRINT "X=";X(I),"Y=";Y(I)
190   NEXT I
200   INPUT "HEADING OF GRAPH",Head$
210   INPUT "X axis HEADING",Xhead$
220   INPUT "Y axis HEADING",Yhead$
230   INPUT "RANGE OF X",Matr(1),Matr(2)
240   INPUT "RANGE OF Y",Matr(3),Matr(4)
250   INPUT "X TICK",Matr(5)
260   INPUT "Y TICK",Matr(6)
270   INPUT "Y CUTS X @",Matr(7)
280   INPUT "X CUTS Y @",Matr(8)
290   Matr(9)=.1
300   Answer$="1"
310   Matr(10)=2
320   Matr(11)=2
330   Matr(12)=2
340   Matr(13)=2
350   Matr(14)=2
360   INPUT "CREATE STORAGE FILE ? (Y/N)",Yn$
370   INPUT "STORAGE FILE NAME",File$
380   IF Yn$="N" THEN GOTO 400
390   CREATE ASCII File$,50
400   ASSIGN @File TO File$
410   OUTPUT @File;N
420   FOR I=1 TO N
430   OUTPUT @File;X(I),Y(I)
440   NEXT I
450   OUTPUT @File;Matr(*),Head$,Xhead$,Yhead$,Answer$
460   ASSIGN @File TO *
470   ASSIGN @File TO File$
480   ENTER @File;N
490   FOR I=1 TO N
500   ENTER @File;X(I),Y(I)
```

```
510   NEXT I
520   ENTER @File;Matr(*),Head$,Xhead$,Yhead$,Answer$
530   ASSIGN @File TO *
540   FOR I=1 TO N
550   PRINT I,X(I),Y(I)
560   NEXT I
570   PRINT "Matr(1)=";Matr(1)
580   PRINT "Matr(2)=";Matr(2)
590   PRINT "Matr(3)=";Matr(3)
600   PRINT "Matr(4)=";Matr(4)
610   PRINT "Matr(5)=";Matr(5)
620   PRINT "Matr(6)=";Matr(6)
630   PRINT "Matr(7)=";Matr(7)
640   PRINT "Matr(8)=";Matr(8)
650   PRINT "Matr(9)=";Matr(9)
660   PRINT "Matr(10)=";Matr(10)
670   PRINT "Matr(11)=";Matr(11)
680   PRINT "Matr(12)=";Matr(12)
690   PRINT "Matr(13)=";Matr(13)
700   PRINT "Matr(14)=";Matr(14)
710   PRINT "Head$     ";Head$
720   PRINT "XHead$    ";Xhead$
730   PRINT "YHead$    ";Yhead$
740   PRINT "Answer$   ";Answer$
750   PRINT
760   PRINT "PROGRAM DONE"
770   MASS STORAGE IS ":HPS290X,700,0"
780   END
```

D6 PROGRAMME V

```
10    PRINT TAB(20);"*****************************"
20    PRINT TAB(20);"*         PROGRAMME V         *"
30    PRINT TAB(20);"*****  *********************"
40    PRINT TAB(20);
50    PRINT TAB(20);"*******.*********************"
60    PRINT TAB(20);"* Programme for calulating  *"
70    PRINT TAB(20);"* the convaying pressure of *"
80    PRINT TAB(20);"* the long distance line    *"
90    PRINT TAB(20);"*****************************"
100   PRINT TAB(20);
110   OPTION BASE 1
120   DIM P(10),Rho(10),Ui(10),Vi(10),Mo(10),Fr(10),X(30),Y(30),K(30)
130   DIM Matr(18),Head$[40],Xhead$[40],Yheads[40]
140   L(1)=390
150   L(2)=682
160   L(3)=476
170   D(1)=.105
180   D(2)=.156
190   D(3)=.200
200   INPUT "No. OF POINTS TO BE PLOTTED",N
210   FOR J=1 TO N
220   READ Rn$
230   DATA 1200A11,1200A12,1200A13
240   DATA 1200A21,1200A22,1200A23
250   DATA 1200A31,1200A32,1200A33
260   DATA 1200A11R,1200A12R,1200A13R
270   DATA 1200A21R,1200A22R,1200A23R
280   DATA 1200A31R,1200A32R,1200A33R
290   DATA 1200A11RR,1200A12RR,1200A13RR
300   DATA 1200A21RR,1200A22RR,1200A23RR
310   MASS STORAGE IS ":HP82290X.700.1"
320   ASSIGN @Path TO Rn$
330   ENTER @Path;Tn$,Pat,P(1),T,F,Ms
340   PRINT "Test No    : ";Tn$
350   PRINT "Pat   [kPa]: ";Pat
360   PRINT "P1    [kPa]: ";P(1)
370   PRINT "TEMP  [ K ]: ";T
380   PRINT "F  [m^2/hr]: ";F*3600
390   PRINT "Ms    [t/hr]: ";Ms
400   PRINT
410   T=1
420    P(I)=P(I)*Pat
430    Rho(I)=P(I)/(.287*T)
440    Ui(I)=F*(P(1)/P(I))/(3.1415*.0529^2)
450    Vi(I)=Ui(I)*3.1415*.0529^2*3600
460    Mo(I)=.5*Rho(I)*Ui(I)^2
470    Fr(I)=Ui(I)^2/(9.81*.105)
480   Ma=Vi(1)*Rho(1)/3600
490   U=Ms/(2.5*Ma)
500   Pow=Pat*(Ma/(Pat/(.287*T)))*LOG(P(1)/Pat)
510   P1=Pat
520   Pt=0
530   FOR I=3 TO 1 STEP -1
540   Pg=100
550   Va=(Ma*.287*300/(3.14159*D(I)^2/4)/2*(1/(P1+Pg)+1/P1))
560   Bet=5.317E-4+194.218*D(I)^
```

```
570   Alp=Bet*L(I)^.5
580   P2=(1.014+(Alp*Va^2)/(9.81*D(I)))*(1+U)
590   Err=ABS(P2-Pg)
600   IF Err<.01 THEN GOTO 630
610   Pg=(P2+Pg)/2
620   GOTO 550
630   P=P2
640   Pt=Pt+P2
650   NEXT I
660   REM                                   *** VARIABLES SELECTION ***
670   X(J)=P(1)-Pat
680   K(J)=Pt-(P(1)-Pat)
690   Y(J)=Pt
700   NEXT J
710   FOR I=1 TO N
720   PRINT "X=";X(I),"Y=";Y(I),"K=";K(I)
730   NEXT I
740   INPUT "HEADING OF GRAPH",Head$
750   INPUT "X axis HEADING",Xhead$
760   INPUT "Y axis HEADING",Yhead$
770   INPUT "RANGE OF X",Matr(1),Matr(2)
780   INPUT "RANGE OF Y",Matr(3),Matr(4)
790   INPUT "X TICK",Matr(5)
800   INPUT "Y TICK",Matr(6)
810   INPUT "Y CUTS X @",Matr(7)
820   INPUT "X CUTS Y @",Matr(8)
830   Matr(9)=.1
840   Answer$="1"
850   Matr(10)=2
860   Matr(11)=2
870   Matr(12)=2
880   Matr(13)=2
890   Matr(14)=2
900   INPUT "CREATE STORAGE FILE ? (Y/N)",Yn$
910   INPUT "STORAGE FILE NAME",File$
920   IF Yn$="N" THEN GOTO 940
930   CREATE ASCII File%,50
940   ASSIGN @File TO File$
950   OUTPUT @File;N
960   FOR I=1 TO N
970   OUTPUT @File;X(I),Y(I)
980   NEXT I
990   OUTPUT @File;Matr(*),Head$,Xhead$,Yhead$,Answer$
1000  ASSIGN @File TO *
1010  ASSIGN @File TO File$
1020  ENTER @File;N
1030  FOR I=1 TO N
1040  ENTER @File;X(1),Y(I)
1050  NEXT I
1060  ENTER @File;Matr(*),Head$,Xhead$,Yhead$,Answer$
1070  ASSIGN @File TO *
1080  FOR I=1 TO N
1090  PRINT I,X(I),Y(I)
1100  NEXT I
1110  PRINT "Matr(1)=";Matr(1)
1120  PRINT "Matr(2)=";Matr(2)
1130  PRINT "Matr(3)=";Matr(3)
1140  PRINT "Matr(4)=";Matr(4)
1150  PRINT "Matr(5)=";Matr(5)
1160  PRINT "Matr(6)=";Matr(6)
1170  PRINT "Matr(7)=";Matr(7)
```

```
570   Alp=Bet*L(I)^.5
580   P2=(1.014+(Alp*Va^2)/(9.81*D(I)))*(1+U)
590   Err=ABS(P2-Pg)
600   IF Err<.01 THEN GOTO 630
610   Pg=(P2+Pg)/2
620   GOTO 550
630   Pi=P2
640   Pt=Pt+P2
650   NEXT I
660   REM                                        *** VARIABLES SELECTION ***
670   X(J)=P(I)-Pat
680   K(J)=Pt-(P(1)-Pat)
690   Y(J)=Pt
700   NEXT J
710   FOR I=1 TO N
720   PRINT "X=";X(I),"Y= ";Y(I),"K=";K(I)
730   NEXT I
740   INPUT "HEADING OF GRAPH",Head$
750   INPUT "X axis HEADING",Xhead$
760   INPUT "Y axis HEADING",Yhead$
770   INPUT "RANGE OF X",Matr(1),Matr(2)
780   INPUT "RANGE OF Y",Matr(3),Matr(4)
790   INPUT "X TICK",Matr(5)
800   INPUT "Y TICK",Matr(6)
810   INPUT "Y CUTS X @",Matr(7)
820   INPUT "X CUTS Y @",Matr(8)
830   Matr(9)=.1
840   Answer$="1"
850   Matr(10)=2
860   Matr(11)=2
870   Matr(12)=2
880   Matr(13)=2
890   Matr(14)=2
900   INPUT "CREATE STORAGE FILE ? (Y/N)",Yn$
910   INPUT "STORAGE FILE NAME",File$
920   IF Yn$="N" THEN GOTO 940
930   CREATE ASCII File$,50
940   ASSIGN @Filec TO File$
950   OUTPUT @Filec;N
960   FOR I=1 TO N
970   OUTPUT @Filec;X(I),Y(I)
980   NEXT I
990   OUTPUT @Filec;Matr(*),Head$,Xhead$,Yhead$,Answer$
1000  ASSIGN @Filec TO *
1010  ASSIGN @File TO File$
1020  ENTER @File;N
1030  FOR I=1 TO N
1040  ENTER @File;X(I),Y(I)
1050  NEXT I
1060  ENTER @File;Matr(*),Head$,Xhead$,Yhead$,Answer$
1070  ASSIGN @File TO *
1080  FOR I=1 TO N
1090  PRINT I,X(I),Y(I)
1100  NEXT I
1110  PRINT "Matr(1)=";Matr(1)
1120  PRINT "Matr(2)=";Matr(2)
1130  PRINT "Matr(3)=";Matr(3)
1140  PRINT "Matr(4)=";Matr(4)
1150  PRINT "Matr(5)=";Matr(5)
1160  PRINT "Matr(6)=";Matr(6)
1170  PRINT "Matr(7)=";Matr(7)
```

```
1180  PRINT "Matr(8)=";Matr(8\
1190  PRINT "Matr(9)=";Matr(9,
1200  PRINT "Matr(10)=";Matr(10)
1210  PRINT "Matr(11)=";Matr(11)
1220  PRINT "Matr(12)=";Matr(12)
1230  PRINT "Matr(13)=";Matr(13)
1240  PRINT "Matr(14)=";Matr(14)
1250  PRINT "Head$     ";Head$
1260  PRINT "XHead$    ";Xhead$
1270  PRINT "YHead$    ";Yhead$
1280  PRINT "Answer$   ";Answer$
1290  PRINT
1300  PRINT "PROGRAM DONE"
1310  MASS STORAGE IS ":HP8290X,700,0"
1320  LOAD "PLOT"
1330  END
```

APPENDIX E

DIMENSIONS OF PIPELINE CONFIGURATIONS INVESTIGATED

E.1 INTRODUCTION

E.2 SCHEMATIC DIAGRAMS

E.1 INTRODUCTION

The dimensions of the pipeline configurations investigated are given in the schematic diagrams in Appendix E.2. The effective *conveying distance* was derived from the horizontal conveying lengths and the equivalent length of the bends as discussed in Appendix F.

The point along the *pipeline* where a change in pipe diameter occurs is also shown in the diagrams.

E.2 SCHEMATIC DIAGRAMS

DIMENSIONS

A = 37.6 m
B = 5.1 m
C = 33.1 m
D = 5.3 m
E = 7.8 m
F = 2.1 m
TOTAL : 91.0 m

O 1 : 105 to 156 mm [100B]
O 2 : 105 to 156 mm [100C]
O 3 : 105 to 156 mm [100D]

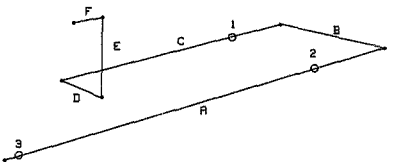


FIGURE E.1: DIMENSIONS OF 100 METRE LOOP

DIMENSIONS

A = 37.6 m
B = 10.5 m
C = 28.5 m
D = 1.3 m
E = 40.0 m
F = 1.4 m
G = 44.4 m
H = 11.3 m
I = 7.8 m
J = 2.1 m

TOTAL : 184.9 m

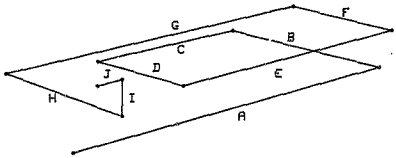


FIGURE E.2: DIMENSIONS OF 200 METRE LOOP

DIMENSIONS

A = 37.6 m
B = 10.5 m
C = 28.5 m
D = 1.3 m
E = 40.0 m
F = 1.4 m
G = 44.4 m
H = 11.3 m
I = 7.8 m
J = 2.1 m

TOTAL : 350.3 m

○ 1 : 185 to 156 mm [400B]

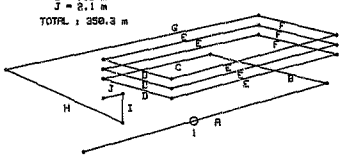


FIGURE E.3: DIMENSIONS OF 400 METRE LOOP

DIMENSIONS

A = 43.9 m
B = 10.1 m
C = 114.8 m
D = 117.1 m
E = 3.2 m
F = 65.7 m
G = 338.8 m
H = 6.0 m
I = 6.0 m
J = 13.8 m
K = 6.0 m
L = 6.0 m
M = 248.6 m
N = 155.3 m
O = 3.1 m
P = 119.8 m
Q = 71.0 m
R = 20.0 m
S = 6.8 m
T = 1.9 m

TOTAL = 1358 m

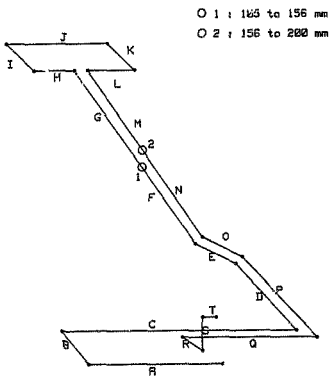


FIGURE E.4: DIMENSIONS OF LONG DISTANCE LINE

APPENDIX F

EFFECTIVE LENGTH OF PIPELINES

F.1 INTRODUCTION

F.2 EQUIVALENT LENGTH OF BENDS

F.3 EFFECTIVE LENGTHS

F.1 INTRODUCTION

The empirical model developed to predict the performance of the long distance line, as discussed in Chapter 10, was based on an effective length of the conveying pipelines. Due to the pressure loss across a bend, which is usually far in excess of any other pressure losses in the conveying system (Ref.16), an equivalent horizontal length for a bend is incorporated.

F.2 EQUIVALENT LENGTH OF BENDS

From recent investigations by Jardine (Ref.5) the equivalent length of a bend was found to be approximately half of the equivalent length as suggested in the model developed by Schuchart (Ref.32).

The investigations by Jardine (Ref.5) were conducted under similar conditions to the experimental investigation described in this report.

The pressure drop across a bend, as suggested by Schuchart (Ref.32), is shown in Equation F.1.

$$\frac{P_{bend}}{P_{straight}} = 210 \cdot \left(\frac{D_b}{D_t}\right)^{-1,15} \qquad (F.1)$$

where D_b = Bend Curvature Diameter
D_t = Pipe Inner Diameter
P_{bend} = Pressure Drop Across a Bend
$P_{straight}$ = Pressure Drop Across a Straight Section Equal in Length to the Bend.

The pressure drop across a bend can be converted into an equivalent length of straight pipeline which has the same pressure drop as the bend. The equivalent length of the bend (L_b) is given by:

$$L_b = (2 \pi R_B) / 4 \qquad (F.2)$$

The dimensions of the bends and the corresponding equivalent lengths are shown in Table F.1.

TABLE F.1: EQUIVALENT LENGTH OF BENDS

PIPE DIAMETER (mm)	BEND RADIUS (mm)	EQUIVALENT LENGTH (m)
105	1850	5,1
156	550	9,6
200	310	14,0

F.3 EFFECTIVE LENGTHS

The effective lengths of the pipeline configurations used in the development of the empirical model to predict the performance of the long distance line are shown in Table F.2. The effective length of the long distance line is given in Table F.3. The dimensions of the pipeline configurations are shown in Appendix E.

TABLE F.2: EFFECTIVE LENGTH OF PIPELINE CONFIGURATIONS

PIPELINE CONFIGURATION	HORIZONTAL LENGTH (m)	NO. OF BENDS	EQUIVALENT LENGTH/BEND (m)	EFFECTIVE LENGTH (m)
100A	91,0	3	5,1	106,3
100D	91,0	3	9,6	119,8
200A	184,9	7	5,1	220,6
200B	184,9	7	9,6	252,1
200C	184,9	7	14,0	282,9
400A	350,3	15	9,6	494,3

TABLE F.3: EFFECTIVE LENGTH OF THE LONG DISTANCE LINE

PIPE DIAMETER (mm)	HORIZONTAL LENGTH (m)	NO. OF BENDS	EQUIVALENT LENGTH/BEND (m)	EFFECTIVE LENGTH (m)
105	354,9	7	5,1	390,6
156	625,1	5	9,6	682,7
200	378,4	7	14,0	476,1
TOTAL	1358,4	20		1549,4

APPENDIX G

PRESSURE DROP FROM FLOWMETER TO THE ROTARY VALVES

G.1 INTRODUCTION
G.2 CALCULATIONS
G.3 CONCLUSIONS

G.1 INTRODUCTION

In this Appendix it is shown that the pressure drop from the flowmeter to the rotary valves, where material was fed into the conveying line, is negligible in relation to the pressure drop across the whole system. The pressure at the flowmeter was thus defined as the conveying pressure.

The maximum pressure drop from the flowmeter to the rotary valves would correspond to a maximum air mass flowrate. The results from test number 100A51, as shown in Appendix A.3, were used in the calculations shown in Appendix G.2.

G.2 CALCULATIONS

The results from the test number 100A51 were:

Air mass flowrate	$\dot{Q}$	= 0,57 kg/s
Pressure at flowmeter	P(1)	= 101,8 kPa
Atmospheric pressure	Pat	= 85,2

The average velocity v is given by:

$$v = \dot{Q} / (\rho A)$$
$$= \dot{Q} / ((p / RT) A)$$
$$= 0,57/((85,2 + 101,8)/(0,287.300). 0,105^2/4)$$
$$= 30,3 \text{ m/s}.$$

The viscosity of air at a temperature of 300 K is $16,84.10^{-6}$ (Ref.20).

Thus the Reynolds number R_e is:

$$R_e = v D / \nu$$
$$= 30,3 . 0,105 / 16,84.10^{-6}$$
$$= 1,89.10^5$$

The friction factor f_L is given by: (Ref.14)

$$f_L = 0,0014 + 0,125/(R_e)^{0,32}$$

$$= 0,0014 + 0,125/(1,89.10^5)^{0,32}$$

$$= 0,00396$$

The pressure drop is derived from Equation G.1 where L_e is the effective length of pipeline. The effective lengths from the flowmeter to the rotary valves was approximately 15,5 metres.

$$p = 4\, f_L \lambda\, L_e\, v^2 / (2.D) \qquad (G.1)$$

Thus:

$$p = 4 \,.\, 0,00396 \,.\, \frac{(101,8 + 85,2)}{0,287.300} \,.\, 15,5.30,3^2/(2.0,105)$$

$$= 2,33 \text{ kPa}$$

The maximum pressure drop from the flowmeter to the rotary valves was thus 2,33 kPa corresponding to a pressure at the flowmeter (ie. conveying pressure) of 101,8 kPa.

G.3 CONCLUSION

The pressure drop from the flowmeter to the rotary valve thus contributed a maximum of 2,28% of the total drop across the system.

Considering that the repeatibility of the results was 6,7%, as shown in Appendix I.3, the pressure drop from the flowmeter to the rotary valve was thus insignificant.

APPENDIX H

MAXIMUM FEEDRATE OF THE ROTARY VALVES

H.1 INTRODUCTION
H.2 CALCULATIONS

H.1 INTRODUCTION

Although the maximum feedrate of the rotary valves, as calculated in Appendix H.2, was in the order of 25 t/h, the maximum product mass flowrate recorded in the receiving hopper was 33,5 t/h. This was attributed to the higher pressure in the blow vessel than the pressure in the conveying pipeline. The material probably had a higher bulk density in the rotary valves than the bulk density of the fluidized material in the blow vessel.

Flow through the leakage spaces in the rotary valves could also explain the high product mass flowrates recorded.

H.2 CALCULATION

The maximum speed (S) of the rotary valves was 31 rpm. The volume (V) of the annulus through which material passed in the rotary valve is given by:

$$V = (d_1^2 - d_2^2) / 4 \cdot L$$

The dimensions of the rotary valve are shown in Figure H.1.

Thus:

$$V = (0,25^2 - 0,075^2) / 4 \cdot 0,325$$
$$= 0,0145 \ m^3$$

The volume throughput (W) of the rotary valves is thus:

$$W = V \cdot S$$
$$= 0,0145.31$$
$$= 0,45 \ m^3/min$$
$$= 27 \ m^3/hr$$

With a bulk density of 930 kg/m^3 for aerated flyash the maximum product mass flowrate would be:

$$\dot{G} = 930 \cdot 27$$
$$= 25110 \text{ kg/h}$$
$$\doteq 25 \text{ t/h}$$

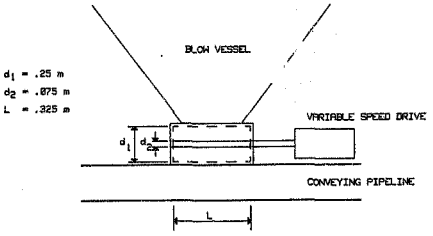


FIGURE H.1: ROTARY VALVE DIMENSIONS

APPENDIX I

ERROR ANALYSIS

I.1 INTRODUCTION
I 2 EXPERIMENTAL ERRORS
I.3 REPEATABILITY OF RESULTS
I.4 EQUATION ERRORS
I.5 MODEL ERRORS

I.1 INTRODUCTION

The accuracy of the results was determined by considering the resolution of the calibration equipment used to calibrate the various instruments recording the data. The number of significant figures recorded for the output signal from the instruments during the calibration also determined the accuracy of the results.

The repeatability of the results is shown by plotting the conveying pressure of the repeated tests against the conveying pressure as calculated from the equations developed in Section 5.2, at the corresponding product and air mass flowrates.

The error in the equations expressing the conveying pressure as a function of product and air mass flowrate for a specific pipeline configuration was determined by plotting the experimentally recorded conveying pressure against the conveying pressure derived from the equation at the corresponding product and air mass flowrate.

Similarly, the error of the empirical model developed to predict the performance of the long distance line was determined by plotting the *calculated conveying pressure (Pmod) against* the experimentally recorded conveying pressure (Pexp) for the p peline configurations from which the model was derived.

I.2 EXPERIMENTAL ERRORS

The experimental uncertainties are summarised in Table I.1. The total uncertainty was derived from the resolution of the calibration instruments and the number of significant figures recorded in the calibration.

TABLE I.1: SUMMARY OF EXPERIMENTAL ERRORS

PARAMETER	UNCERTAINTY
Conveying pressure	0,1602 kPa
Product mass flowrate	0,070 t/h
Temperature	0,64 ^{o}C
Air mass flowrate	1,762.10^{-3} kg/s

I.2.1 CONVEYING PRESSURE

The conveying pressure was recorded with Pressure Transducer 1, as specified in Appendix C. The mercury manometer used to calibrate the pressure transducer had a resolution of 0,5 units (or 0,5 . 1,02 = 0,51mm). The uncertainty (W_{p1}) was thus:

$$W_{p1} = \rho \cdot g \cdot h$$
$$= 13{,}6 \cdot 9{,}81 \cdot 0{,}51$$
$$= 68{,}0 \text{ Pa}$$

Three significant figures were recorded for the voltage signal from the pressure transducer. The uncertainty (W_{p2}) was thus 0,0005 V. From the calibration equation the corresponding uncertainty in terms of pressure was determined as shown below.

The slope of the calibration curve for Pressure Transducer 1, as shown in Appendix C, was 184,585 kPa/V.

Thus:

$$W_{p2} = 184{,}585 \cdot 0{,}0005$$
$$= 92{,}2 \text{ Pa}$$

The total uncertainty (W_p) in the conveying pressure is given by:

$$W_p = W_{p1} + W_{p2}$$
$$= 68{,}0 + 92{,}2$$
$$= 160{,}2 \text{ Pa}$$

I.2.2 PRODUCT MASS FLOWRATE

Two methods were used to determine the product mass flowrate. At high air mass flowrates the difference in mass of the receiving hopper was divided by the corresponding time interval. The only experimental error was thus due to the uncertainty of the mass as recorded in the receiving hopper. The time interval was accurately recorded from the computer in-built clock.

There was no uncertainty in the mass of the 40 kg calibration weights. The uncertainty of the load cell output signal was 0,0005 V. Thus from the calibration curve, the uncertainty (W_L) is:

$$W_L = 0{,}0005 \cdot 908{,}008$$
$$= 0{,}45 \text{ kg}$$

The product mass flowrate is derived from:

$$\dot{G} = G / T$$

Thus:

$$\frac{d\dot{G}}{dG} = \frac{1}{T}$$

The average time interval to record the product mass flowrate was 300 sec.

Thus:

$$\frac{d\dot{G}}{dG} = \frac{1}{300}$$

The uncertainty (W) in the product mass flowrate was

$$W_{G1} = [\,[\,(d\dot{G})/(dG)\,.\,W_L\,]^2\,]^{0,5}$$
$$= [\,[\,1/300\,.\,0,45\,]^2\,]^{0,5}$$
$$= 0,013 \text{ kg/s}$$
$$= 0,047 \text{ t/h}$$

At low air mass flowrates, plugs of material entered the receiving hopper. The product mass flowrate was derived from the slope of the mass versus time trace. The protractor used to measure the slope had a resolution of $0,5^{o}$. From a typical set of results, 51^{o} correspond to 7,1 t/h.

Thus the uncertainty (W_{G2}) in product mass flowrate was thus:

$$W_{G2} = 7,1\,.\,0,5/51$$
$$= 0,070 \text{ t/h}$$

I.2.3 TEMPERATURE

The resolution of the alcohol thermometer used to calibrate the temperature resistor was $0,5^{o}C$. Thus the corresponding uncertainty of the temperature resistor (W_{T1}) was $0,5^{o}C$. The voltage signal was recorded to within + 0,0005 V. From the slope of the calibration curve, the uncertainty is given by:

$$W_{T2} = 278,514\,.\,0,0005$$
$$= 0,14^{o}C$$

Thus the total uncertainty (W_T) of the temperature resistor was:

$$W_T = W_{T1} + W_{T2}$$
$$= 0,5 + 0,14$$
$$= 0,6^{o}C.$$

The uncertainty (W) in the product mass flowrate was

$$W_{G1} = [\,[\,(d\dot{G})/(dG)\,.\,W_L\,]^2\,]^{0,5}$$
$$= [\,[\,1/300\,.\,0,45\,]^2\,]^{0,5}$$
$$= 0,013 \text{ kg/s}$$
$$= 0,047 \text{ t/h}$$

At low air mass flowrates, plugs of material entered the receiving hopper. The product mass flowrate was derived from the slope of the mass versus time trace. The protractor used to measure the slope had a resolution of $0,5^o$. From a typical set of results, 51^o correspond to 7,1 t/h.

Thus the uncertainty (W_{G2}) in product mass flowrate was thus:

$$W_{G2} = 7,1\,.\,0,5/51$$
$$= 0,070 \text{ t/h}$$

I.2.3 TEMPERATURE

The resolution of the alcohol thermometer used to calibrate the temperature resistor was $0,5^oC$. Thus the corresponding uncertainty of the temperature resistor (W_{T1}) was $0,5^oC$. The voltage signal was recorded to within + 0,0005 V. From the slope of the calibration curve, the uncertainty is given by:

$$W_{T2} = 278,514\,.\,0,0005$$
$$= 0,14^oC$$

Thus the total uncertainty (W_T) of the temperature resistor was:

$$W_T = W_{T1} + W_{T2}$$
$$= 0,5 + 0,14$$
$$= 0,6^oC.$$

I.2.4 AIR MASS FLOWRATE

The air mass flowrate ($\dot{Q}$) was derived from:

$$\dot{Q} = \dot{V} \cdot \rho$$
$$= \dot{V} \cdot p / (R T)$$

where

$\dot{V}$ = volumetric flowrate
p = pressure
R = 0,287 (universal constant)
T = temperature

The uncertainty in the volumetric flowrate was obtained from the resolution of the inclined manometer (i.e, 0,5mm).

From the inclined manometer an average height of 149 mm corresponded to a volumetric flowrate of 22,8 m^3/min. Thus the uncertainty ($W_{\dot{V}}$) is given by:

$$W_{\dot{V}} = 22,8 \cdot 0,5/149$$
$$= 0,0765 \ m^3/min.$$

The uncertainty in the air mass flowrate is given by:

$$W_{\dot{Q}1} = [(\frac{d\dot{Q}}{d\dot{V}} \cdot W_{\dot{V}})^2 + (\frac{d\dot{Q}}{dp} \cdot W_p)^2 + (\frac{d\dot{Q}}{dT} \cdot W_T)^2]^{0,5} \quad (I.1)$$

The various terms in Equation I.1 are:

$$\frac{d\dot{Q}}{d\dot{V}} = \frac{p}{R\,T}$$

$$= 86 / (0,287 \cdot 300)$$
$$= 0,9988$$

$$\frac{d\dot{Q}}{dp} = \dot{V} \cdot \frac{1}{R\,T}$$

$$= 22,8 \cdot 1 / (0,287.300)$$
$$= 0,2648$$

$$\frac{d\dot{Q}}{dT} = -\dot{V}\,\frac{p}{R\,T^2}$$
$$= - 22,8 \cdot 86 / (0,287.300^2)$$
$$= - 0,0759$$

Thus, substituting in Equation I.1:

$$W_{Q1} = [(0,9988 \cdot 0,0765)^2 + (0,2648 \cdot 0,1602)^2]^{0,5}$$
$$= 0,09999 \text{ kg/min}$$
$$= 0,00167 \text{ kg/s}$$

The additional uncertainty in air mass flowrate (W_{Q2}) from the calibration curve is:

$$WQ2 = 661,413 [m^3/h/V] \cdot 0,0005 [V]$$
$$= 0,331 \text{ m}^3/\text{hr}$$
$$= 9,194 \cdot 10^{-5} \text{ kg/s}$$

Thus the total uncertainty in air mass flowrate is:

$$W_Q = W_{Q1} + W_{Q2}$$
$$= 1,67.10^{-3} + 9,194.10^{-5}$$
$$= 1,762.10^{-3} \text{ kg/s}$$

I.3 REPEATABILITY OF RESULTS

The repeatability is shown in Figures I.1 to I.5 where the conveying pressures from the repeated test are plotted against the conveying pressure as calculated with the equations developed in Section 5.2 at the same product and air mass flowrate. The percentage error as defined in Equation I.3 and the correlation coefficients are summarised in Table I.2.

$$\% \text{ error} = \left(\frac{|P(equ) - P(exp)|}{P(exp)} \right) . 100 \qquad (I.3)$$

TABLE I.2: REPEATABILITY OF RESULTS

PIPELINE CONFIGURATION	AVERAGE % ERROR	CORRELATION COEFFICIENT
100A	6,7	0,930
100B	6,6	0,985
100C	5,2	0,890
200A	5,9	0,985
200C	10,5	0,961

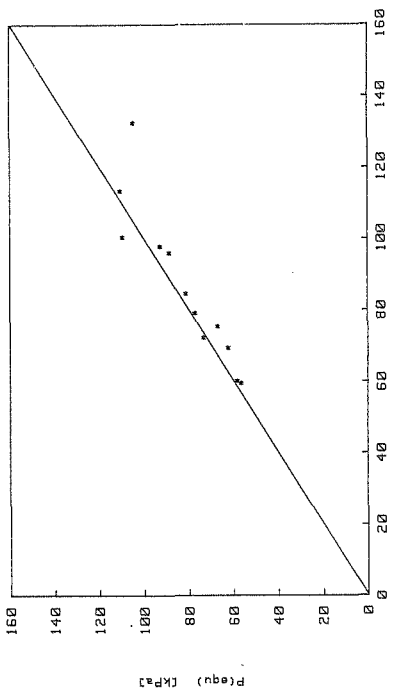


FIGURE I.1: P(equ) VERSUS P(exp) [100A]

100B

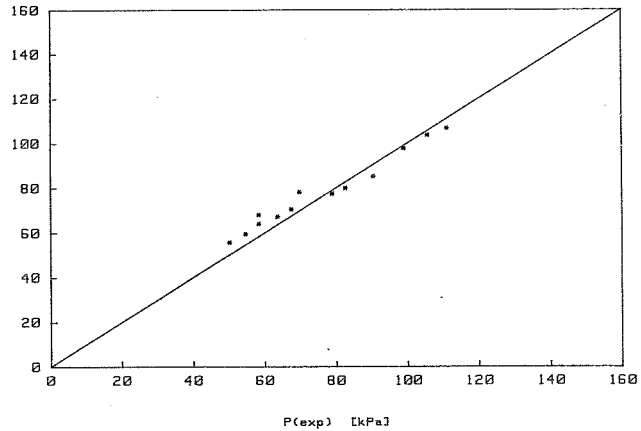


FIGURE I.2: P(equ) VERSUS P(exp) [100B]

100C

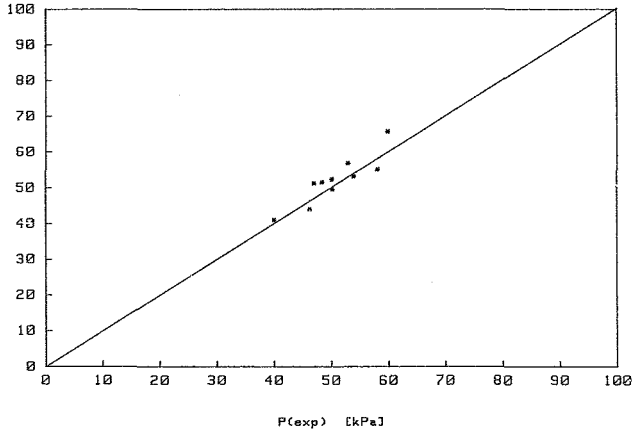


FIGURE I.3: P(equ) VERSUS P(exp) [100C]

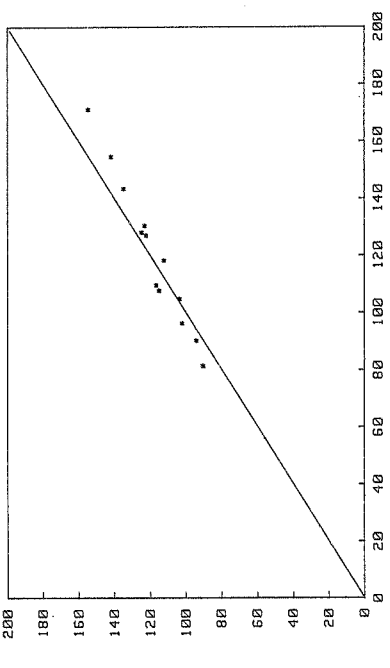


FIGURE I.4: P(equ) VERSUS P(exp) [200A]

FIGURE I.5: P(equ) VERSUS P(exp) [200C]

I.4 EQUATION ERRORS

The errors in the equations developed in Section 5.2 are summarised in Table I.3. The graphs in Figures I.6 to I.13 show the conveying pressures as calculated with the equations, plotted against the experimentally recorded conveying pressure. The errors are mainly due to the square root model of the equations not fitting the data. At high air mass flowrates, a linear model would fit the data more accurately.

The experimental uncertainties as discussed in Appendix I.2 also contributed to the errors in the equation.

TABLE I.3: EQUATION ERRORS

PIPELINE CONFIGURATIONS	AVERAGE % ERROR	CORRELATION COEFFICIENT
100A	5,9	0,975
100B	4,9	0,983
100C	7,6	0,897
100D	5,7	0,945
200A	3,6	0,978
200B	7,8	0,919
200C	11,3	0,916
400A	6,4	0,938

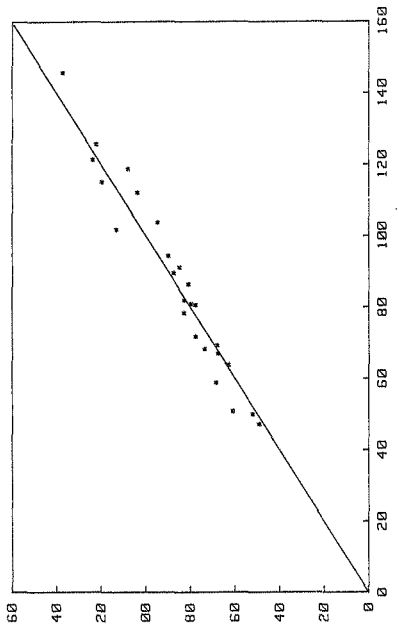


FIGURE I.6: P(equ) VERSUS P(exp) [100A]

100B

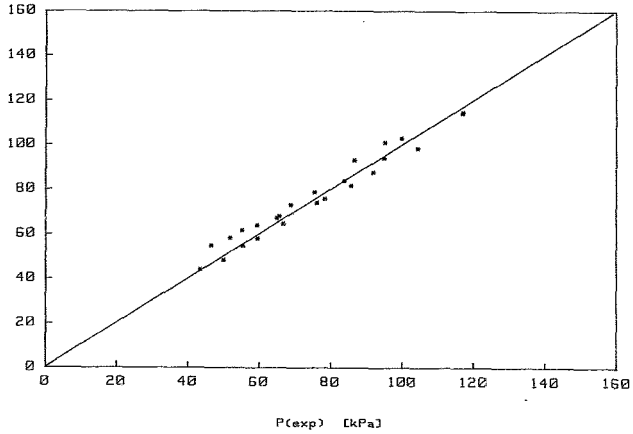


FIGURE I.7: P(equ) VERSUS P(exp) [100B]

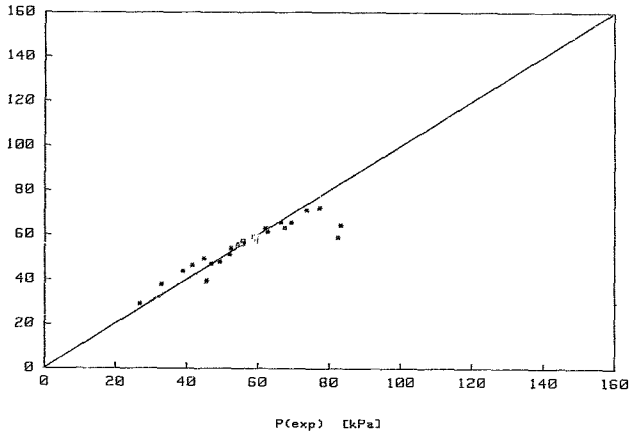


FIGURE I.8: P(equ) VERSUS P(exp) [100C]

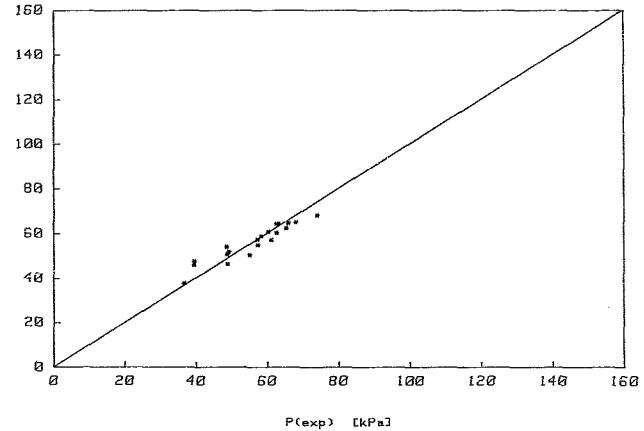


FIGURE I-9: P(equ) VERSUS P(exp) [100D]

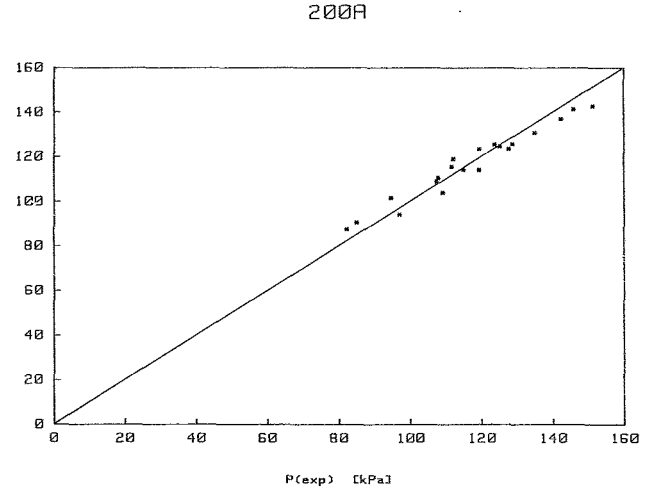


FIGURE I.10: P(equ) VERSUS P(exp) [200A]

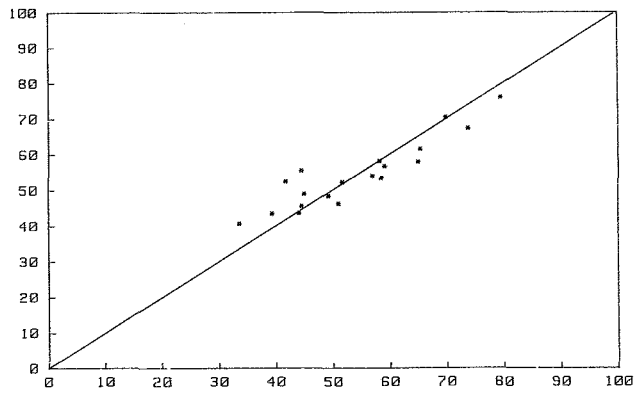


FIGURE I.11: P(equ) VERSUS P(exp) [200B]

FIGURE I.12: P(equ) VERSUS P(exp) [200C]

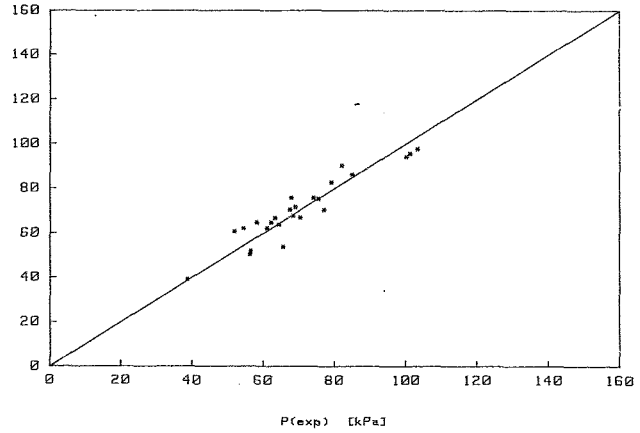


FIGURE I.13: P(equ) VERSUS P(exp) [400A]

I.5 MODEL ERRORS

The errors in the model developed to predict the performance of the long distance line, as discussed in Chapter 10, was determined by plotting pressure from the model against the experimentally recorded conveying pressure for the results from which the model was derived.

The errors are summarised in Table I.4.

TABLE I.4: MODEL ERRORS

PIPELINE CONFIGURATION	AVERAGE % ERROR	CORRELATION COEFFICIENT
100A	16,9	0,794
100D	25,4	0,870
200A	20,7	0,987
200B	12,9	0,919
200C	9,0	0,916
400A	13,7	0,935

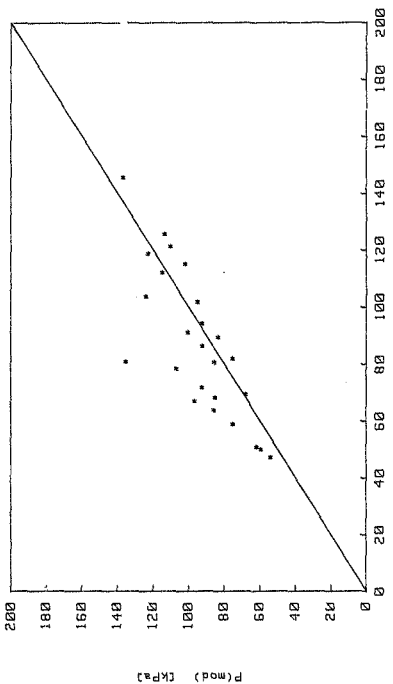


FIGURE I.14: P(mod) VERSUS P(exp) [100A]

FIGURE I.15: P(mod) VERSUS P(exp) [100D]

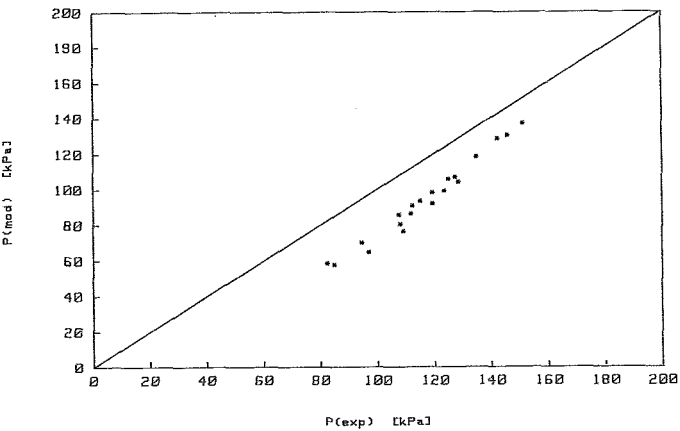


FIGURE I.16: P(mod) VERSUS P(exp) [200A]

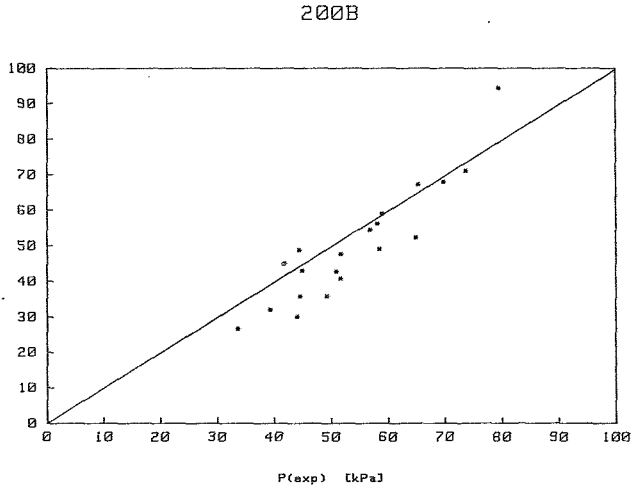


FIGURE I.17: P(mod) VERSUS P(exp) [200B]

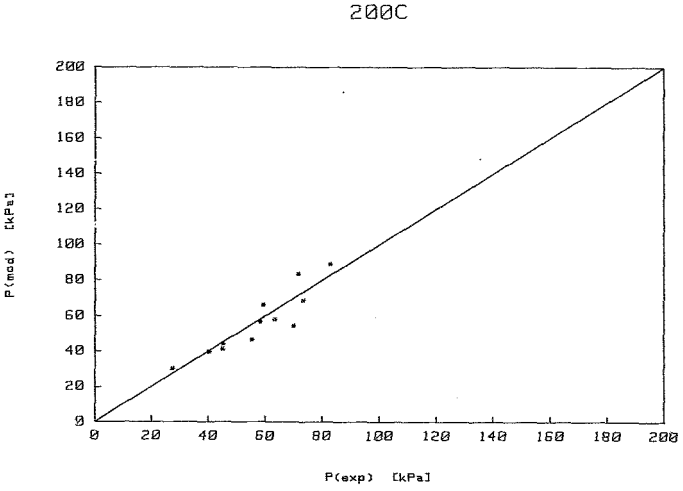


FIGURE I.18: P(mod) VERSUS P(exp) [200C]

FIGURE I.19: P(mod) VERSUS P(exp) [400A]

REFERENCES

1. BIRD, D.R. **Pneumatic transport of solids in pipes.** Lecture course. University of the Witwatersrand. September 1981.

2. BRITISH STANDARDS 1042: **Measurement of fluid flow in pipe.** Part 2A, 1973.

3. CHAMBERS, A.J., MARCUS, R.D. **Pneumatic conveying calculations.** Proc 2nd International Conference, Bulk Solids Materials Storage Handling and Transportation, Wollonyong, July 1986.

4. HUNKE, H. **Beitrug zur Optimalen Auslengung Pneumatischer Sonderanlagen fur den Baustoff Naturanhydrit anhand von Betriebsuersuchen mit Grossen Sonderlangen.** Dissertation, Technical University, Berlin.

5. JARDINE, K.J. **An investigation into the system characteristics of a pneumatic conveying system when transporting flyash for the use in the backfilling of coal mines.** MSc Dissertation, University of the Witwatersrand, Johannesburg, 1986.

6. KANO, T. **Reduction of power consumption in pneumatic conveying of granular materials.** Bulk Solids Handling, Vol.5, No.3, June 1985.

7. KLINTWORTH, J. MARCUS, R.D. **A review of low-velocity pneumatic conveying systems.** Bulk Solids Handling, Vol.5, No.4, August 1985.

8. KLINZING, G. **Gas-solid transport.** McGraw-Hill, USA, 1981.

9. KONRAD, K. **Dense phase pneumatic conveying through long pipelines: effect of significantly compressible air flow on pressure drop.** Journal of Powder Technology, 48 (1986), pp 193-203.

10. KONRAD, K., HARRISON, D., NEDDERMAN, R.M., DAVIDSON, J.F. **Prediction of the pressure drop for horizontal dense phase pneumatic conveying.** 5th International Conference, Pneumatic Transport of Solids in Pipes. London. 1980.

11. MARCUS, R.D. **Drag reducing flow in dilute phase pneumatic conveying.** MSc dissertation, University of the Witwatersrand, Johannesburg.

12. MARCUS, R.D. **Experimental observations obtained from long distance pneumatic conveying studies.** *Materials Handling Research Unit*, University of the Witwatersrand, Johannesburg.

13. MARCUS, R.D. *Pneumatic transport of solids.* Part 1. University of the Witwatersrand, Johannesburg.

14. MARCUS, R.D., CHAMBERS, A.J., RATCLIFF, S. **Design and operation of pneumatic conveying systems.** Lecture course, University of the Witwatersrand, Johannesburg. 1986.

15. MARCUS, R.D., DICKSON, A.J., RALLIS, C.J. **Some aspects of dilute phase pneumatic conveying of gas-solid suspensions.** The South African Mechanical Engineer. Vol.28, April 1978, pp 131-136.

16. MARCUS, R.D., HILBERT, J.D., KLINZING, G.E. **Flow through bends and acceleration zones in pneumatic conveying systems.** Bulk Solids Handling, Vol.5, No.4. August 1985.

17. MARCUS, R.D. RIZK, R., CHAMBERS, A.J. **Design and optimization of long distance pneumatic conveying systems.** *2nd International* Conference, Bulk Materials Storage Handling and Transportation, Wollongong, 1986.

18. MARCUS, R.D., RIZK, F., KLINZING, G., LEUING, C.S. **Pneumatic transport handbook,** In Press.

19. MARCUS, R.D., WIGGILL, C.R., RIZK, F. **Parameters influencing long distance pneumatic conveying systems.** Bulk Solids Handling, Vol.5, No.4. August 1985.

20. MASSEY, B.S. **Mechanics of fluids.** 5th Edition, Van Nostraud Reinhold. UK. 1983.

21. MEIJERS, S.J. **An investigation into the measurement of slip velocity for dilute phase gas/solids suspensions and the progression of the state diagram.** PhD Thesis, University of the Witwatersrand, Johannesburg, 1986.

22. MUSCHELKNAUTZ, E., KRAMBROCK, W. **Chemical engineering technology,** 41 (1969), 21 p 1164.

23. OWEN, P.R. **Pneumatic Transport.** *Journal of Fluid Mechanics,* Vol.39, Part 2, pp 407 - 432, 1969.

24. PERKINS, D.E. **Selecting and sizing pneumatic conveying systems.** Plant Engineering *Journal.* July 1980, pp 93 - 96.

25. PETERS, T.W. **Shirebrook pneumatic coal transportation scheme.** Mining *Technology,* December 1977.

26. RAMACHANDRAN, P.S., BULKHARD, D.G., LAUER, B.E. **Indian journal of technology.** 8(1970) p 199.

27. RIZK, F. **A comparison between horizontal and vertical pneumatic conveying systems considering the optimal operating condition.** *Journal of* Powder and Bulk Solids Technology. 7(1983) 3, pp 15-16.

28. ROSE, H.E., DUCKWORTH, R.A. **The Engineer** 478, March 1969.

29. ROSE, H.E., DUCKWORTH, R.A. ***Transportation* of solid particles in liquids and gases.** The *Engineer,* 1961, 14. March 21/28.

30. RUSKI, H.J. **The *influence* of stepped pipelines in pneumatic long distance *transport* of building materials.** Proc. Int. Conf. Pneumatic Conveying Technology, Jersey, Channel Islands. March 1987.

31. ROSSETTI, S.L., PFEFFER, R. A.I.Ch E.J. 18, 31 (1972).

32. SHUCHART, P. Chemical Engineering Technology, 40 (1963), pp 21 - 22.

33. SNOW, C.L. Long distance pneumatic conveying of dried slimes. MSc Dissertation, University of the Witwatersrand, Johannesburg, 1984.

34. SOO, S.L. Long distance pneumatic transportation. Journal of Pipelines 4(1984), pp 79 - 85.

35. SOO, S.L. Long distance pneumatic transportation. Pneumatic transport of solids in pipes, South African Institute of Materials Handling, University of the Witwatersrand.

36. STOESS (Jr), H.A. Pneumatic pipelines. Journal of pipelines, 1 (1981) 3-10. Elsevier scientific publishing company, Amsterdam.

37. STOESS, P.E. Pneumatic conveying. 2nd Edition, John Wiley and Sons, New York, 1983.

38. The Engineering Equipment Users Association : Pneumatic Handling of Powdered Materials. EEUA Handbook No.15, Constable & Co. Ltd. 1963.

39. TWEEDY, D. Pneumatic conveying in the mining industry. Pneumatic Conveying Research Group, University of the Witwatersrand, Johannesburg, 3 July 1979.

40. UNDERHILL, L.G. Introstat. Third Edition, Juta & Co. Cape Town, 1981.

41. VOGEL, R. Pneumatic conveying becomes more acceptable. School of Mechanical Engineering, University of the Witwatersrand, Johannesburg.

42. WEN, C.J., O'BRIEN, W.S. Pneumatic conveying and transporting. Chemical Processing and Engineering, Vol.8, pp 89 - 134. Marcel Dekker Inc. New York, 1976.

Author Bettman Richard
Name of thesis Long Distance Pneumatic Conveying. 1987

PUBLISHER:
University of the Witwatersrand, Johannesburg
©2013

LEGAL NOTICES:

Copyright Notice: All materials on the University of the Witwatersrand, Johannesburg Library website are protected by South African copyright law and may not be distributed, transmitted, displayed, or otherwise published in any format, without the prior written permission of the copyright owner.

Disclaimer and Terms of Use: Provided that you maintain all copyright and other notices contained therein, you may download material (one machine readable copy and one print copy per page) for your personal and/or educational non-commercial use only.

The University of the Witwatersrand, Johannesburg, is not responsible for any errors or omissions and excludes any and all liability for any errors in or omissions from the information on the Library website.